The Development of Analytical Methods for Investigations of Dynorphin A 1-17 Metabolism in the Central Nervous System and Peripheral Tissues and Transport at the Blood Brain Barrier

By

Courtney D. Kuhnline Sloan

B.S., Investigative and Medical Sciences and Chemistry, Saint Louis University, 2005

M.S., Pharmaceutical Chemistry, The University of Kansas, 2008

Submitted to the Department of Pharmaceutical Chemistry and the faculty of the Graduate School of the University of Kansas in partial fulfillment of the requirements for the degree of Doctor of Philosophy.

_____

Chairperson- Dr. Susan M. Lunte

_____

Dr. Kenneth L. Audus

_____

Dr. John F. Stobaugh

_____

Dr. Teruna J. Siahaan

_____

Dr. Jane V. Aldrich

Dissertation Defense: February 11, 2011

The Dissertation Committee for Courtney Kuhnline Sloan

certifies that this is the approved version of the following dissertation:

The Development of Analytical Methods for Investigations of Dynorphin A 1-17 Metabolism, in the Central Nervous System and Peripheral Tissues, and Transport at the Blood Brain Barrier

_____

Chairperson- Dr. Susan M. Lunte

Date approved:_____

This dissertation is dedicated to my parents, Pam and Mike Kuhnline,
for always pushing me to do my absolute best at everything I have ever attempted,
and to my husband, Patrick, for his continual encouragement and willingness to spend our first months as a married couple with me buried under my thesis.

This work was possible because of the unconditional love and support I have been so fortunate to have from each of you.

Abstract

Dynorphin A 1-17 (Dyn A 1-17) is an endogenous neuropeptide that acts preferentially at the kappa opioid receptor. Elevated concentrations of Dyn A 1-17 have demonstrated neurotoxicity via a non-opioid mechanism, potentially mediated by NMDA (N-methyl-D-aspartate) receptors. This neurotoxicity has further been implicated in a variety of conditions including neuropathic pain, stress, depression, and neurological disorders including; Alzheimer's and Parkinson's disease. Unlike traditional small molecule neurotransmitters, peptides can undergo enzymatic degradation once released into the extracellular space and these metabolites can then go on to exhibit their own unique properties *in vivo*, often at sites far distal to their releasing cells. The investigation of dynorphin metabolism is especially crucial at blood brain barrier, where a peptide metabolite may exhibit substantially different transport properties. Traditional methods for the quantification of neuropeptides are immunoassays such as ELISA (enzyme linked immunosorbent assay) and RIA (radioimmunoassay). While these techniques have excellent limits of detection, cross-reactivity between related species is a significant issue. Therefore, it is essential to develop analytical methodologies capable of simultaneously determining the concentrations of both the parent peptide and its metabolites.

In this thesis, the metabolism of Dyn A 1-17 in both the central nervous system and peripheral tissues as well as with an *in vitro* cell culture model of the blood brain barrier (BBB) is investigated. Methods for the separation and detection of Dyn A 1-17 and four of its key metabolites; Dyn A 1-6, Dyn A 1-8, Dyn A 1-13, and Dyn A 2-17 were developed using capillary electrophoresis (CE) with copper complexation and UV detection and liquid chromatography-tandem mass spectrometry (LC-MS/MS). Dyn A 1-6 was found to be a major metabolite in the above mentioned systems and therefore its permeability at the BBB was

investigated using bovine brain microvessel endothelial cells (BBMECs). The effect of this peptide on the permeability of the low molecular weight, low permeability compound fluorescein was also explored.

In addition to CE and LC-MS/MS, microchip electrophoresis is also investigated. More specifically the development of an immunoaffinity microchip electrophoresis system was begun. Online immunoaffinity enables sample clean-up and preconcentration on the separation device. By combining immunoaffinity with highly efficient electrophoretic separations, an integrated device to investigate dynorphin metabolism is fabricated. Miniaturization decreases analysis time, significantly improving temporal resolution. Additionally preconcentration will improve limits of detection, making the detection of endogenous concentrations of dynorphin peptides from biological samples feasible. Towards this goal, antibody screening and some initial microchip electrophoresis studies with amperometric and laser-induced fluorescence detection were investigated. Future directions include the incorporation of this device with on-line microdialysis sampling and the development of an immunoaffinity microchip electrophoresis system for investigating neuropeptides implicated in neuropathic pain.

Acknowledgments

I might be listed as the author on this thesis, but it was not a solitary effort by any means. There are many people without whom, this work would not have been possible and for all of you I am truly grateful.

First, I would like to thank my advisor, Dr. Susan Lunte for allowing me to work in her lab during my time at KU. Thank you for listening to my interests and then assigning me a project that not only nurtured those interests but challenged me. You have given me more opportunities than I could ever have asked for while in graduate school. I am fairly certain my family thinks all I did was travel during my time here because of all of the conferences I was lucky enough to attend. Because of you I am a better scientist, teacher, and presenter. Thank you for always seeing the positive in my work, even if I didn't see it at the time.

I also must gratefully acknowledge Dr. Terry Phillips of the NIH for welcoming me into his lab for six months and teaching me a plethora of things about antibodies. My experience in your lab and in Washington, D.C. was an amazing opportunity and I truly appreciate all of your mentorship. I also must thank your lovely wife Jennifer for several wonderful dinners and your colleague Dr. Heather Kalish for all her assistance in the lab.

Thanks to my committee members for taking time out of their busy schedules to be here today: Dr. Teruna Siahaan and Dr. Jane Aldrich and especially to my readers Dr. John Stobaugh and Dr. Ken Audus.

A special note of thanks to people who have helped me in the lab or contributed to this project directly: Dr. Kelly Desino, Dr. Dan Mudra, and Dr. Rebecca Nofsinger for teaching me about mass spec and how to be a responsible user of a shared instrument; Glen Bisbee and Scott

Toerber, amazingly talented engineers with the Waters corporation; Dr. Kshitij Patkar and Dr. Kelly Desino for teaching me the brain isolation procedures; Giuseppe and Dulan for later helping me with the isolation; Sara Thomas for the rat tissue harvests and the rest of Craig Lunte's lab for letting me live my last year in the mass room in your lab; and the Forrest lab for letting me use your plate reader and occasionally your cell culture lab.

Thank you to Nancy Helm for all of your help and friendship. Thanks to Ann and Karen for help with a variety of things, and Nicole for making my mass spec duties a little less stressful. Thank you to Gary Weber for help with posters, room reservations, and the always fun game of "Do you know where Sue is?"

The graduate school experience would not be complete without the other people who surround you on a day-to-day basis in the lab. I am so lucky to have had such a wonderful "lab family": Dr. Celeste Frankenfeld, Dr. Pradyot Nandi, Dr. David Fischer, Dr. Matthew Hulvey, Dr. Philip Livanec, Dhara Desai, Ryan Grigsby, Jessica Creamer, Anne Regel, Tom Linz, Dulan Gunasekara, and David Scott; undergraduates Emilie Mainz and Derek Jensen; and visiting scientists galore: Dr. Wendell Coltro, Dr. Mercedes Vasquez, Dr. Nobuyuki Suzuki (Nobusan), Dorothy Chrzaszcz, Jonas Bloedt, Emer Duffy, Christa Snyder, Giuseppe Caruso and Dr. Fracassi da Silva----- thank you all.

I do not think I would have stayed sane without the help of Dr. Matt Hulvey. You are definitely the post doc extraordinaire and if I can be half as helpful to the students in the Bailey lab I will consider myself a success. Your friendship and support will never be forgotten.

To Dave, Pradyot, and Ryan- thanks for letting me hang out when there were no girls in the lab and for always being willing to take a random lunch or dinner trip to find some new

exotic (& of course spicy) food to try! Dave and Pradyot, thanks for always being up for a philosophical discussion about just about anything, especially one that eventually led us to the Phoggy Dog. Ryan, thank you for all of your help in the lab, when you leave the place may seriously fall apart.

I owe a special thank you to the ladies of the Lunte Lab especially Dr. Celeste Frankenfeld, Dhara Desai, and Jessica Creamer for occupying the desk across from me and always being a sounding board for the "problem of the day". Celeste, without you I may never have figured out how to get started in the lab. Dhara, you are truly the little sister I never had and I miss you! Thanks for always making me laugh. Jess, you made the end of grad school more fun that I thought it could be and for that I am so happy. Thanks to Jess and Anne for numerous coffee runs and trips out for great food. While in grad school I also had the pleasure of mentoring two undergraduate students: Dorothy Chrzaszcz and Emilie Mainz. Thank you for helping me hone my lab training and teaching skills and for always being so enthusiastic about research. You both served as wonderful reminders of how exciting and interesting research can be. All of you are amazing women and scientists and I am so happy to have worked with each of you.

I also must thank the friends that I was lucky enough to find at KU. You have all formed a much needed support system throughout this crazy journey. So here it goes (in no particular order): Dr. Diana Sperger, Dr. Kelly Desino, Taryn Bagby, Dr. Bob Berendt, Dr. Brooke Barrett, Dr. Natalie Ciaccio, Maria (Thorson) Feeney, Dr. Daniel Mudra, Dr. Rebecca Nofsinger, Shuang Cai, Shara Thati, Talia Martin, Sarah Pyszczynski, Elodie Dempah, Dr. Joseph Lubach and Dr. Loren Schieber. Thank you to the incoming class of 2005 for being there at the beginning when we were buried in organic and being told we should know this from kindergarten (Dr. Brooke

Barrett, Maria (Thorson) Feeney, Dr. Natalie Ciaccio, Dr. Rosemary Ndolo, Alana Toro-Ramos, Barlas Buyuktimkin, Dr. Prakash Manikwar, Dr. Aaron Markham, Dennis Nguyen, Dr. Reza Esfandiary, Stephen Goldman, Dr. Julian Kissman, David Hart, and Dr. Andi Skinner). Thank you to Brooke, Maria, and Natalie- our prelim study group, and especially Brooke for sharing a love of all things organization.

Thank you Kelly Desino (and family) for your friendship and encouragement over the past 5 years and for introducing me to the art of stamping. Thank you Diana Sperger and Tim Davey for always being up for a night out or an impromptu bar crawl. Diana, thanks for being the best roommate in grad school for a month and for bringing Sam and Penelope along! Thank you Taryn and Tom Bagby for being wonderful friends and for letting me crash in your spare room and invade your lives for a month.

Thank you to my two best friends who I was lucky enough to meet on the first day of college: Elizabeth Lindeman and Sormarie Colon-LeFranc for always knowing how to make me laugh and for being able to pick up right where we left off no matter how much time has passed.

Of course none of this would be possible without the unending support, encouragement, and love I have received from my family. I am fortunate to have a very close extended family and for their love and encouragement I consider myself very lucky.

I want to thank my dad for always pushing me to do my best, for instilling in me a belief that I could be anything I wanted (even when I thought I wanted to be the first female president despite my intense hatred for arguing and debating or a veterinarian despite my fear of animals), and for improving my memory and recall one line of the Gettysburg address at a time.

I want to thank my mom for answering an infinite number of “emergency” phone calls at all hours only to find out I was just worried or stressed, for setting an excellent example of how to work hard to achieve your dreams, and for explaining to me at a young age that until I was all grown up, school was my job and it was important for me to work hard and succeed at my job. I don’t think you ever intended for me to stay in school this long, but without that message I may not have made it this far.

I also want to thank my brother for being the best younger brother a girl could have. Jake, you inspire me every day by your passion to help people. I only hope I can make half the impact in this world that you are. Thanks for always knowing how to make me laugh.

I want to thank all of the members of the Sloan family: Rick and Debbie you are the best mother- and father- in-law I could have ever imagined. Everyone should be as lucky to inherit such a huge group of brother- and sister-in-laws: Jim, Kori, Anna & baby; Bill, Ashlee (you’re a Sloan to me) & Madi; Peter & Rebecca; Mary (& Allen), Tricia, and Dennis. Thank you all for welcoming me into your life and your family.

Last but obviously not least, I will forever be grateful to my husband for his support throughout this challenging process. Pat you have been the best friend, boyfriend, fiancé, and now husband, and without you this road would have been so much more difficult. Thank you for always being understanding when lab and class consumed my life and energy and for making many trips between Champaign and Lawrence over the past five and a half years. I’m so excited to start the next chapter of our life together under one roof. Thank you for knowing when to encourage me, when to just listen to me complain, when to push me forward, and when to tell me to “just relax”.

Table of Contents

Chapter One:

Overall Thesis Objective and Chapter Summaries

1.1 Research Objectives

There is a continuing interest in the determination of peptides in biological samples. With the increasing interest in identifying *in vivo* signaling molecules and disease biomarkers, the development of analytical methods for the determination of peptides in plasma, urine, cerebrospinal fluid (CSF), and microdialysates is essential. Most endogenous peptides are present at low nM to pM concentrations within these complex matrices. Exogenously delivered bio-therapeutics are also becoming increasingly popular. The analytical methods by which these protein and peptide-based drugs are determined must be sensitive, quantitative, and robust.

This thesis explores a variety of techniques for peptide analysis including capillary electrophoresis (CE), microchip electrophoresis (ME), liquid chromatography with mass spectrometric detection (LC-MS/MS), enzyme-linked immunosorbent assay (ELISA), and immunoaffinity microchip electrophoresis (IAME). In particular, the need for analytical methods capable of simultaneously detecting the parent peptide as well as its metabolites is addressed. The work presented here is focused on a specific family of opioid peptides, the dynorphins, although much of it has applicability towards the determination of other neuropeptides, especially those which possess a high isoelectric point (pI).

1.2 Thesis Outline and Chapter Objectives:

1.2.1 Chapter Two

This chapter is a review of analytical methods for the quantitation of endogenous peptides. A variety of techniques are covered that have been employed for the determination of peptides in plasma, urine, tissues, and microdialysis samples. The review briefly describes matrix-assisted laser desorption ionization, radioimmunoassays, and ELISAs. However, the primary focus is on separation-based analyses including LC, CE, and ME. A variety of detection methods are also covered including UV, laser

induced fluorescence (LIF), amperometry, and mass spectrometry. Examples from the literature are given for a variety of biological matrices.

1.2.2 Chapter Three

The development of capillary electrophoresis methods for the separation of dynorphin A 1-17 (Dyn A 1-17) and four of its key metabolites is presented. Buffer optimization is discussed in detail. Phytic acid was used to circumvent adsorption of high pI peptides to the capillary wall. Additionally, resolution of closely related peptide metabolites was overcome using cyclodextrins. An on-capillary copper complexation technique was explored in an effort to improve limits of detection with UV and also to render the peptides electroactive for future applications using microchip electrophoresis with electrochemical detection. The *in vitro* metabolism of Dyn A 1-17 was investigated in human plasma as well as rat brain and spinal cord slices.

1.2.3 Chapter Four

This chapter is focused on the development of a quantitative LC-MS/MS technique for Dyn A 1-17 and its metabolites. Two mass spectrometry instruments, a Quattro micro (Waters) and an API 2000 (AB Sciex), were evaluated. Optimization for dynorphin peptides was performed on each. The tunable parameters and settings of the two were compared. The remainder of the chapter is focused on the optimization of the liquid chromatographic separation of the dynorphins and the challenges associated with the analysis of peptides in biological matrices. In particular ion suppression in the presence of a cell compatible solution, phosphate buffered saline with ascorbic acid (PBSA), was observed and modifications to this buffer were necessary for adequate ionization. This chapter lays the groundwork for the *in vitro* investigations of Dyn A 1-17 metabolism presented in Chapter 5.

1.2.4 Chapter Five

The LC-MS/MS method developed in Chapter 4 was applied to *in vitro* studies of Dyn A 1-17 metabolism. Initially the *in vitro* studies were performed in central nervous system (CNS) tissues, namely in rat brain and spinal cord slices. The metabolism was then investigated in the presence of an *in vitro* blood brain barrier (BBB) model consisting of a primary culture of bovine brain microvessel endothelial cells (BBMECs). The identification of Dyn A 1-6 as a key metabolite in each of these systems led to further investigations of this peptide's transport across the BBB. Directional and temperature dependence of this transport are addressed as well as the effect of this peptide on the transport of the low molecular weight, membrane impermeant molecule fluorescein.

1.2.5 Chapter Six

This chapter is a review of immunoaffinity capillary and microchip electrophoresis techniques as well as preliminary work towards the development of an immunoaffinity microchip system for investigating dynorphin metabolism. In moving towards micro total analysis systems (μTAS) for continuous monitoring of peptides, considerable improvements must be made in sensitivity and selectivity. In particular, neuropeptides are present *in vivo* at low nanomolar-picomolar concentrations. While immunoassays address the necessary limits of detection for these species, cross-reactivity with structurally homologous species can hinder accuracy. This is of particular importance when trying to study neuropeptide metabolism. As demonstrated in Chapter 2, electrophoresis offers a highly efficient separation format for such studies. Miniaturization can further improve temporal resolution of such techniques. However, sample clean-up and preconcentration are often essential for analysis in biological matrices, especially for the determination of low abundant peptides. Therefore, incorporation of an immunoaffinity port into a microchip electrophoresis device can combine the high specificity of immunoassay with the high resolving power of electrophoresis. For future applications involving *in vivo*

microdialysis studies, such devices have the added benefits of small sample volume consumption and fast separation times, making near-real time monitoring of neurochemical processes a conceivable reality.

1.2.6 Chapter Seven

This chapter gives an overview of the research presented in this thesis. The Dyn A 1-17 metabolites identified by both CE and LC-MS/MS are summarized. Future work towards the development of an integrated immunoaffinity microchip electrophoresis system for *in vitro* and *in vivo* investigations of dynorphin metabolism and transport at the blood brain barrier is described. Also, additional experiments involving IAME techniques for biologically related analytes such as an "immunoaffinity pain microchip" are addressed.

Chapter Two:

Analytical Strategies for the Determination of Peptides in Physiological Samples

2.1 Introduction

Peptides are involved in a plethora of signaling pathways *in vivo* including pain perception, blood pressure regulation, and neurotransmission. They can act as neurotransmitters, hormones, antibiotics, toxins, enzyme inhibitors, and immune modulators. Endogenous peptides have been implicated as potential biomarkers for a variety of diseases including neurological disorders such as Alzheimer's and Parkinson's diseases, diabetes, arthritis, neuropathic pain and some cancers. Exogenously delivered biotherapeutics are also gaining popularity, and thus their stability and pharmacokinetic properties *in vivo* must be investigated. Additionally, much of the work in the proteomics arena is focused on the analysis of peptide fragments, used to determine structural information about key proteins of physiological interest.

The analysis of peptides is therefore an important analytical pursuit for a variety of scientific areas including pharmaceutics, neurochemistry, clinical testing, biomarker discovery, proteomics, and peptidomics. More specifically, this analysis must be applied to *in vivo* and *in vitro* samples which are complicated matrices, containing other protein and peptide components that can interfere with analysis and diminish sensitivity. This chapter will therefore discuss analytical methods for the determination of peptides in biological samples. In particular, methods for analyzing known peptides in blood, urine, and cerebrospinal fluid (CSF) will be addressed, as well as the analysis of microdialysates from a variety of tissues and animal models. Common methods for sample preparation will be briefly described as they apply to biological samples. Primarily, mass spectrometric- and separation-based techniques will be discussed, although a brief discussion of immunoassays is also included.

2.2 Sample preparation

Several key challenges exist with the analysis of peptides, specifically those in biological fluids. The first, of course, is accurately determining the concentration of analyte(s) of interest in complicated matrices such as blood, urine, and cerebral spinal fluid, all of which contain a variety of salts, amino acids, peptides, and proteins that can interfere with analysis. In addition to these body fluids, peptides can be sampled from tissues via microdialysis, studied in tissue homogenates, and investigated with *in vitro* samples such as cell culture. Therefore, clean-up and desalting prior to analysis is often necessary. There are four commonly employed sample preparation methods that can aid in decreasing the effects of matrix components on analysis: solid phase extraction (SPE), protein precipitation (PP), liquid-liquid extraction (LLE), and immunoaffinity purification.

Protein precipitation is likely one of the simplest and least expensive sample clean-up procedures. PP is easily employed by the addition of at least twice the volume of either an organic (usually acetonitrile) or an acidic solution. Due to the fact that co-precipitation of peptides is possible, PP can risk loss of the analyte(s) of interest. This method is also often incorporated with other sample clean-up methods because remaining matrix components can still cause interference with subsequent analysis.

Liquid-liquid extraction relies on the different solubility of a compound in aqueous versus organic solvent. This method is difficult to employ for most peptides due to their inherent polarity. However, certain applications of LLE are beneficial, specifically when the peptide of interest is cyclic or contains modified N- and/or C-termini. Solid phase extraction (SPE) can be performed with a variety of materials including non-polar, polar, ion-exchange and mixed

materials, making this method selective and versatile. In addition to selecting the appropriate material for the desired application, solvents and elution solutions are also optimized for recovery of the peptides of interest. SPE can also conveniently be incorporated online prior to reverse phase LC with column switching techniques.

Immunoaffinity purification is a sample clean-up method with high specificity for the compounds of interest. For example, antibodies immobilized on magnetic beads can be used prior to analysis [1]. While offline immunoaffinity can be utilized, an advantage of such a technique is the various ways to incorporate online cleanup directly to the analysis method. For example, antibody modified affinity columns can be used prior to RP HPLC with the use of column switching. Antibodies can also be immobilized into capillaries or reservoirs for clean-up prior to analysis by capillary or microchip electrophoresis.

For many biological matrices, especially blood, large proteins such as albumin are responsible for a large portion of the matrix interference. Simple methods such as molecular weight cut-off filters can significantly reduce interference from these proteins. Care must be taken to determine recovery of the peptides of interest and account for loss following filtration. In addition to sample preparation to remove interfering matrix components, peptide adsorption to vials, pipette tips, as well as instrument components can interfere with accurate analysis, especially in low concentration samples. This issue will be very compound specific and will need to be addressed on a case-by-case basis during the method development phase for each peptide. In this thesis, the adsorption of dynorphin peptides to the wall of a fused silica capillary during analysis by CZE and the addition of ion-pairing agents in the sample and run buffer to prevent this (Chapter 3) [2] is discussed. In addition, silanization of glass side-by-side diffusion

chambers is employed in Chapter 5 to prevent dynorphin adsorption during cellular transport assays.

Sample stability is another important consideration in peptide analysis, both at room temperature, during sample prep and analysis, as well as during storage (typically frozen). Most reports have included various enzyme inhibitors to prevent degradation. As can be seen in Figure 2.1, the stability of bradykinin is significantly improved with the inclusion of both an ACE-inhibitor and an N-carboxypeptidase inhibitor (captopril and MEGETPA specifically) [3].

2.3 Analytical Techniques for Peptide Analysis

2.3.1 Immunoassays

Historically immunoassays have been employed for the quantitation of peptides. These methods are highly sensitive, and are typically aimed at the quantitation of one particular compound. Despite their sensitivity, cross-reactivity with peptides of similar structure or sequence can generate false results. This is especially problematic when sampling from a biological fluid that will likely contain other peptides. Assays are also time consuming and expensive. Radioimmunoassays (RIA) in particular are expensive due to the use of radiolabeled compounds and carry some risk of handling such reagents. Enzyme-linked immunosorbent assays (ELISAs) circumvent the use of radiolabeled compounds, but are still relatively expensive. Nevertheless, immunoassays have extensively been employed for the determination of peptides from a variety of biological fluids. Immunoassays have been reported for the detection of peptides in blood [4], plasma [5], urine [6, 7], and CSF [8-11]. A recent report describes a novel radioimmunoassay (RIA) for the quantitation of the iron regulatory peptide

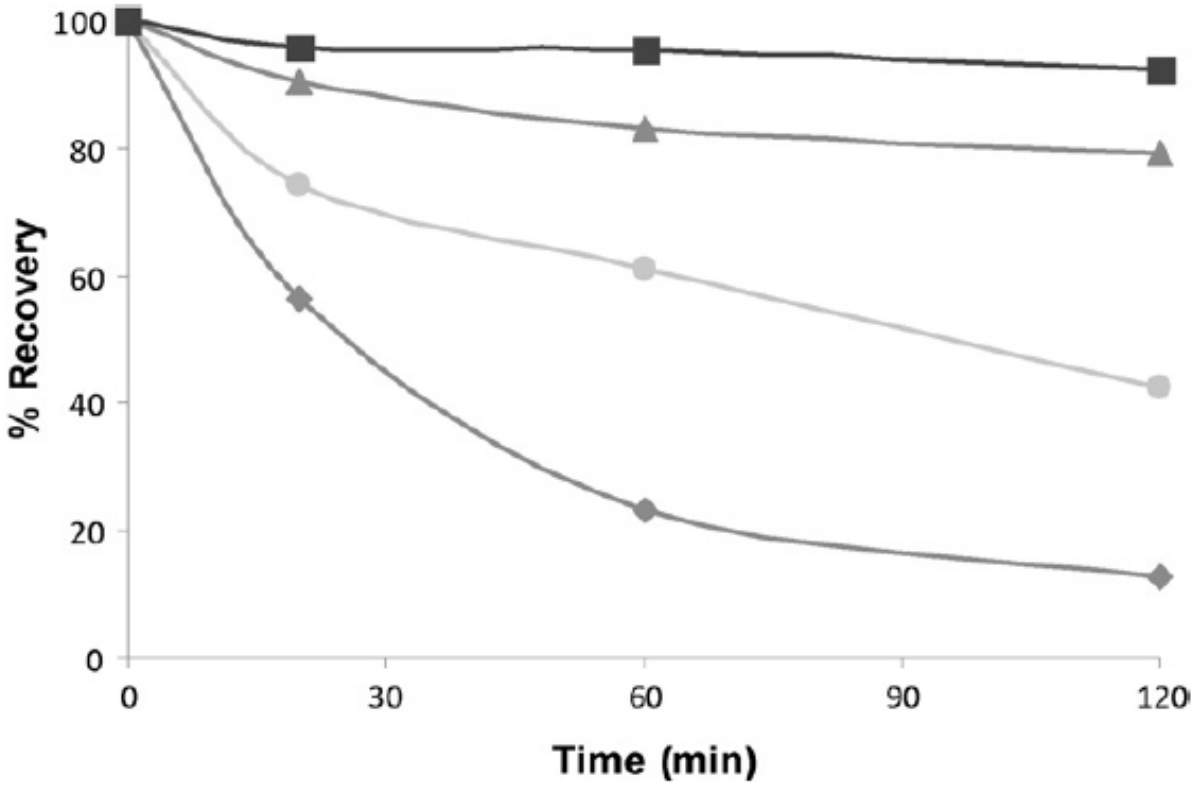

Figure 2.1 Bradykinin degradation in bovine plasma is inhibited by the addition of both the ACE-inhibitor captopril and the N-carboxypeptidase inhibitor MEGETPA (square data points) as compared to the stability of bradykinin in plasma without inhibitors (diamond data points). Full inhibition was not achieved with captopril alone (1 mM – circle data points or 2 mM- triangle data points). Reprinted with permission from [12].

hepcidin in human plasma, verifying the peptide's relationship to iron levels in patients with chronic kidney disease [5]. Patient hepcidin levels increased dramatically 24 hours post I.V. iron infusion (Figure 2.2).

In addition to the expense and time, immunoassays are typically employed for the detection of a single analyte. In most cases of peptide analysis, it is desirable to detect several related peptides simultaneously. For example, the investigation of peptide metabolism is essential for understanding the unique role of metabolites *in vivo*. Therefore, the remainder of this review will focus on methods that are capable of monitoring several related peptides in a single assay. This includes mass spectrometry- and separation-based methods for determining peptides in physiological fluids. In addition to the techniques discussed in the following sections, many researchers have found that a combination of separation techniques aids in the analysis of such complicated samples. Two dimensional chromatography [13-16], immunoaffinity CE [17, 18] and ME [19-21], and on-line CE-LC separations [22] have all been employed to improve limits of detection and decrease interferences from matrix components. Of particular importance to the work in this thesis is the increased combination of immunoaffinity purification on-line with electrophoretic separations.

2.3.2 Matrix assisted laser desorption ionization mass spectrometry (MALDI MS)

Matrix assisted laser desorption ionization mass spectrometry ionizes samples that have been co-crystallized with a compound which is usually a UV-adsorbing weak organic acid. Molecules are transferred to the gaseous phase following UV laser excitation. MALDI mass spectrometry is most often paired with time-of-flight (TOF) mass analyzers. Most MALDI MS

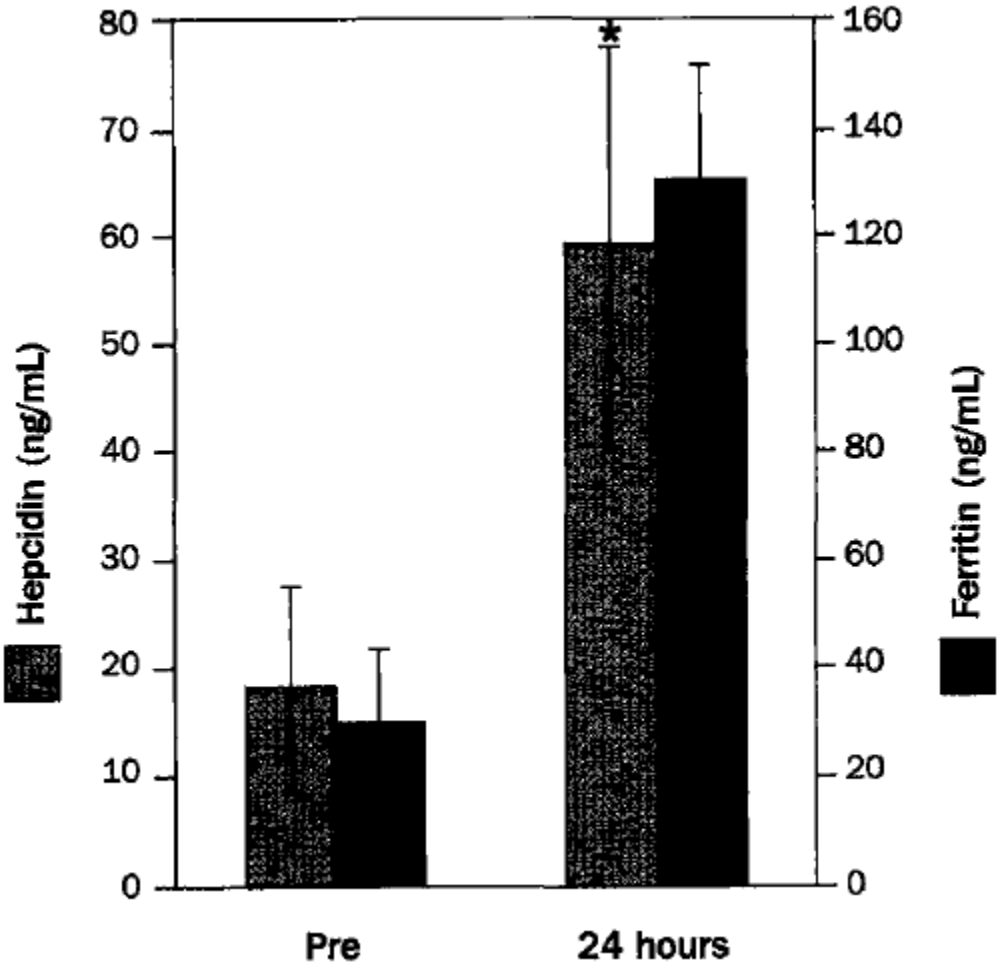

Figure 2.2 Hepcidin (grey bars) and ferritin (black bars) concentrations in patients with chronic kidney disease pre- and post-IV treatment with 200 mg iron sucrose. Reprinted with permission from [5].

applications are qualitative in nature and achieve accurate peptide identification in biological samples.

There are some semi-quantitative techniques reported, however; most reports utilize MALDI for its sensitivity, ionization interested readers should consult the following review [25]. MALDI also offers an attractive alternative of intact peptides and proteins, molecular weight determination, and wide mass range. One advantage of MALDI over electrospray ionization (ESI) is the increased ability to ionize samples in the presence of salts and buffers that are common contaminants in biological samples without signal suppression. De-salting prior to spotting on MALDI plates however, is still a common sample preparation technique. Additionally, ionization by MALDI is highly dependent upon the matrix chosen and sensitivity is both highly compound and matrix dependent. A variety of matrix components have been investigated to enhance ionization of peptides from biological samples [23, 24]. A detailed discussion of these processes is beyond the scope of this review, however; for the analysis of cyclic peptides which typically exhibit decreased ionization by ESI when compared to linear peptides. For example, the metabolism of the peptide cyclotide kalata B1 in plasma was characterized by both LC-MS and MALDI and the limits of detection were improved by two orders of magnitude with MALDI [26].

MALDI mass spectrometry has been applied extensively to studies investigating peptide metabolism in a variety of tissues, such as the degradation of neurotensin in human and rat plasma [27]. Chait and Kreek developed MALDI methods for the identification of dynorphin metabolites in both human and rhesus monkey blood *ex vivo* [28-30]. Additionally, the group investigated the *in vivo* metabolism of the peptide Dyn A 1-17 in rat striatum [31]. Reed *et al*

examined the biotransformation of the opioid peptide β-endorphin in the rat striatum via microdialysis [32]. The opioid activity of the identified peptide fragments (Figure 2.3) was further evaluated. In addition to the *in vivo* metabolism, the work also characterized β-endorphin degradation in rat cerebrospinal fluid and rat brain striatum slices. MALDI has also been used by others to analyze neuropeptide content in rat brain slices. Different neuropeptide patterns were exhibited between animals previously identified as low and high cocaine responders, suggesting a link between neuropeptide expression and addictive behavior [33]. MALDI has also been applied to the analysis of peptide biomarkers in urine [34, 35].

In addition to traditional peptide identification studies, recent work has focused on molecular imaging capabilities of MALDI (IMS). Several recent reviews are published on advances in this area [36, 37]. Direct analysis of peptides within tissue sections generates a three-dimensional representation of peptide distribution within whole organs, thus rendering not only molecular information, but also spatial localization [38]. For definitive peptide identification additional techniques, such as LC-MS/MS and MALDI-MS/MS, are often employed after MALDI imaging analysis is completed. Seeley and Caprioli reported the use of IMS for determining β-amyloid distribution in a mouse model of Alzheimer's disease [39]. Like traditional staining techniques, IMS enables the localization of these peptides in specific brain regions, but the technique also differentiates between various amyloid isoforms that are present in the disease model (Figure 2.4).

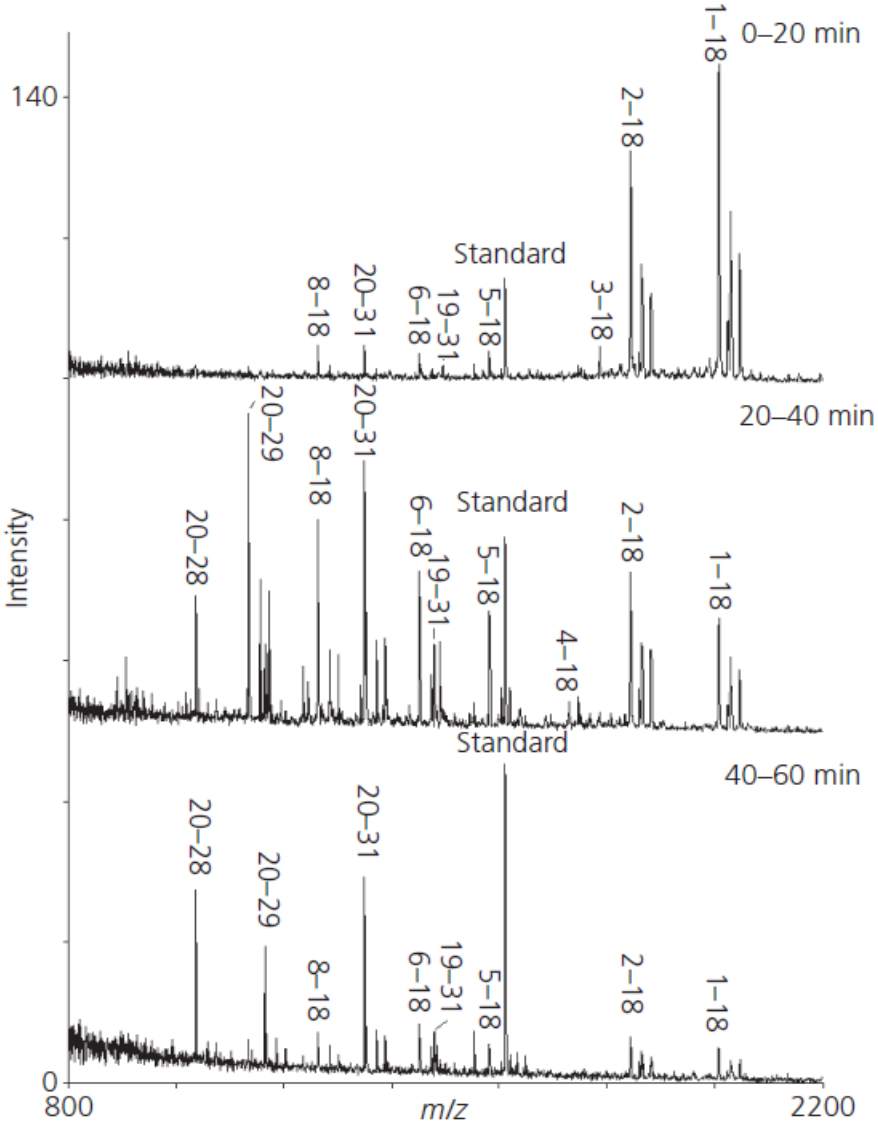

Figure 2.3 MALDI mass spectra of microdialysis samples from the rat brain striatum following microinfusion of β-endorphin. The appearance of new metabolites was observed with increased time. Reprinted with permission from [32].

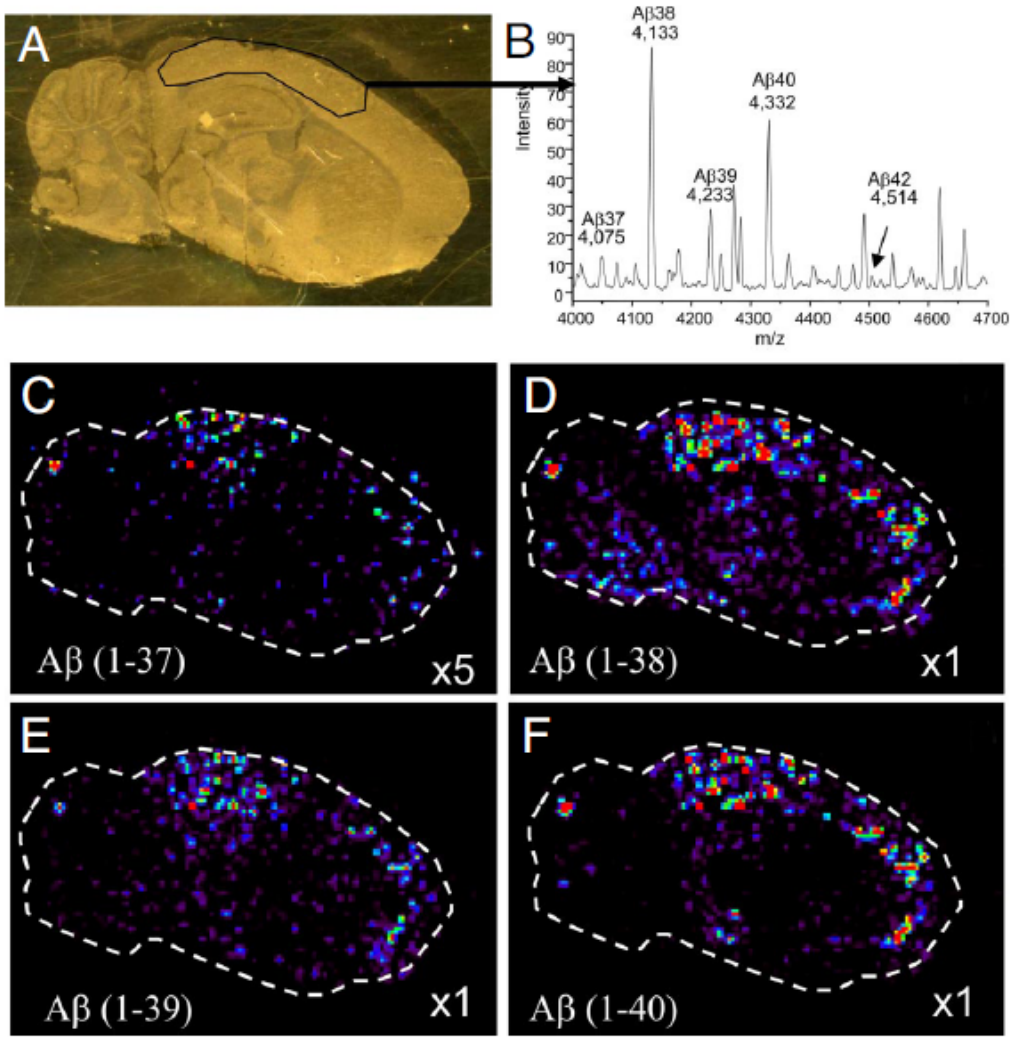

Figure 2.4 Imaging mass spectrometry (IMS) of β-amyloid plaques in an Alzheimer's disease model. Not only can plaque localization be determined, but also the molecular composition of those plaques. Reprinted with permission from [39].

2.3.3 Liquid chromatography

Liquid chromatography (LC) is a commonly employed separation technique for peptide analysis. Most applications utilize reverse phase stationary phases (C8 and C18 are common), and retention is based on the interaction of hydrophobic moieties on the peptide with the column stationary phase. LC can be paired with a variety of detectors including UV, fluorescence, and though not as common, electrochemical. UV detection is by far the most commonly employed mode of detection; however, the lack of specificity is a significant drawback, especially when sample matrices are complicated. Fluorescence and electrochemical detection both require derivatization of samples prior to analysis, as peptides lacking tryptophan residues are not inherently fluorescent and those lacking tyrosine residues are not electroactive. Nevertheless, there are still reports of peptide quantitation using these techniques. LC with UV detection has been employed for the quantitation of enkephalin and vasopressin analogs spiked into human urine [40]. Thompson *et al* utilized LC-UV for the determination of leucine enkephalin metabolism and transport at the blood brain barrier [41-43].

Weber's group has extensively evaluated the ability of peptides to form complexes with copper (II) ions, rendering even des-tyrosine peptides electroactive. They were able to detect a pharmaceutically relevant peptide in bovine serum using this method [44]. The peptide investigated, TP9201, is both cyclic and N-amidated preventing the applicability of most fluorescent labeling schemes for this analysis. Pre-column complexation with copper was utilized by Kennedy's group for the determination of vasopressin and bradykinin in rat microdialysates using capillary LC with electrochemical detection. The authors report concentration detection limits in the low picomolar range [45].

LC with fluorescence detection enabled the determination of leucine enkephalin (0.31 nmol/mL) in spiked human plasma following pre-column derivatization with NDA/CN^- [46]. Quantitative analysis of the opioid peptide drug DADLE and two cyclic prodrugs of the same peptide was achieved in rat plasma also employing pre-column NDA/CN^- derivatization [47]. SPE was used prior to peptide labeling, and the reported limit of quantitation was 6 ng/mL. In the work of Schwartz and Matuszewski a peptide-doxorubicin conjugate was evaluated as a prodrug approach to deliver the cytotoxic drug doxorubicin using LC with fluorescence detection [48]. Following I.V. administration stability was evaluated in chilled human plasma that contained the additive EDTA which prevented further *ex vivo* metabolism of the peptide-drug conjugate (Figure 2.5).

Matrix interference is often a significant issue with UV, electrochemical, and fluorescence detection due to the lack of specificity with all three of these detection methods. Sample clean-up is essential and often long gradient separations are required to separate peptides of interest from interfering species to accurately determine peptide concentrations. For these reasons, mass spectrometry is the most attractive detector for the analysis of peptides in biological fluids, and several reviews have been published on the topic [49-51]. The selectivity of mass spectrometry and the improved sensitivity and specificity gained from tandem mass spectrometry techniques make it an attractive mode of detection following LC separation. In LC-MS applications, special considerations must be taken when selecting a mobile phase system. Non-volatile buffers, for example, are not compatible with MS. Narrow-bore columns as well as capillary columns are more often employed in these systems to increase ionization efficiency due to decreased volumetric flow rate. Most applications involve direct coupling of the LC flow to electrospray ionization sources (ESI), and many also utilize tandem mass spectrometry

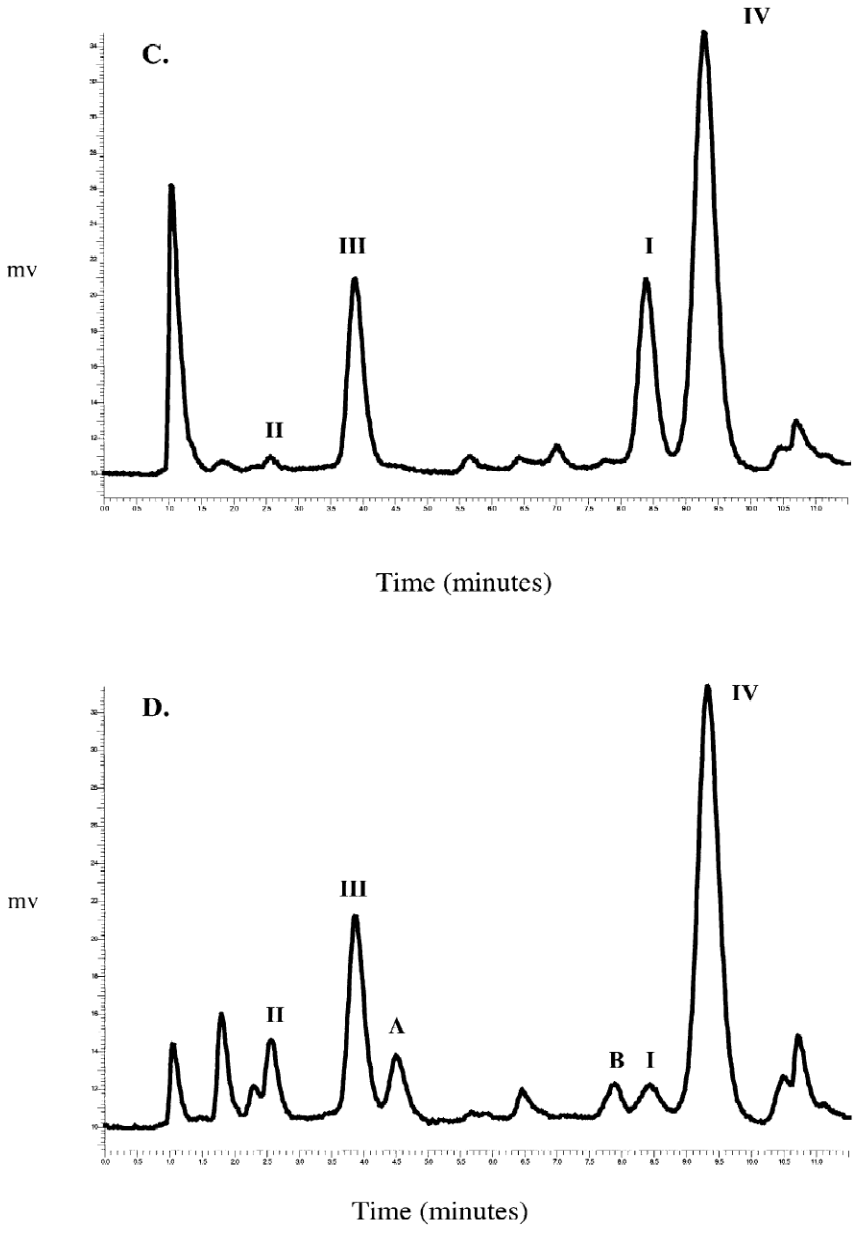

Figure 2.5 A- Human plasma 45 min post I.V. dose of compound I; B- Human plasma 2.5 hours post I.V. dose of compound I. Compounds I-IV (I= doxorubicin-conjugate, II-doxorubicin, III=leucine-doxorubicin, IV=internal standard). Reprinted with permission from [48].

functionality for the increased sensitivity and specificity as well as the improvements in quantitation.

Of all the body fluids, blood products are by far the most commonly analyzed. Its removal from patients is relatively non-invasive, and therefore much of the work towards identifying disease biomarkers has focused on peptide determination in plasma or serum. Drug plasma levels are also crucial for assessing pharmacokinetic properties of therapeutics, making assays that enable accurate and sensitive high throughput quantitation of peptides from this matrix essential for drug development. Researchers investigating melanotan-II, a synthetic peptide analog thought to have therapeutic potential for the treatment of obesity, were able to determine concentrations in both mouse plasma and brain homogenates following isoperitoneal (I.P.) administration of the peptide [52]. The method employed protein precipitation with acetonitrile prior to LC-MS/MS analysis and improvements over previously reported limits of detection were achieved in both plasma and brain tissue: 0.5 ng/ml and 2.5 ng/mL respectively versus 5 ng/mL and 40 ng/mL as previously reported [53]. Work by van den Broek and colleagues has utilized LC coupled to tandem MS for a variety of assays to quantitate peptide biomarkers in human serum and plasma [3, 12, 54, 55].

Pharmaceutical applications of exogenously administered peptides typically utilize LC-MS/MS for determination of drug plasma concentrations. Due to the high potency and therefore low dose of these drugs, analytical methods for the determination of these compounds in plasma must achieve excellent limits of detection. Muraro *et al* generated a plasma concentration-time profile of a synthetic parathyroid hormone analog in rat plasma after I.V. administration (Figure 2.6) [56]. The method enabled lower limits of detection of 0.2 ng/mL for the synthetic peptide.

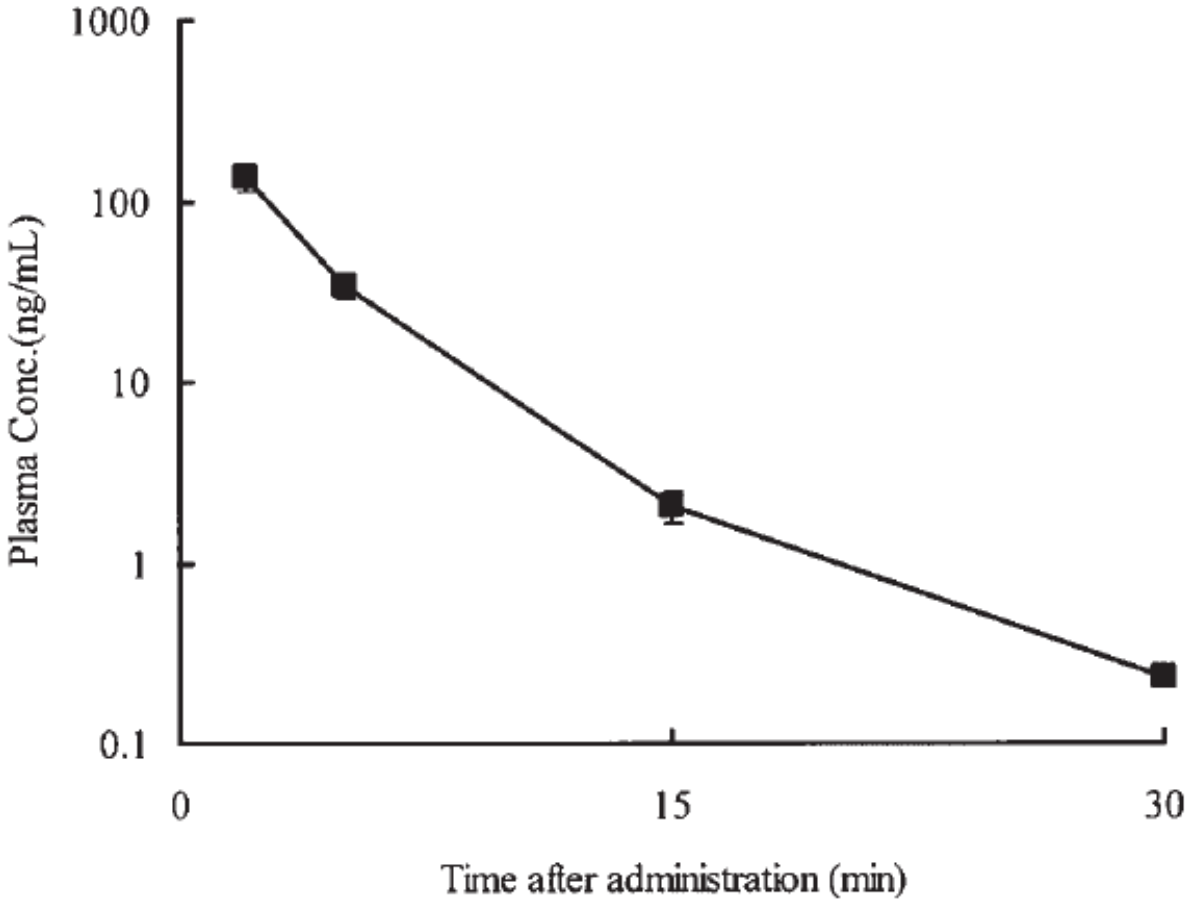

Figure 2.6 Plasma concentration-time profile in rat of [M_1]-PTH(1-14)NH_2 after I.V. administration (100 μg/kg). Reprinted with permission from [56].

Determination of the HIV inhibitor, sifuvirtide, was accomplished in HIV+ human plasma by LC-MS/MS with a simple protein precipitation sample clean-up procedure [57]. A lower limit of quantitation of 9.75 ng/mL was reported. Quantitative determination of a peptide drug in clinical trials is described by Lovgren *et al* with lower limit of quantitation reported as 5.0 pg/mL in human plasma [13]. The method employed a cyano column-C4 reverse-phase column-C18 reverse phase column couple to remove phospholipids known to cause ion suppression. The LC system was further coupled with an ESI-triple quadrupole mass spectrometer for tandem MS.

While blood (plasma and serum specifically) is by far the most extensively investigated biological fluid, urine has received considerable attention as a body fluid for screening biomarkers of disease. Very few intact proteins are found in the urine, therefore smaller peptide metabolites can more easily be identified [58-60]. The determination of type II collagen degradants by LC-MS/MS is described by multiple groups [61-63]. Type II collagen is known to degrade in patients afflicted with osteoarthritis, and as such is a potential biomarker for osteoarthritis for both diagnosis and progression. It is thought that metalloproteinases are responsible for this degradation, and therefore proteolytic peptide fragments of type II collagen are of interest as disease biomarkers. In these studies, immunoaffinity chromatography was performed online with a quantitative LC-MS/MS method to determine collagen peptides in rat and human urine [62]. The experimental set-up is shown in Figure 2.7. The potential with this method is a clinical assay for earlier diagnosis of osteoarthritis. C-reactive protein is another peptide investigated extensively as a biomarker in urine by LC-MS/MS [14, 58-60, 64].

The application of mass spectrometry to the quantitation of peptides in the central nervous system has also been employed. LC-MS/MS has been used for monitoring the release of

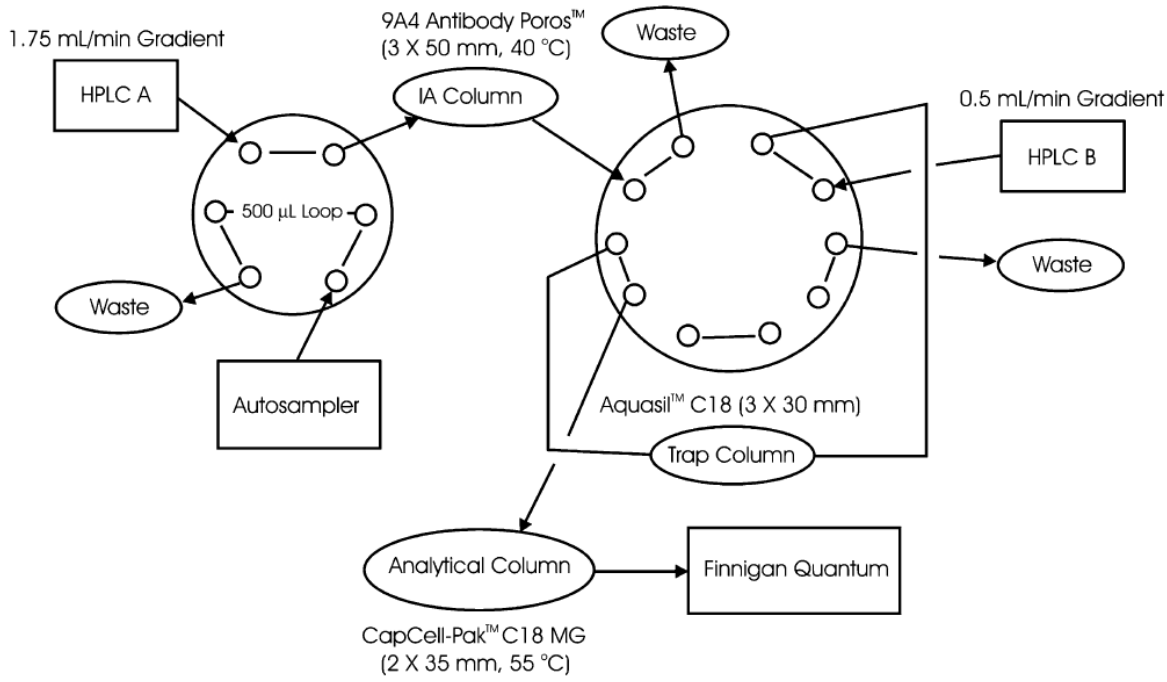

Figure 2.7 Immunoaffinity column switching diagram. Immunoaffinity (IA) column was functionalized with antibodies to the neoepitope of type II collagen (NET2C). At t = 0 min, 500 µL urine was injected onto the IA column (diverted to waste), at t = 1.7 min the sample was eluted from the IA column and focused on the trap column, and at t = 4.3 min gradient elution off the trap column and through the analytical column to the mass spectrometer was performed. Reprinted with permission from [62].

neuropeptides into the extracellular space following microdialysis sampling [65-67] and for the analysis of peptides in cerebral spinal fluid (CSF) [68-71]. *In vitro* investigations of blood brain barrier transport characteristics of endogenous neuropeptides [72] and synthetic peptide analogs [73-74] have also been explored using LC with tandem mass spectrometry.

2.3.4 Electrophoresis

Electrophoresis is also a convenient format for the separation of peptides since they are charged species. Separation occurs based on each compound's mass to charge ratio. Advantages of this mode of separation include small sample volumes, efficient separations with high resolution, and the potential for miniaturization which decreases sample volume further and improves assay time and often sensitivity. The simplest format of capillary electrophoresis is capillary zone electrophoresis (CZE); however, variations to this technique can be made to improve resolution and alter peptide electrophoretic behavior.

Capillary electrophoresis can be modified in rather simple ways to alter migration order and resolution, thereby improving the separation of peptides from interfering substances for each specific application. For example, surfactants can be incorporated to reverse the electroosmotic flow for faster detection of anionic species, modifiers such as cyclodextrins can improve resolution of closely related species, capillaries can be modified to prevent adsorption issues and alter electroosmotic flow, and transient isotachophoresis (tITP) can be used prior to CZE to preconcentrate samples thereby improving limits of detection. Similar modifications can be made in the microchip format as well, and the selection of microchip material can also be optimized for each desired application. Additionally a variety of detection schemes can be employed. Below a discussion of both capillary and microchip electrophoresis details other

important advantages of the two techniques as well as applications of each to peptide analysis in physiological fluid.

2.3.4.1 Capillary electrophoresis (CE)

A variety of detection modes can be employed with CE for the analysis of peptides including: UV [75], fluorescence [75, 76], electrochemical [77-79] and mass spectrometry [80, 81]. As with LC, UV detection is the most common; however, since this is a universal detector, matrix interference can be problematic. Nevertheless, CE with UV has still been employed for a variety of biological applications, simply because of its ease of operation and inclusion in most commercially available instrumentation. Most studies involve spiking the biological matrices of interest with known concentrations of peptide(s). Stroink *et al* utilized CZE coupled with online size exclusion chromatography (SEC) and a reverse-phase C18 trapping column for the detection of spiked enkephalins in human cerebral spinal fluid [22]. Angiotensin II and gonadorelin have been determined in plasma following spiking [82, 83]. Even when these peptides were spiked into plasma, sample clean-up by SPE was still necessary, and transient isotachophoresis was also incorporated prior to CZE for preconcentration.

One important application for which CE has been explored is for the determination of peptides in the central nervous system (CNS). Not surprisingly, perhaps, one of the most recent interests in neurochemistry is the development of sensitive assays for biomarkers linked to Alzheimer's disease. Aggregated forms of β-amyloid (Aβ) peptides are found in the plaques of patients with Alzheimer's disease as determined post mortem. Aβ peptides were investigated in CSF using CE with UV detection [84]. Sample preparation, storage conditions, and background electrolyte selection were optimized to prevent aggregation. As is demonstrated in Figure 2.8 A,

the separation of five amyloid peptide standards was achieved. The presence of Aβ 1-40 in the CSF of an Alzheimer's patient is confirmed following de-salting and 20-fold concentration of the sample (Figure 2.8 B).

Fluorescence and electrochemical (EC) detection have been utilized with CE; however, both typically require sample derivatization prior to analysis. Most labeling techniques require reaction with amine groups such as the peptide N-terminus or lysine residues. Therefore peptides with modified N-termini or those lacking a lysine residue will not be detected. Copper complexation however, is an attractive technique for the detection of peptides electrochemically [85-88]. It does not require an amine for the reaction and it is selective over amino acids residues and peptides of less than 3 amino acids in sequence. Complexation can be carried out on-capillary so that additional sample dilution is not necessary. CE-EC with copper complexation has been utilized by our group previously for the quantitation of enkephalin and angiotensin peptides spiked in human plasma [89, 90]. Non-aqueous CE has also been performed with electrochemical detection for the determination of leucine enkephalin and methionine enkephalin [91]. Conductivity detection has also been employed for the analysis of peptides [92-94]. In one particular example, cytochrome c and apomyoglobin were digested on-capillary with trypsin [95].

Determination of peptides in physiological fluids has also been performed using CE with fluorescence detection. The metabolism and transport of substance P at the blood brain barrier has been investigated by Freed *et al* utilizing CE-LIF [96, 97]. Samples were derivatized prior to CE analysis by NDA/CN^-. Peptide hormones [98] and carnosine-related peptides [99] have also been determined in the CSF by CE with LIF following pre-capillary derivatization with fluorescein isothiocyante (FITC) and 3-(4-carboxybenzoyl) quinoline-2-carboxaldehyde

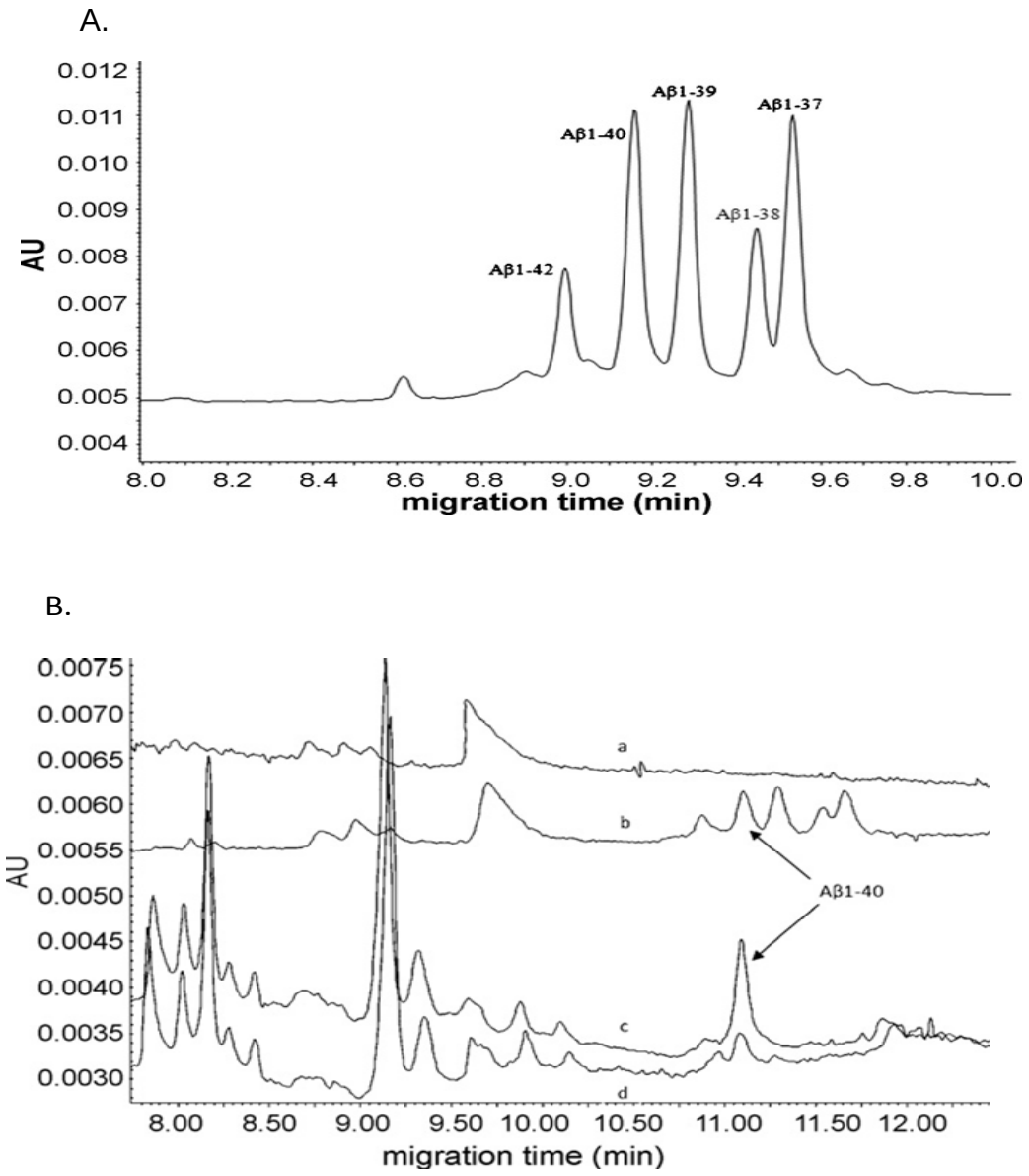

Figure 2.8 A. CE separation of 5 amyloid peptides using 1,4-diaminobutane (DAB) as a dynamic capillary coating to slow electroosmotic flow (EOF) and improve resolution. B. Electropherograms of CSF from a patient with Alzheimer's disease (AD). CSF from an AD patient (A), CSF from an AD patient, spiked with 5 amyloid peptides (B), CSF from an AD patient, desalted and concentrated, Aβ 1-40 confirmed by spiking (C), and CSF from an AD patient, desalted and concentrated (D). Reprinted with permission from [84].

(CBQCA), respectively. Sheeley *et al* exploited the high resolving power of CE to separate D-amino acid-containing peptides from their L-amino acid counterparts [100]. While mass spectrometry would not distinguish between these two compounds because their masses are identical, CE-LIF does. Peptides were derivatized with fluorescamine prior to separation and then were resolved under MEKC conditions employing the surfactant sodium dodecyl sulfate (SDS) as well as gamma cyclodextrin to further improve resolution. The D-amino acid-containing peptide, NdWFa, and its counterpart, NWFa, were then detected in the neurons of the abdominal ganglia of *Aplysia californica*.

CE has also been employed with mass spectrometric detection. Online coupling of CE to MS uses electrospray ionization (ESI), while offline CE-MS analysis is typically accomplished with matrix-assisted laser desorption ionization. CE-ESI-MS uses either a sheath- or sheathless-flow to directly couple the CE flow to the ion spray source. Special care must be taken when selecting a background electrolyte (BGE) in these applications due to the need for a highly volatile solvent for ESI. Typical BGEs such as sodium phosphate, for example, are incompatible with electrospray ionization. With CE-MALDI-MS, the CE eluent is spotted directly onto MALDI plates for identification of peptide samples. Several reviews on the coupling of CE to mass spectrometry can be consulted for more detailed information [80, 81, 101-103].

Several CE-MS methods have been applied to the determination of polypeptides in urine as potential biomarkers for renal diseases and prostate cancer [104-107]. Kaiser *et al* were able to establish polypeptide patterns using CE with ESI-TOF MS [108]. The method developed was applied to the analysis of urine from patients with various renal diseases. As can be seen in Figure 2.9, urine polypeptide distribution patterns differ between healthy patients and those with diabetic nephropathy, minimal change disease (MCD), and focal segmental glomerulosclerosis

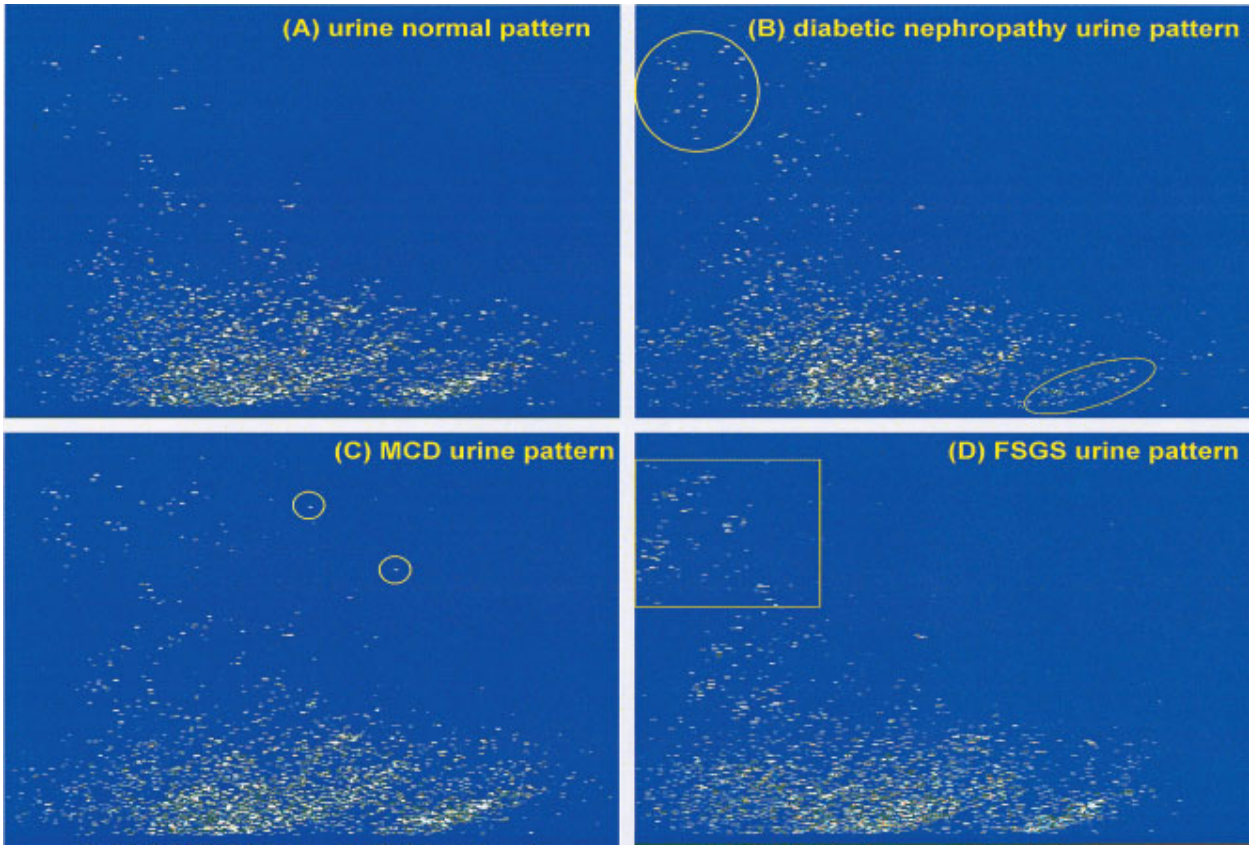

Figure 2.9 Differing polypeptide patterns in urine samples of A- healthy patients, B-diabetic nephropathy, C-minimal change disease, and D-focal-segmental glomerulosclerosis. Reprinted with permission from [108].

(FSGS). To obtain structural information about the polypeptides, offline coupling of CE to a MALDI TOF-TOF instrument was subsequently performed.

CE-MS has also been applied to the analysis of blood and plasma. Work by Cao and co-workers separated α- and β-hemoglobin in human blood using CE-ESI-MS [104]. Neuropeptides were analyzed by on-line SPE-CE-ESI-MS in human plasma [109]. Plasma samples were subjected to protein precipitation with acetonitrile and ultafiltration with a molecular weight cut-off filter prior to solid phase extraction on a C18 microcartridge and analysis by CE-ESI-MS. Limits of detection ranged from 0.1 to 10 ng/mL depending on the peptide.

2.3.4.2 Immunoaffinity capillary electrophoresis (ICE or IACE)

In addition to offline sample clean-up techniques, online incorporation of immune-based sample preconcentration is widely explored in conventional CE [110-113]. Antibody immobilization at the capillary inlet or into a small frit attached to the capillary enables biological samples to interact with selected antibodies prior to electrophoresis. This effectively cleans the sample of any extraneous matrix components while simultaneously concentrating the peptides or proteins of interest at the head of the separation capillary.

Kalish and Phillips used immunoaffinity CE for the determination of inflammatory secretions from single cells [114]. Eleven different cytokines and chemokines were determined in single astrocytes following stimulation with vasoactive intestinal peptide (VIP). The same group also reported the detection of neurotrophins in the serum of head trauma patients when previously such determinations have only been possible directly from brain tissue or CSF [115].

Guzman and coworkers have pioneered the use of this technique for the analysis peptide biomarkers and for proteomics [111, 116]. In one such example, immunoaffinity-CE-MS is used to differentiate between endogenous erythropoietin (EPO) and exogenously administered EPO analogs [117, 118].

Immunoassays can also be performed on-capillary in solution. Work by Kennedy's group examined the insulin content of single islets of Langerhans by a capillary-based competitive immunoassay with LIF detection [119, 120]. In these instances, detection of the free-labeled compound (in this case insulin) and the insulin-antibody complex are detected (Figure 2.10). The effect of glucose and calcium stimulation on insulin secretion were also evaluated in these cells (Figure 2.11)

2.3.4.3 Microchip electrophoresis (ME)

Microchip electrophoresis is a miniaturized form of CE. Channels are fabricated from a variety of materials including glass, plastics, and polymers. Separations by microchip electrophoresis boast numerous advantages over the conventional format: decreased reagent consumption and analysis time, for example. Other features such as their small footprint and portability, the ability for mass production and fabrication from disposable materials, and integration of multiple processes on a single device have fueled the exploration of such devices for clinical diagnostics. Reviews of the application potential for microchip devices in the analysis of biomolecules are already published [121, 122].

The most commonly employed modes of detection for ME are fluorescence and electrochemical; however, there are some reports of mass spectrometric detection as well.

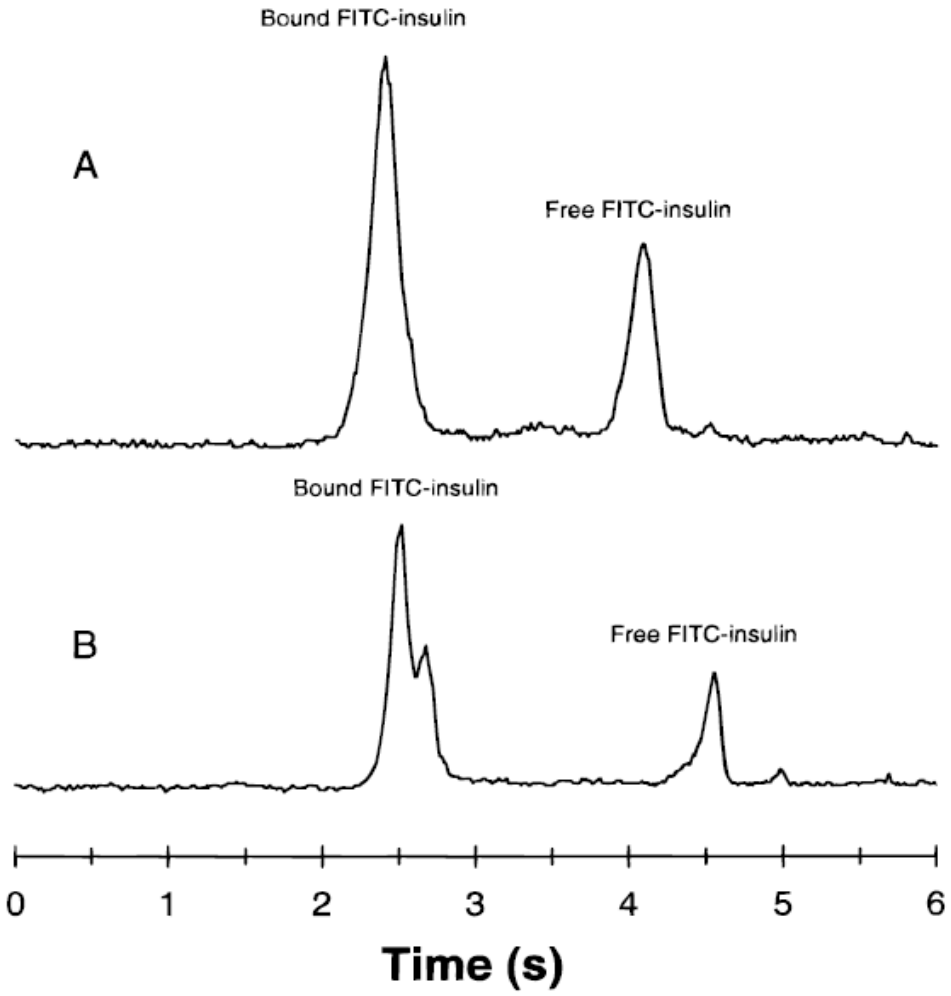

Figure 2.10 Electropherogram of bound FITC-insulin and free FITC-insulin following on-capillary immunoassay. Injection times: A- 400 ms and B- 80 ms. Reprinted with permission from [119].

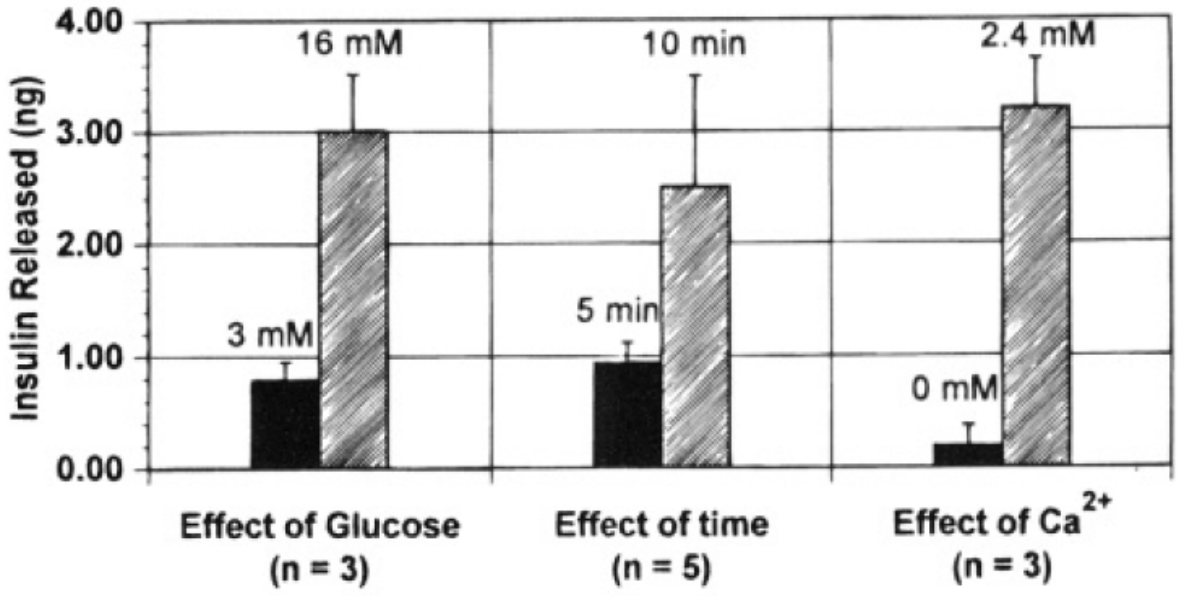

Figure 2.11 Insulin release from single islet of Langerhans following both glucose and calcium stimulation. Reprinted with permission from [120].

Electrochemical detection can be miniaturized without a loss in sensitivity. Amperometry is commonly employed due to simplicity of electrode integration within the microchip device, especially when polymer substrates such as PSMS (poly (dimethylsiloxane)) are used. Work in our lab employed the previously mentioned copper complexation technique to leucine enkephalin peptides offline prior to analysis on PDMS microchips with both carbon paste and carbon fiber working electrodes in a dual electrode format [123, 124]. Conductivity detection has also been illustrated for the detection of peptides; however, the application of these devices for physiological samples has not yet been extensively explored [125-129].

Both fluorescence and chemiluminescence have been utilized for on-chip analysis of peptides. Huynh *et al* performed on-chip derivatization of peptides with naphthalene 2,3-dicarboxaldehyde/2-mercaptoethanol (NDA/2ME) from microdialysate, enabling subsequent ME separation with laser induced fluorescence, and demonstrating the utility of these devices for integrated sample preparation, separation, and on-line sampling [130]. Microchip analyses have also been performed for the determination of carnosine-related peptides in both human CSF and canine plasma following derivatization with a chemiluminescent label [131]. The same group analyzed the intracellular sulfhydryl protein hemoglobin in single human red blood cells [132]. Cells were injected and lysed on-chip and their contents separated and determined downstream following on-chip labeling.

While these examples highlight the use of microchips for the determination of peptides in "real" biological samples, much of the work in this arena thus far is still in its early stages of development. Techniques for sample concentration prior to analysis as well as improved clean-up of matrix constituents are currently being explored by numerous groups to advance the microchip platform in these research areas. One such technique, involving antibody

immobilization within miniaturized devices, has received considerable attention in the past decade and is discussed in further detail in the next section of this chapter.

2.3.4.4 Immunoaffinity Microchip Electrophoresis

Much of the work with microchips for the analysis of physiological samples has incorporated sample-cleanup and preconcentration on the microchip device itself. To this end, immunoaffinity microchip electrophoresis has been extensively explored. As mentioned at the beginning of this chapter, immunoassays have long been the standard method for quantitation of peptides and proteins. However, the need to analyze more than one peptide simultaneously and often peptides of similar structure renders cross-reactivity a significant drawback to these techniques. Analytical researchers have, however, found convenient means for exploiting the antibody-antigen reaction in combination with electrophoretic separation.

Online incorporation of immunoaffinity preconcentration and sample purification to both CE and ME is quickly becoming a go-to method for peptide and protein analysis [110-113]. This work has been pioneered in part by the work of Dr. Terry Phillips. Work in his lab has demonstrated the potential of these methods for the analysis of clinical samples ranging from skin biopsies to tears [17-21, 114, 115, 133]. In one report, the use of an immunoaffinity microchip electrophoresis system with LIF detection enabled the quantitation of twelve neuropeptides simultaneously in just two minutes [19] as can be seen by the electropherogram in Figure 2.12. Additionally, brain-derived neurotrophic factor (BDNF) concentrations were determined in human skin biopsies. These levels are related to atopic inflammatory events and can distinguish between patients who experienced no allergic reaction to severe atopic

dermatitis. The relationship between the location of the tissue biopsy (i.e. distance from the skin lesion) was also explored (Figure 2.13) [21].

The inclusion of sample preconcentration on a microchip device is essential for the application of such methodologies to the analysis of complex samples. Progress in this area, in combination with work towards miniaturized detectors, on-chip derivatization, and on-line sampling, such as the coupling of microdialysis directly to the separation device, will enable the development of fully functional micro total analysis systems for fast, portable assays.

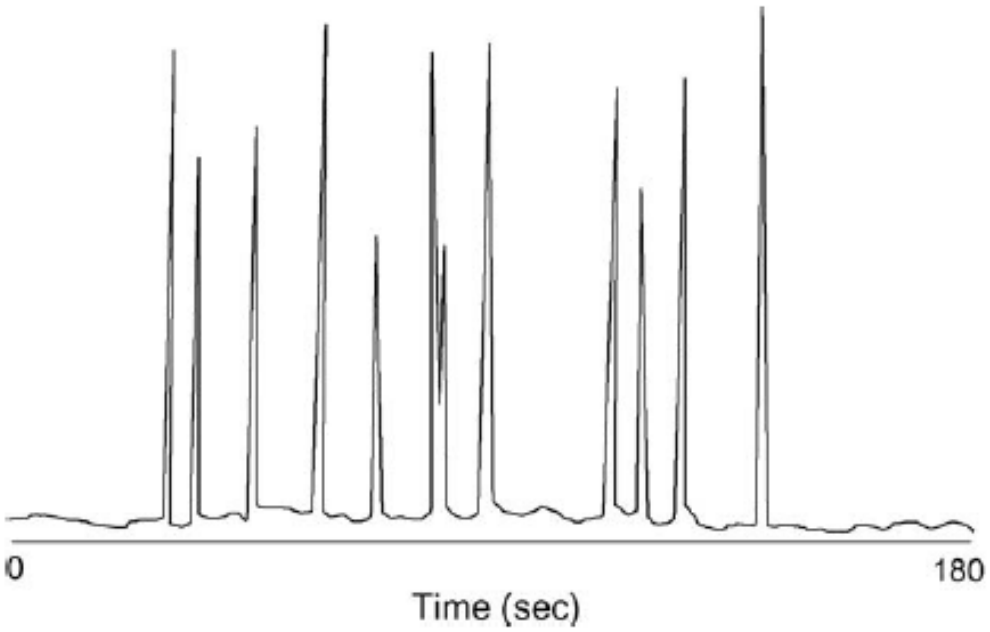

Figure 2.12 Electropherograms of neuropeptide standards (SP, CGRP, BDNF, IL-1β, VIP, NY, NT-4, β-endorphin, ACTH, CRH, IL-6, and TNF-α) following immunoaffinity microchip electrophoresis. Reprinted with permission from [19].

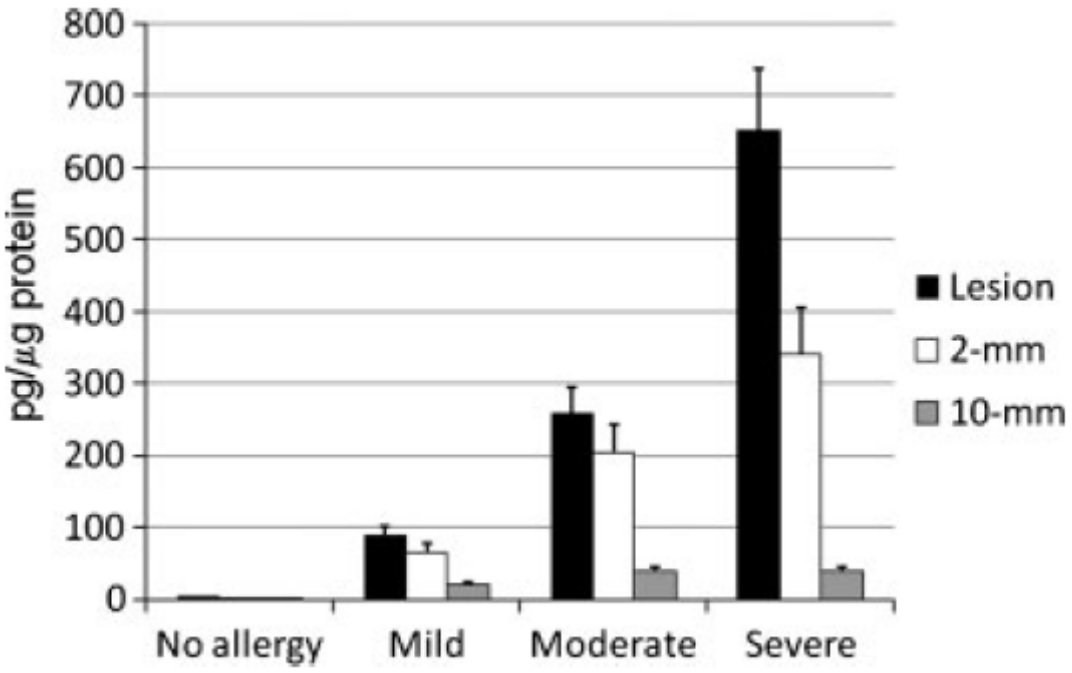

Figure 2.13 Effect of distance from skin lesion on BDNF concentration in patients with varying degrees of atopic dermatitis. Reprinted with permission from [21].

2.4 Summary

This chapter reviews a variety of separation-based techniques for the determination of peptides from physiological solutions. Sample preparation is briefly addressed as well as immunoassays which have long been the gold standard for peptide and protein quantitation. The applications of these methods to the analysis of blood, urine, CSF, microdialysate, and cell culture studies are also described and examples are presented.

Each of the methods discussed in this review has advantages and disadvantages for the determination of peptides in physiological fluids. Both ELISA and RIA boast excellent limits of detection, enabling the determination of endogenous concentrations of low abundance peptide biomarkers. However, the expense and problems associated with cross-reactivity limit their applicability for simultaneous determination of similar peptides. This is especially problematic for investigating peptide metabolism. MALDI mass spectrometry can simultaneously monitor a plethora of peptides without suffering ion suppression to the same extent as other ionization methods, such as electrospray. Imaging capabilities with this technique make it not only a tool for molecular identification, but also spatial localization within organs. Its quantitative abilities are limited, however, making this a method primarily used for peptide identification.

Separation-based techniques offer advantages over immunoassays and MALDI MS in that they can be paired with various detectors often enabling quantitative analysis while also simultaneously determining multiple peptides within a given sample. Liquid chromatography, capillary electrophoresis, and microchip electrophoresis are described in this chapter as they apply to peptide analysis. UV, electrochemical, fluorescence, and mass spectrometric detection have been employed to varying degrees with most of these separation techniques.

Liquid chromatography is a robust separation technique that has been used extensively for peptide analysis. Specifically LC-MS/MS has seen extensive use for peptide analysis and is considered the gold standard of analytical techniques in most industrial applications such as pharmaceutics. Instrumentation and columns can be costly, and long gradients are often necessary for peptides. Electrophoresis offers an attractive separation for peptides which are charged species. The highly efficient separations and low sample volumes are advantageous when analysis of volume-limited samples (such as microdialysis) is desired. The low injection volumes can be problematic when very low abundance peptides are the analytes of interest, and therefore pairing CE with sensitive detectors is especially advantageous. Miniaturization of the separation device decreases the sample volume requirements even further and offers faster analysis times and portability as additional advantages. Resolution of structurally related peptides can be problematic in these microchip devices; however, various substrate and design options offer the users flexibility.

UV detection is the most commonly used detection method with both LC and CE. Its use is simple and most commercially available instrument comes outfitted with such detectors. For peptide analysis, however, it is limited primarily by its selectivity, especially when analyzing biological samples containing interfering substances. Electrochemical detection requires an electroactive moiety, such as tyrosine. Its applications to peptide analysis have been extended by derivatizing strategies such as copper complexation. This detection method has seen extensive application in microfluidic devices due to its inherent scalability. Miniaturization of electrodes does not impact its sensitivity in the same way decreased pathlength decrease UV absorbance. Similarly, fluorescence detection typically necessitates a derivatization or labeling step unless peptides contain tryptophan. Limits of detection with this method of detection are excellent. A

limiting factor of many labeling chemistries is the requirement of a specific amino acid residue (often lysine) or an unmodified N-terminus.

Mass spectrometry has been paired with LC, CE, and to a lesser extent ME. This detection method offers the advantages of both specificity and sensitivity especially when tandem mass spectrometry is employed. Most reports of LC or CE mass spectrometry employ electrospray ionization. One of the concerns when using ESI is its propensity for ion suppression from matrix components. Samples must therefore be adequately de-salted and rid of additional proteins and lipids prior to detection.

Each of the techniques presented in this chapter has its own set of advantages and disadvantages. Careful selection of the best analytical tool(s) is essential for quantifying peptides in complicated biological matrices. Many of these techniques are best employed in tandem, used to supplement, confirm, and validate each report. The development of hybrid techniques such as immunoaffinity CE and two-dimensional separations promises to advance the area of peptide determination.

2.5 References

[1] Whiteaker, J. R., Zhao, L., Zhang, H. Y., Feng, L., Piening, B. D., Anderson, L., Paulovich, A. G., *Analytical Biochemistry* 2007, *362*, 44-54.

[2] Kuhnline, C. D., Lunte, S. M., *Journal of Separation Science* 2010, *33*, 2506.

[3] van den Broek, I., Sparidans, R. W., Schellens, J. H. M., Beijnen, J. H., *Journal of Chromatography B* 2010, *878*, 590-602.

[4] Tamm, N. N., Seferian, K. R., Semenov, A. G., Mukharyamova, K. S., Koshkina, E. V., Krasneselsky, M. I., Postnikov, A. B., Serebryanaya, D. V., Apple, F. S., Murakami, M. M., Katrukha, A. G., *Clinical Chemistry* 2008, *54*, 1511-1518.

[5] Busbridge, M., Griffiths, C., Ashby, D., Gale, D., Jayantha, A., Sanwaiya, A., Chapman, R. S., *British Journal of Biomedical Science* 2009, *66*, 150-157.

[6] Hanson, D. A., Weis, M. E., Bollen, A., Maslan, S. L., Singer, F. R., Eyre, D. R., *Journal of Bone and Mineral Research* 1992, *7*, 1251-1258.

[7] Teni, T. R., Bandivdekar, A. H., Sheth, A. R., Sheth, N. A., *Clinical Chemistry* 1989, *35*, 1376-1379.

[8] Mouedden, M. E., Vanermeeren, M., Meert, T., Mercken, M., *Journal of Neuroscience Methods* 2005, *145*, 97-105.

[9] Maruyama, M., Arai, H., Sugita, M., Tanji, H., Higuchi, M., Okamura, N., Matsui, T., Higuchi, S., Matsushita, S., Yoshida, H., Sasaki, H., *Experimental Neurology* 2001, *172*, 433-436.

[10] Gloeckner, S. F., Meyne, F., Wagner, F., Heinemann, U., Krasnianski, A., Meissner, B., Zerr, I., *Journal of Alzheimer's Disease* 2008, *14*, 17-25.

[11] Okamura, N., Arai, H., Higuchi, M., Tashiro, M., Matsui, T., Itoh, M., Iwatsubo, T., Tomita, T., Sasaki, H., *Neurosci. Lett.* 1999, *273*, 203-207.

[12] van den Broek, I., Sparidans, R. W., Schellens, J. H. M., Beijnen, J. H., *Journal of Chromatography B* 2010, *878*, 1085-1092.

[13] Lovgren, U., Johansson, S., Jensen, L. S., Ekstrom, C., Carlshaf, A., *Journal of Pharmaceutical and Biomedical Analysis* 2010, *53*, 537-545.

[14] Rogatsky, E., Balent, B., Goswami, G., Tomuta, V., Jayatillake, H., Cruikshank, G., Vele, L., Stein, D. T., *Clinical Chemistry* 2006, *52*, 872-879.

[15] Rogatsky, E., Tomuta, V., Jayatillake, H., Cruikshank, G., Vele, L., Stein, D. T., *Journal of Separation Science* 2007, *30*, 226-233.

[16] Xu, Y., Mehl, J. T., Bakhtiar, R., Woolf, E. J., *Analytical Chemistry* 2010, *82*.

[17] Phillips, T. M., *Luminescence* 2001, *16*, 145-152.

[18] Phillips, T. M., Smith, P., *Biomedical Chromatography* 2003, *17*, 182-187.

[19] Phillips, T. M., Wellner, E. F., *Journal of Chromatography A* 2006, *1111*, 106-111.

[20] Phillips, T. M., Wellner, E. F., *Electrophoresis* 2007, *28*, 3041-3048.

[21] Phillips, T. M., Wellner, E. F., *Electrophoresis* 2009, *30*, 2307-2312.

[22] Stroink, T., Wiese, G., Teeuwsen, J., Lingeman, H., Waterval, J. C. M., Bult, A., de Jong, G. J., Underberg, W. J. M., *Electrophoresis* 2003, *24*, 897-903.

[23] Rechthaler, J., Allmaier, G., *Rapid Communications in Mass Spectrometry* 2002, *16*, 899-902.

[24] Schurenberg, M., Dreisewerd, K., Hillenkamp, F., *Analytical Chemistry* 1999, *71*, 221-229.

[25] Zaluzec, E. J., Gage, D. A., Watson, J. T., *Protein Expression and Purification* 1995, *6*, 109-123.

[26] Colgrave, M. L., Jones, A., Craik, D. J., *Journal of Chromatography A* 2005, *1091*, 187-193.

[27] Kokko, K. P., Dix, T. A., *Analytical Biochemistry* 2002, *308*, 34-41.

[28] Chou, J. Z., Chait, B. T., Wang, R., Kreek, M. J., *Peptides* 1996, *17*, 983-990.

[29] Chou, J. Z., Kreek, M. J., Chait, B. T., *American Society for Mass Spectrometry* 1994, *5*, 10-16.

[30] Yu, J., Butelman, E. R., Woods, J. H., Chait, B. T., Kreek, M. J., *The Journal of Pharmacology and Experimental Therapeutics* 1996, *279*, 507-514.

[31] Reed, B., Zhang, Y., Chait, B. T., Kreek, M. J., *Journal of Neurochemistry* 2003, *86*, 815-823.

[32] Reed, B., Bidlack, J. M., Chait, B. T., Kreek, M. J., *Journal of Neuroendocrinology* 2008, *20*, 606-616.

[33] Romanova, E. V., Lee, J. E., Kelleher, H. L., Sweedler, J. V., Gulley, J. M., *The AAPS Journal* 2010, *12*, 443-454.

[34] Anderson, D. S., Heeney, M. M., Roth, U., Menzel, C., Fleming, M. D., Steen, H., *Analytical Chemistry* 2010, *82*, 1551-1555.

[35] Lapolla, A., Seraglia, R., Molin, L., WIlliams, K., Cosma, C., Reitano, R., Sechi, A., Ragazzi, E., Traldi, P., *Journal of Mass Spectrometry* 2008, *44*, 419-425.

[36] McDonnell, L. A., Corthals, G. L., Willems, S. M., van Remoortere, A., van Zeijl, R. J. M., Deelder, A. M., *Journal of Proteomics* 2010, *73*, 1921-1944.

[37] Goodwin, R. J. A., Pennington, S. R., Pitt, A. R., *Proteomics* 2008, *8*, 3785-3800.

[38] Andersson, M., Groseclose, M. R., Deutch, A. Y., Caprioli, R. M., *Nature Methods* 2008, *5*, 101-108.

[39] Seeley, E. H., Caprioli, R. M., *Proceddings of the National Academy of Science* 2008, *105*, 18126-18131.

[40] Suchankova, J., Soukupova, K., Tesarova, E., Bosakova, Z., Coufal, P., *Chromatographia* 2003, *60*, S119-S124.

[41] Thompson, S. E., Audus, K. L., *Peptides* 1993, *15*, 109-116.

[42] Thompson, S. E., Audus, K. L., *Pharmaceutical Research* 1994, *11*, 1366-1369.

[43] Thompson, S. E., Cavitt, J., Audus, K. L., *Journal of Cardiovascular Pharmacology* 1994, *24*, 818-825.

[44] Woltman, S. J., Chen, J., Weber, S. G., Tolley, J. O., *Journal of Pharmaceutical and Biomedical Analysis* 1995, *14*, 155-164.

[45] Shen, H., Witowski, S. R., Boyd, B. W., Kennedy, R. T., *Analytical Chemistry* 1999, *71*, 987-994.

[46] De Montigny, P., Riley, C. M., Sternson, L. A., Stobaugh, J. F., *Journal of Pharmaceutical and Biomedical Analysis* 1990, *8*, 419-429.

[47] Yang, J. Z., Bastian, K. C., Moore, R. D., Stobaugh, J. F., Borchardt, R. T., *Journal of Chromatography B* 2002, *780*, 269-281.

[48] Schwartz, M. S., Matuszewski, B. K., *Journal of Chromatography B* 2002, *780*, 171-182.

[49] Harald, J., Walden, M., Schafer, S., Genz, S., Forssmann, W., *Analytical Bioanalytical Chemsitry* 2004, *378*, 883-897.

[50] van den Broek, I., Sparidans, R. W., Schellens, J. H. M., Beijnen, J. H., *Journal of Chromatography B* 2008, *872*, 1-22.

[51] Lanckmans, K., Sarre, S., Smolders, I., Michotte, Y., *Talanta* 2008, *74*, 458-469.

[52] Hatziieremia, S., Kostomitsopoulos, N., Balafas, V., Tamvakopoulos, C., *Rapid Communications in Mass Spectrometry* 2007, *21*, 2431-2438.

[53] Trivedi, P., Jiang, M., Tamvakopoulos, C., Shen, X., Yu, H., Mock, S., Fenyk-Melody, J., Van der Ploed, L. H. T., Guan, X., *Brain Research* 2003, *977*, 221-230.

[54] van den Broek, I., Sparidans, R. W., Schellens, J. H. M., Beijnen, J. H., *Journal of Chromatography B* 2007, *854*, 245-259.

[55] van den Broek, I., Sparidans, R. W., Schellens, J. H. M., Beijnen, J. H., *Rapid Communications in Mass Spectrometry* 2010, *24*, 1842-1850.

[56] Murao, N., Ishigai, M., Yasuno, H., Shimonaka, Y., Aso, Y., *Rapid Communications in Mass Spectrometry* 2007, *21*, 4033-4038.

[57] Che, J., Meng, Q., Chen, Z., Hou, Y., Shan, C., Cheng, Y., *Journal of Pharmaceutical and Biomedical Analysis* 2010, *51*, 927-933.

[58] Fierens, C., Stockl, D., Baetens, D., De Leenheer, A. P., Thienpont, L. M., *Clinical Chemistry* 2003, *49*, 992-994.

[59] Fierens, C., Thienpont, L. M., Stockl, D., Willekens, E., De Leenheer, A. P., *Journal of Chromatography A* 2000, *896*, 275-278.

[60] Fierens, C., Thienpont, L. M., Stockl, D., De Leenheer, A. P., *Rapid Communications in Mass Spectrometry* 2000, *14*, 936-937.

[61] Nemirovskiy, O., Li, W. W., Szekely-Klepser, G., in: Rai, A. J. (Ed.), *The Urinary Proteome: Methods in Molecular Biology* 2010, pp. 253-270.

[62] Berna, M., Scmalz, C., Duffin, K., Mitchell, P., Chambers, M., Achermann, B., *Analytical Biochemistry* 2006, *356*, 235-243.

[63] Li, W., Nemirovskiy, O., Fountain, S., Mathews, W. R., Szekely-Klepser, G., *Analytical Biochemistry* 2007, *369*, 41-53.

[64] Aguiar, M., Masse, R., Gibbs, B. F., *Analytical Biochemistry* 2006, *354*, 175-181.

[65] Behrens, H. L., Chen, R., Li, L., *Anal Chem* 2008, *80*, 6949-6958.

[66] Klintenberg, R., Andren, P. E., *Journal of Mass Spectrometry* 2005, *40*, 261-270.

[67] Nydahl, K. S., Pierson, J., Nyberg, F., Caprioli, R. M., Andren, P. E., *Rapid Communications in Mass Spectrometry* 2003, *17*, 838-844.

[68] Fanciulli, G., Azara, E., Wood, T. D., Delitala, G., Marchetti, M., *Journal of Chromatography B* 2007, *852*, 485-490.

[69] Fanciulli, G., Azara, E., Wood, T. D., Dettori, A., Delitala, G., Marchetti, M., *Journal of Chromatography B* 2006, *833*, 204-209.

[70] Matsumoto, A., Matsumoto, R., Kadoyama, K., Nishimoto, T., Matsuyama, S., Midorikawa, O., *Int J Pept Res Ther* 2009, *15*, 205-210.

[71] Pan, S., Rush, J., Peskind, E. R., Galasko, D., Chung, K., Quinn, J., Jankovic, J., Leverenz, J. B., Zabetian, C., Pan, C., Wang, Y., Oh, J. H., Zhang, J., Montine, T., Zhang, J., *Journal of Proteome Research* 2007, *7*, 720-730.

[72] Chappa, A. K., Audus, K. L., Lunte, S. M., *Pharmaceutical Research* 2006, *23*, 1201-1208.

[73] Ouyang, H., Andersen, T. E., Chen, W., Nofsinger, R., Steffansen, B., Borchardt, R. T., *Journal of Pharmaceutical Sciences* 2008, *98*, 2227-2236.

[74] Chappa, A. K., *Pharmacedutical Chemistry*, The University of Kansas, Lawrence 2007.

[75] Solinova, V., Kasicka, V., Koval, D., Barth, T., Ciencialova, A., Zakova, L., *Journal of Chromatography B* 2004, *808*, 75-82.

[76] Garcia-Campana, A. M., Taverna, M., Fabre, H., *Electrophoresis* 2007, *28*, 208-232.

[77] Rose, M. J., Lunte, S. M., Carlson, R. G., Stobaugh, J. F., *Journal of Pharmaceutical and Biomedical Analysis* 2003, *30*, 1851-1859.

[78] Wang, A., Fang, Y., *Electrophoresis* 2000, *21*, 1281-1290.

[79] Ye, J., Baldwin, R. P., *Anal Chem* 1994, *66*, 2669-2674.

[80] Herrero, M., Ibanez, E., Cifuentes, A., *Electrophoresis* 2008, *29*, 2148-2160.

[81] Stutz, H., *Electrophoresis* 2005, *26*, 1254-1290.

[82] Waterval, J. C. M., Hommels, G., Bestebreurtje, P., Versluis, C., Heck, A. J. R., Bult, A., Lingeman, H., Underberg, W. J. M., *Electrophoresis* 2001, *22*.

[83] Waterval, J. C. M., Krabbe, H., Teeuwsen, J., Bult, A., Lingeman, H., Underberg, W. J. M., *Electrophoresis* 1999, *20*, 1909-1916.

[84] Verpillot, R., Otto, M., Klafki, H., Taverna, M., *Journal of Chromatography A* 2008, *1214*, 157-164.

[85] Hauer, H., Dukes, G. R., Margerum, D. W., *Journal of the American Chemical Society* 1973, *95*, 3515-3522.

[86] Kirksey, J., S. T. , Neubecker, T. A., Margerum, D. W., *Journal of the American Chemical Society* 1979, *101*, 1631-1633.

[87] Margerum, D. W., *Pure & Applied Chemistry* 1983, *55*, 23-34.

[88] Margerum, D. W., Chellappa, K. L., Bossu, F. P., Burce, G. L., *Journal of the American Chemical Society* 1975, *97*, 6894-6896.

[89] Gawron, A. J., Lunte, S. M., *Electrophoresis* 2000, *21*, 3205-3211.

[90] Lacher, N. A., Garrison, K. E., Lunte, S. M., *Electrophoresis* 2002, *23*, 1577-1584.

[91] Psurek, A., Matysik, F., Scriba, G. K. E., *Electrophoresis* 2006, *27*, 1199-1208.

[92] Abad-Villar, E. M., Kuban, P., Hauser, P. C., *Journal of Separation Science* 2006, *29*, 1031-1037.

[93] Baltussen, E., Guijt, R. M., van der Steen, G., Baltussen, S., van Dedem, G. W. K., *Electrophoresis* 2002, *23*, 2888-2893.

[94] Gong, X. Y., Dobrunz, D., Kumin, M., Wiesner, M., Revell, J. D., Wennemers, H., Hauser, P. C., *Journal of Separation Science* 2008, *31*, 565-573.

[95] Schuchert-Shi, A., Hauser, P. C., *Analytical Biochemistry* 2009, *387*, 202-207.

[96] Freed, A. L., Cooper, J. D., Davies, M. I., Lunte, S. M., *Journal of Neuroscience Methods* 2001, *109*, 23-29.

[97] Freed, A. L., Audus, K. L., Lunte, S. M., *Peptides* 2002, *23*, 157-165.

[98] Chen, Y., Xu, L., Zhang, L., Chen, G., *Analytical Biochemistry* 2008, *380*, 297-302.

[99] Huang, Y., Duan, J., Chen, H., Chen, M., Chen, G., *Electrophoresis* 2005, *26*, 593-399.

[100] Sheeley, S. A., Miao, H., Ewing, M. A., Rubakhin, S. S., Sweedler, J. V., *The Analyst* 2005, *130*, 1198-1203.

[101] Monton, M. R. N., Terabe, S., *Analytical Sciences* 2005, *21*, 5-13.

[102] Schiffer, E., Mischak, H., Novak, J., *Proteomics* 2006, *6*, 5615-5627.

[103] Schmitt-Kopplin, P., Englemann, M., *Electrophoresis* 2005, *26*, 1209-1220.

[104] Cao, P., Moini, M., *Journal of the American Society of Mass Spectrometry* 1998, *9*, 1081-1088.

[105] Julian, B. A., Wittke, S., Novak, J., Good, D. M., Coon, J. J., Kellmann, M., Zurbig, P., Schiffer, E., Haubitz, M., Moldoveanu, Z., Calcatera, S. M., Wyatt, R. J., Sykora, J., Sladkova, E., Hes, O., Mischak, H., McGuire, B. M., *Electrophoresis* 2007, *28*, 4469-4483.

[106] Schiffer, E., Vlahou, A., Pertrolekas, A., Stravodimos, K., Tauber, R., Geschwend, J. E., Neuhaus, J., Stolzenburg, J., Conaway, M. R., Mischak, H., Theodorescu, D., *Clinical Cancer Research* 2009, *15*, 4935-4943.

[107] Theodorescu, D., Filser, D., Wittke, S., Mischak, H., Krebs, R., Walden, M., Ross, M., Eltze, E., Bettendorf, O., Wulfing, C., Semjonow, A., *Electrophoresis* 2005, *26*, 2797-2808.

[108] Kaiser, T., Wittke, S., Just, I., Krebs, R., Bartel, S., Filser, D., Mischak, H., Weissinger, E. M., *Electrophoresis* 2004, *25*, 2044-2055.

[109] Hernandez, E., Benavente, F., Sanz-Nebot, V., Barbosa, J., *Electrophoresis* 2008, *29*, 3366-3376.

[110] Amundsen, L. K., Siren, H., *Electrophoresis* 2007, *28*, 99-113.

[111] Guzman, N. A., Blanc, T., Phillips, T. M., *Electrophoresis* 2008, *29*, 3259-3278.

[112] Hou, C., Herr, A. E., *Electrophoresis* 2008, *29*, 3306-3319.

[113] Moser, A. C., Hage, D. S., *Bioanalysis* 2010, *2*, 769-790.

[114] Kalish, H., Phillips, T. M., *Journal of Separation Science* 2009, *32*, 1605-1612.

[115] Kalish, H., Phillips, T. M., *Journal of Chromatography B* 2010, *878*, 194-200.

[116] Guzman, N. A., Phillips, T. M., *Analytical Chemistry* 2005, 61A-67A.

[117] Benavente, F., Hernandez, E., Guzman, N. A., Sanz-Nebot, V., Barbosa, J., *Analytical Bioanalytical Chemistry* 2007, *377*, 2633-2639.

[118] Gimenez, E., Benavente, F., de Bolos, C., Nicolas, E., Barbosa, J., Sanz-Nebot, V., *Journal of Chromatography A* 2009, *1216*, 2574-2582.

[119] Tao, L., Kennedy, R. T., *Analytical Chemistry* 1996, *68*, 3899-3906.

[120] Schultz, N. M., Huang, L., Kennedy, R. T., *Analytical Chemistry* 1995, *67*, 924-929.

[121] Dolnik, V., Liu, S., *Journal of Separation Science* 2005, *28*, 1994-2009.

[122] Gawron, A. J., Martin, R. S., Lunte, S. M., *European Journal of Pharmaceutical Sciences* 2001, *14*, 1-12.

[123] Gawron, A. J., Martin, R. S., Lunte, S. M., *Electrophoresis* 2001, *22*, 242-248.

[124] Martin, R. S., Gawron, A. J., Fogarty, B. A., Regan, F. B., Dempsey, E., Lunte, S. M., *The Analyst* 2001, *126*, 277-280.

[125] Guigt, R. M., Baltussen, E., van der Steen, G., Frank, H., Billiet, H., Schalkhammer, T., Laugere, F., Vellekoop, M., Berthold, A., Sarro, L., van Dedem, G. W. K., *Electrophoresis* 2001, *22*, 2537-2541.

[126] Abad-Villar, E. M., Kuban, P., Hauser, P. C., *Electrophoresis* 2005, *26*, 3609-3614.

[127] Galloway, M., Stryewski, W., Henry, A., Ford, S. M., Llopis, S., McCarley, R. L., Soper, S. A., *Analytical Chemistry* 2002, *74*, 2407-2415.

[128] Laugere, F., Guijt, R. M., Bastemeijer, J., van der Steen, G., Berthold, A., Baltussen, E., Sarro, P., van Dedem, G. W. K., Vellekoop, M., Bossche, A., *Analytical Chemistry* 2003, *75*, 306-312.

[129] Shadpour, H., Hupert, M. L., Patterson, D., Liu, C., Galloway, M., Stryewski, W., Goettert, J., Soper, S. A., *Analytical Chemistry* 2007, *79*, 870-878.

[130] Huynh, B. H., Fogarty, B. A., Nandi, P., Lunte, S. M., *Journal of Pharmaceutical and Biomedical Analysis* 2006, *42*, 529-534.

[131] Zhao, S., Huang, Y., Shi, M., Huang, J., Liu, Y., *Analytical Biochemistry* 2009, *393*, 105-110.

[132] Zhao, S., Huang, Y., Ye, F., Shi, M., Liu, Y., *Journal of Chromatography A* 2010, *1217*, 5732-5736.

[133] Wellner, E. F., Kalish, H., *Electrophoresis* 2009, *29*, 3477-3483.

Chapter Three:

Separation of dynorphin A metabolites and dynorphin-copper complexes by capillary electrophoresis with UV detection

Published as:

C.D. Kuhnline and S. M. Lunte, Evaluation of an on-capillary copper complexation methodology for the investigation of in vitro metabolism of dynorphin A 1–17, **J. Sep. Sci.** 33, 16. 2506-2514, 2010.

3.1 Introduction

Dynorphin A 1-17 (Dyn A 1-17) is an endogenous opioid peptide with selectivity for the kappa opioid receptor. The structures of dynorphin and its major metabolites are shown in Figure 3.1. The investigation of dynorphin analogs as potential therapeutics for treatment of cocaine abuse and peripheral pain management has also revealed a neurotoxic component to this peptide's *in vivo* activity [1]. Elevated levels of dynorphin have been implicated in a variety of neurodegenerative disorders including Alzheimer's disease [2], Parkinson's disease [3], and neuropathic pain [4], as well as stress and depression [5]. It is hypothesized that the neurotoxic effects are non-opioid in nature and may arise from activation of the N-methyl-D-aspartate (NMDA) receptor [6, 7]. Once released into the extracellular space, dynorphin is subject to enzymatic degradation with each metabolite exhibiting its own unique biological effects. It is possible that one (or more) of these metabolites is responsible for the neurotoxicity of dynorphin. Therefore, methods to study the metabolism of dynorphin *in vivo* are necessary to further elucidate the mechanisms of neurotoxicity.

The most common method for quantitation of dynorphin *in vivo* is radioimmunoassay (RIA). However, a major drawback to this approach is that cross-reactivity with metabolites can lead to falsely elevated results [8]. To circumvent this issue, chromatographic separation can be performed prior to the immunoassay. In one report, HPLC/RIA was employed to investigate the metabolism of Dyn A 1-13 in human blood [9]. This process took over 24 hours and involved solid phase extraction for sample clean-up and relatively long LC gradients (>20 min), followed by fraction collection prior to RIA. Another disadvantage of RIA is the use of expensive radioactive reagents and assay kits, as well as the costs associated with the disposal of radioactive waste. A variety of other methods have been used to quantify opioid peptides such

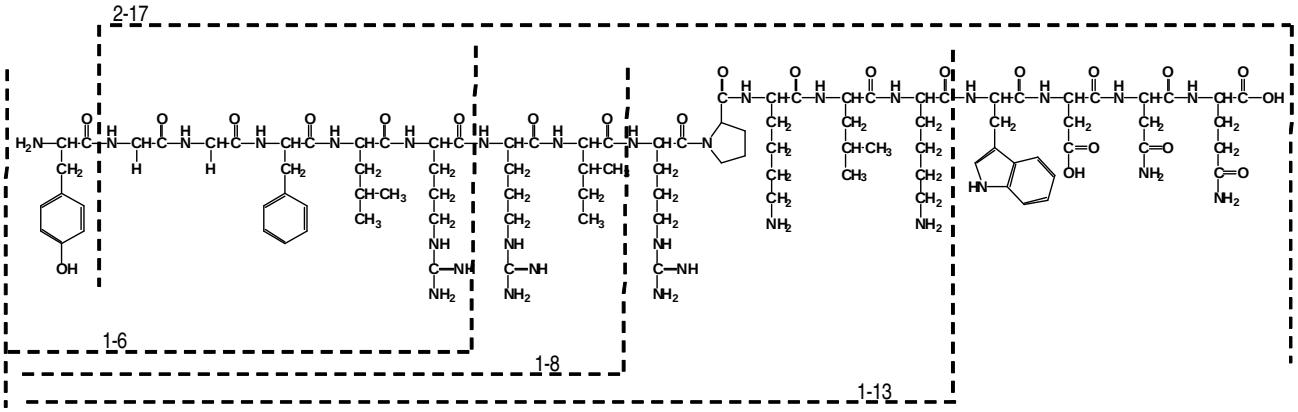

Figure 3.1 Structure of Dynorphin A 1-17 (Y-G-G-F-L-R-R-I-R-P-K-L-K-W-D-N-Q) with metabolites of interest (1-6, 1-8, 1-13, 2-17) indicated by dotted lines.

as the enkephalins, endomorphins, and smaller dynorphin peptides including HPLC with UV detection [10], LC-MS [3, 11], CE-UV [12, 13], CE-LIF [13, 14], and CE-MS [15-19]. A review of these methods is provided in Chapter 2 of this thesis. Qualitative and semi-quantitative MALDI methods have also demonstrated potential for monitoring dynorphin peptides [20-23]. Mass spectrometry provides conclusive metabolite identification; however, the instrument requirements are expensive.

Capillary electrophoresis provides several advantages for monitoring peptides of biological and pharmacological interest [24, 25]. Highly efficient and fast separations are possible without the use of organic modifiers, separations can be performed at high pH, and various complexation strategies can be employed on-capillary. The small volume requirements of CE enable the analysis of volume-limited samples and allow the use of expensive separation additives. In this work, on-capillary copper complexation was investigated for the detection of dynorphin peptides. Performing this complexation on-capillary is advantageous over pre- or postcolumn derivatization methods because sample dilution is avoided. This is especially important for the analysis of expensive compounds and volume-limited biological samples such as microdialysis samples.

In the late 1970s and early 1980s, Margerum and co-workers extensively characterized the coordination of Cu (II) with nitrogens in the peptide backbone [26-29]. This method is based on the biuret reaction, and can be used to improve UV detection of peptides as well as for the electrochemical detection of non-tyrosine containing peptides. Weber's group exploited this method for postcolumn derivatization of peptides to enable electrochemical detection following LC separation [30-33]. In a separate report, Kennedy's group achieved picomolar detection limits of neuropeptides from microdialysis samples following precolumn derivatization with

copper and both UV and electrochemical detection [34]. Previous work in our group has applied on-capillary copper complexation for the amperometric detection of enkephalin and angiotensin peptides [35-37]. A major advantage of this approach is that it is selective for peptides in the presence of amino acids because at minimum a tripeptide is required for complexation. Additionally, in contrast to many fluorescence derivatization techniques based on reactions with primary amines, N-terminally modified and cyclic peptides are also capable of forming complexes with copper.

In this chapter, a capillary electrophoresis based separation of Dyn A 1-17 and four previously identified metabolites is described. Phytic acid and various forms of cyclodextrins are investigated as run buffer additives to prevent peptide adsorption and improve resolution between metabolites. The copper complexation method is applied to *in vitro* metabolism in human plasma as well as rat brain and spinal cord. To the best of our knowledge, this is the first report of studying dynorphin metabolism with capillary electrophoresis.

3.2 Materials and Methods

3.2.1 Reagents

All dynorphin peptides (Dyn A 1-17, 2-17, 1-13, 1-8 and 1-6) were obtained from Bachem Biosciences, Inc. (King of Prussia, PA, USA). Capillaries were obtained from Polymicro Technologies (Phoenix, AZ, USA). Sodium tetraborate, phytic acid, D, L tartaric acid, copper (II) sulfate, β-cyclodextrin, and (2-hydroxypropyl)-β-cyclodextrin were all purchased from Sigma-Aldrich (St. Louis, MO USA). Sulfobutyl ether-beta-cyclodextrin was obtained from Dr. Stella's laboratory at the University of Kansas. Mesityl oxide which was used

as a neutral marker for electroosmotic flow (EOF) determination was also purchased from Sigma-Aldrich (St. Louis, MO USA). Human plasma was obtained at Watkins Health Center (University of Kansas, Lawrence, KS, USA). Brain and spinal cord samples were obtained from male Wistar rats (Charles River, Wilmington, MA, USA).

3.2.2 Human plasma samples

Human plasma was obtained from a healthy volunteer at Watkins Health Center and used 1-2 hours after withdrawal. Plasma was diluted 1:10 in 100 mM sodium tetraborate with 25 mM phytic acid, pH 9.0, to slow enzyme activity and prevent the capillary from clogging. Dyn A 1-17 was added at a concentration of 200 μM and kept at room temperature to further retard enzyme activity. An initial aliquot was taken at t = 0 and subsequent aliquots were taken approximately every 40 minutes, corresponding to a 25-minute separation and flushes with NaOH and run buffer between runs. The run buffer for plasma analysis consisted of 100 mM sodium tetraborate, 25 mM phytic acid, 3 mM tartaric acid, 2 mM cupric sulfate, and 20 mM sulfobutyl ether-beta-cyclodextrin (SBE_4-β-CD), pH 9.0.

3.2.3 Rat brain and spinal cord slices

The brains and spinal cords of male Wistar rats were removed on the day of analysis and kept in ice cold artificial cerebrospinal fluid (aCSF) prior to experiments. Animals that could no longer be used for studies due to their weight were graciously donated by Dr. Craig Lunte's laboratory at the University of Kansas. Tissue slices were prepared with a clean razor blade in a petri dish on a bed of ice. The tissue slices were exposed to dynorphin at room temperature to slow enzyme activity. For brain samples, a 5 mm by 5 mm section was bathed in 100 mM sodium tetraborate with 25 mM phytic acid, pH 9.0 that was spiked with 200 μM Dyn A 1-17.

Immediately, an aliquot was removed and analyzed by the optimized copper-complexation method. Subsequent aliquots were removed at approximately 40-minute intervals to permit a 25-min CE separation followed by flushes with NaOH and run buffer. Similarly, a 5 mm length of spinal cord was prepared and bathed in buffer spiked with Dyn A 1-17. Aliquots were removed every 40 minutes. The run buffer for rat tissue slice analysis consisted of 100 mM sodium tetraborate, 25 mM phytic acid, 3 mM tartaric acid, 2 mM cupric sulfate, and 20 mM SBE_4-β-CD, pH 9.0.

3.2.4 Capillary electrophoresis analysis

Separations were performed on a Beckman Coulter PACE/MDQ (Brea, CA, USA) with UV detection at 200 nm and 280 nm. The system was controlled using 32 Karat software, and all subsequent data analysis was performed with this software as well. Fused-silica capillaries (50 μm id x 360 μm od) were obtained from Polymicro Technologies (Phoenix, AZ, USA). A 50 cm capillary (40 cm to detector) was used for native dynorphin and a 60 cm capillary (50 cm to detector) was used for the dynorphin-copper complexes. A small window was burned through the polyimide coating 10 cm from the capillary end for UV detection. Pressure injections were performed at 6.9 kPa for 5.0 seconds, and a separation voltage of 25 kV was applied with the anode at the injection end.

Buffers were prepared in 18 MΩ deionized (D.I.) H_2O and adjusted to pH 9.0 with the addition of NaOH. Dynorphin stock solutions were prepared at a concentration of 1mg/mL in 18 MΩ D.I. H_2O and kept frozen until use when they were diluted to desired concentrations in sodium tetraborate (50 or 100 mM) with 25 mM phytic acid (pH 9.0). Native dynorphin separations were accomplished using an optimized background electrolyte consisting of 50 mM

sodium tetraborate, 25 mM phytic acid, and 5 mM (2-hydroxypropyl) beta-cyclodextrin (HP-β-CD), pH 9.0. Separation of the copper complexes was achieved using 100 mM sodium tetraborate, 25 mM phytic acid, 3 mM D,L tartaric acid, 2 mM cupric sulfate, and 20 mM SBE_4-β-CD, also pH 9.0.

3.3 Results and Discussion

3.3.1 Separation optimization of native dynorphin peptides

To study the metabolism of dynorphin *in vitro*, this work focused on the development of an electrophoretic separation of Dyn A 1-17 from four previously identified metabolites-two of which, in particular, have been implicated in neurotoxicity and neuropathic pain (1-13 and 2-17). Initially 50 mM sodium phosphate, pH 7.0, and 50 mM tetraborate, pH 9.0, were investigated as possible background electrolytes. Under these conditions dynorphin peptides were not detected. Upon repeated injections very broad peaks with inconsistent migration times were observed; however, virtually no separation was seen between metabolites of interest. To reduce adsorption of the basic peptides onto the capillary wall, phytic acid was added to the background electrolyte. Phytic acid is a polyanion and acts as an ion-pairing agent to shield positively charged amino acid side chains from interaction with the silanol groups on the capillary wall [38-41]. This has been used previously by our group to prevent adsorption of substance P metabolites [42]. In addition to preventing peptide adsorption at the capillary wall, phytic acid has also been shown to improve resolution [39-41].

Ion-pairing with highly basic peptides was also shown to result in longer migration times due to an overall change in their net charge [38-39]. Phytic acid concentrations of 15, 20, and 25

mM were evaluated in the run buffer and sample buffer, and 25 mM was determined to be sufficient to prevent analyte adsorption while keeping currents low enough to avoid excessive Joule heating. The structure of phytic acid and representative electropherograms of the concentration comparison can be seen in Figure 3.2. Although incomplete resolution of Dyn A 1-17 and 2-17 was still observed, higher phytic acid concentrations were not investigated due to high background currents resulting in increased noise and occurrence of bubble formation.

There are several aromatic residues present in dynorphin that are capable of forming inclusion complexes with cyclodextrin, specifically Tyr^{1}, Phe^{4}, and Trp^{14}. To further improve the resolution of Dyn A 1-17 and the des-Tyr metabolite, 5 mM HP-β-CD was included in the optimized run buffer. The final optimized separation is shown in Figure 3.3 along with the structure of HP-β-CD. The UV response at 200 nm was linear over the concentration range of 2.5-50 μM (R^2= 0.991-1.000, 5 concentrations, n=3 for each).

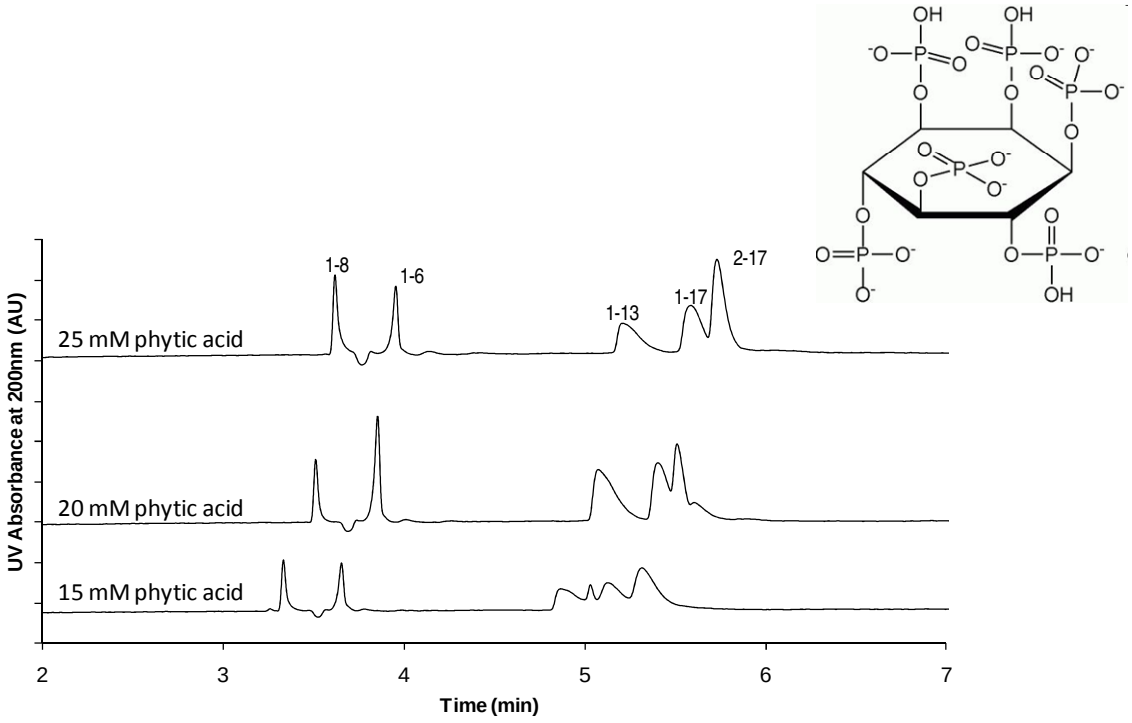

Figure 3.2 Representative electropherograms demonstrating the effect of phytic acid (structure shown from food-info.net) concentration on peak shape, migration time and resolution. Buffer: 50 mM sodium tetraborate, 15, 20, or 25 mM phytic acid, pH 9.0. Peptides are 100 μM in 50 mM sodium tetraborate, various phytic acid concentrations, pH 9.0.

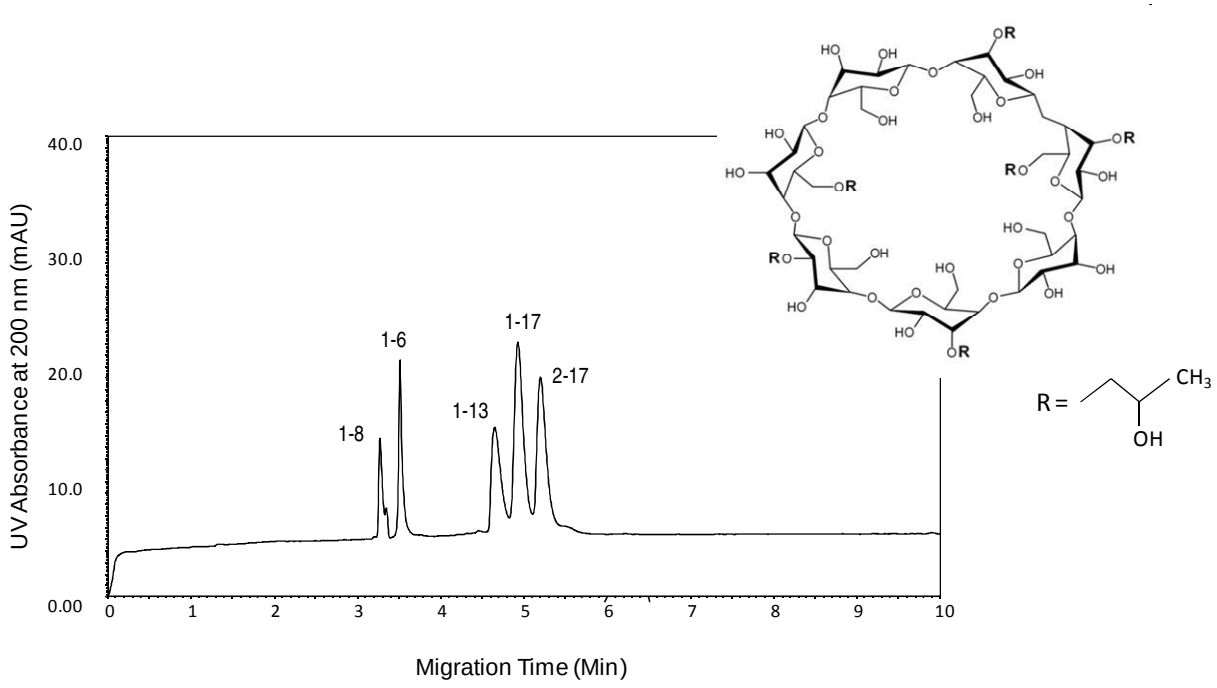

Figure 3.3 Optimized separation of native dynorphin peptides upon inclusion of HP-β-CD (structure shown from http://astrobiology.berkeley.edu). Buffer: 50 mM sodium tetraborate, 25 mM phytic acid, 5 mM HP-β-CD, pH 9.0. Peptides are 100 μM in 50 mM sodium tetraborate, 25 mM phytic acid, pH 9.0.

3.3.2 Separation optimization of copper-complexed dynorphin peptides

It has been shown that, at basic pH, peptides can form complexes with copper (II) via nitrogens in the peptide backbone. The complexation typically begins at the N-terminus, and the reaction of Cu(II) with a model peptide is demonstrated in Figure 3.4. Copper complexation has been shown to effectively improve UV sensitivity while also rendering peptides electroactive [26-37]. As shown in Figure 3.5, complexation could be confirmed based on the shift in migration time seen with Dyn A 1-17 in copper-containing buffer (4.56 +/- 0.14 min versus 3.98 +/- 0.08 min, n=3 for each). This later migration time is due to the increase in overall negative charge on the peptide following complexation due to resonance delocalization at the dynorphin-copper coordinate sites [26-29]. Inclusion of copper in the run buffer causes minimal if any

The previously optimized 25 mM phytic acid was included in both run buffer and sample buffer during the optimization of the dynorphin-copper complex separation. On-capillary complexation was performed using conditions previously optimized in our group employed for both enkephalin and angiotensin peptides [35-37]. The run buffer therefore included 50 mM sodium tetraborate, 25 mM phytic acid, 3 mM tartaric acid, and 2 mM cupric sulfate. However, under these conditions, the resolution between all five peptides was decreased compared to native dynorphin peptides. Copper complexation increases the overall negative charge on each peptide, reducing the differences in their mass-to-charge ratio, and thus, their electrophoretic mobilities. All of the Cu (II)-peptides migrated later, with Dyn A 1-6 and 1-8 co-migrating, followed by 1-13, 1-17 and 2-17 co-migrating. This resolution was improved somewhat when the EOF was decreased by increasing the concentration of sodium tetraborate to 100 mM.

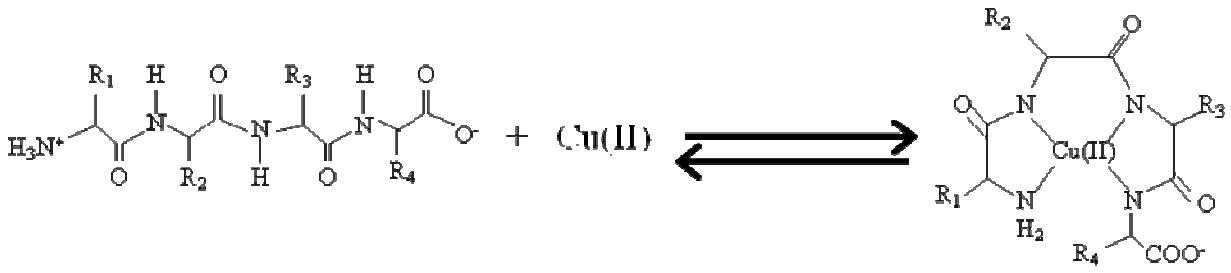

Figure 3.4 Schematic of model 4-amino acid peptide with copper (II).

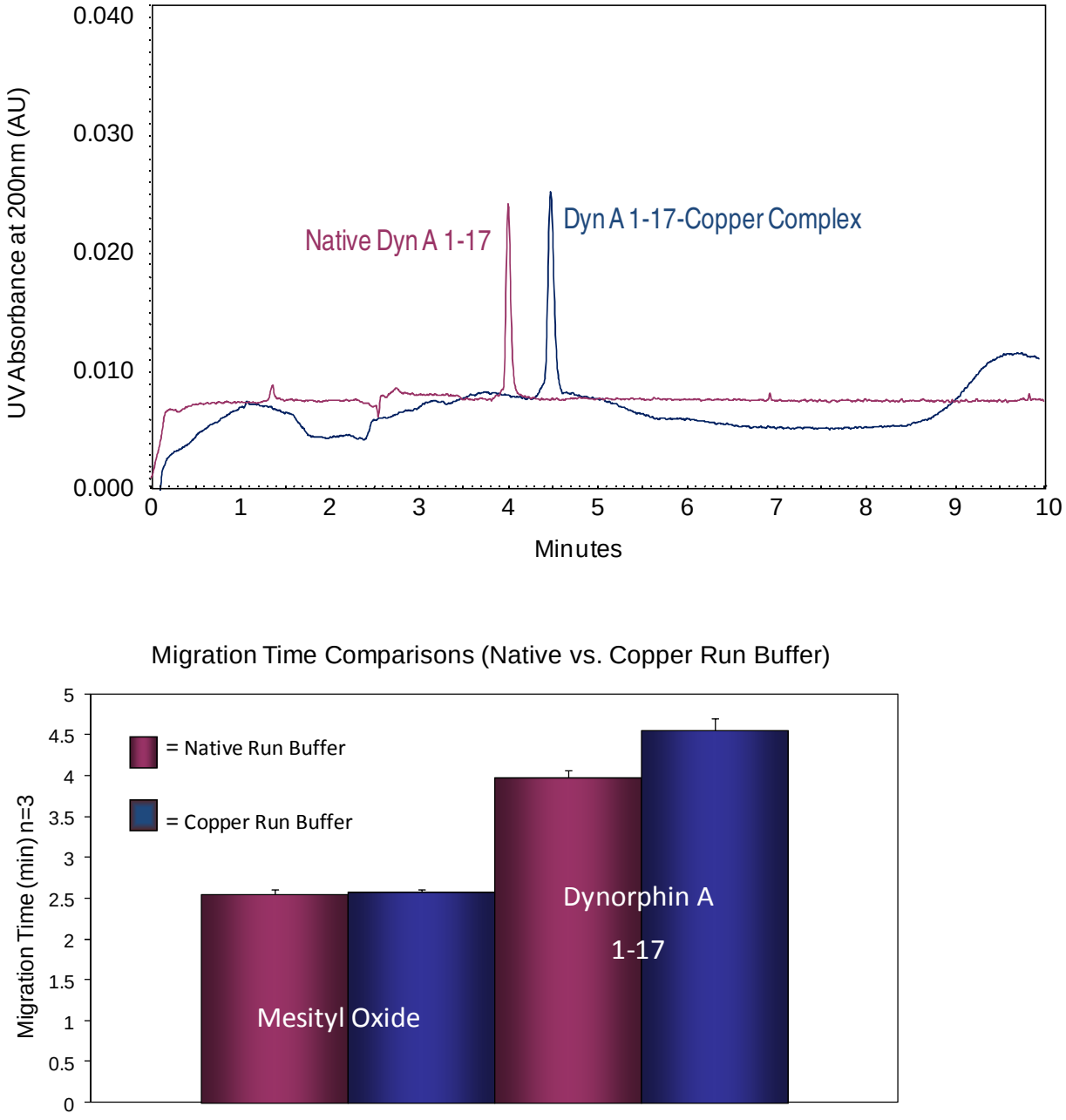

Figure 3.5 Comparison of migration time of Dyn A 1-17 with (blue) and without (purple) copper run buffer. Native run buffer: 50 mM sodium tetraborate, 25 mM phytic acid, pH 9.0, Copper

run buffer: 50 mM sodium tetraborate, 25 mM phytic acid, 2 mM $CuSO_4$, 3 mM tartaric acid, pH 9.0. Peptides were 100 μM. Average migration times are reported, n = 3.

To further improve the separation of the Cu (II) complexed peptides, several different types of beta-cyclodextrins were investigated. Beta-cyclodextrins consist of seven oligosaccharides in a cyclic arrangement. Inclusion complexes between hydrophobic amino acid residues and the cyclodextrin core form on capillary [43-44]. In particular, three aromatic amino acid residues in the dynorphin sequence- Tyr^1, Phe^4, and Trp^{14} -could complex with cyclodextrin. Changes in the substitution on the hydrophilic exterior of cyclodextrins alter their mobility on capillary. HP-β-CD was evaluated at both 5 and 10 mM, unsubstituted beta-cyclodextrin (β-CD) was investigated at 5 and 10 mM, and SBE_4-β-CD was evaluated at 2, 10, 15, and 20 mM. The structures of these cyclodextrins as well as comparisons of the resulting electropherograms can be seen in Figure 3.6.

Not surprisingly, sulfobutyl-ether-beta- cyclodextrin exhibited the most significant improvements in resolution due to its negative charge. Interaction with the hydrophobic core resulted in a higher negative electrophoretic mobility for the peptide complex. The effect of SBE_4-β-CD concentration on the separation of dynorphin metabolites is shown in Figure 3.7 and 3.8. The optimal concentration of SBE_4-β-CD was determined to be 20 mM and was included in all subsequent studies. Under these conditions, UV response at 200 nm was linear over a range of 20-75 μM (R^2=0.9808-0.9915, 5 concentrations, n=3 for each). The optimized separation is shown in Figure 3.9.

In general, copper complexation increased the peak heights and areas of dynorphin peptides when detected at both 200 and 280 nm. Detection was most sensitive at 200 nm;

however, 280 nm offered more selectivity for copper-complexed peptides. The calculated peak efficiencies for native dynorphin and dynorphin-copper complexes are reported in Table 3.1. As can be seen in this table, the overall the separation efficiency improved upon complexation.

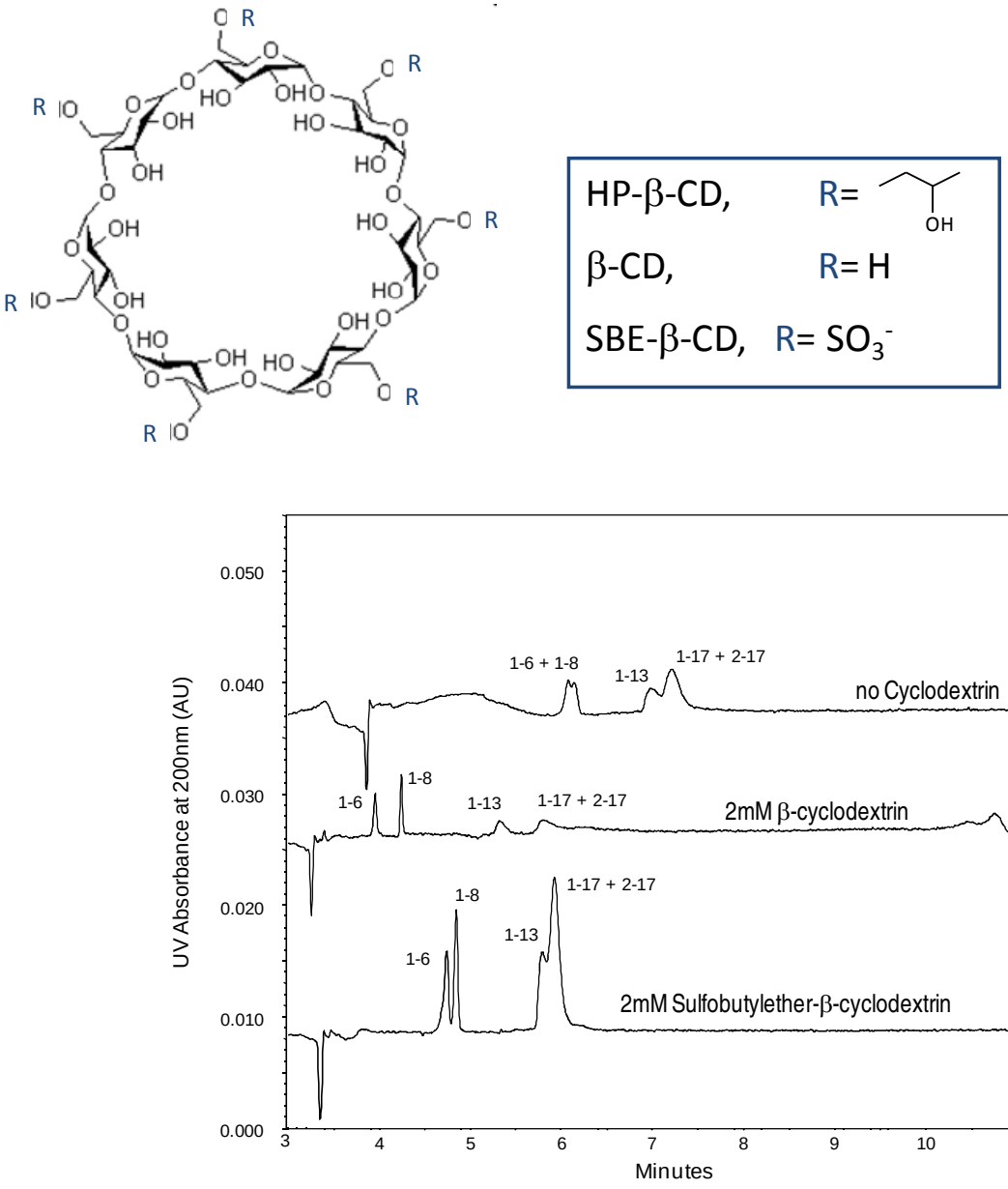

Figure 3.6 Representative electropherograms demonstrating the effect of various cyclodextrins (structure shown from http://astrobiology.berkeley.edu) on resolution of dynorphin-copper complexes. Buffer: 50 mM sodium tetraborate, 25 mM phytic acid, 2 mM $CuSO_4$, 3 mM tartaric acid, pH 9.0. Peptides are 100 μM in 50 mM sodium tetraborate, 25 mM phytic acid, pH 9.0.

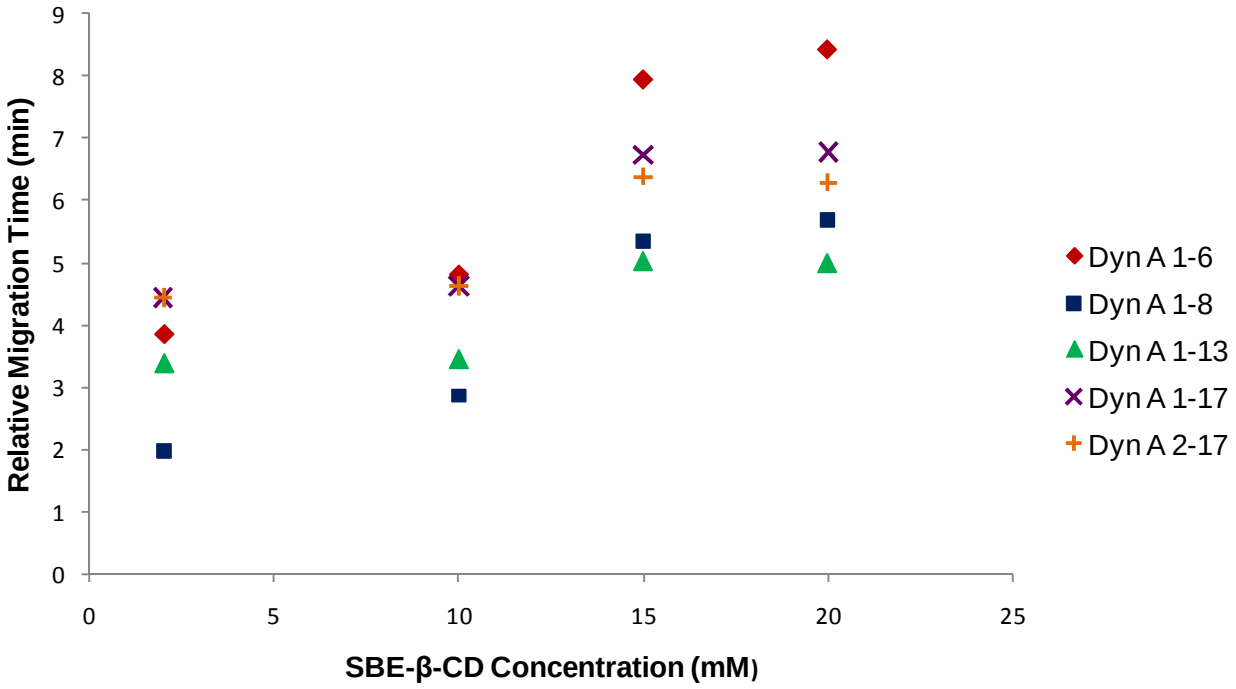

Figure 3.7 Effect of SBE-β-CD on relative migration time. Run buffer contained 100 mM sodium tetraborate, 25 mM phytic acid, 3 mM tartaric acid, 2 mM cupric sulfate, and specified amount of SBE-β-CD. Peptides are 100 μM in 100 mM sodium tetraborate, 25 mM phytic acid. Migration times are based on averages of triplicate runs, relative to mesityl oxide a neutral marker.

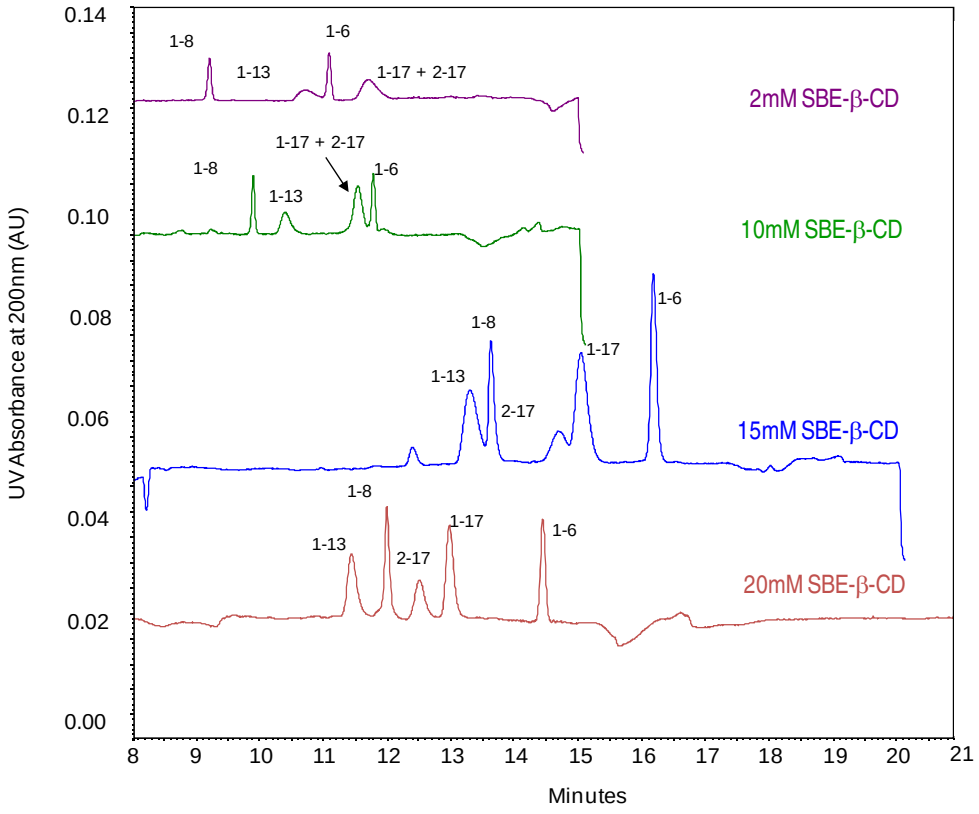

Figure 3.8 Electropherogram overlays demonstrating the effect of SBE-β-CD on relative migration time. Run buffer contained 100 mM sodium tetraborate, 25 mM phytic acid, 3 mM tartaric acid, 2 mM cupric sulfate, and specified amount of SBE-β-CD. Peptides are 100 μM in 100 mM sodium tetraborate, 25 mM phytic acid.

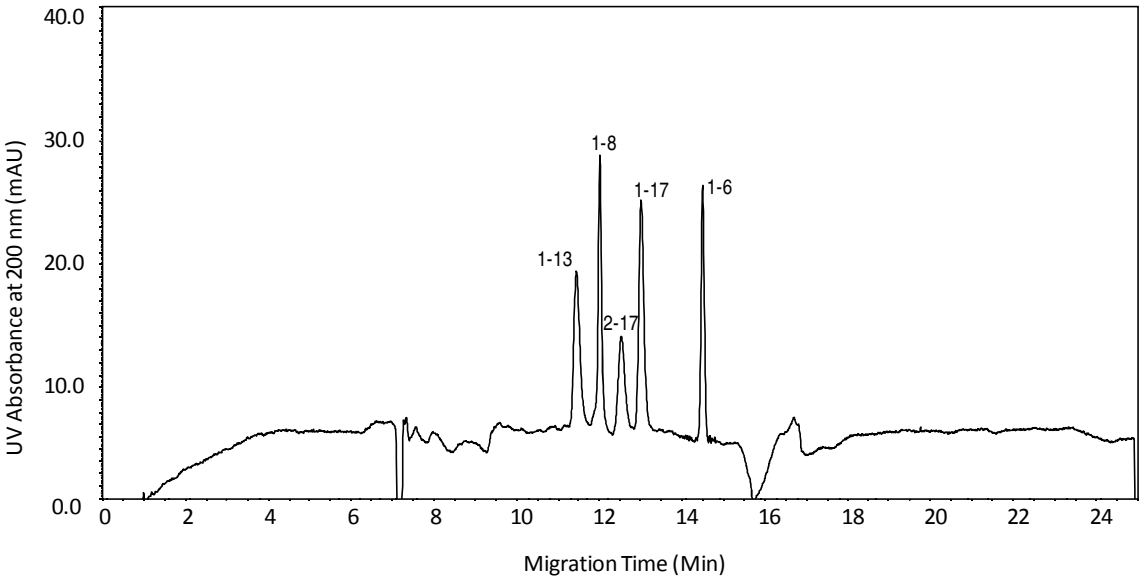

Figure 3.9 Optimized separation of dynorphin-copper complexes. Buffer: 100 mM sodium tetraborate, 25 mM phytic acid, 20 mM SBE-β-CD, 3 mM tartaric acid, 2 mM $CuSO_4$, pH 9.0. Peptides are 100 μM in 100 mM sodium tetraborate, 25 mM phytic acid, pH 9.0.

Peptide	Native Dynorphin (N)	Dynorphin-Copper Complexes (N)
Dyn A 1-6	1200	19000
Dyn A 1-8	18000	17000
Dyn A 1-13	4100	4700
Dyn A 1-17	5000	10000
Dyn A 2-17	2300	9000

Table 3.1. Effect of copper complexation on separation efficiency.

Each peptide was 100 μM (n=3) in sodium tetraborate buffer with 25 mM phytic acid. Run buffer conditions: Native (50 mM sodium tetraborate, 25 mM phytic acid, 5 mM HP-β-CD, pH 9.0, Complexes (100 mM sodium tetraborate, 25 mM phytic acid, 2 mM $CuSO_4$, 2 mM tartaric acid, 20 mM SBE_4-β-CD, pH 9.0).

Efficiency (N) was calculated using the following equation: $N=16(t_R/w_b)^2$.

3.3.3 Analysis of *in vitro* dynorphin metabolism in biological tissues of interest

The analytical methods described above were then used to monitor the metabolism of dynorphin A 1-17 *in vitro* in biological tissues of interest. Metabolic enzymes can vary greatly from tissue to tissue and species to species. The neurotoxic effects of dynorphin peptides have generated an interest in the downstream effects of its metabolic processing since it may be a metabolite that is producing these effects. More specifically, the role of dynorphin and its metabolites on the generation of neuropathic pain is of importance. In particular, the transport and metabolism of this peptide at the blood brain barrier is of interest and could provide insight into the mechanism of dynorphin neurotoxicity.

In these studies, the metabolism of Dyn A 1-17 was investigated in several tissues, including human plasma, rat brain, and rat spinal cord, using the optimized copper complexation method. A 1:10 dilution of human plasma was spiked with Dyn A 1-17 (200 μM). The metabolism was then monitored at 40-minute intervals. As can be seen in Figure 3.10, at time t = 0, only one peak is present in the electropherogram. The migration time of this peak corresponds with that of Dyn A 1-17. This peak was present only after spiking with dynorphin and was not observed in the plasma blank. Therefore, it has been identified as the parent peptide. At time t = 160, two new peaks appear in the electropherogram. The early migrating metabolite is identified as Dyn A 1-13 and the later migrating peak as Dyn A 1-6. Again these peaks were identified based on injections of single metabolite standards and migration time comparisons.

A similar experiment was performed to examine the metabolism of dynorphin in brain and spinal cord tissue slices. A 5 mm x 5 mm section of each tissue was removed and bathed in a buffer solution spiked with Dyn A 1-17 (200 μM). The metabolism of Dyn A 1-17 was monitored over time, and these electropherograms can be seen in Figure 3.11 (rat brain slice) and 3.12 (rat spinal cord slice). In the rat brain slice, at time t = 0, one dominant peak is observed for

the parent peptide. The peptide is rapidly degraded in the presence of the brain tissue sample as can be seen by the complete absence of the 1-17 peak after 40 minutes. At this same time, a later migrating peak also appears, and based on migration time, it is identified as Dyn A 1-6. An early migrating peak also appears at this time point. The migration time of this new peak does not correspond to that of any of the metabolites that were investigated in this study. Interestingly, this early migrating unidentified metabolite also appears over time in the rat spinal cord sample. However, in the spinal cord slice, the metabolism of Dyn A 1-17 is considerably slower and only a small decrease in peak height of the parent compound is observed after 160 minutes.

One of the limitations of CE for the analysis of basic peptides is the potential for analyte adsorption to the negatively charged silanol groups at the capillary wall [45]. Dynorphin is a highly basic peptide (pI= 11.4) [46] that has been shown to adsorb rapidly to glass and plastic surfaces [47]. While the use of polymer modified capillaries has been explored for separations of basic drugs and proteins, these are expensive and time-consuming to produce in house [48-49]. A less expensive alternative employs an ion-pairing buffer additive. Phytic acid is a polyanion that acts to shield the positive charges on basic amino acid residues from the capillary wall. Kostel *et al* were able to prevent substance P adsorption to capillaries by including phytic acid in the run buffer [42].

Resolution of closely related species can also be problematic in these applications. Micellar electrokinetic chromatography (MEKC) has been used to improve the resolution of opioid peptide analogs, providing an additional mode of separation within a bare fused silica capillary [12]. In addition, cyclodextrins have been exploited as run buffer additives and have

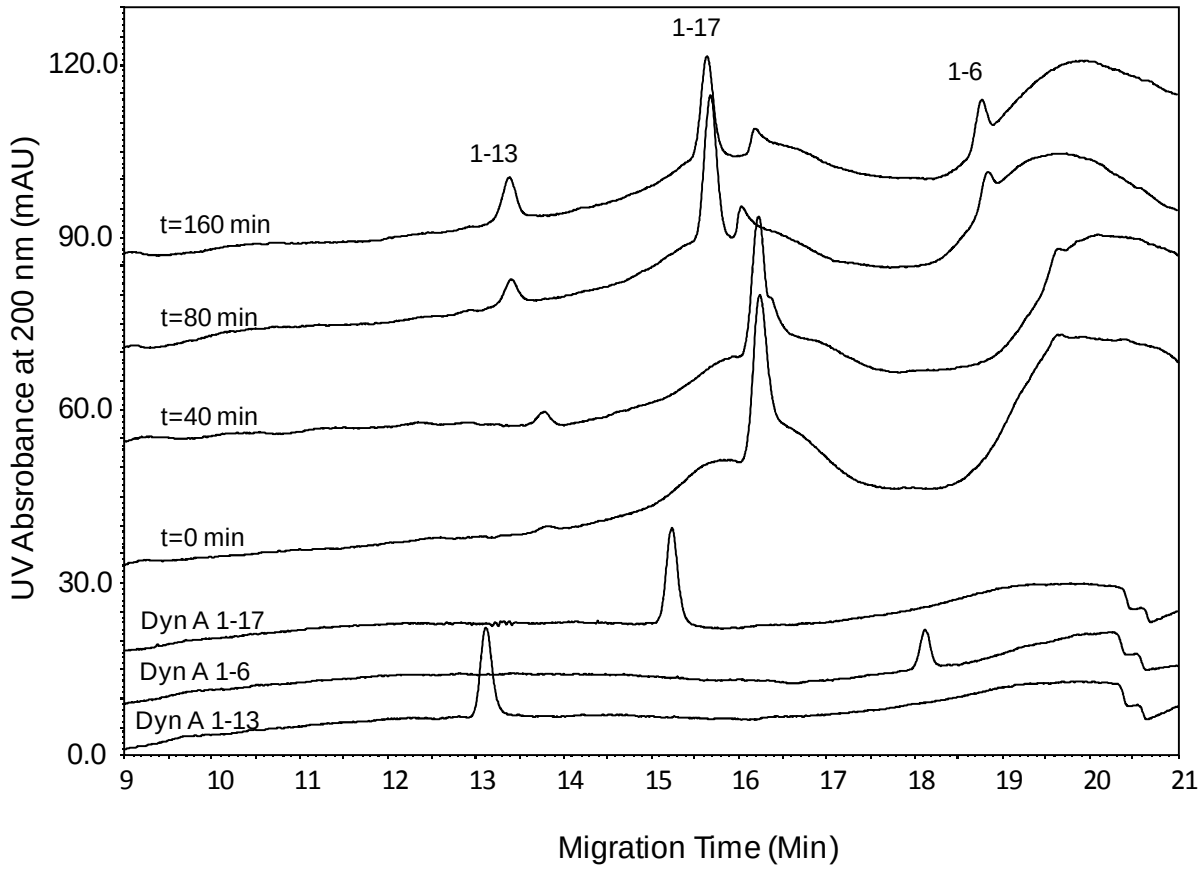

Figure 3.10 Metabolism of Dyn A 1-17 in a 1:10 dilution of human plasma.

Metabolites (1-6 and 1-13) were identified based on migration times of standard injections of each peptide. Separation conditions same as those in Figure 3.9

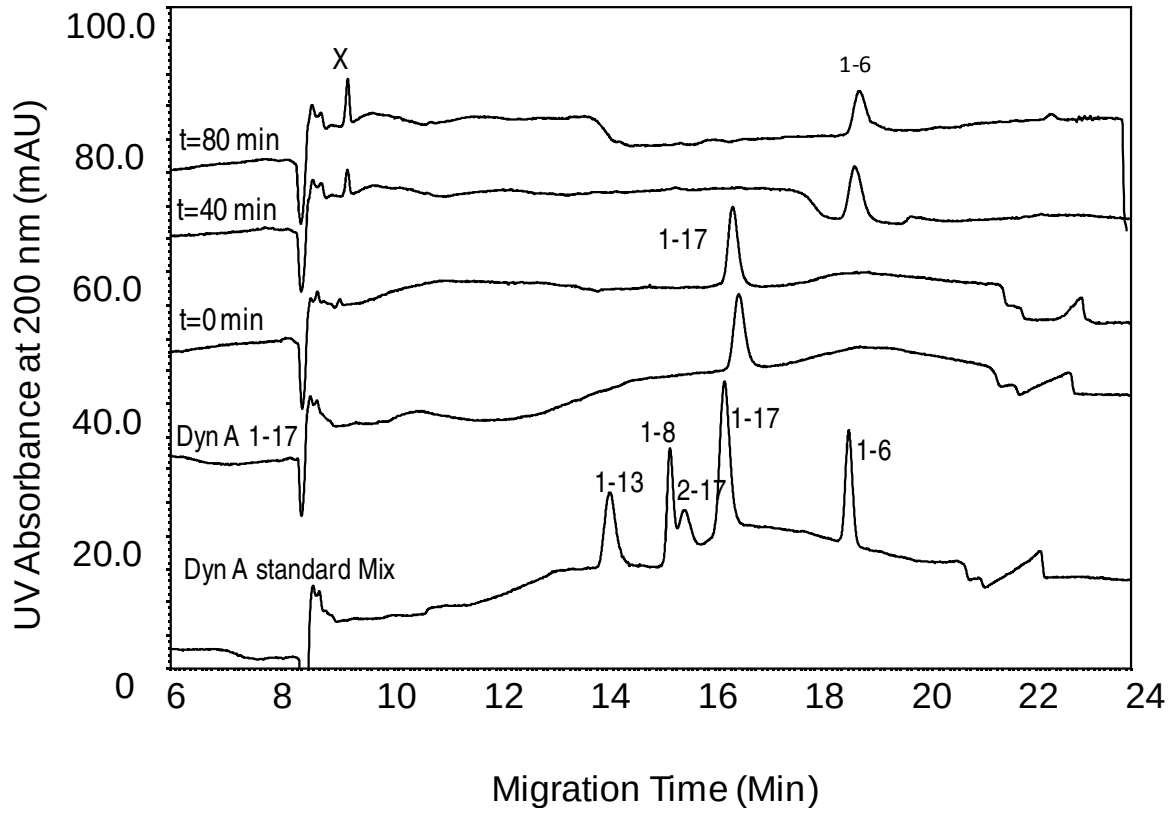

Figure 3.11 Metabolism of Dyn A 1-17 in rat brain slice. Metabolites were identified based on standard single injections of each peptide. X = unidentified metabolite. Separation conditions same as in Figure 3.9.

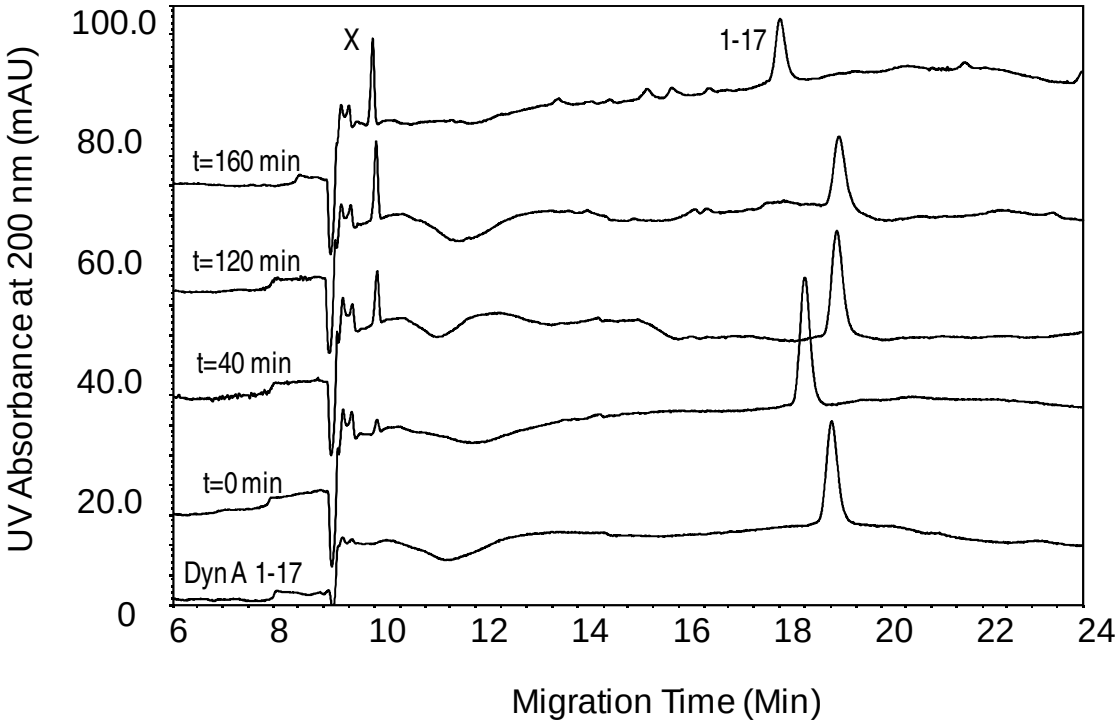

Figure 3.12 Metabolism of Dyn A 1-17 in rat spinal cord slice. Metabolites were identified based on standard single injections of each peptide. X = unidentified metabolite. Separation conditions same as in Figure 3.9.

been shown to improve resolution for peptide metabolites and enantiomers of relevant pharmaceuticals [43, 44]. In this work, various forms of beta-cyclodextrin were investigated to improve resolution of closely related metabolites, and sulfobutyl-ether-β cyclodextrin was found to be optimal. The optimized separation has been used to examine *in vitro* metabolism of Dyn A 1-17 in human plasma as well as in rat brain and spinal cord.

Previous reports of dynorphin metabolism have identified a variety of metabolites present in blood. Kreek's group investigated the *in vitro* metabolism of Dyn A 1-17 in both human and rhesus monkey blood using MALDI [20-21, 23]. Human or monkey blood was spiked with Dyn A 1-17, and three major metabolites were identified, one opioid (Dyn A 1-6) and two non-opioid (Dyn A 2-17 and 7-17) peptides. These major metabolites were further degraded to 2-6, 8-17, 9-17, 11-17, 3-17, and 4-17. The Dyn A 1-6 and 7-17 fragments arise from cleavage at paired basic amino acid residues Arg(6)-Arg(7). The endopeptidase responsible for this metabolite has been termed dynorphin A converting enzyme (DCE) [50, 51]. Cleavage of the N-terminal tyrosine to produce Dyn A 2-17 is likely the result of nonspecific aminopeptidase activity [52, 53]. While the metabolism products were similar in human and monkey blood, their time course differed considerably, with metabolism occurring much faster in rhesus monkeys.

The studies presented here detected the generation of two major metabolites over a 160 time period. The metabolites Dyn A 1-6 and Dyn A 1-13 were identified based on single injections of metabolite standards and correlating migration times. The presence of Dyn A 1-6 agrees well with the aforementioned studies performed in the Kreek lab [20, 21, 23], demonstrating the utility of CE in monitoring dynorphin metabolism. It is thought that the peptidase responsible for the cleavage of the N-terminal tyrosine is membrane-bound [52]. The studies presented in this paper were done in plasma as opposed to whole blood. This is a

possible explanation for why Dyn A 2-17 was not observed in this work, but was reported previously [20, 21, 23].

Due to the neurotoxicity of Dyn A 1-17, its metabolism has also been studied in the brain. Several enzymes have been implicated in the metabolism of opioid peptides in the brain. In the early 1980's an aminopeptidase from Sprague Dawley rat brains was purified by Berg and Marks and shown to cleave the N-terminal tyrosine from enkephalin and dynorphin peptides [52, 53]. However, the reactivity of this enzyme decreased with increasing size of the peptide, suggesting a conformational component to the availability of the tyrosine residue for enzymatic cleavage. As mentioned previously, the endopeptidase responsible for cleavage at the paired basic amino acids- Arg^6 and Arg^7- is termed dynorphin A converting enzyme and has been isolated and purified from human cerebrospinal fluid and human spinal cord tissue [50, 51].

Kreek's group investigated the metabolism of dynorphin A 1-17 in the striatum of Fischer rats using microdialysis [22]. MALDI was employed for identification following direct infusion of Dyn A 1-17. Dyn A 1-7, 8-17, 1-6, and 9-17 were observed. Interestingly, the counterpart metabolites (7-17 and 1-8) were not detected. Andren's group has also investigated the metabolism of dynorphin using microdialysis and nanoLC/ESI-TOF MS [3]. Their study compared dynorphin metabolism in the brains of healthy Sprague Dawley rats and those with unilateral 6-OHDA lesions to mimic Parkinson's disease. Several metabolites were found in the brains of the lesioned rats that were not present in healthy rats, exemplifying the importance of these metabolic events and their potential role in various neurological disorders.

To examine the metabolism of Dyn A in the central nervous system, *in vitro* studies with both rat brain and rat spinal cord slices were performed in this work. In the rat brain slice the

appearance of two metabolites was observed, however only one could be identified by standard injections and migration time correlation. This metabolite is Dyn A 1-6, suggesting the presence of dynorphin converting enzyme in the rat brain. The earlier migrating metabolite does not correspond to any of the metabolites investigated in this study. Interestingly, Dyn A 1-6 does not appear in studies with the rat spinal cord but, again, an unidentified early migrating metabolite is present. The time course of the metabolism in all three tissues also varies. Parent peptide is still present after 160 minutes in both the plasma and the spinal cord. In the rat brain, however, the peak for Dyn A 1-17 is completely absent by the 40-minute time point. Differences in the metabolic kinetics between species and tissues have been previously reported. For example, Kreek's group found the metabolism of Dyn A 1-17 to be much faster in monkey blood than in human blood [20, 23].

3.4 Summary

A method for on-capillary copper complexation of dynorphin peptides has been developed. The method described here demonstrates the usefulness of capillary electrophoresis for examining peptide degradation in a single assay where the parent peptide and metabolites are detected simultaneously following electrophoretic separation. It is clear that the metabolism of dynorphin is a complex process that varies between tissues and species. Capillary electrophoresis provides a convenient format for the separation and detection of the parent peptide and its metabolites.

The use of on-capillary complexation improves the efficiency of these separations and has the potential to render even the des-tyrosine metabolites electroactive, making amperometric

detection feasible. Future work will focus on electrochemical detection of the peptides to improve limits of detection. Additionally, transferring this separation to a microchip device for even faster analysis is being explored. In these studies, metabolism was slowed by diluting the plasma and performing the analysis at room temperature. In a microchip format, these steps could potentially be avoided, enabling a more physiologically relevant investigation of dynorphin metabolism. The length of time for the CE runs is the limiting factor with respect to temporal resolution, and microchip electrophoresis would improve this from 40 minutes to less than 5 minutes. This miniaturized format would enable direct coupling to microdialysis sampling, making near real-time monitoring of dynorphin metabolism *in vivo* possible. Microchip analysis of dynorphin peptides will be further discussed in Chapter 6 of this thesis.

3.5 References

[1] Hauser, K. F., Aldrich, J. V., Anderson, K. J., Bakalkin, G., Christie, M. J., Hall, E. D., Knapp, P. E., Scheff, S. W., Signh, I. N., Vissel, B., Woods, A. S., Yakovleva, T., Shippenberg, T. S., *Frontiers in Bioscience* 2005, *10*, 216-235.

[2] Yakovleva, T., Marinova, Z., Kuzmin, A., Seidah, N. G., Haroutunian, V., Terenius, L., Bakalkin, G., *Neurobiology of Aging* 2006, *14*, 1700-1708.

[3] Klintenberg, R., Andren, P. E., *Journal of Mass Spectrometry* 2005, *40*, 261-270.

[4] Lai, J., Ossipov, M. H., Vanderah, T. W., Malan, J., T. P. , Porreca, F., *Molecular Interventions* 2001, *1*, 160-167.

[5] Shirayama, Y., Ishida, H., Iwata, M., Hazama, G., Kawahara, R., Duman, R. S., *Journal of Neurochemistry* 2004, *90*, 1258-1268.

[6] Hauser, K. F., Knapp, P. E., Turbek, C. S., *Experimental Neurology* 2001, *168*, 78-87.

[7] Nardo, L., Soong, Y., Wu, D., Young, I. R., Walker, D., Szeto, H. H., *Am J Physiol Endocrinol Metab* 2002, *282*, 1301-1307.

[8] Ghazarossian, V. E., Chavkin, C., Goldstein, A., *Life Sciences* 1980, *27*, 75-86.

[9] Mueller, S., Hochhaus, G., *Pharmaceutical Research* 1995, *12*, 1165-1170.

[10] Partilla, J. S., You, J., Rothman, R. B., *Journal of Chromatography B* 1995, *667*, 49-56.

[11] Prokai, L., Kim, H., Zharikova, A., Roboz, J., Ma, L., Deng, L., Simonsick Jr., W. J., *Journal of Chromatography A* 1998, *800*, 59-68.

[12] Furtos-Matei, A., Day, R., St.-Pierre, S. A., St-Pierre, L. G., Waldron, K. C., *Electrophoresis* 2000, *21*, 715-723.

[13] Solinova, V., Kasicka, V., Koval, D., Barth, T., Ciencialova, A., Zakova, L., *Journal of Chromatography B* 2004, *808*, 75-82.

[14] Garcia-Campana, A. M., Taverna, M., Fabre, H., *Electrophoresis* 2007, *28*, 208-232.

[15] Hernandez, E., Benavente, F., Sanz-Nebot, V., Barbosa, J., *Electrophoresis* 2007, *28*, 3957-3965.

[16] Herrero, M., Ibanez, E., Cifuentes, A., *Electrophoresis* 2008, *29*, 2148-2160.

[17] Lee, E. D., Muck, W., Henion, J. D., *Journal of Chromatography* 1988, *458*, 313-321.

[18] Sanz-Nebot, V., Benavente, F., Hernandez, E., Barbosa, J., *Analytica Chimica Acta* 2006, *577*, 68-76.

[19] Stutz, H., *Electrophoresis* 2005, *26*, 1254-1290.

[20] Chou, J. Z., Chait, B. T., Wang, R., Kreek, M. J., *Peptides* 1996, *17*, 983-990.

[21] Chou, J. Z., Kreek, M. J., Chait, B. T., *American Society for Mass Spectrometry* 1994, *5*, 10-16.

[22] Reed, B., Zhang, Y., Chait, B. T., Kreek, M. J., *Journal of Neurochemistry* 2003, *86*, 815-823.

[23] Yu, J., Butelman, E. R., Woods, J. H., Chait, B. T., Kreek, M. J., *The Journal of Pharmacology and Experimental Therapeutics* 1996, *279*, 507-514.

[24] Kasicka, V., *Electrophoresis* 2010, *31*, 122-146.

[25] Scriba, G. K. E., Psurek, A., in: Schmitt-Kopplin, P. (Ed.), *Capillary Electrophoresis: Methods and Protocols*, Humana Press Inc., Totowa 2008, pp. 483-506.

[26] Hauer, H., Dukes, G. R., Margerum, D. W., *Journal of the American Chemical Society* 1973, *95*, 3515-3522.

[27] Kirksey, J., S. T. , Neubecker, T. A., Margerum, D. W., *Journal of the American Chemical Society* 1979, *101*, 1631-1633.

[28] Margerum, D. W., *Pure & Applied Chemistry* 1983, *55*, 23-34.

[29] Margerum, D. W., Chellappa, K. L., Bossu, F. P., Burce, G. L., *Journal of the American Chemical Society* 1975, *97*, 6894-6896.

[30] Chen, J., Logman, M., Weber, S. G., *Electroanalysis* 1999, *11*, 331-336.

[31] Chen, J., Weber, S. G., *Analytical Chemistry* 1995, *67*, 3596-3604.

[32] Tsai, H., Weber, S. G., *Analytical Chemistry* 1992, *64*, 2897-2903.

[33] Woltman, S. J., Chen, J., Weber, S. G., Tolley, J. O., *Journal of Pharmaceutical and Biomedical Analysis* 1995, *14*, 155-164.

[34] Shen, H., Witowski, S. R., Boyd, B. W., Kennedy, R. T., *Analytical Chemistry* 1999, *71*, 987-994.

[35] Gawron, A. J., Lunte, S. M., *Electrophoresis* 2000, *21*, 2067-2073.

[36] Gawron, A. J., Lunte, S. M., *Electrophoresis* 2000, *21*, 3205-3211.

[37] Lacher, N. A., Garrison, K. E., Lunte, S. M., *Electrophoresis* 2002, *23*, 1577-1584.

[38] Kornfelt, T., Vinther, A., Okafo, G. N., Camilleri, P., *Journal of Chromatography A* 1996, *726*, 223-228.

[39] Okafo, G. N., Birrell, H. C., Greenway, M., Haran, M., Camilleri, P., *Analytical Biochemistry* 1994, *219*, 201-206.

[40] Okafo, G. N., Perrett, D., Camilleri, P., *Biomedical Chromatrography* 1994, *8*, 202-204.

[41] Veraart, J. R., Schouten, Y., Gooijer, C., Lingeman, H., *Journal of Chromatography A* 1997, *768*, 307-313.

[42] Kostel, K. L., Freed, A. L., Lunte, S. M., *Journal of Chromatography A* 1996, *744*, 241-248.

[43] Armstrong, D. W., Ward, T. J., Armstrong, R. D., Beesley, T. E., *Science* 1986, *232*, 1132-1135.

[44] Talt, R. J., Thompson, D. O., Stella, V. J., Stobaugh, J. F., *Analytical Chemistry* 1994, *66*, 4013-4018.

[45] Lauer, H. H., McManigill, D., *Analytical Chemistry* 1985, *58*, 166-170.

[46] Marinova, Z., Vukojevic, V., Surcheva, S., Yakovleva, T., Cebers, G., Pasikova, N., Usynin, I., Hugonin, L., Fang, W., Hallberg, M., Hirschberg, D., Bergman, T., Langel, U., Hauser, K. F., Pramanik, A., Aldrich, J. V., Graslund, A., Terenius, L., Bakalkin, G., *The Journal of Biological Chemistry* 2005, *280*, 26360-26370.

[47] Ho, W. K. K., Cox, B. M., Chavkin, C., Goldstein, A., *Neuropeptides* 1980, *1*, 143-152.

[48] Cifuentes, A., Santos, J. M., deFrutos, M., Diez-Masa, J. C., *Journal of Chromatography A* 1993, *652*, 161-170.

[49] Towns, J. K., Bao, J., Regnier, F. E., *Journal of Chromatography* 1992, *599*, 227-237.

[50] Silberring, J., Castello, M. E., Nyberg, F., *The Journal of Biological Chemistry* 1992, *267*, 21324-21328.

[51] Nyberg, F., Nordstrom, K., Terenius, L., *Biochemical and biophysical research communications* 1985, *131*, 1069-1074.

[52] Benuck, M., Berg, M. J., Marks, N., *Journal of Neurochemical Research* 1984, *9*, 733-749.

[53] Berg, M. J., Marks, N., *Journal of Neuroscience Research* 1984, *11*, 313-321.

Chapter Four:

Development of an LC-MS/MS method for the quantitation of dynorphin peptides in biological matrices

4.1 Introduction

Liquid chromatography in conjunction with tandem mass spectrometry is a popular means for separation and quantitation of peptides and proteins. Several reviews have recently been published on this topic [1, 2]. LC-MS/MS has been employed for the analysis of naturally occurring peptides in both *in vitro* [3] and *in vivo* metabolism studies as well as for the investigation of peptide transport across biological barriers such as the blood brain barrier [4-6]. The use of LC-MS/MS has also been employed for the determination of the stability, pharmacokinetics, and pharmacodynamics of peptide-based pharmaceuticals [7-9]. While MALDI has advanced as a qualitative means for identifying peptides in biological matrices [10-13], more quantitative techniques are often desirable for the aforementioned applications. In particular, electrospray ionization (ESI) enables direct coupling of LC flow to the ionization source of mass spectrometers, creating a means for sample de-salting prior to detection, increased through-put, and automation [1, 2].

Under ESI conditions, compounds that carry a charge in solution are transferred into the gas phase as evaporation of the volatile solvents used in liquid chromatography occurs. Charge repulsion, within the aerosol droplet, results in the release of single ions into the gaseous phase. ESI is a gentle ionization process and can be performed in either positive or negative mode depending on the application and compounds of interest. A schematic of the ionization process can be seen in Figure 4.1. Peptides and proteins will produce multiply charged ions under ESI conditions enabling their detection on instruments with somewhat limited mass to charge (m/z) range. For example, a peptide with a molecular weight of 3000 is above the 1800 limit of the instrument employed for the majority of these studies; however, a doubly charged ion of this

peptide has a mass to charge ratio of 1501 [(MW + 2)/number of charges = 3002/2) and will therefore be detected.

A variety of experiments can be performed using a triple quadrupole mass spectrometer including precursor ion scans, product ion scans, neutral loss or gain, and multiple reaction monitoring. In this work, precursor and product ion scans were used in the optimization of instrument parameters for the analytes of interest. Precursor ion(s) are identified in the first quadrupole. For small compounds this would be the molecular mass (plus 1 for the addition of a proton), but for peptides there are typically multiple ions representing multiple charge states (Figure 4.2). These precursor ions are then fragmented in the collision cell and the product ions are identified (Figure 4.3). The information gained from these scans is in the form of a mass spectrum, and the identified precursor ions are then used in additional experiments such as multiple reaction monitoring or MRM.

MRM is most often employed for quantitation, improving sensitivity and enabling high specificity for the analytes of interest. In the first quadrupole, the precursor ion is selected. This ion is then collisionally dissociated (by an inert gas) in the second quadrupole, and the third quadrupole scans for these specific product ions (Figure 4.4). The conversion of one precursor ion to one product ion is called a transition. By focusing on only a handful of specific transitions (typically one to two per analyte), dwell time on the ions of interest is increased, improving sensitivity in comparison to the data collected in scan mode. Data is presented in this case not as a spectra, but instead as a chromatogram, where ion intensity is plotted on the y-axis versus time on the x-axis. A total ion chromatogram (TIC) can be viewed, which is a sum of all ions detected from all the specified transitions, or each transition can be observed separately in an extracted ion chromatogram (XIC). Multiple reaction monitoring not only improves selectivity,

but with the inclusion of an appropriate internal standard (IS), more accurate quantitation can be achieved correcting for ion suppression [1]. Ideally an internal standard is an isotopically-labeled version of the analyte of interest; however, these compounds are expensive and their use is not always practical or feasible.

This chapter will discuss important analytical considerations for peptide analysis via LC-MS/MS including method development, internal standard selection, and specific challenges when sampling from biologically compatible matrices. In particular, this chapter will lay the groundwork for Chapter 4 in which the metabolism of Dyn A 1-17 is investigated in the presence of rat brain and spinal cord as well as bovine brain microvessel endothelial cells, a blood brain barrier mimic.

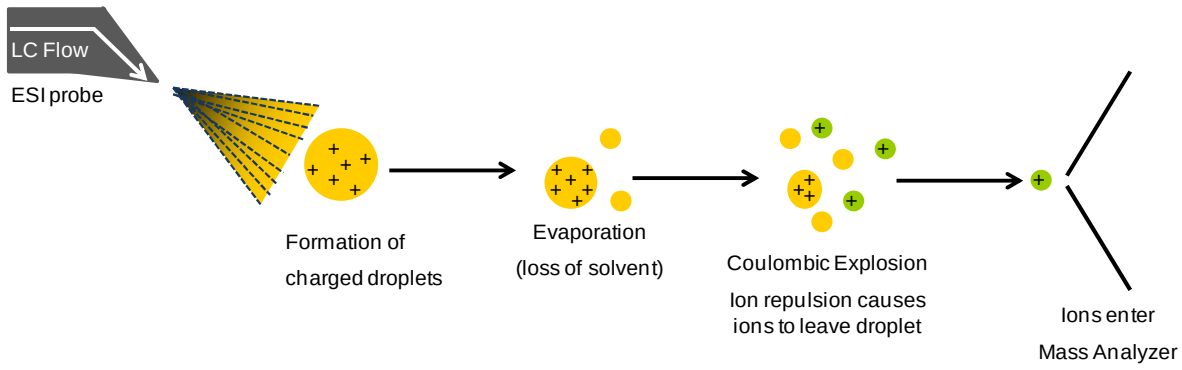

Figure 4.1 Cartoon depiction of electrospray ionization, modified from Waters website (www.waters.com).

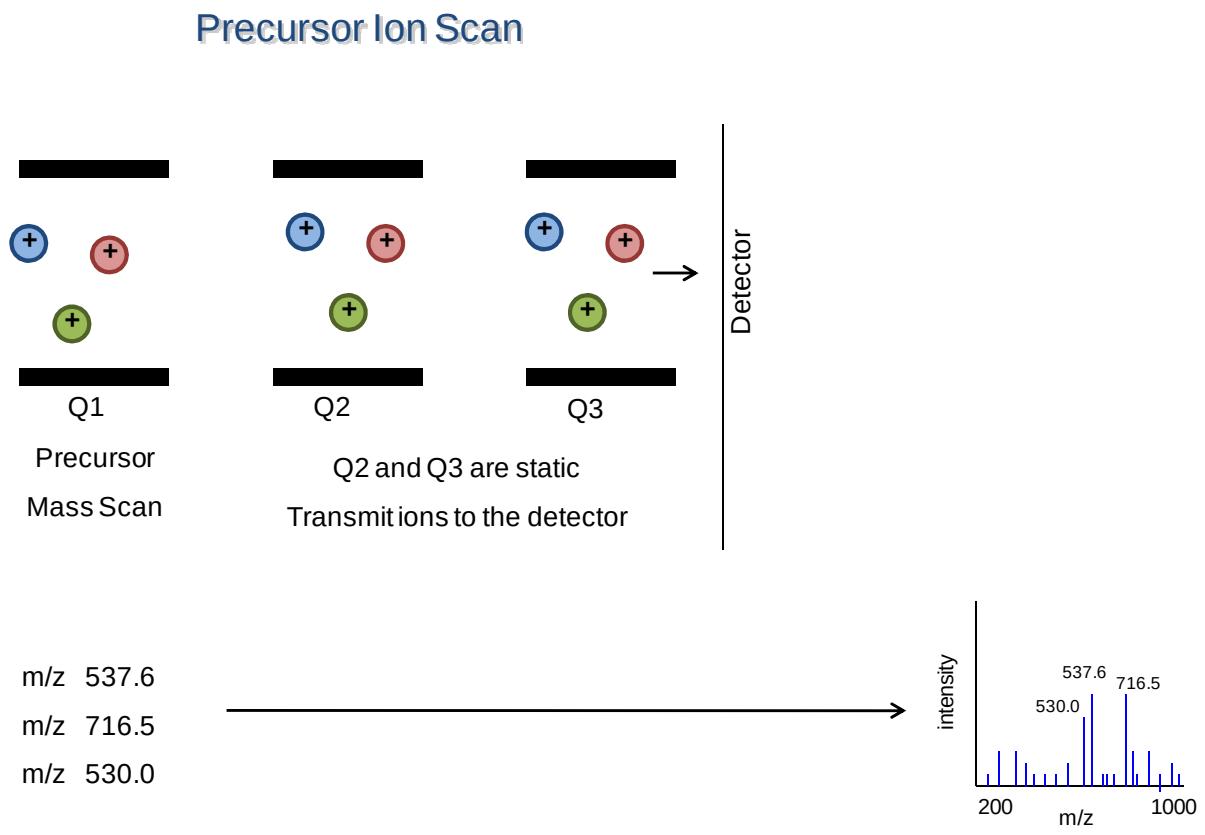

Figure 4.2 Cartoon depiction of a precursor ion scan. Experiments are performed to identify precursor ions (multiple charge states in the case of peptides). Precursor ion scans are typically performed to optimize voltages prior to precursor mass selection for use in MRM experiments. Example values are given for Dyn A 1-17: 537.6 (4+ charge state) and 716.5 (3+ charge state) and bradykinin: 530.0 (2+ charge state) precursor ions.

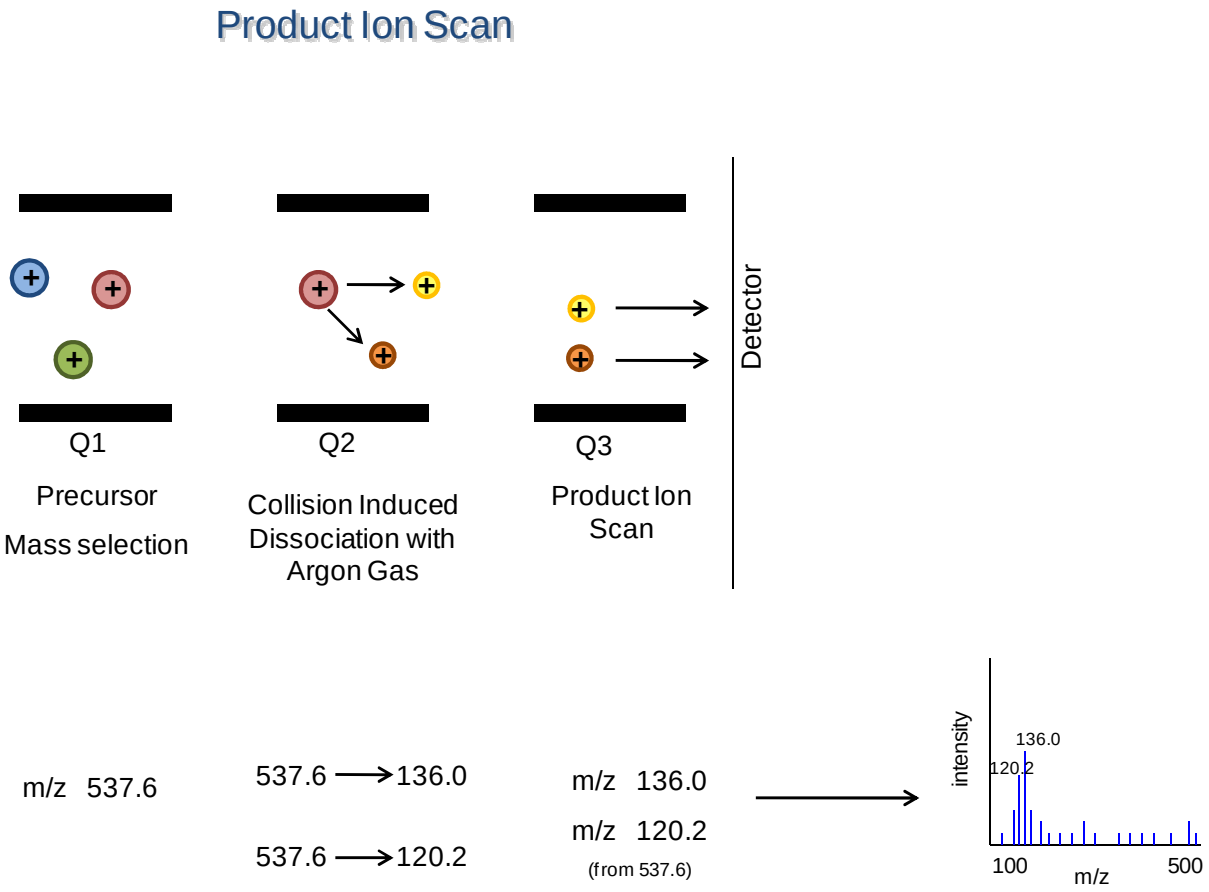

Figure 4.3 Cartoon depiction of a product ion scan. These are typically preformed to tune CID parameters for optimization prior to MRM. Example transitions shown are for Dyn A 1-17 (the parent 4+ ion 537.6 is fragmented to 136.0 and 120.2).

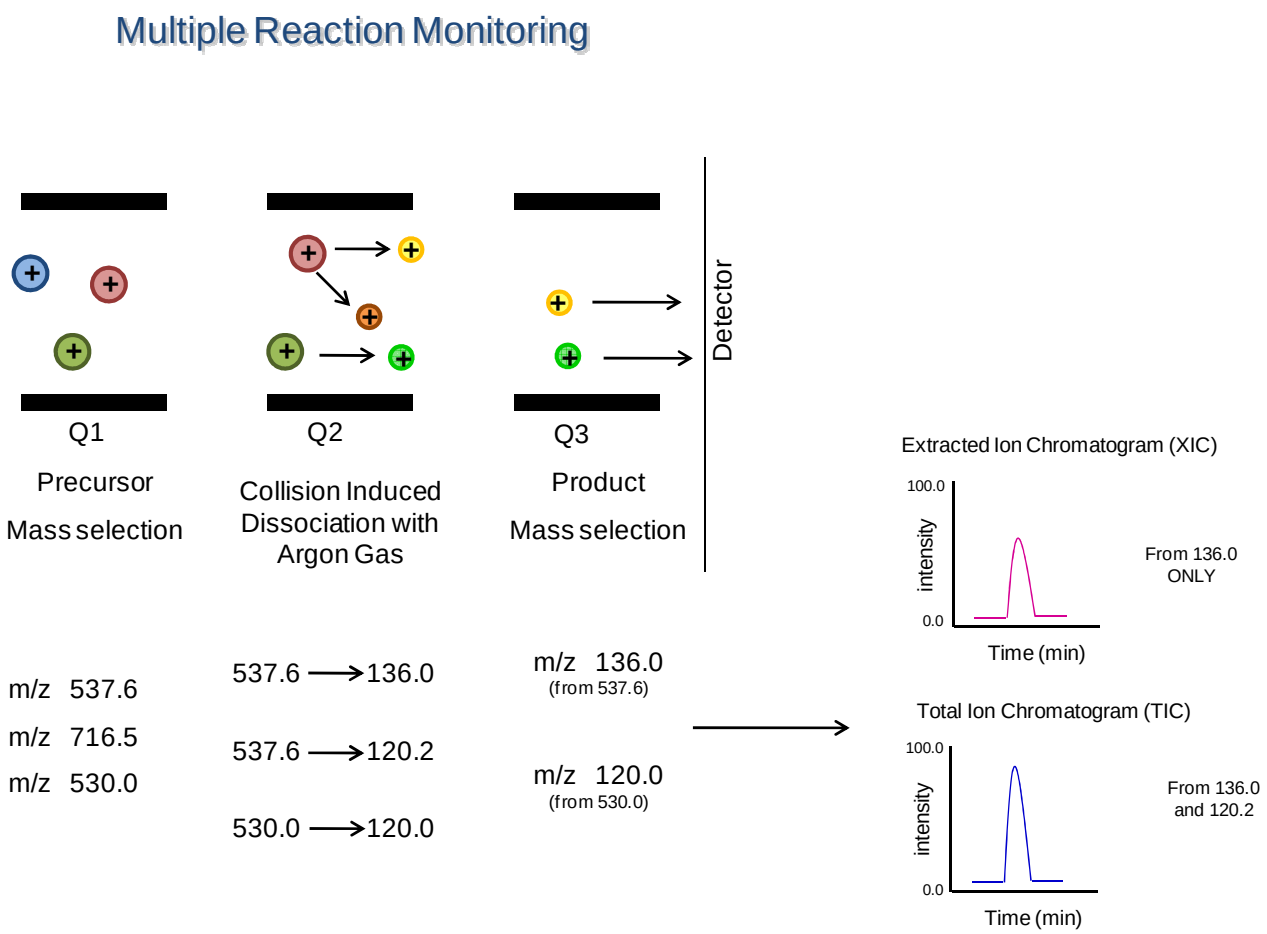

Figure 4.4 Cartoon depiction of multiple reaction monitoring. These experiments are typically performed when quantitation of known analytes of interest is desired. Two chromatograms are shown on the right, one for the XIC for Dyn A 1-17 and for the TIC for Dyn A and the IS.

4.2 Materials and Methods

4.2.1 Reagents

All dynorphin peptides (Dyn A 1-17, 2-17, 1-13, 1-8, and 1-6) were obtained from Bachem Biosciences, Inc. (King of Prussia, PA, USA). Bradykinin was purchased from Sigma-Aldrich (St. Louis, MO USA). Fisher Optima acetonitrile (LC-MS grade) was used for all mobile phases containing organic (Fisher Scientific, Fair Lawn, NJ, USA). Formic acid was purchased from Acros Organics (Morris Plains, NJ, USA) at 99.9% purity. All aqueous mobile phases were made from 18 MΩ deionized (D.I.) water from a benchtop Milli-Q Synthesis A10 Water Purification System (Millipore, Billerica, MS, USA), filtered with 0.2 μm Magna nylon filters from Osmonics (Minnetonka, MN, USA). Minimum Essential Media and Ham's F12 were purchased from Life Technologies, Invitrogen Corporation (Carlsbad, CA, USA). All other reagents were purchased from Sigma Aldrich (St. Louis, MO, USA).

4.2.2 Liquid Chromatography-Tandem Mass Spectrometry Instrumentation

Two LC-MS/MS systems were used for the studies in this dissertation. The first was a Waters Micromass Quattro micro triple quadrupole mass spectrometer with a Waters 2690 HPLC system (Waters, Milford, MA, USA) on the front end. The LC system included a refrigerated autosampler and a column oven as well as an external diverter valve. The system was operated using MassLynx 3.5 software. The second system consisted of an API 2000 triple quadrupole mass spectrometer (AB Sciex, Foster City, CA, USA) with a Shimadzu Prominence LC (Shimadzu, Japan) complete with two LC20-AD pumps with a solvent mixer, a CMB-20ALite controller, degasser (DGU-20A3), autosampler (Sil20A-HT), and column heater (CTO-20A). The system was operated using Analyst 1.5 software. Analyst was also used for data

analysis of quantitative experiments. A 1.0 x 50 mm C18 analytical column with 5 μm particles and the corresponding guard column (Vydac Microbore, C-18 MS columns, Grace Davidson Discovery Sciences, Deerfield, IL, USA) were utilized for all experiments.

With both instruments a variety of parameters are considered tunable for each compound of interest investigated. In general these parameters are voltages– responsible for guiding the ions through the pathway of the instrument, gas flows– which aid in the transport of ions through the mass spectrometer and prevent contaminants from entering the instrument, and temperature settings– which aid in the desolvation of charged droplets and the entrance of ions into the gaseous phase. A detailed discussion about the different instrumental parameters and configurations follows.

4.2.2.1 Waters Micromass Quattro micro

There are two categories of parameters for which a user can optimize the ionization and fragmentation of their compounds of interest: the source parameters and the analyzer parameters. Two source parameters, the cone voltage and capillary voltage are extremely compound specific, and therefore can be set for each analyte of interest. The capillary voltage (kV) is applied to the ESI probe and contributes to the formation of charge aerosol droplets as the LC eluent exits the end of the stainless steel capillary. The cone voltage (V) is applied to the sample cone, the first orifice of entrance into the portion of the mass spectrometer that is under vacuum. The cone voltage must be carefully optimized so as to prevent in source decay of the analytes of interest. For example, if the cone voltage is tuned to a value higher than necessary, fragmentation of peptides can occur at the ion source, decreasing the amount of intact molecule available for entrance to the spectrometer thus reducing sensitivity.

The remaining source parameters are tunable for a series of compounds, in this case, for an entire family of dynorphin peptides. The extractor parameter (V) is a voltage applied to the extraction cone which rests behind the sample cone. It is responsible for directing and focusing the ions into the first quadrupole. The RF lens value (V) is the voltage applied to the hexapole (collision cell). It guides ions into the collision cell. The locations of these applied voltages along the mass spec quadrupoles can be seen in Figures 4.5 and 4.6. In addition to these voltages, the source and desolvation temperatures (°C) and the cone and desolvation gas flows (L/h) must be optimized. The source temperature settings aid in the evaporation of the LC eluent from the charged droplet. The temperature must be sufficiently high to improve sensitivity while preventing this evaporation from occurring too rapidly which hinders ionization. Both the cone gas and desolvation gas are nitrogen gas (from a liquid nitrogen source) which surround the cone and probe respectively and aid in eluent evaporation.

In addition to the source parameters, a variety of settings on the analyser are also tunable. These values will have different values depending on the experiment being performed. The resolution values (LM and HM 1 and 2) are most often set to 15; however, when performing MRMs the resolution can be sacrificed to some degree in order to improve sensitivity. For example, decreasing these values to the range of 10.0-13.0 can bring the peak width at half height from 0.5 to around 1.0 increasing sensitivity. In MS1 scan mode, the entrance and exit values are set to 50 and no collision energy is applied. This allows ions to pass through the quadrupoles, reaching the detector more quickly. When MS/MS experiments are performed the entrance and exit values are lowered to extend the dwell time of the ions within the collision cell, resulting in more complete fragmentation. Also during these experiments, collision energy is applied and optimized for each compound of interest. Similarly, ion energy 1 and 2 are

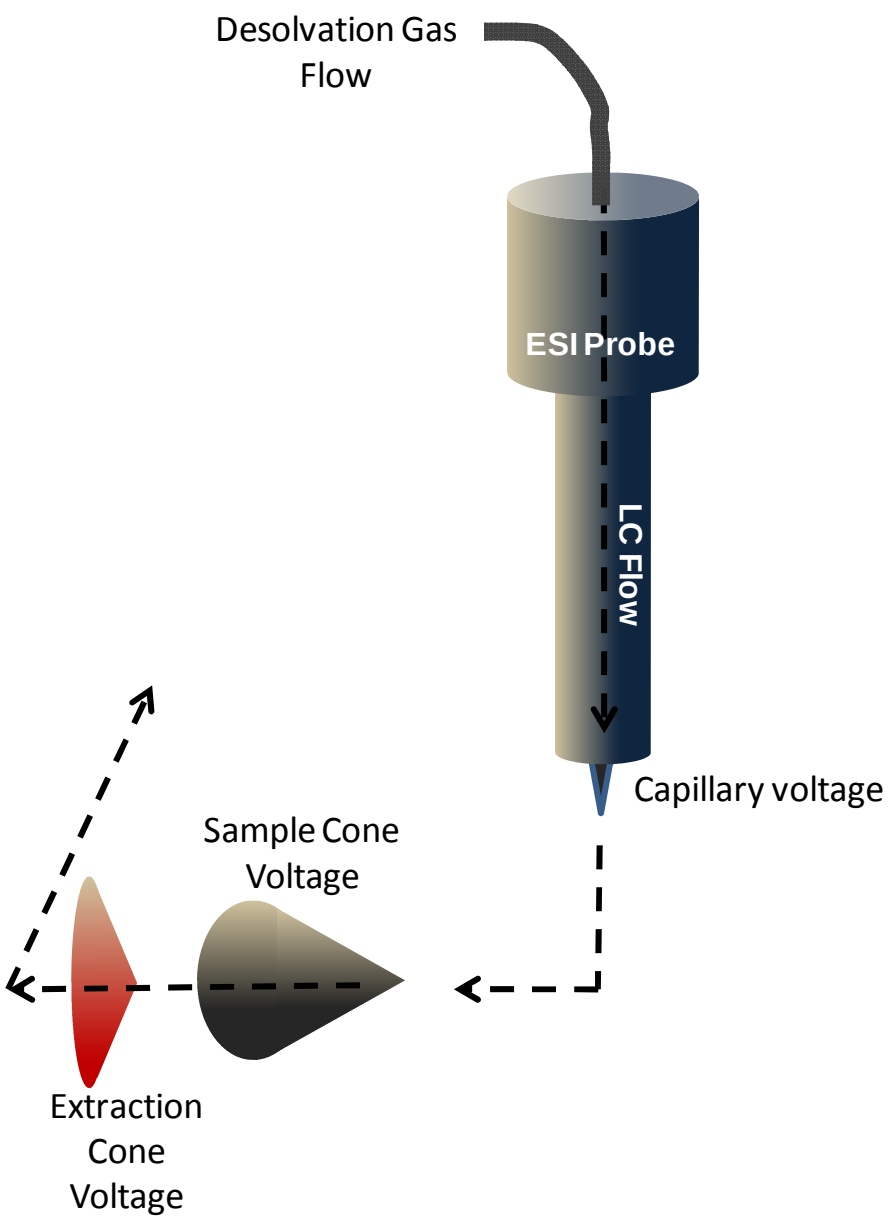

Figure 4.5 Diagram of the Z-spray ionization source on the Waters Quattro micro. Figure modified from www.waters.com.

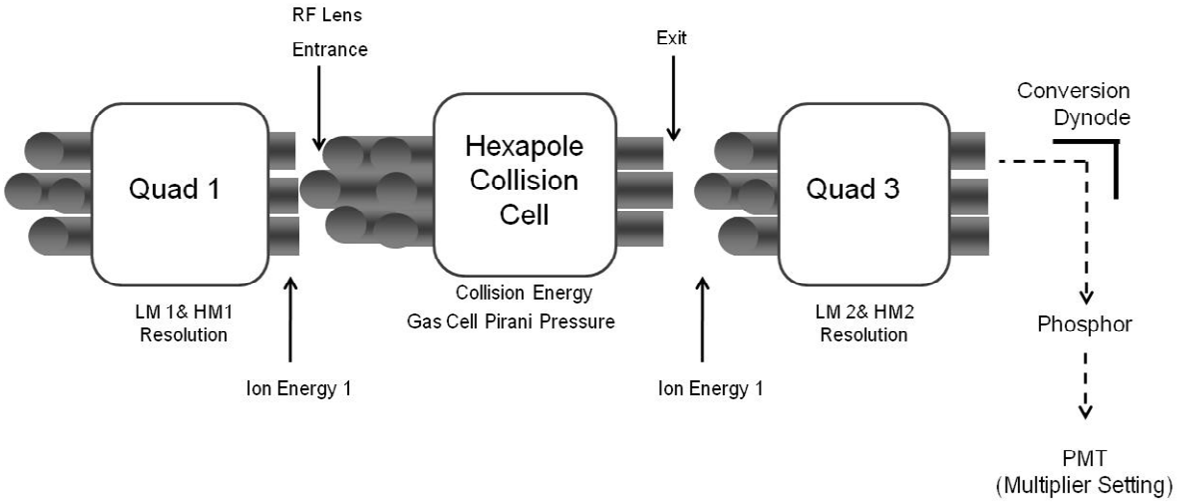

Figure 4.6 Diagram of the quadrupole "rail" on the Waters Quattro micro featuring a hexapole collision cell. Figure modified from Waters user manual.

Source Parameters	Units	Range	Recommended Values	
Capillary Voltage	kV	2.5-4	3	
Cone Voltage	V	10-150	60	
Extractor	V	0-4	3	
RF Lens	N/A	0-5	0.2	
Source Temperature	℃	70-120	120	
Desolvation Temperature	℃	150-450	350	highly dependent on flow rate
Cone gas	L/h	50-200	1-100	
Desolvation gas	L/h	0-1200	700	highly dependent on flow rate
Analyser Parameters	**Units**	**Range**	**Recommended Value MS1**	**Recommended Value MS2**
LM1 and HM1 Resolution	N/A		15	15 (13 to increase ionization)
Ion Energy 1	N/A		0.5	0-3
Entrance	N/A		50	-5 to 5
Collision	N/A		1	1-200
Exit	N/A		50	1 to 5
LM2 and HM2 Resolution	N/A		15	15 (13 to increase ionization)
Ion Energy 2	N/A		3	0-3
Cell Pirani Pressure	mbar		1 e-4 (argon)	3.6 e-3 (argon)
Multiplier Voltage	V		650	650

Table 4.1 Tunable Mass Spec Parameters for the Waters Quattro micro instrument.

optimized differently for MS1 versus MS/MS experiments. These values are applied to exit of quad 1 and quad 3, respectively. A summary of these tunable values can be seen in Table 4.1.

4.2.2.2 Applied Biosystems API 2000

With the API 2000, the following parameters are tunable during method development for specific compounds. Their location along the quadrupole can be seen in Figures 4.7 and 4.8. The declustering potential (DP) controls the difference in potential between the skimmer (held at ground) and the orifice plate. This potential difference decreases the occurrence of solvent cluster ions, resulting in more efficient ionization. The entrance potential (EP) parameter controls the difference between voltage on quadrupole zero (Q0) and ground, guiding the ions into the Q0 region which is under high pressure. The EP parameter also aids in focusing the ions as they enter Q0. All other ion path voltages are dependent on the EP value, and therefore this is one of the first parameters optimized. The collision cell entrance potential is a mass-dependent parameter that controls the potential difference between Q0 and the entrance of quadrupole 2 (Q2). It focuses ions into the collision cell. During MS/MS scans this parameter is optimized for the precursor ion. The collision cell exit potential similarly is used to focus and accelerate ions as they leave Q2. This parameter is optimized for the product ion in MS/MS scans. Two parameters control how the precursor ions fragment in the collision cell: the collision energy (CE) and the collisionally activated dissociation (CAD) gas. The CE parameter controls the energy that the precursor ions receive as they enter the second quadrupole. The CAD parameter control the pressure of the collision gas in the collision cell during MS/MS scans. Both the CE and CAD parameters control the product ions produced and are very compound specific. They are optimized to the lowest setting that will generate a reproducible fragment ion with the highest sensitivity.

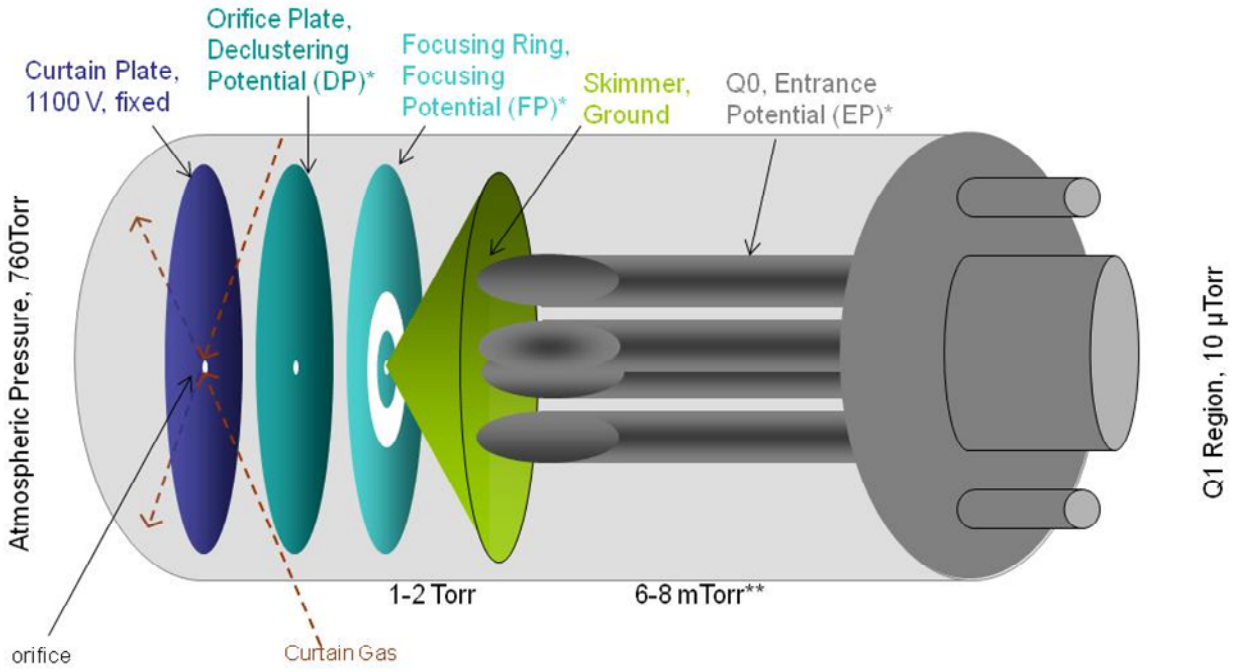

Figure 4.7 Diagram of the ionization source on the API 2000. Figure modified from training materials at the API training course.

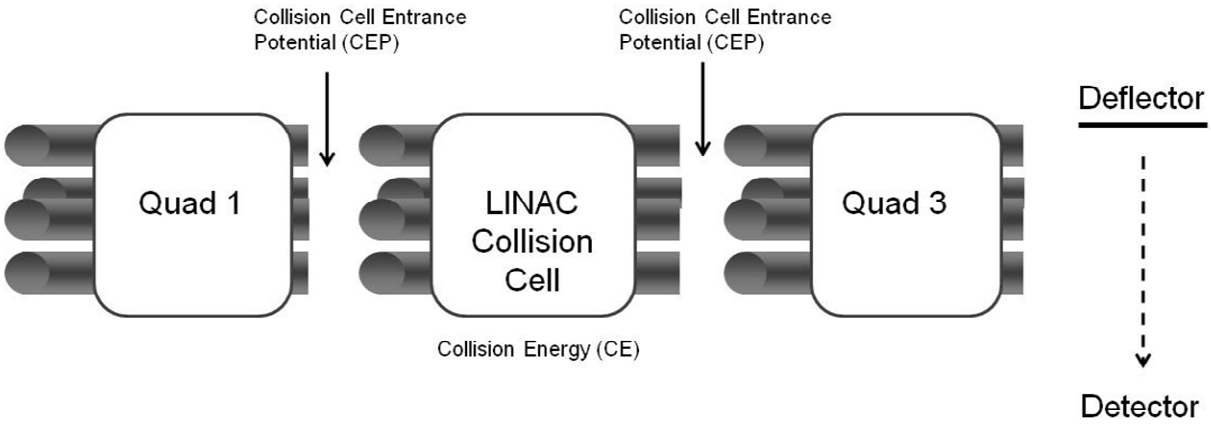

Figure 4.8 Diagram of the quadrupole "rail" on the API 2000. Figure modified from training materials at the API training course.

Three gases are optimized by flow injection analysis because they are dependent upon the mobile phase and flow rate employed: curtain gas (CUR), gas 1 and gas 2 (GS1 and GS2). The curtain gas flow prevents contaminants from entering the ion path by flowing in an outward direction from behind the curtain plate and in front of the orifice. The highest setting that does not compromise sensitivity should be utilized. Two additional gas parameters are optimized using FIA: gas 1 and gas 2. The GS1 parameter controls the nebulizer gas on the TurboIonSpray probe. It aids in the generation of small droplets and is crucial for maintaining stable flow at the probe. This parameter plays a significant role in sensitivity and is greatly influenced by the position of the probe in the source. The GS2 parameter controls the auxiliary gas and aids in the evaporation of spray droplets. This parameter works in conjunction with the temperature setting (TEM) to vaporize the LC solvent. Lastly the ion spray voltage controls the potential applied to the needle in the source. It is responsible for the ionization of the sample and also contributes to the stability of the spray and the sensitivity. The acceptable values for these parameters are summarized in Table 4.2.

4.3 Results and Discussion

4.3.1 Optimization of mass spectrometric parameters for Dyn A 1-17 (API 2000 system)

Prior to infusing compound, the ion spray must be adjusted so as to prevent spraying directly down the orifice of the instrument. This is crucial for protecting the instrument from contaminants that will ultimately diminish sensitivity. The spot size will depend on the flow rate and volatility of the mobile phase composition and should be aimed directly below the curtain

Compound-Dependent Parameters	Units	Range	Typical Optimized Ranges	Typical Value	Step Size
Declustering Potential (DP)	V	0 to 400	20 to 200	50	5 or 10 V
Entrance Potential (EP)	V	2 to 15		10	
Collision Cell Entrance Potential (CEP)	V	0 to 188	10 to 70	mass dependent	1 V
CAD Gas (CAD)	N/A	0 to 12		5	
Collision Energy (CE)	V	5 to 130		No typical value	5V
Collision Cell Exit Potential (CXP)	V	0 to 55	0 to 20	mass dependent	0.5 V
Source-Dependent Parameters	**Units**	**Range**	**Typical Optimized Ranges**	**Typical Value**	**Step Size**
Nebulizer Gas (GS1)	N/A	0 to 90	40 to 60		
Auxillary or Turbo Gas (GS2)	N/A	0 to 90	45 to 65		
Temperature of the Turbo Gas (TEM)	℃	0 to 750		600	25℃
Curtain Gas (CUR)	N/A	10 to 50		10	
IonSpray Voltage	V	4500 to 5500		5000	

Table 4.2 Tunable mass spec parameters for the API 2000.

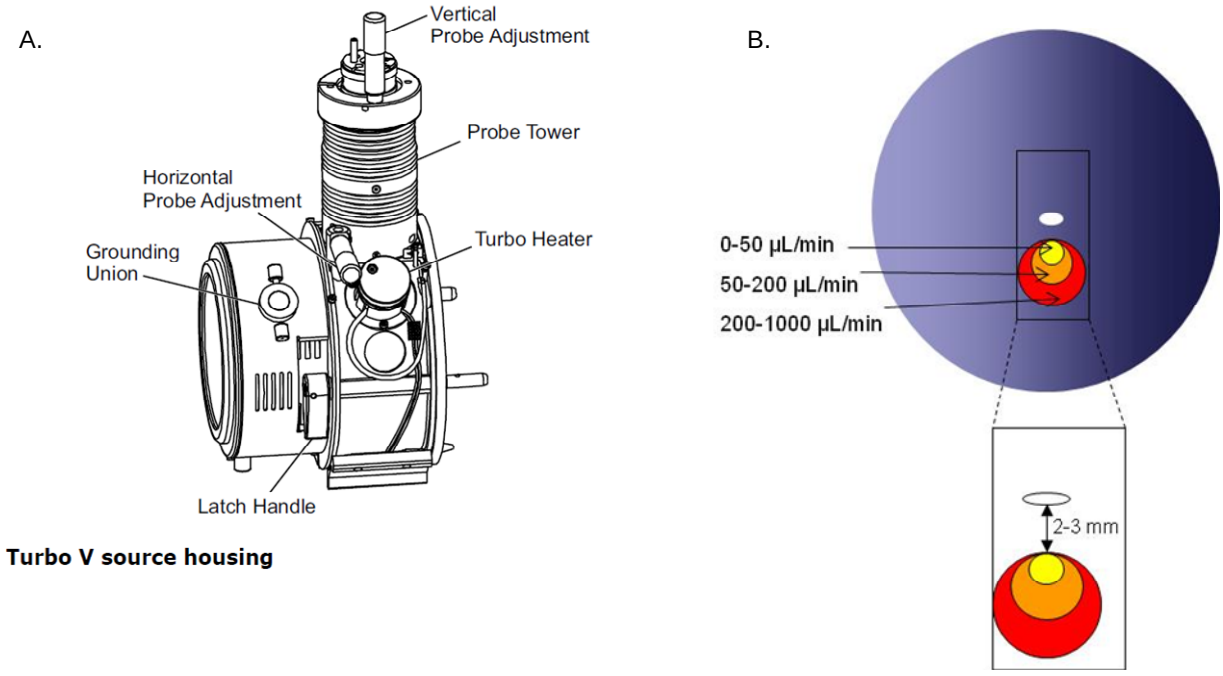

Figure 4.9 A. Diagram of the ion source housing on the API 2000 indicating the vertical and horizontal probe adjustments used to optimize the electrospray location on the curtain plate (from appliedbiosystems.com). B. Depiction of the electrospray location on the curtain plate. Figure modified from training materials at the API training course.

plate orifice as shown in Figure 4.9. Once this is achieved, compound tuning can commence. In these studies, one micromolar peptide standards were prepared from stock solutions in H_2O with 0.1% v/v formic acid and infused via the integrated syringe pump at a flow rate of 20 μL/min. A scan of the first quadrupole was performed over a user defined m/z range. In order to determine if the peptide concentration was sufficiently high for compound-dependent parameter optimization a stable total ion chromatogram (TIC) was obtained with an intensity of at least 1.0 e^6 and no higher than 1.0 e^8. Figure 4.10A shows the TIC for an infusion of Dyn A 1-17 and an internal standard (bradykinin). The corresponding spectrum (Figure 4.10 B) depicts the multiply charged ions present for each peptide. Dyn A 1-17 has a molecular weight of 2147.52 and both the 3+ and 4+ ions (716.5 and 537.6 respectively) were detected. For bradykinin (MW=1060.21) only the 2+ ion (530.8) was detected. In these studies, bradykinin was chosen as an internal standard because it has a high pI (12) similar to Dyn A 1-17 (pI 11.5) and was found to behave similarly during chromatographic separation. It was advantageous to use bradykinin over another dynorphin peptide due to their structural differences so that there was no possible appearance of bradykinin as a metabolite of Dyn A 1-17.

Next all compound-dependent parameters were optimized using the automated tune function within the Analyst software. In the case of Dyn A 1-17 where two precursor ions were observed, the 537.6 m/z was utilized because it was the most intense. Again 1 μM solutions of Dyn A 1-17 and bradykinin were infused together at a flow rate of 20 μL/min. During the infusion, each tunable parameter is ramped through a range of values and the setting that yields the highest ion intensity is saved in a tune method. These parameters include: declustering potential (DP), entrance potential (EP), collision cell entrance potential (CEP), collision cell exit potential (CXP), collision energy (CE), and collisionally activated dissociation gas (CAD).

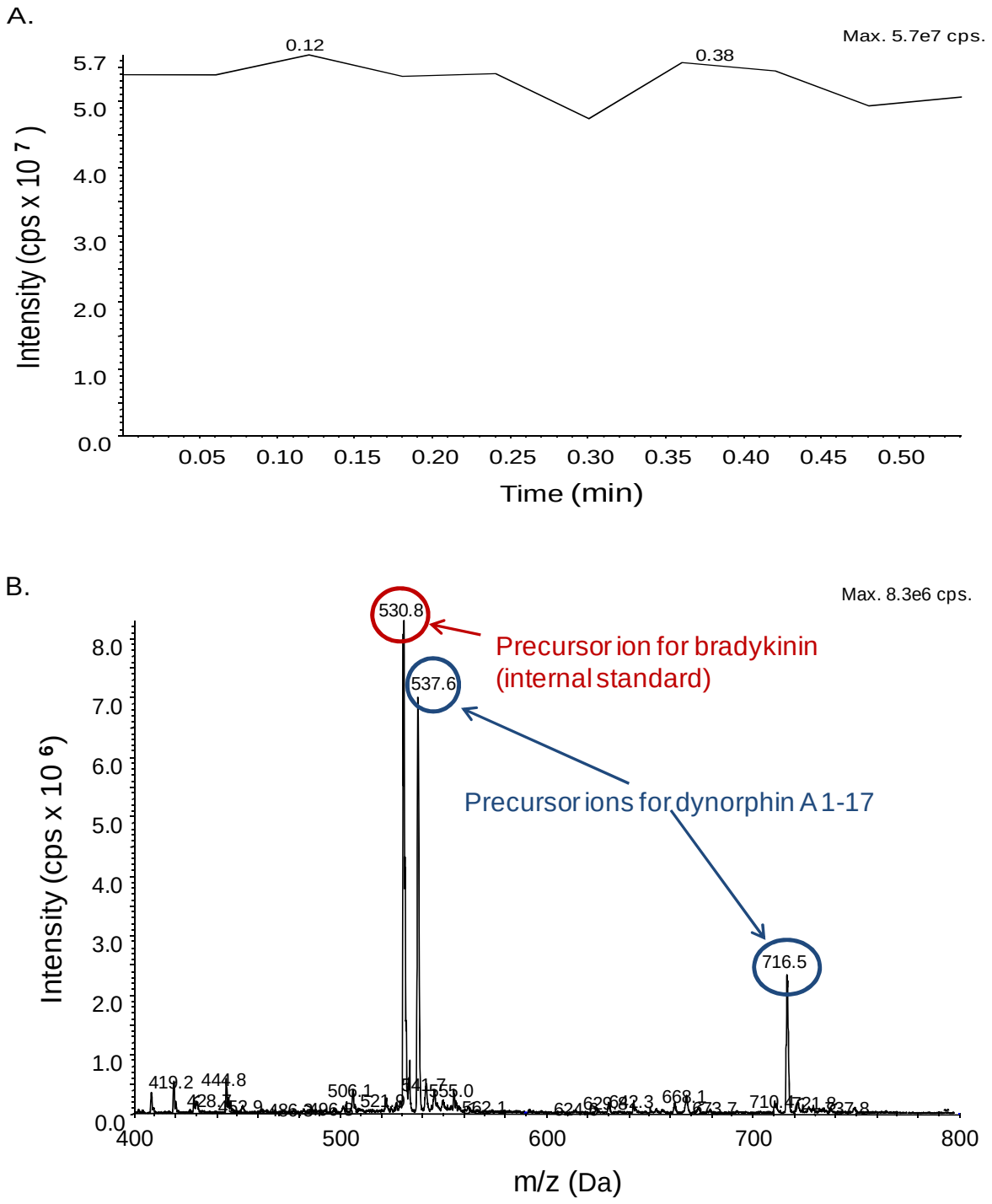

Figure 4.10 A. Total Ion Chromatogram (TIC) of a 1 ìM Dyn A 1-17 and bradykinin mixture in H_2O and 0.1% formic. MS Scan, infusion at 20 ìL/min. B. Mass spectrum of a 1 ìM Dyn A 1-17 and bradykinin mixture in H_2O + 0.1% formic. MS Scan, infusion at 20 ìL/min.

Each of these parameters was described in detail in Section 4.2.2.2, and Table 4.2 summarizes the acceptable values for these parameters. DP, EP, and CEP are optimized to generate the most intense precursor ions, whereas optimal CXP and CE values are determined for the four most intense product ions of each compound. Dyn A 1-17 produced several fragments including: m/z 91.2, 120.1, 130.1, and 136.0 with the 537.6 to 136.0 transition being the most intense (Figure 4.11). Bradykinin produced 98.1, 112.1, 120.1, and 157.1 with the 530.8 to 120.1 transition being the most intense transition (Figure 4.12).

Once the voltage optimization was complete and the most intense transition for each peptide is determined, further optimization is performed. The optimized voltage parameters are applied during all source parameter optimization. There are several source parameters optimized for each of these transitions and they include: curtain gas (CUR), gas 1 (GS1), gas 2 (GS2), temperature (TEM), and ion spray voltage (IS). These are all dependent on the LC conditions (mobile phase composition and flow rate) and for this reason optimization is carried out using flow injection analysis (FIA). A discrete amount (10 μL) of a 1 μM peptide solution is injected via the LC autosampler into the mobile phase stream, which consists of 50:50 v/v acetonitrile: water (ACN: H_2O) and is set at a flow rate of 200 μL/min. Source parameters are then optimized with one value applied during each injection. Typically three values for each parameter are investigated, and each FIA takes a total of 1 minute. With these parameters optimized, a new method is saved that combines all of the voltage and source parameters. The optimized voltage and source parameters for Dyn A 1-17 and bradykinin are summarized in Table 4.3. Next, the LC conditions are optimized and these conditions are added to the acquisition method within the Analyst program to create a fully functional MRM method.

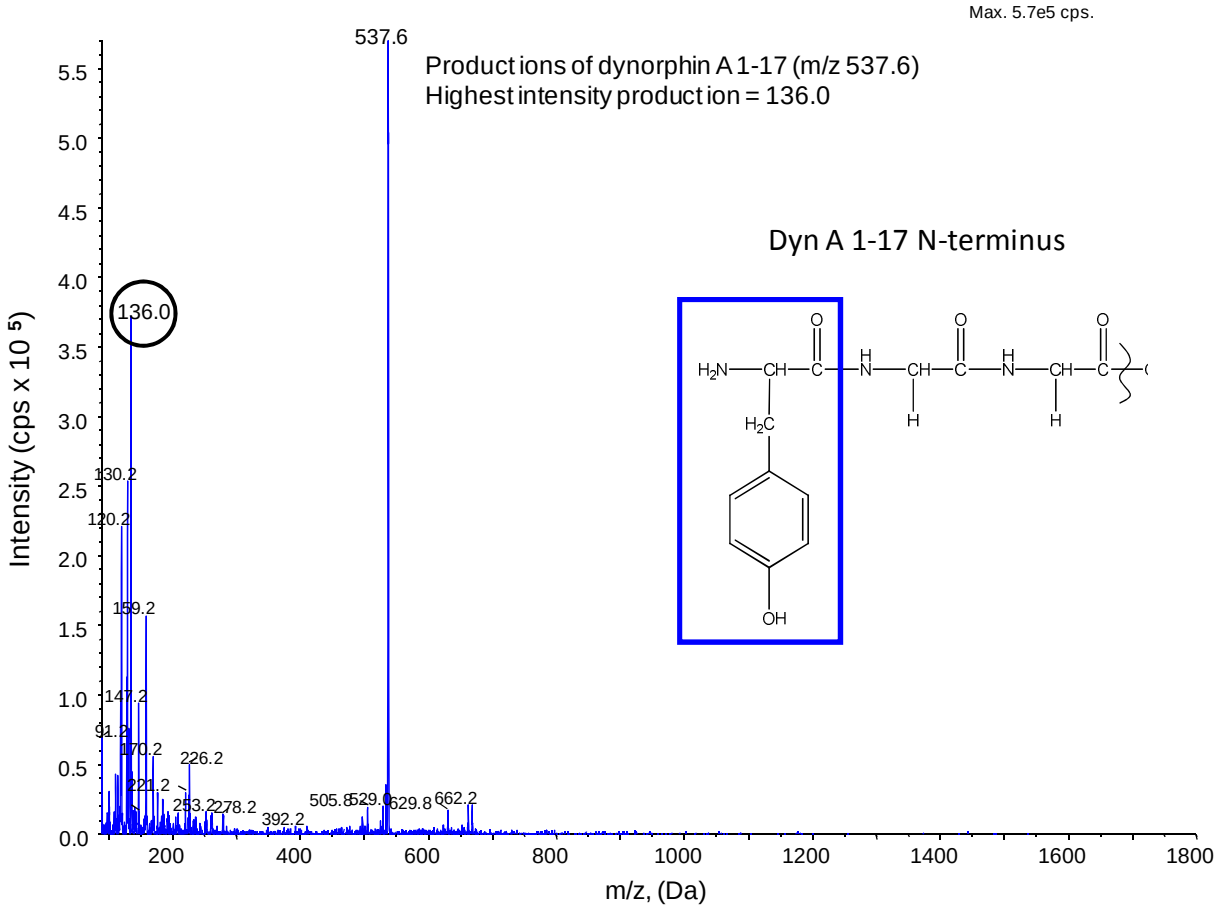

Figure 4.11 MS/MS of 1 ìM Dyn A in H_2O + 0.1% formic. Collision energy optimization during an infusion at 20 ìL/min. Inset structure is the N-terminus of Dyn A 1-17 and the boxed portion corresponds to the 136.0 product ion.

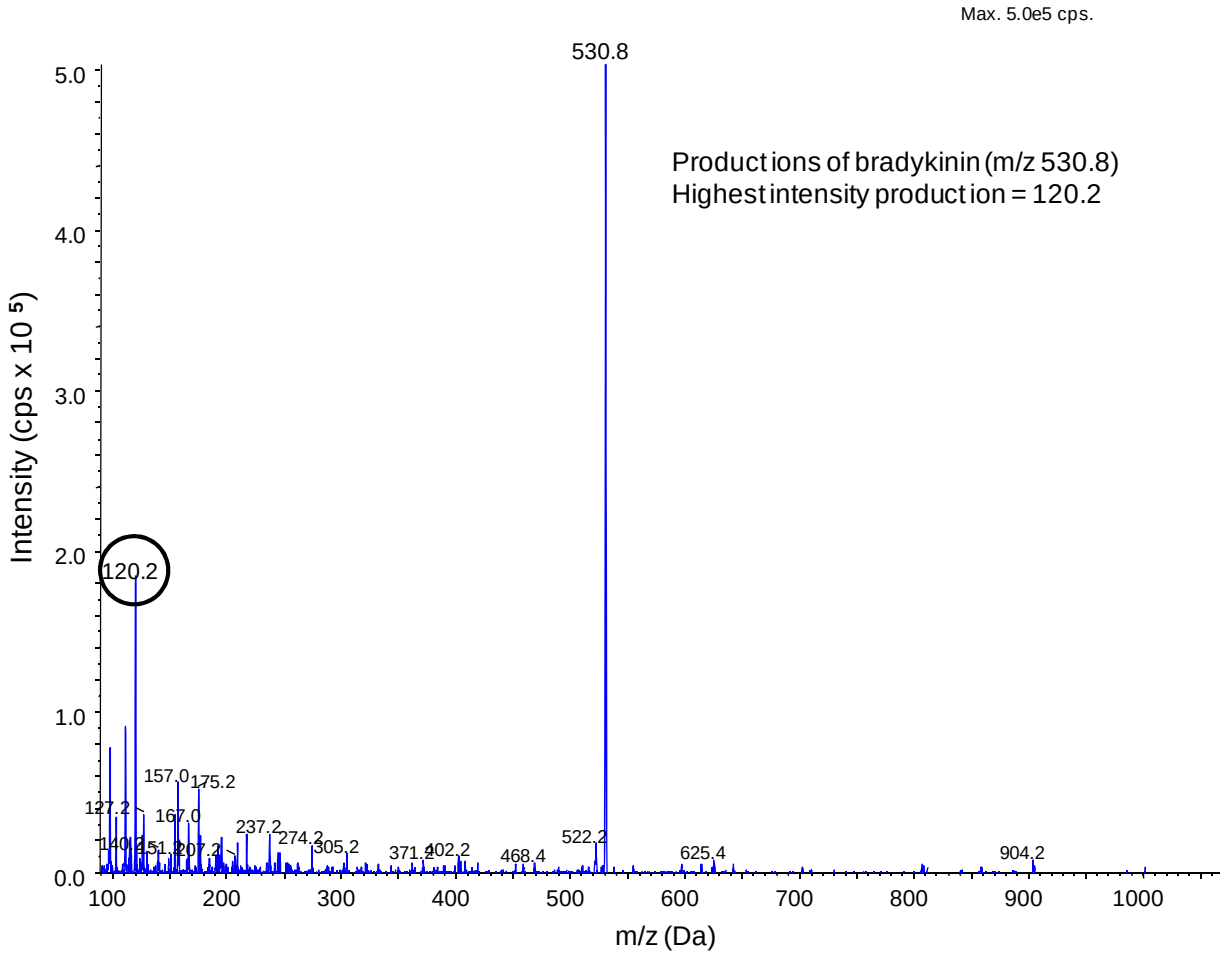

Figure 4.12 MS/MS of 1 ìM bradykinin in H_2O + 0.1% formic. Collision energy optimization during an infusion at 20 ìL/min.

Peptide	DP	FP	EP	CEP	CE	CXP	CUR	IS	GS1	GS2	CAD
BK	86	320	9.5	20	91	4	30	3000	40	50	4
Dyn A 1-17	71	270	9	28	43	6	30	5500	40	50	6

Table 4.3. Optimized mass spec parameters (API 2000) for Dyn A 1-17 and the internal standard bradykinin (BK).

4.3.2 Optimization of liquid chromatography conditions for Dyn A 1-17

Previous work in our group with substance P and dynorphin analogs [3, 4, 14] utilized a step gradient that ramped from 100% aqueous to 100% acetonitrile over the course of one minute. This method was therefore used as a starting point for developing a chromatographic system for Dyn A 1-17 and bradykinin (I.S.). A 1.0 x 50 mm C18 analytical column with 5 μm particles and the corresponding guard column were employed. The mobile phase conditions utilized were as follows: 100% mobile phase A from 0 to 5 minutes, a linear ramp to 100% mobile phase B from 5 to 6 minutes, hold at 100% B from 6 to 15 minutes, a linear return to 100% A from 15 to 16 minutes, and a column re-equilibration step, holding at 100% A from 16 to 22 minutes (curve shown in Figure 4.13 inset). Mobile phase A consisted of 95% H_2O, 5% ACN with 0.1% formic acid and mobile phase B consisted of 90% ACN, 10% H_2O with 0.1% formic acid.

Under these conditions, a late eluting peak (18.21 min) was observed (Figure 4.13). This peak shifted with respect to the mobile phase return to 95% aqueous conditions, always eluting approximately 2 minutes after this return was programmed (data not shown). Thus it was determined that Dyn A 1-17 is not soluble at this high organic content and precipitation of Dyn A 1-17 was occurring at the head of the column. When aqueous mobile phase conditions were restored the peptide was resolubilized resulting in a second peak. The method was adjusted so that the final composition of mobile phase B was only 30% ACN, 70% H_2O, 0.1% formic acid (gradient curve in Figure 4.14 insert). The second peak disappeared and Dyn A 1-17 eluted at 7.81 min in a similar fashion to the internal standard which eluted at 7.73 min (Figure 4.14).

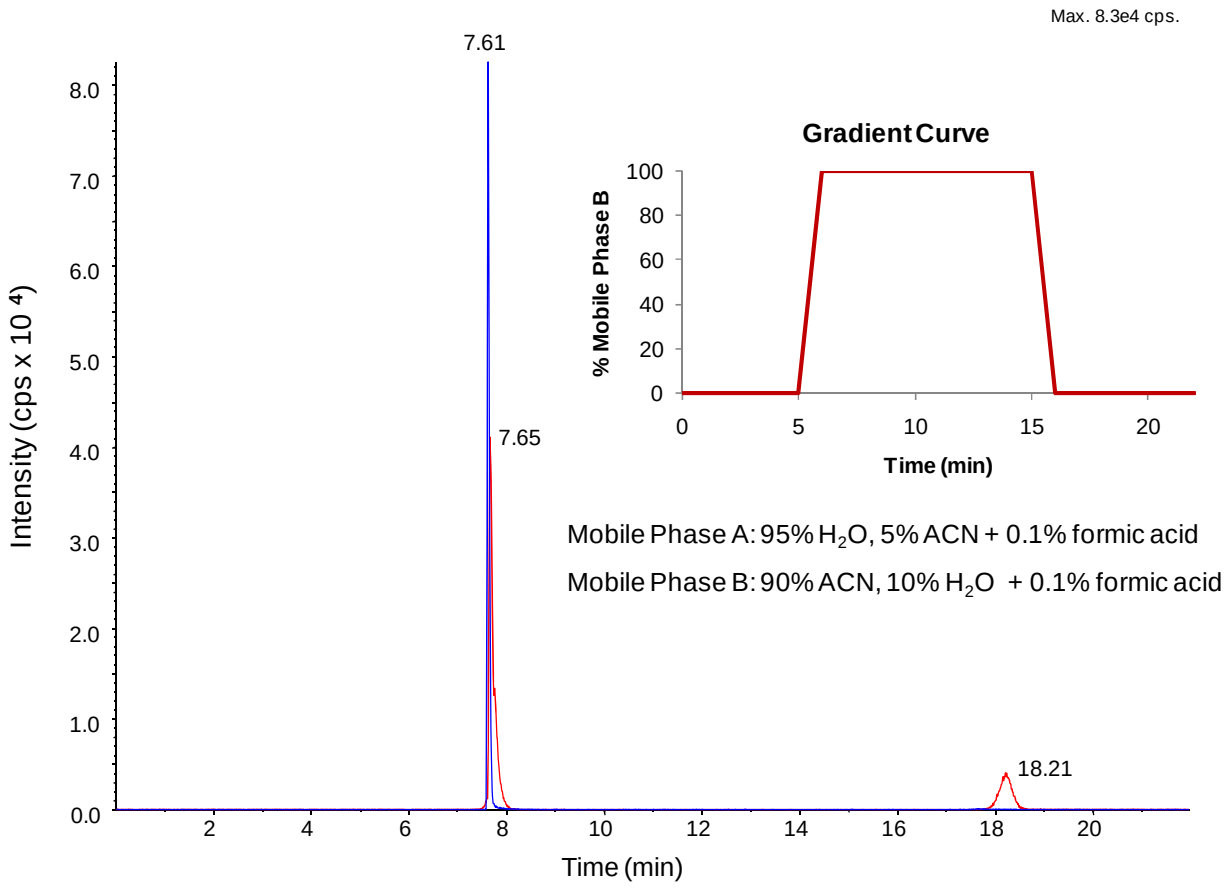

Figure 4.13 Extracted Ion Chromatograms (XIC) of 1 ìM bradykinin (blue trace) and 0.25 ìM Dyn A (red trace) in H_2O + 0.1% formic. Second peak observed only in Dyn A 1-17 trace. LC gradient curve shown: mobile phase A is 95% H_2O, 5% ACN with 0.1% formic acid. Mobile phase B is 90% ACN, 10% H_2O with 0.1% formic acid.

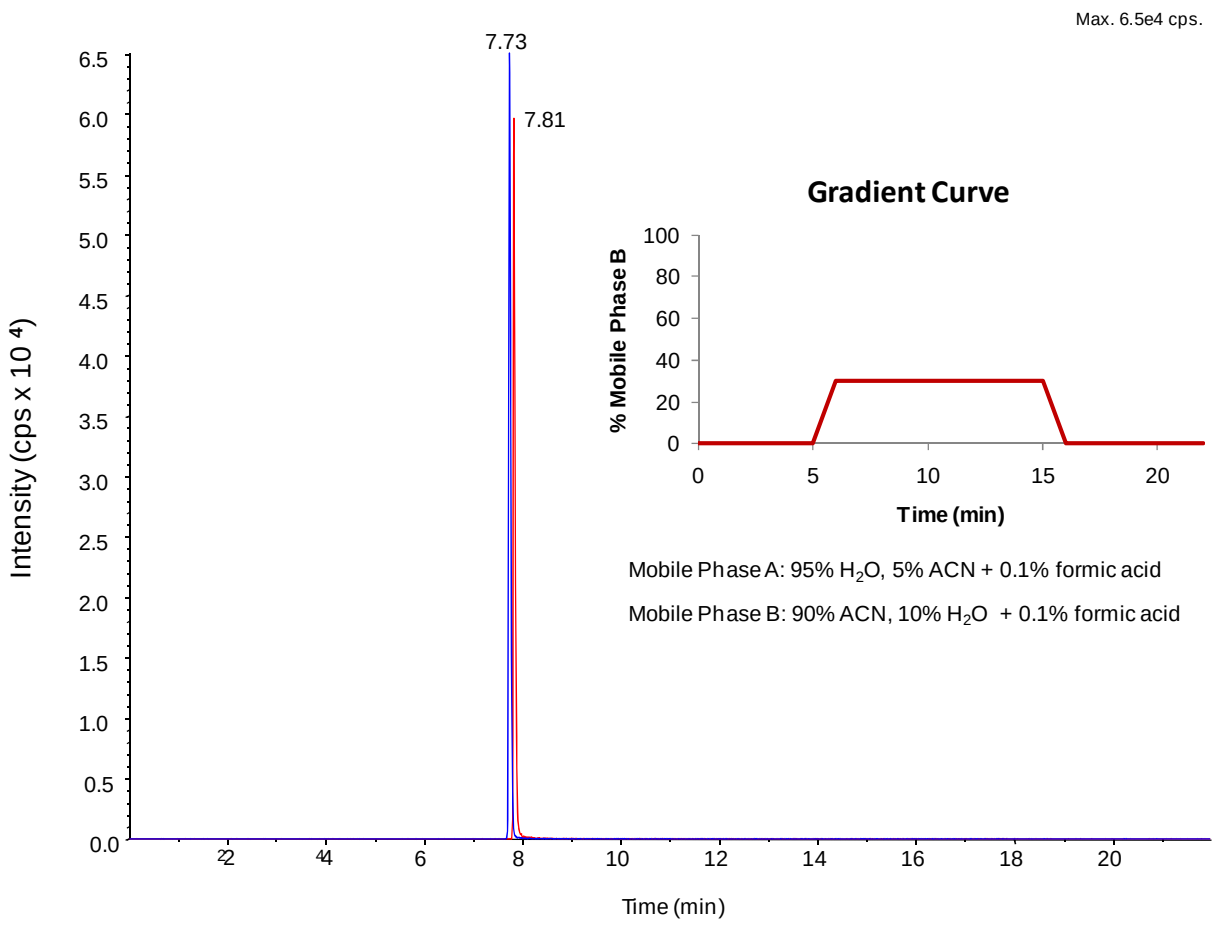

Figure 4.14 Extracted Ion Chromatograms (XIC) of 1 ìM bradykinin (blue trace) and 0.25 ìM Dyn A (red trace) in H_2O + 0.1% formic. LC gradient curve shown: Mobile phase A is 95% H_2O, 5% ACN with 0.1% formic acid. Mobile phase B is 90% ACN, 10% H_2O with 0.1% formic acid.

Using this LC method, a calibration plot for Dyn A 1-17 standards in H_2O with 0.1% formic acid was generated. A linear response was obtained between 0.025 and 1 μM with an R^2 value of 0.9984 as can be seen in Figure 4.15. The ultimate goal of this project, however is to develop an LC-MS/MS method for quantitation of Dyn A 1-17 transport and metabolism with an *in vitro* BBB mimic. Such studies require the use of high salt solutions to maintain cell viability and tight junction integrity for the duration of the studies (typically 2-4 hours). Therefore, it was necessary to characterize the LC-MS/MS when sampling Dyn A 1-17 from these types of matrices.

4.3.3 Characterization of Dyn A 1-17 ionization in cell compatible matrices

In order to maintain healthy cells during transport and metabolism studies, experiments must be carried out under appropriate conditions. Transport media must maintain isotonicity, tight junction integrity, and physiological pH (7.4), as well as provide an energy source (typically glucose) for studies lasting longer than one hour [15, 16]. Sampling from high salt content matrices present several analytical challenges for LC-MS. First, high salt solutions are incompatible with electrospray ionization as significant damage to the ESI probe can occur. Additionally, high salt samples tend to contaminate the front end and eventually the quadrupoles of mass spectrometers, if precautions in sample preparation and method development are not taken.

The first line of defense against such damage to expensive mass spectrometry equipment is the use of a diverter valve. This allows the LC flow to be directed to waste at the beginning of a run in order to de-salt such samples, since salts will elute with the void volume of the column. Prior to the retention time of the analytes, the LC flow is directed back to the mass spectrometer

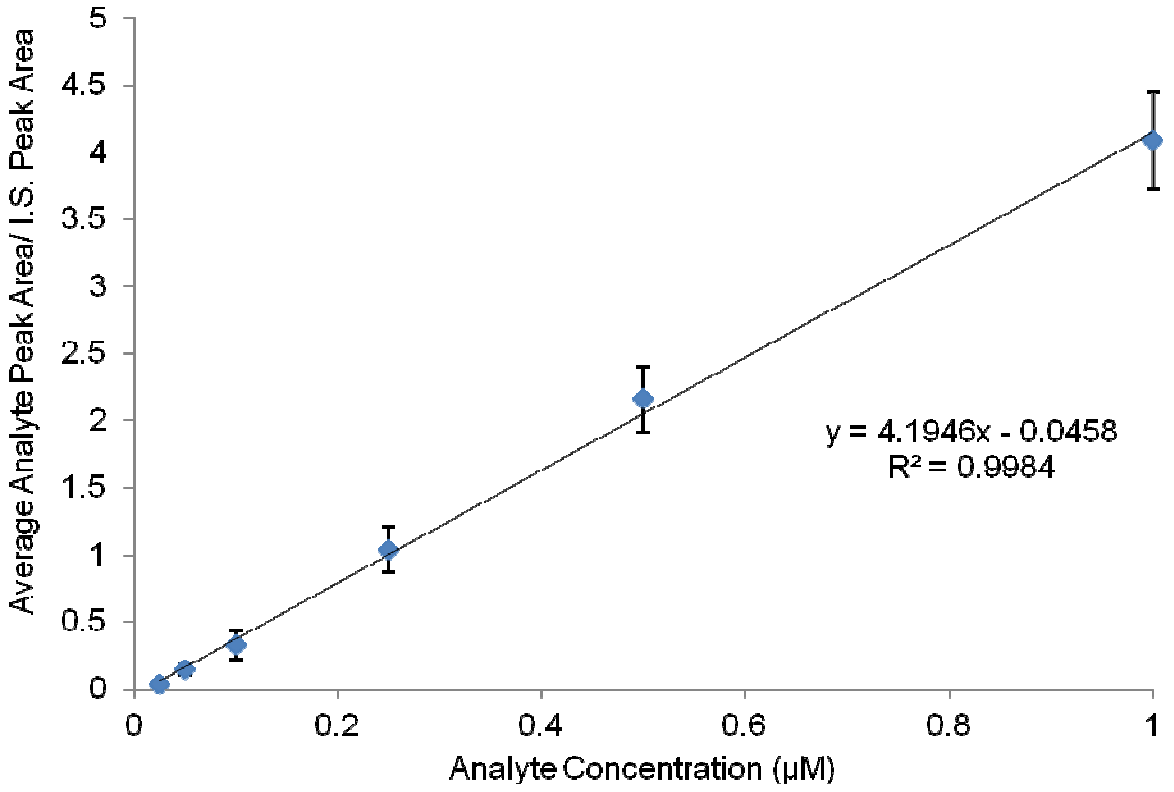

Figure 4.15 Calibration plot of Dyn A 1-17 standards in H_2O with 0.1% formic (n=3 at each concentration). Linear response from 0.025 – 1 ìM.

for analysis. The flow is then diverted back to waste following the elution of all compounds of interest so as to prevent any lipid-based cellular components from entering the mass spec and contaminating the source. The retention time of Dyn A 1-17 and the internal standard was such that diversion for the first five minutes of the LC run was feasible. At 5 minutes, the LC flow was routed to the mass spectrometer and then flow was diverted back to waste again at 12 minutes.

A second line of defense is to dilute samples in mobile phase to decrease the salt concentration. In these experiments, standards of Dyn A 1-17 were prepared in phosphate buffered saline with ascorbic acid (PBSA) and cell experimental media. Aliquots (60 μL) were removed and diluted with 48 μL H_2O with 0.1% formic and 12 μL of internal standard (10 μM stock). Therefore the resulting concentration of Dyn A 1-17 was always half that of the original standard, and this value could be used for the creation of a calibration plot.

Previous work concerning the transport and metabolism of Substance P and Dyn A 1-11 amide analogs by BBMEC used media composed of a 50:50 mixture of Minimum Essential Media (MEM) and Ham's F12 with 10 mM HEPES [3-4, 14]. However, for Dyn A 1-17, significant ion suppression was observed in the presence of this cell compatible solution, and considerable run to run variation was observed, as demonstrated by the overlay of chromatograms in Figure 4.16. Samples of lower concentration (25-100 nM) were analyzed and only peaks for the internal standard were observed (data not shown).

In order to identify the component responsible for this ion suppression and obviate the problem, PBSA alone was investigated. This is also commonly employed for cell transport studies and consists of phosphate buffered saline supplemented with $MgSO_4$, $CaCl_2$, ascorbic

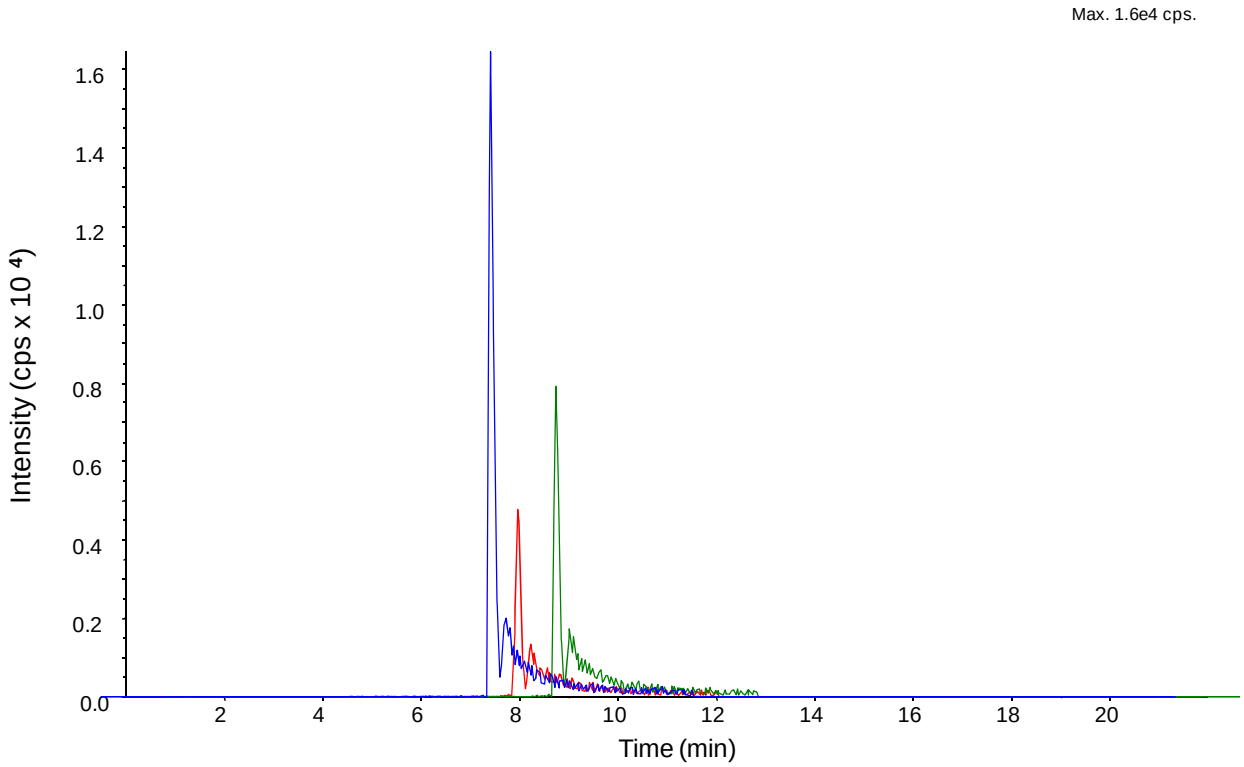

Trace Color	Run Number	Retention Time (t_R)
Blue	1	7.93
Red	2	7.96
Green	3	7.95

Figure 4.16 XIC for 500 nM Dyn A 1-17 (n=3) in experimental cell media. Chromatograms are shifted so that peaks can be more easily viewed. Actual retention times are listed above.

acid, and glucose. Although the peak intensity did not vary as drastically from run to run in the presence of PBSA as compared to the experimental cell media, the peak area was still diminished in comparison to standards in H_2O with formic acid and Dyn concentrations of less than 500 nM were not detected.

Overlays of the triplicate injections of Dyn A 1-17 in PBSA are shown in Figure 4.17. As can be seen in Figure 4.18, the peak area of the internal standard was not significantly affected by the presence of these solutions, suggesting that a structural component of dynorphin was responsible for this observed signal suppression. The formation of strong phosphate and sulfate adducts with positively charged side chains of peptides has been reported previously [17]. Chait and co-workers observed the formation of strong ionic complexes in the presence of phosphate and sulfate at low concentrations (approximately 0.050 mM) relative to the quantities included in PBSA and cell experimental media used in these studies (~10 mM).

In an attempt to improve the ionization efficiency of Dyn A 1-17, the phosphate concentration was decreased by a factor of 10. To maintain isotonicity the concentrations of NaCl and KCl were increased, and to aid in buffering of the system, 10 mM HEPES was included. To prevent sulfate adduct formation, magnesium chloride was substituted for the magnesium sulfate typically included in PBSA. Magnesium and calcium are essential components included in the cell media to maintain tight junction integrity. Glucose, ascorbic acid, and calcium chloride concentrations were not altered. This new cell culture media will be referred to as modified phosphate buffered saline (mPBSA) in this dissertation. Upon modification of the PBSA media, improvements were seen in peak area as well as run to run reproducibility. Overlays of triplicate injections of Dyn A 1-17 in mPBSA are shown in Figure 4.19. Also important to note, Dyn A 1-17 was stable in modified PBSA over the course of 5

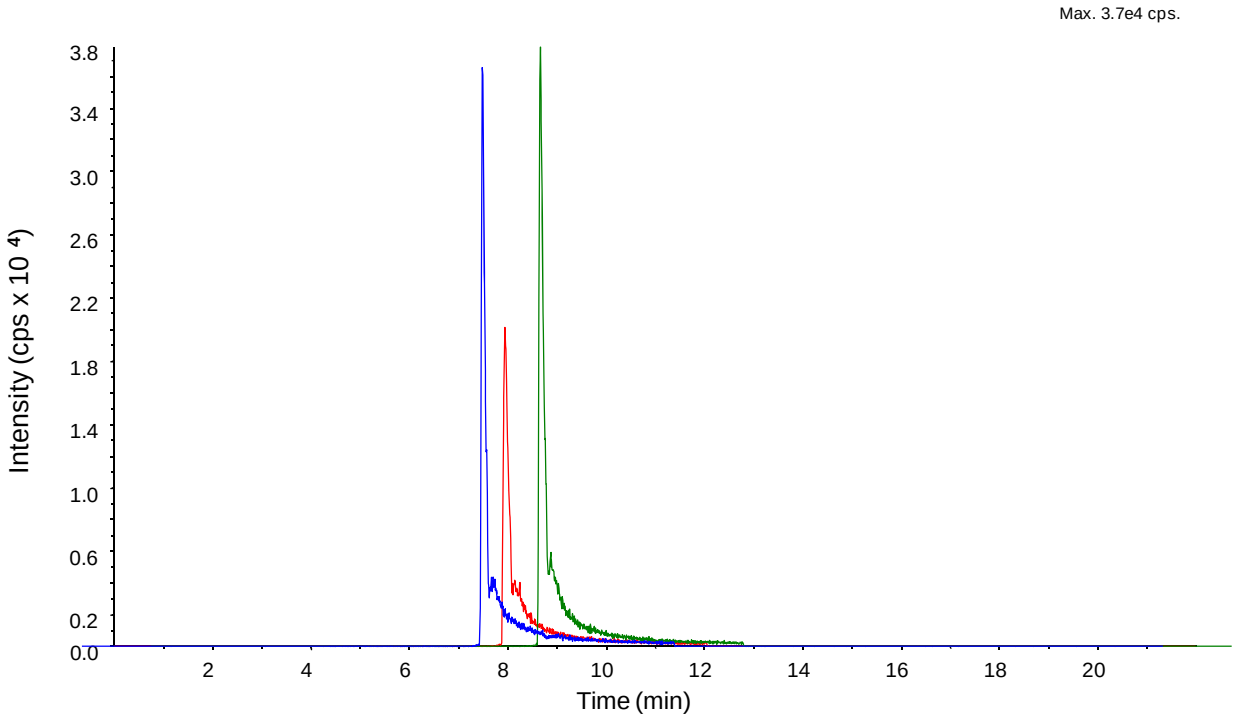

Trace Color	Run Number	Retention Time (t_R)
Blue	1	8.14
Red	2	7.94
Green	3	7.92

Figure 4.17 XIC for 500 nM Dyn A 1-17 in PBSA (n=3). Chromatograms are shifted so that peaks can be more easily viewed. Actual retention times are listed above.

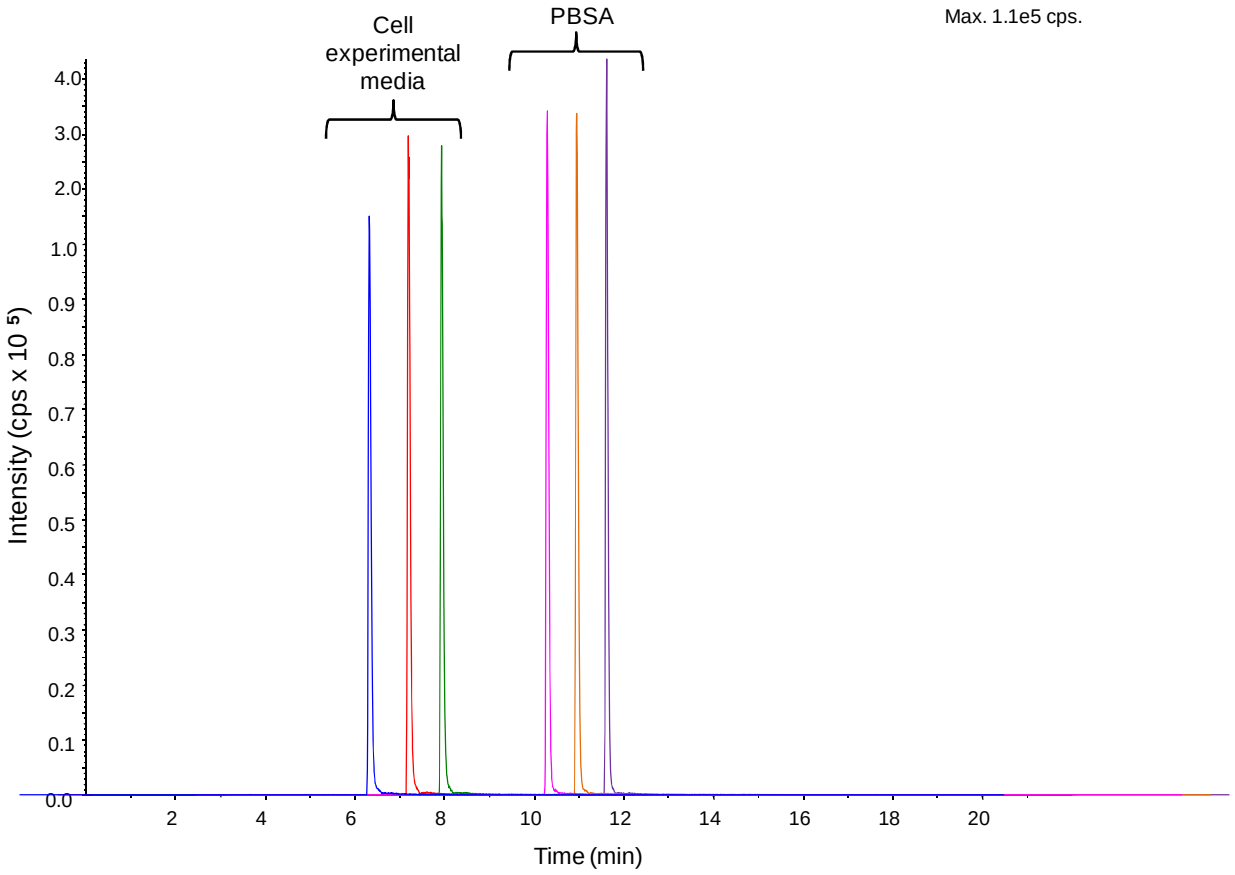

Trace Color	Run Number	Retention Time (t_R)
Blue	1	7.81
Red	2	7.82
Green	3	7.82
Pink	1	8.07
Orange	2	7.82
Purple	3	7.82

Figure 4.18 XIC for the internal standard bradykinin (1 ìM) in cell experimental media and PBSA. Chromatograms are shifted so that peaks can be more easily viewed. Actual retention times are listed above.

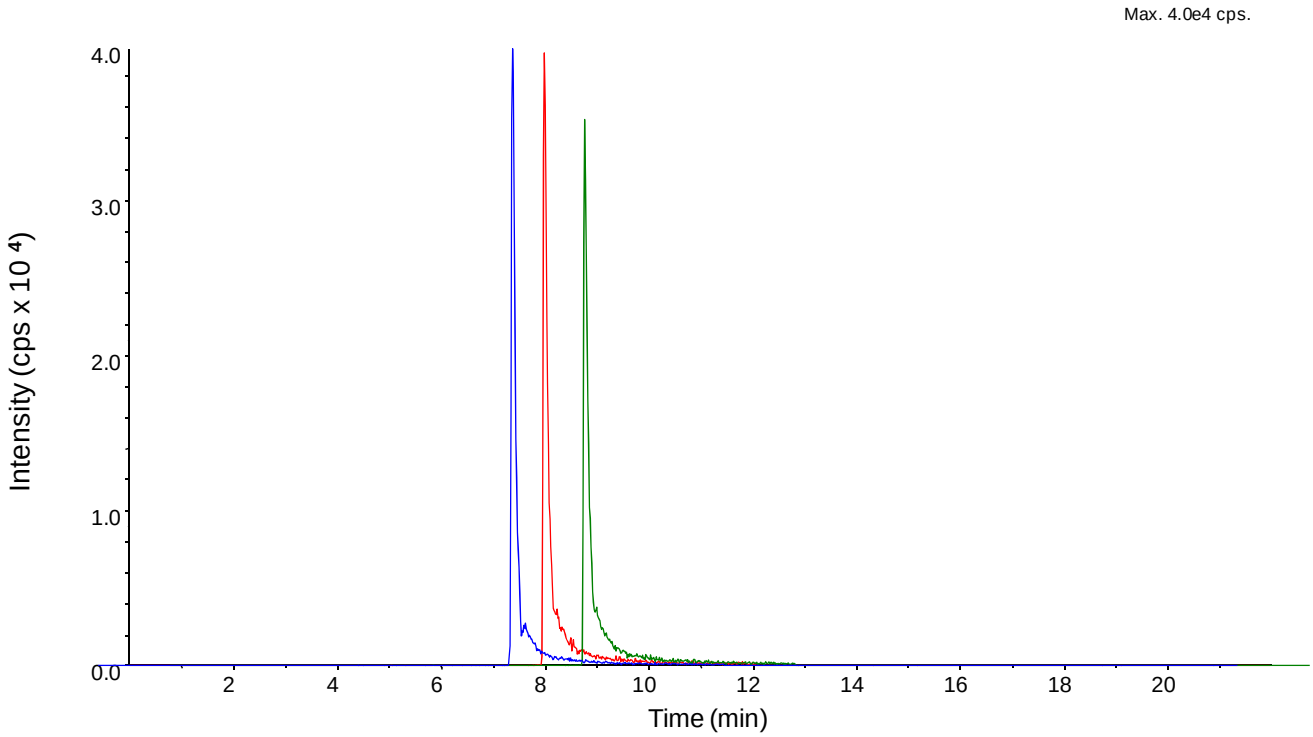

Trace Color	Run Number	Retention Time (t_R)
Blue	1	7.99
Red	2	7.99
Green	3	7.99

Figure 4.19. XIC for 500 nM Dyn A 1-17 in modified PBSA. Chromatograms are shifted so that peaks can be more easily viewed. Actual retention times are listed above.

hours at both room temperature and at 37°C. A comparison of matrix effects on peak area for Dyn A 1-17 and bradykinin in various cell compatible medias can be seen in Figure 4.20.

4.3.4 Optimization of LC-MS/MS parameters for dynorphin metabolites

Once an appropriate media was identified for cell transport and metabolism studies, the tuning procedure outlined in Section 4.2.2.2 was repeated for a mixture of dynorphin metabolites utilizing bradykinin as an internal standard. Briefly the compounds were infused and all source parameters were optimized using the automated tune function within the Analyst software. Next flow injection analysis was performed to optimize the LC flow-dependent parameters. Three of the metabolites of interest retain the N-terminal sequence of Dyn A 1-17 and therefore had similar fragmentation patterns, with the 136 product ion again being the most intense. The des-tyrosine metabolite Dyn A 2-17 produced a unique fragmentation spectrum however, and the 120 product ion was found to be the most predominant. The optimized mass spectrometry parameters for each of the dynorphin metabolites are summarized in Table 4.4, and the precursor and product ions for all analytes of interest are in Table 4.5.

In addition to tuning each compound to determine optimal ionization and CID parameters, LC gradient optimization was also performed. It was found that in order to chromatographically separate Dyn A 1-17 from its metabolites, increasingly shallow gradients (decreased %B/min) must be utilized. This however had a negative impact on peak shape (Figure 4.21). In particular the peak for Dyn A 1-6 was found to be extremely broad under all gradient conditions. It also exhibited a very irreproducible retention time. By decreasing the organic content at the beginning of the gradient, retention of Dyn A 1-6 was achieved and the peak shape and retention time for this peptide were improved as can be seen in Figure 4.22.

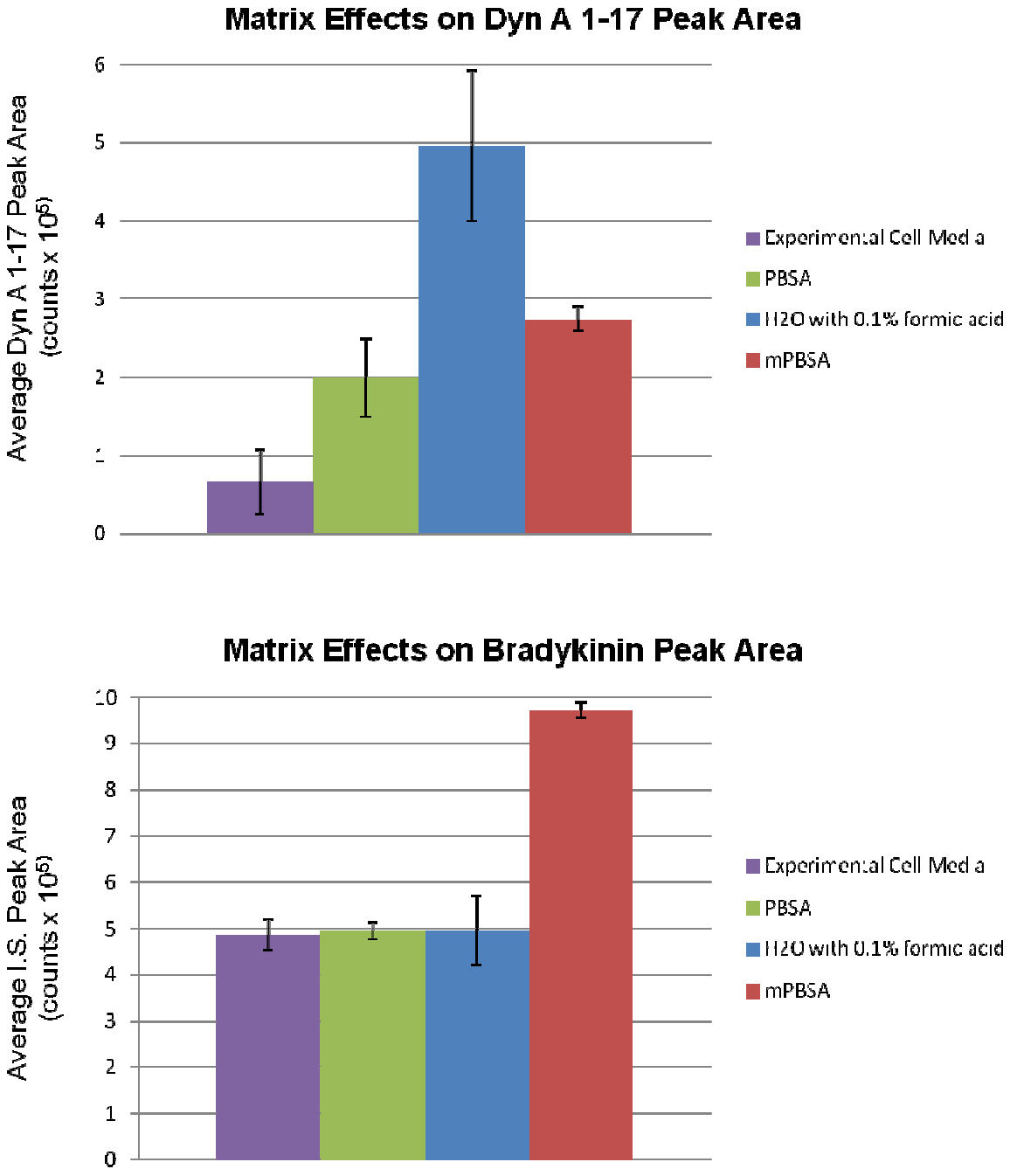

Figure 4.20. Peak area comparison for 500 nM Dyn A 1-17 (top) and 1 ìM bradykinin (bottom) in H_2O with formic acid, experimental cell media, PBSA, and mPBSA. Average peak areas are reported for each, n=3.

Peptide	DP	FP	EP	CEP	CE	CXP	CUR	IS	GS1	GS2	CAD
Dyn A 2-17	71	180	8.5	20	77	6	30	5500	40	50	6
Dyn A 1-13	51	370	12	10	27	4	40	3000	40	50	6
Dyn A 1-8	71	60	10.5	18	45	6	30	3000	40	50	6
Dyn A 1-6	41	330	8.5	36	23	6	30	5500	50	50	6

Table 4.4. Optimized mass spec parameters (API 2000) for the dynorphin metabolites.

Peptide	Molecular Weight	Precursor Ion (m/z)	Charge State	Product Ion (m/z)
BK	1060.22	530.8	2+	120.1
Dyn A 2-17	1984.34	496.96	4+	120.1
Dyn A 1-17	2147.52	537.63	4+	136.2
Dyn A 1-13	1603.98	401.85	4+	136.1
Dyn A 1-8	981.2	491.34	2+	136.1
Dyn A 1-6	711.82	356.72	2+	136.1

Table 4.5. Summary of dynorphin ionization (precursor ions, charge state and product ions) following optimization of API 2000 parameters.

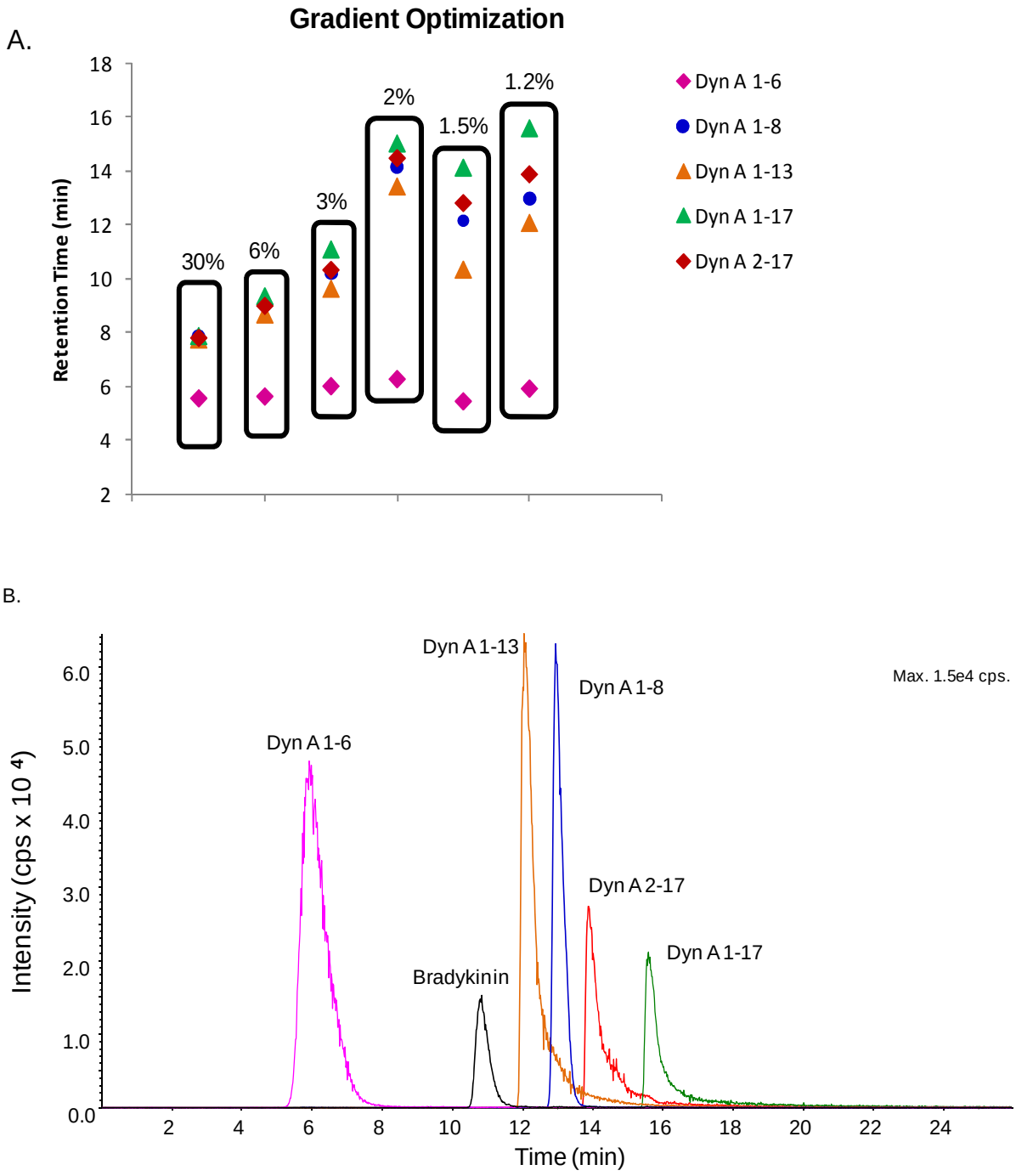

Figure 4.21. A. Effect of gradient steepness on peptide retention time (values indicate %B/min). B. Overlay of extracted ion chromatograms for dynorphin peptides under shallow gradient conditions of 1.2 %B/min.

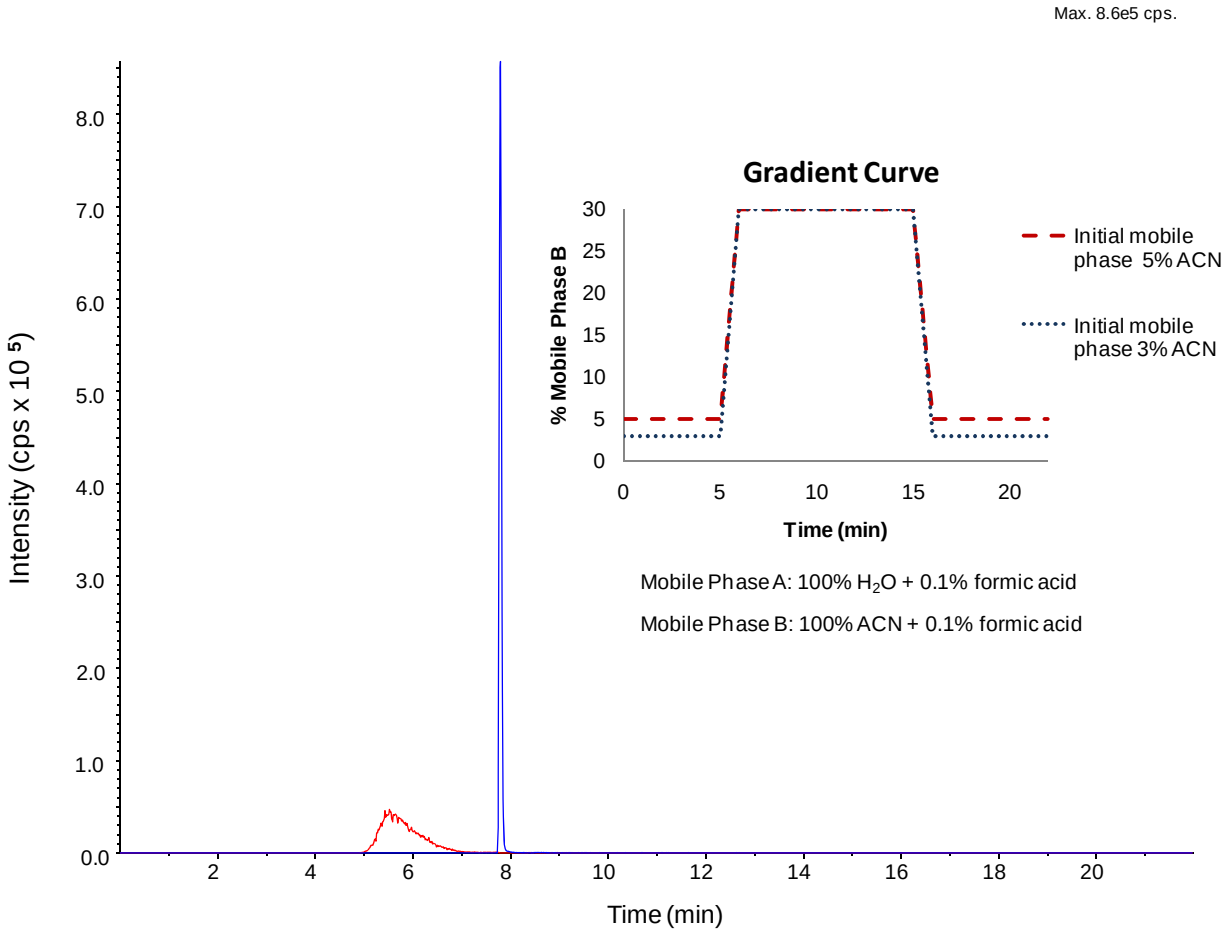

Figure 4.22. Effect of starting mobile phase composition on Dyn A 1-6 peak shape and retention time. Starting conditions of 5% acetonitrile (red trace) and 3% acetonitrile (blue trace).

Superior peak shapes were observed for all the peptides at the steeper step "gradient". Ion suppression due to the co-elution of dynorphin peptides was not observed utilizing the short step gradient. This method increased through-put by maintaining shorter run times and relied primarily on the mass spectrometer to separate each compound based on its specific transitions as can be seen in the extracted ion chromatograms in Figure 4.23. Additionally, there was no cross-talk observed from one run to the next indicating that the ions were adequately cleared from the quadrupole from run to run.

Final optimized LC conditions consisted of the following: initial conditions of 97% A, 3% B from 0 to 5 minutes, a linear ramp from 3 to 30% B from 5 to 6 minutes, holding at 30% B from 6 to 15 minutes, a linear return to initial conditions from 15 to 16 minutes, and column equilibration from 15 to 22 minutes holding at 3% B, where mobile phase A consisted of 100% H_2O with 0.1% formic acid and mobile phase B consisted of 100% ACN with 0.1% formic acid (Figure 2.24). Calibration plots for each metabolite were constructed using this optimized method, and the results are summarized in Table 4.6. The smaller metabolites exhibited better sensitivity and lower limits of detection, supporting the hypothesis that more basic residues in the peptide chain contribute to ion suppression due to phosphate adduct formation.

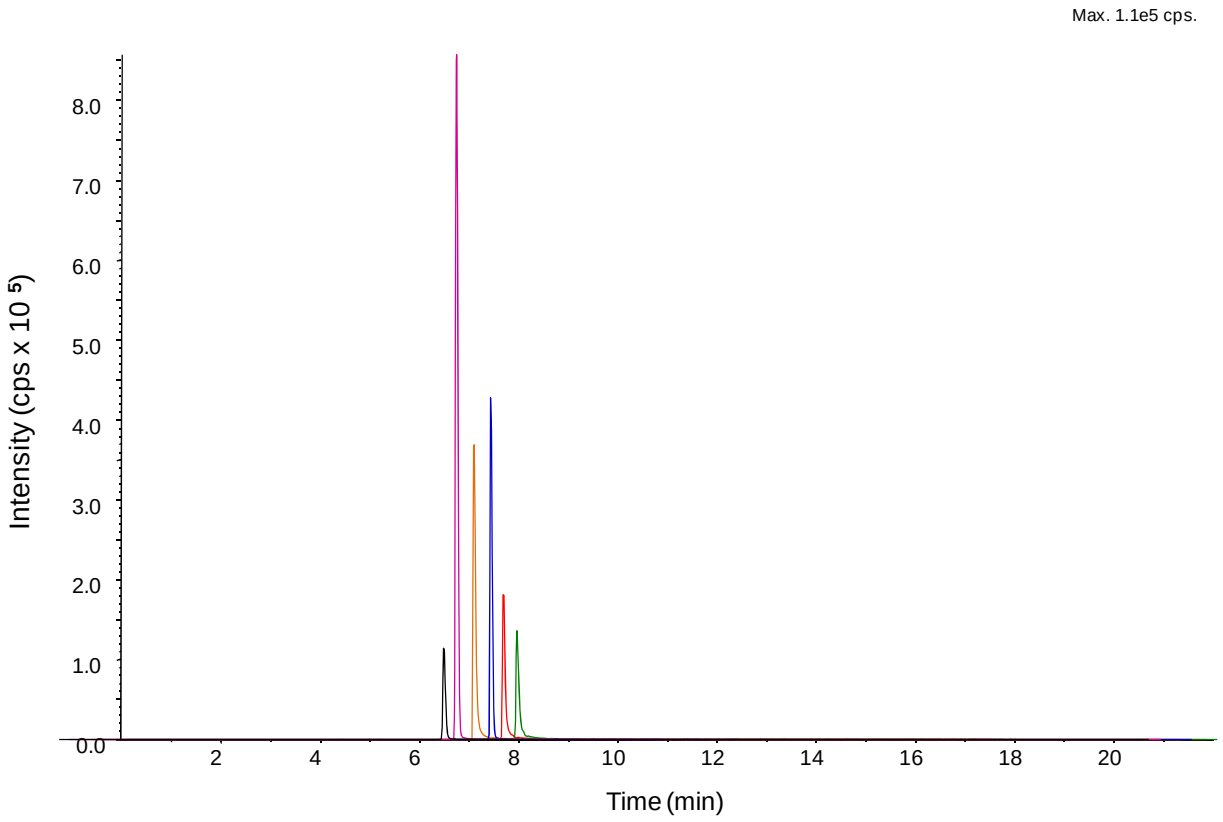

Peptide	Trace Color	Retention Time (t_R)
Dyn A 1-6	Pink	7.79
Dyn A 1-8	Blue	7.84
Dyn A 1-13	Orange	7.71
Dyn A 1-17	Red	7.84
Dyn A 2-17	Green	7.79
Bradykinin	Black	7.75

Figure 4.23 Extracted ion chromatograms for each dynorphin metabolite and the internal standard bradykinin with optimized mass spec and LC parameters. Chromatograms are shifted so that peaks may be more easily viewed. Actual retention times are listed above.

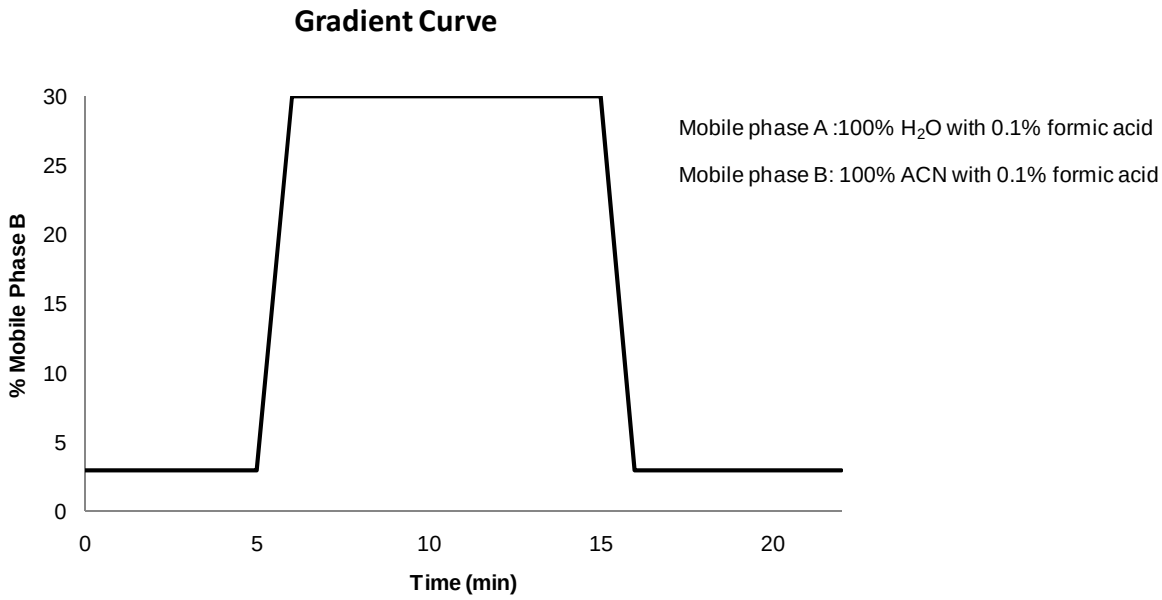

Figure 4.24 Final optimized gradient conditions. Initial conditions of 97% A, 3% B from 0 to 5 minutes, a linear ramp from 3 to 30% B from 5 to 6 minutes, holding at 30% B from 6 to 15 minutes, a linear return to initial conditions from 15 to 16 minutes, and column equilibration from 15 to 22 minutes holding at 3% B.

Peptide	Linear Range in mPBSA (μM)	R^2	LOD	LLOQ
Dyn A 1-6	0.001- 5	0.9994	0.2 nM	0.6 nM
Dyn A 1-8	0.001- 5	0.9968	0.1 nM	0.3 nM
Dyn A 1-13	0.1-5	0.9963	32 nM	108 nM
Dyn A 2-17	0.5-5	0.9831	30 nM	102 nM
Dyn A 1-17	0.1-5	0.9844	45 nM	116 nM
	in H_2O + 0.1% formic			
Dyn A 1-17	0.025-1	0.9984	1 nM	4 nM

Table 4.6. Linearity, limit of detection (LOD, S/N =3), and lower limit of quantitation (LLOQ, S/N = 10) for Dyn A 1-17 and metabolites (n=3 at each concentration, 6 point calibration plots).

4.4 Summary

This chapter described the method development necessary for LC-MS/MS determination of Dyn A 1-17 and several of its key metabolites. Ionization and LC conditions were optimized for each of the peptides in a cell compatible media to enable investigations of dynorphin metabolism and transport at the blood brain barrier and further investigations of metabolism in the CNS. Modifications of the typically employed PBSA were necessary to improve ionization conditions for the highly basic dynorphin peptides. Specifically dilution of the phosphate and sulfate concentrations was necessary to prevent adduct formation. Chapter 4 will discuss in detail the application of this method to *in vitro* studies of metabolism and transport.

4.5 References

[1] John, H., Walden, M., Schafer, S., *Analytical Bioanalytical Chemsitry* 2004, 378, 883-897.

[2] van den Broek, I., Sparidans, R. W., Schellens, J. H. M., Beijnen, J. H., *Journal of Chromatography B* 2008, 872, 1-22.

[3] Chappa, A. K., Cooper, J. D., Audus, K. L., Lunte, S. M., *Journal of Pharmaceutical and Biomedical Analysis* 2007, 43, 1409-1415.

[4] Chappa, A. K., Audus, K. L., Lunte, S. M., *Pharmaceutical Research* 2006, 23, 1201-1208.

[5] Lanckmans, K., Sarre, S., Smolders, I., Michotte, Y., *Talanta* 2008, 74, 458-469.

[6] Wu, Q., Liu, C., Smith, R. D., *Rapid Communications in Mass Spectrometry* 1996, 10, 835-838.

[7] Wei, H., Wen, J., Rui, X., Houwen, L., Fan, G., Wu, Y., *Analytical Bioanalytical Chemsitry* 2009, 395, 1461-1469.

[8] Murao, N., Ishigai, M., Yasuno, H., Shimonaka, Y., Aso, Y., *Rapid Communications in Mass Spectrometry* 2007, 21, 4033-4038.

[9] Siskos, A., Katsila, T., Balafas, E., Kostomitsopoulos, N., Tamvakopoulos, C., *Journal of Proteome Research* 2009, 8, 3487-3496.

[10] Chou, J. Z., Chait, B. T., Wang, R., Kreek, M. J., *Peptides* 1996, 17, 983-990.

[11] Chou, J. Z., Kreek, M. J., Chait, B. T., *American Society for Mass Spectrometry* 1994, 5, 10-16.

[12] Reed, B., Zhang, Y., Chait, B. T., Kreek, M. J., *Journal of Neurochemistry* 2003, 86, 815-823.

[13] Yu, J., Butelman, E. R., Woods, J. H., Chait, B. T., Kreek, M. J., *The Journal of Pharmacology and Experimental Therapeutics* 1996, 279, 507-514.

[14] Chappa, A. K., *Pharmacedutical Chemistry*, The University of Kansas, Lawrence 2007.

[15] Audus, K. L., Borchardt, R. T., *Pharmaceutical Research* 1986, 3, 81-87.

[16] Gumbleton, M., Audus, K. L., *Journal of Pharmaceutical Sciences* 2001, 90, 1681-1698.

[17] Chowdhury, S. K., Katta, V., Beavis, R. C., Chait, B. T., *American Society for Mass Spectrometry* 1990, 1, 382-388.

Chapter Five:

Investigation of the metabolism of Dyn A 1-17 and the blood brain barrier transport of its key metabolite, Dyn A 1-6

5.1 Introduction

5.1.1 The blood brain barrier

The blood brain barrier (BBB) consists of a network of endothelial cells connected by intracellular tight junctions that are responsible for maintaining brain homeostasis (Figure 5.1) [1-3]. It serves not only as a physical barrier, but also as a metabolic one, due to its expression of various metabolic enzymes [4-9]. The barrier possesses a number of features including efflux transporters [10-12], decreased pinocytosis, minimal fenestration, and high electrical resistance effectively protecting the brain from external substances [13, 14]. In addition to protecting the central nervous system from xenobiotics, the barrier is integrated with nutrient transporters to maintain proper levels of essential compounds such as amino acids [15]. The characterization of the behavior of endogenous substances at the blood brain barrier is important when investigating their potential role as biomarkers for neurodegenerative diseases. In particular the metabolism and transport of neuropeptides at the blood brain barrier will provide insight into their role in central nervous system (CNS) disorders.

5.1.2 Dynorphin and the blood brain barrier

Upregulation of dynorphin has been implicated in a variety of neurological disorders including Alzheimer's [16], Parkinson's disease [17], neuropathic pain [18], stress and depression [19]. This opioid peptide has been show to exhibit preferential binding to the kappa-opioid receptor and at elevated concentrations has been shown to be neurotoxic. Most reports investigating the pharmacology of dynorphin employ immuno-based techniques for quantitation. These methods have notoriously low limits of detection, essential for studying endogenous levels of neuropeptides; however, cross-reactivity with related peptides and metabolites can

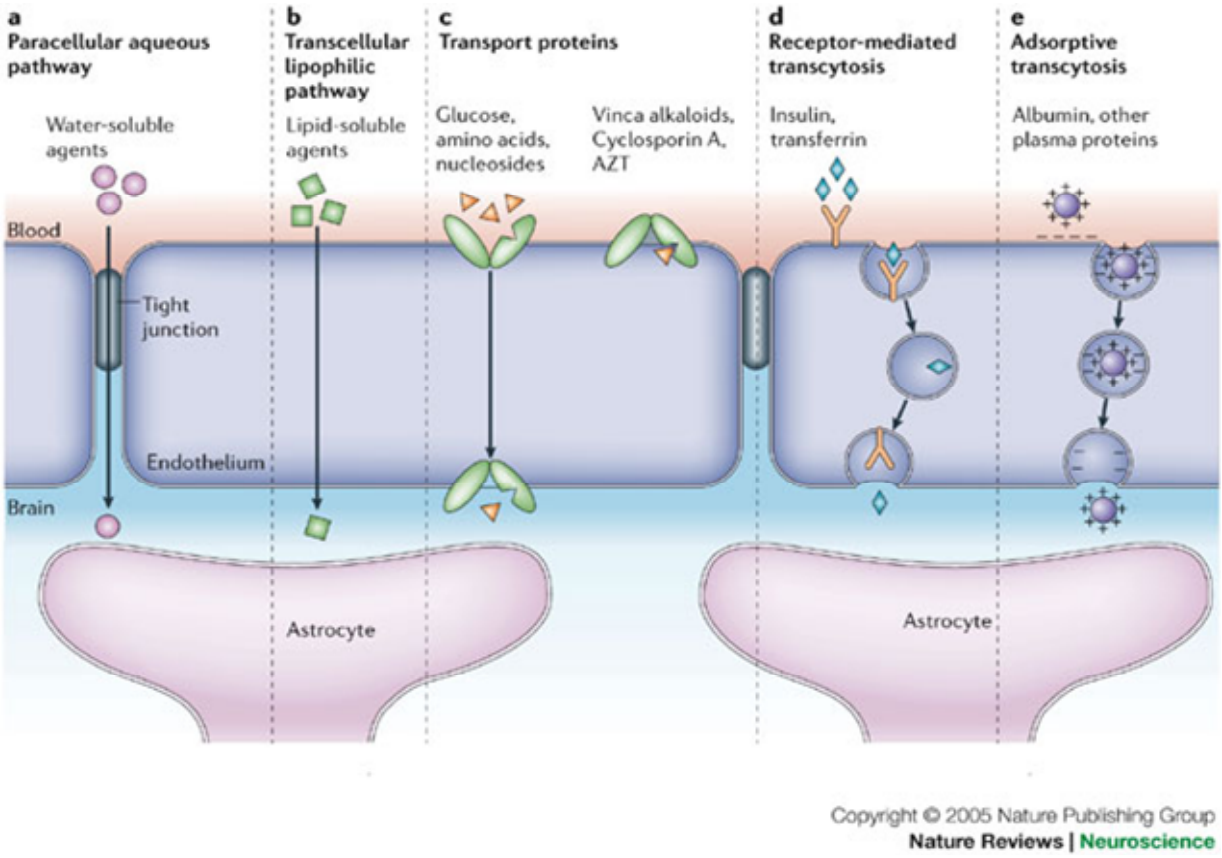

Figure 5.1 Schematic of the BBB with depictions of possible transport mechanism indicated by a-e. Used with permission from [3].

significantly compromise their accuracy [20]. Reported elevated levels of dynorphin may in fact be due to detection of a metabolite. Therefore it is essential to gain a clear understanding of the differing roles of the parent peptide and metabolites, since it is possible a metabolite may in fact be responsible for the reported neurotoxic effects. Of particular interest in this work is the potential for dynorphin metabolites to display unique transport properties and therefore physiological effects at the blood brain barrier. This chapter will therefore describe the investigation of the metabolism of Dyn A 1-17 in tissues of the central nervous system and by cells that create an *in vitro* model of the blood brain barrier. The transport of the major metabolite (Dyn A 1-6) at the blood brain barrier is also investigated.

5.1.3 Methods for studying the blood brain barrier

A variety of *in vivo* and *in vitro* methods exist for studying a peptide's behavior at the blood brain barrier. *In vivo* methods include microdialysis sampling and brain perfusion studies. Continuous monitoring is possible utilizing microdialysis sampling, and experiments can be performed on anesthetized or awake, freely-moving animals.

Microdialysis is also useful for examining site specific metabolism of peptides [17, 21-23]. Peptides of interest can be included in the perfusate and delivered directly to the brain in order to study *in vivo* metabolism. Additionally, if the peptides of interest are delivered peripherally, the transport across the blood brain barrier can be characterized by sampling via the microdialysis probe [24]. The effect of peripherally administered compounds on the permeability or metabolism of the peptide of interest as well as on the release of neurotransmitters can also be investigated. For example, peripheral administration of various

metabolic inhibitors can be used to further characterize a peptide's metabolism at the BBB. A major concern that must be addressed when using microdialysis to measure peptide transport into the brain is the generally low recovery of these compounds across the probe membrane [25]. In addition, quantitation from such samples is difficult due to low sample volumes.

In situ rat brain perfusion directly delivers compounds of interest to the brain via the carotid artery [26]. Compounds (often radiolabelled) are delivered directly to the brain at constant concentration, and the rate of infusion can be manipulated. The perfusions are stopped at various times and brain uptake is typically determined by scintillation counting when radiolabeled compounds are used. If metabolism is a concern or interest, chromatographic separations are usually employed. From these data points, uptake kinetics can then be determined. This method avoids metabolism by liver enzymes as well as peripherally circulating enzymes.

In vitro cell culture models of the BBB simplify the biological aspects of the blood brain barrier considerably by enabling the investigation of a compound's behavior at the brain endothelium as opposed to whole brain [14]. An i*n vitro* cell culture model of the BBB was developed by Audus and Borchardt using primary cultures isolated from the grey matter of bovine brains (Figure 5.2) [13]. A variety of enzymes have been identified at the BBMEC monolayer, including angiotensin converting enzyme, and various peptidases and hydrolases, which have been shown previously to cause peptide metabolism [4, 5, 27]. These cells exhibit many of the physical characteristics typical of the BBB including tight junctions, decreased pinocytosis, and minimal fenestration. Efflux transporters, as well as specific uptake transport systems, are also expressed by this cell line. These cells have been extensively characterized, making this a useful model for investigating BBB transport.

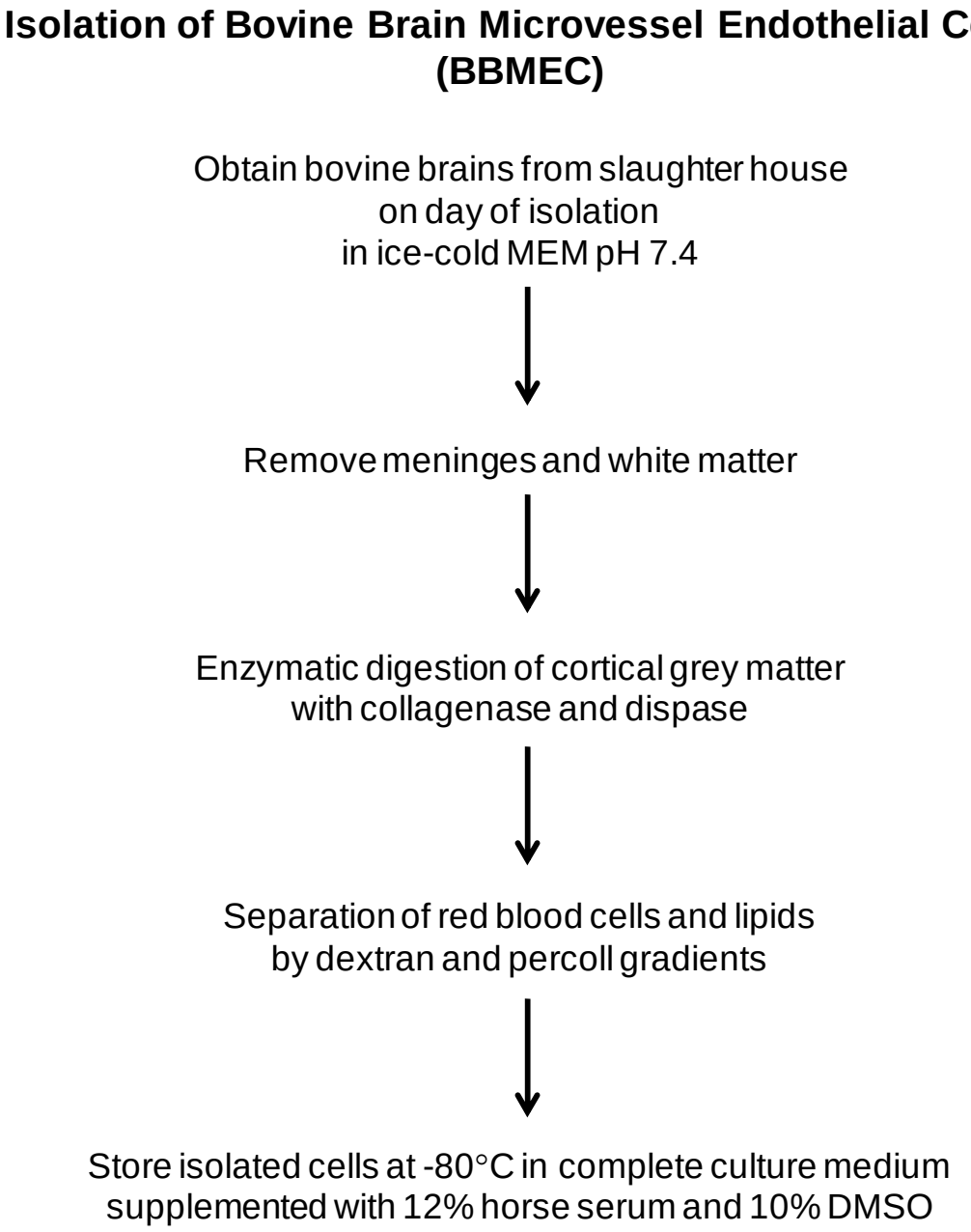

Figure 5.2 Summary of the BBMEC isolation procedure.

The isolated endothelial cells are grown on polycarbonate membranes and mounted in Side-by-Side™ diffusion chambers to perform permeability screening (Figure 5.3). An advantage of this *in vitro* method for investigating BBB permeability is the ability of the experimentalist to manipulate a variety of variables including temperature and compound concentration. Experiments performed at 4°C exhibit the effect of reduced ATP activity on transport, indicating when active processes are involved in compound permeation. Bi-directional permeability can also be investigated by spiking either the apical (blood side) or basolateral (brain side) chambers and monitoring transport in either direction. Additionally, peptide metabolism can be characterized by growing BBMECs in 12-well culture plates and incubating the cells with the peptide in cell media (Figure 5.4).

Recent work with *in vitro* models of the BBB has focused on the development of immortalized brain endothelial cell lines [28]. This decreases the time necessary to reach confluency (7 versus 14 days) as well the workload on the laboratory scientist. The isolation procedures for primary cells are very time and labor intensive as is evident by the method described in this chapter. Additionally, the role of other cell types on the behavior of the brain endothelium, specifically on the formation of tight junctions, is of interest. This has driven the development of co-culture systems. Specifically the role of astrocytes on tight junction formation has been investigated using co-cultures with Transwell® systems and endothelial cells grown in astrocyte-stimulated media [14, 29-31].

This chapter utilized the BBMEC primary cell culture model to investigate the metabolism of Dyn A 1-17. The experimental set-up is shown in Figure 5.3. The BBB transport of the major metabolite, Dyn A 1-6, was then examined using Side-By-Side™ diffusion chambers. The *in vitro* model simplifies the BBB investigations (in comparison to *in vivo*

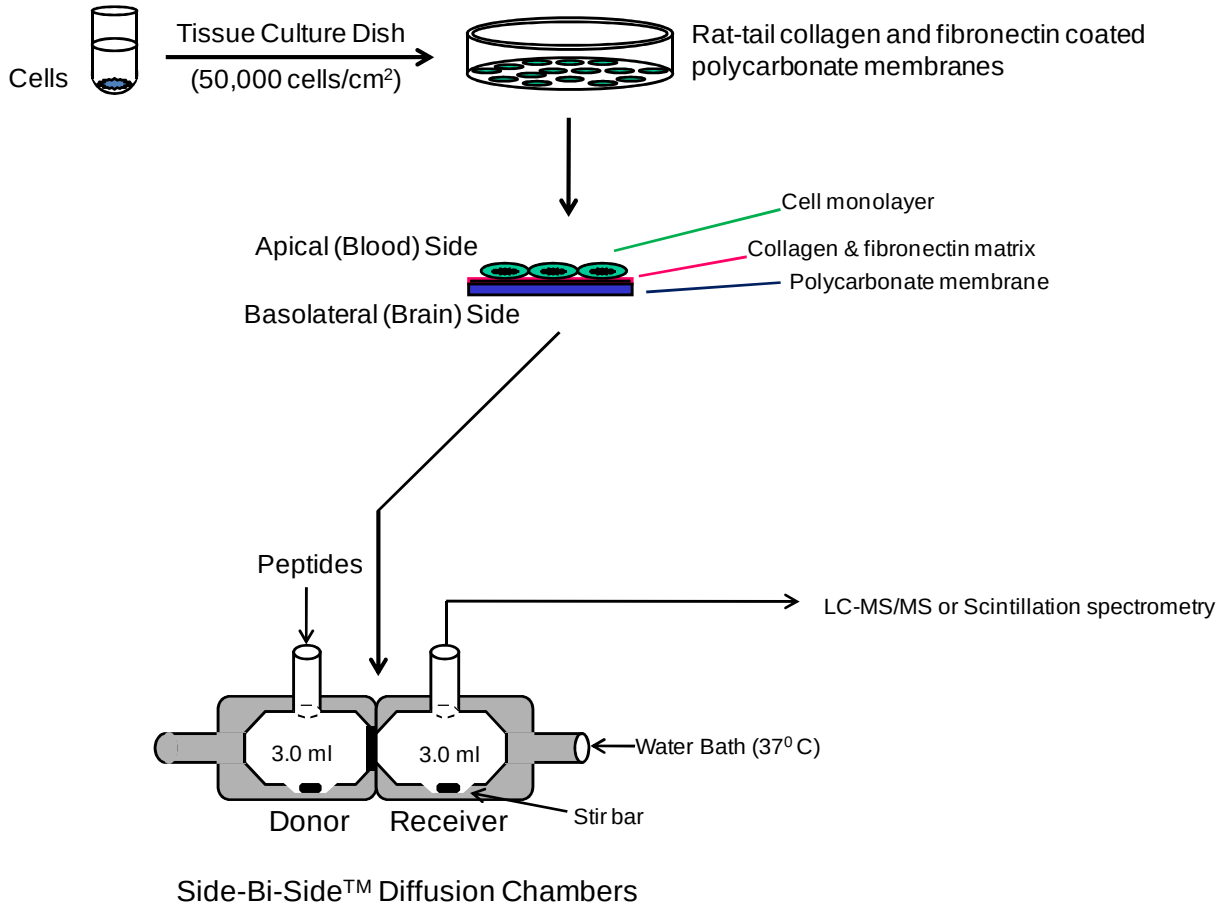

Figure 5.3 Experimental set-up for BBMEC permeability study with Side-By-Side™ diffusion chambers. Donor and receiver indicate the typical apical to basolateral experiment at 37°C.

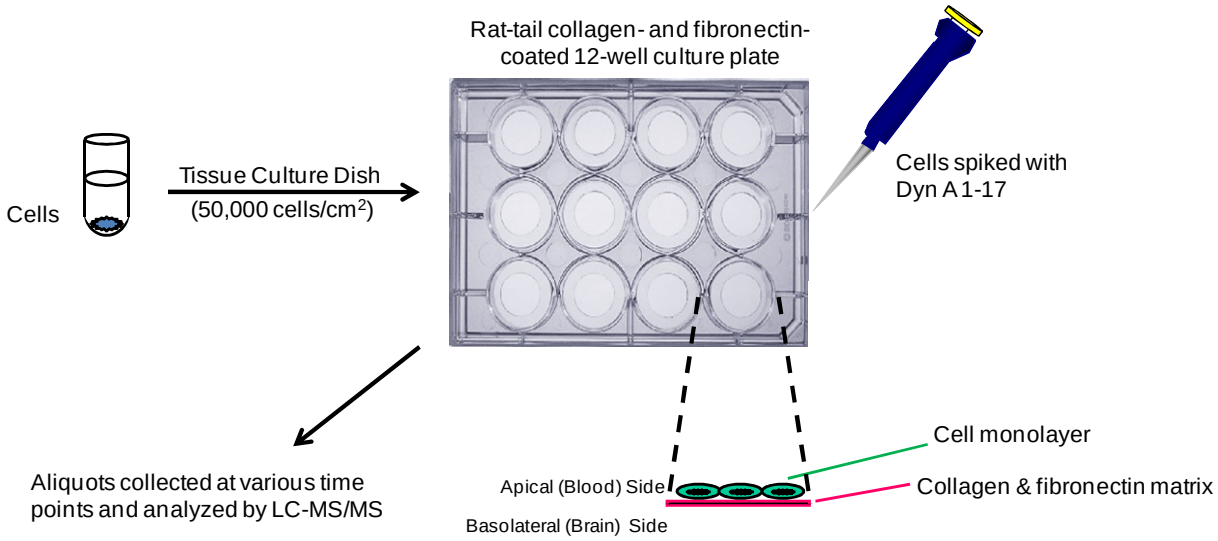

Figure 5.4. Experimental set-up for BBMEC metabolism studies.

techniques such as microdialysis) by focusing exclusively on the role of the brain endothelium on peptide metabolism.

5.1.4 Analytical methods for quantifying peptides of interest

A detailed discussion of analytical methods for the quantitation of peptides is included in Chapter 2 of this thesis; therefore, a brief discussion of the methods utilized for investigating metabolism and transport at the blood brain barrier follows. One of the simplest methods for determining the transport of compounds across the BBB is the use radiolabeled compounds and scintillation counting [15, 32]. This is most often employed in competitive studies that are done to determine if saturable, carrier-mediated processes are responsible for a peptide's permeation. In these studies a radiolabeled peptide is added to the diffusion chamber and its permeability is determined. Then the effect of un-labeled peptide on the permeation of the radiolabeled compound is evaluated. Alterations in the permeation of the labeled compound indicate the two species are competing for the same transport system. This method, however, can be costly due to the expense of producing labeled compounds. Radiolabeled peptides are also not always commercially available and safety considerations must be addressed before handling such compounds.

Other popular methods include a separation method (LC or CE) coupled with UV [5, 33-34], fluorescence [21], or mass spectrometric [35] detection. In general, the sensitivity of an analysis method using UV detection is low due to wavelengths employed (typically 210 nm for peptides). Fluorescence detection, although highly sensitive, requires labeling as peptides lacking a tryptophan residue are not natively fluorescent. Labeling must also be accomplished following assay completion because structural modifications to the peptide will alter its behavior

(its metabolic stability and permeability) *in vitro*. Fluorescent tagging of peptides is usually accomplished at a particular amino acid residue (such as lysine) and therefore only peptides and metabolites containing these residues are tagged, thus limiting the applicability of this approach.

Improved specificity can be achieved by employing mass spectrometric detection. Peptides can be detected without any labeling. Typically, LC-MS/MS is performed with the direct coupling of the LC eluent to the electrospray ionization (ESI) source, providing a means for online sample de-salting prior to analysis [35]. Multiple reaction monitoring significantly improves the detector selectivity for the peptides of interest and provides more accurate quantitation results. Important considerations for developing LC-MS/MS methods for dynorphin peptides are covered in detail in Chapter 4 of this thesis.

This chapter employs liquid chromatography with tandem mass spectrometry for the investigation of Dyn A 1-17 metabolism in the central nervous system and in the presence of BBMECs. The method does not require any labeling of the dynorphin peptides and minimal sample preparation is necessary. Improved limits of detection were achieved using LC-MS/MS in comparison to the CE-UV method described in Chapter 3. This method was then utilized to examine the BBB transport of Dyn A 1-6, the predominant metabolite identified from the metabolism studies, using the BBMEC culture system and Side-By-Side^{TM} diffusion chambers.

5.2 Materials and Methods

5.2.1 Reagents

All dynorphin peptides (Dyn A 1-17, 2-17, 1-13, 1-8, and 1-6) were obtained from Bachem Biosciences, Inc. (King of Prussia, PA, USA). Bradykinin was purchased from Sigma-Aldrich (St. Louis, MO USA). Fisher Optima acetonitrile (LC-MS grade) was used for all mobile phases containing organic (Fisher Scientific, Fair Lawn, NJ, USA). Formic acid was purchased from Acros Organics (Morris Plains, NJ, USA) at 99.9% purity. All aqueous mobile phases were made from 18 MΩ deionized (D.I.) water from a benchtop Milli-Q Synthesis A10 Water Purification System (Millipore, Billerica, MS, USA), filtered with 0.2 μm Magna nylon filters from Osmonics (Minnetonka, MN, USA). Minimum Essential Media and Ham's F12 were purchased from Life Technologies, Invitrogen Corporation (Carlsbad, CA, USA). All other reagents were purchased from Sigma Aldrich (St. Louis, MO, USA).

5.2.2 Metabolism studies in at central nervous system tissues

The brains and spinal cords of male Wistar rats (350-400 grams) were removed on the day of the study and kept in ice cold mPBSA prior to experiments. Animals that could no longer be used for microdialysis studies were graciously donated by Dr. Craig Lunte's laboratory at the University of Kansas. Tissue slices were prepared with a sterile razor blade in a petri dish on a bed of ice. For the metabolism studies, the tissue slices were exposed to dynorphin at room temperature (instead of 37 °C) to slow enzyme activity. For brain tissue slices, a 5 mm by 5 mm section was bathed in mPBSA spiked with 25 ìM Dyn A 1-17. Aliquots (50 μL) were collected at various time points over a 4 hour period, mixed with 50 μL of ice-cold aqueous 0.1% formic acid solution, and centrifuged on a table-top centrifuge for 2.5 min. Following centrifugation a

60 μL aliquot was removed and further diluted with 48 μL H_2O with 0.1% formic acid. Prior to analysis by LC-MS/MS, 12 μL of a 10 μM bradykinin solution was added to serve as an internal standard for quantitation. Similarly, a 5 mm length of spinal cord (width approximately 2 mm) was prepared and bathed in mPBSA spiked with 25 ìM Dyn A 1-17. Following the metabolism study, the brain and spinal cord slices were homogenized in PBSA and analyzed for total protein content by the Pierce BCA assay (Pierce, Rockford, IL, USA). Metabolism results are expressed as ìM dynorphin peptides per mg of protein.

5.2.3 Isolation and maintenance of bovine brain microvessel endothelial primary cultures

Microvessel endothelial cells were isolated from the cortical grey matter of bovine brains by enzymatic digestion and centrifugation as described by Audus and Borchardt in 1986 [13]. Briefly, bovine brains were obtained from a slaughter house in DeSoto, KS and transported to the laboratory in ice cold minimum essential medium (MEM), pH 7.4. Collagenase and dispase digestions in conjunction with centrifugation steps and both dextran and percoll gradients were used to isolate the endothelial cells from red blood cells and lipids. Following isolation the bovine brain microvessel endothelial cells were stored at -80 °C for up to 6 weeks in complete culture medium supplemented with 12% horse serum and 10% DMSO.

BBMECs were thawed and then seeded, at a density of approximately 50,000 cells/cm^2, on polycarbonate culture plates or 0.4 μm polycarbonate membranes (Nuclepore Track-etch, 13 mm, Whatman, United Kingdom) that were pre-coated with rat tail collagen and fibronectin. The plating medium consisted of 50% Minimum Essential Medium (MEM) and 50% Ham's F12 supplemented with 100 μg/mL streptomycin, 100 μg/mL penicillin G, 13 mM sodium bicarbonate, 10 mM HEPES, 10% platelet poor horse serum, 150 μg/mL heparin, and 50 μg/mL

polymixin B. Seventy two hours after plating, the media was changed. The changing medium consisted of 50% Minimum Essential Medium (MEM) and 50% Ham's F12 supplemented with 100 μg/mL streptomycin, 100 μg/mL penicillin G, 13 mM sodium bicarbonate, 10 mM HEPES, 10% platelet poor horse serum, 100 μg/mL heparin, and 0.5% endothelial cell growth supplement (ECGs). The changing medium was then replaced every 48 hours. The cells were grown to confluency (12-14 days after seeding) at 37 °C in an atmosphere of 5% CO_2 and 95% relative humidity.

5.2.4 Metabolism studies in the presence of BBMECs

BBMECs were seeded onto 12-well polycarbonate cell culture plates at a density of approximately 50,000 cells/cm^2. Cells were grown until a confluent monolayer formed (typically 12 to 14 days after seeding) as determined by light microscopy. Metabolism studies were performed in modified phosphate-buffered saline supplemented with $CaCl_2$, $MgCl_2$, glucose and ascorbic acid, pH 7.4 (mPBSA) which was previously described in Chapter 4. Before beginning each metabolism study, the growth medium was aspirated off and the cells were rinsed three times with pre-warmed (37 °C) mPBSA. The 12-well plate was kept in a benchtop incubator (Boekel, Feasterville, PA, USA), maintained at 37 °C and stirred continuously by a shaker (Stovall Belly Dancer, Cole Palmer, Vernon Hills, IL, USA). Cells were incubated with Dyn A 1-17 at varying concentrations and 60 μL aliquots were removed at various timepoints over the span of four hours. Aliquots were placed directly into autosampler vials containing 48 μL H_2O with 0.1% formic acid and were frozen (-20 °C) until analyzed. Prior to analysis, the samples were thawed, vortexed, and 12 μL internal standard (10 μM bradykinin) was added and analysis was performed via LC-MS/MS.

5.2.5 BBMEC permeability studies

BBMECs were grown on 0.4 μm polycarbonate membranes in a petri dish at a density of approximately 50,000 cells/cm^2. Cells were grown until a confluent monolayer formed (typically 12 to 14 days after seeding) as determined by light microscopy. Transport studies were performed in modified phosphate-buffered saline supplemented with $CaCl_2$, $MgCl_2$, glucose and ascorbic acid, pH 7.4 (mPBSA). Before beginning each study, the growth medium was aspirated off and the cells were then rinsed three times with pre-warmed (37 °C) mPBSA. The membranes were then removed and mounted in Side-by-Side™ diffusion chambers (Crown Glass Inc., Somerville, NJ, USA). Prior to studies, the diffusion chambers were silanized with Sigmacote (Sigma Aldrich, St. Louis, MO, USA) to prevent peptide adsorption to the chamber walls during the study.

Chambers were then pre-warmed (37°C) and rinsed three times with mPBSA. Following membrane placement, one side of the diffusion chamber was filled with 3 mL of mPBSA and examined for leaks. If the membrane was mounted correctly and no leaks were present, the other side of the chamber was filled with 3 mL of mPBSA as well. The chamber temperature was maintained for the duration of the study by external circulating water baths (at either 37 °C or 4 °C depending on the experiment) and each chamber was stirred constantly at 600 rpm by Teflon coated magnetic stir bars driven by an external console. The donor side was then spiked with the peptide of interest and 60 μL aliquots were removed from the receiver side at various time points and then replaced with an equal volume of mPBSA to prevent changes in volume that could affect flux. Studies typically lasted 2-4 hours. Samples were collected directly into autosampler vials pre-filled with 48 μL H_2O with 0.1% formic acid and then stored at -20 °C until use. Upon

thawing, samples were vortexed and 12 μL internal standard (10 μM bradykinin) was added and analysis was performed using an LC-MS/MS.

Upon completion of the transport study, fluorescein or [^{14}C]-sucrose were added to the apical side of the monolayer and utilized to test the monolayer integrity. These low permeability markers do not readily cross the blood brain barrier and are an indicator of monlayer integrity. Fluorescein samples were placed directly into a 96-well plate and analyzed by a fluorescence microplate spectrophotometer (Molecular Devices, Sunnydale, CA, USA) at excitation and emission wavelengths of 490 and 520 nm respectively. Sucrose samples were mixed with 10 mL of scintillation fluid and analyzed by liquid scintillation counting (Beckman, Fullerton, CA, USA).

For studies determining the permeability of fluorescein without Dyn A 1-6 pre treatment, chambers were filled with the modified media (mPBSA), and the cells were allowed to equilibrate for 5 minutes. After the equilibration period, fluorescein was added to the apical side of the cell membranes such that the final concentration was 10 ìM. Immediately a 100 ìL aliquot was removed from the donor chamber and collected into a 96 well plate. Additional 100 ìL aliquots were taken from the receiver chamber (t=10, 20, 30, and 60), and a final sample was taken from the donor chamber after 60 minutes as well. These fluorescence values were determined on a microplate spectrophotometer. The permeability of fluorescein was then determined using the following equation:

$$P_{app} = (ÄQ/Ät)/ A \times C_0$$

Where, ÄQ/Ät is the linear appearance of fluorescein in the receiver chamber, A is the cross sectional area of the cell monolayer (0.636 cm^2), and C_0 is the initial concentration in the donor chamber at t=0 (in this case, 10 ìM).

In the Dyn A 1-6 transport studies, 20 ìL of mPBSA was removed from the donor chamber and replaced with 20 ìL of a Dyn A 1-6 stock solution, resulting in 18.6 ìM peptide in the chamber. Bi-directional studies were performed by adding Dyn A 1-6 to either the apical (blood) or basolateral (brain) side of the mounted monolayers at 37°C. Aliquots (60 ìL) were taken from the receiver chamber at various time points over a 4 hour period. Studies done at 4°C were carried out in the apical to basolateral direction over a 2 hour period at the same concentration. All samples were collected into autosampler vials containing H_2O with formic acid. Mass balance samples were collected from the receiver chamber at the start and finish of each experiment. Quantitation was performed via LC-MS/MS. Peptide permeability was calculated with the same equation described above for fluorescein.

5.2.6 Liquid chromatography-tandem mass spectrometry instrumentation

An API 2000 triple quadrupole mass spectrometer (AB Sciex, Foster City, CA, USA) equipped with a Shimadzu Prominence LC (Shimadzu, Japan) consisting of two LC20-AD pumps with a solvent mixer, a CMB-20ALite controller, degasser (DGU-20A3), autosampler (Sil20A-HT), and column heater (CTO-20A) was employed for these studies. The system used Analyst 1.5 software for control and data analysis. A 1.0 x 50 mm C18 analytical column with 5 µm particles and the corresponding guard column, 1.0 x 10 mm (Vydac Microbore, C-18 MS columns, Grace Davidson Discovery Sciences, Deerfield, IL, USA) were utilized for all experiments.

5.2.7 Analysis of metabolism and permeability studies by LC-MS/MS

Transport samples were analyzed by the LC-MS/MS protocol described extensively in Chapter 4. Briefly, 60 μL aliquots were diluted with 48 μL H_2O with 0.1% formic, and prior to analysis 12 μL of a 10 μM bradykinin solution was added to serve as an internal standard for quantitation. Sample de-salting and separation were achieved using a 1.0 x 50 mm C18 analytical column with 5 μm particles and the corresponding guard column, 1.0 x 10 mm (Grace Davidson Discovery Sciences, Deerfield, IL, USA). The mobile phase was diverted to waste for the first 5 minutes of the LC run, then to the mass spectrometer from 5 to 12 minutes and again back to waste for the remainder of the run. The LC gradient program was as follows: initial conditions of 97% A, 3% B from 0 to 5 minutes, a linear ramp from 3 to 30% B from 5 to 6 minutes, holding at 30% B from 6 to 15 minutes, a linear return to initial conditions from 15 to 16 minutes, and column equilibration from 15 to 22 minutes holding at 3% B. Mobile phase A consisted of 100% H_2O with 0.1% formic acid. Mobile phase B consisted of 100% ACN with 0.1% formic acid. Multiple reaction monitoring was performed by the API 2000 and all ionization conditions and transitions were optimized previously (Chapter 4).

5.3 Results and Discussion

5.3.1 *In vitro* metabolism of Dyn A 1-17 in central nervous system tissues

Elevated concentrations of dynorphin have been implicated in a variety of neurological disorders. Due to cross-reactivity exhibited by immunoassays, these reportedly elevated concentrations may, in fact, be indicative of an increase in a dynorphin metabolite instead. It is therefore possible that it is a metabolite and not the parent peptide that is actually responsible for

these neurotoxic effects. Consequently, elucidating the metabolic profile of Dyn A 1-17 in the central nervous system is essential to understanding the role it plays *in vivo*. Toward this end, i*n vitro* metabolism studies were performed with both rat brain and spinal cord slices.

To ascertain that accurate results were attainable in modified PBSA (mPBSA), the stability of Dyn A 1-17 in mPBSA was determined at room temperature and at 37°C over ten hours. The dynorphin concentration remained constant throughout (data not shown). There was no appearance of metabolites over time, however, the Dyn A 1-17 standards did contain peaks for the Dyn A 1-8, 1-13, and 2-17 metabolites even at the initial (t = 0) timepoint. The concentrations of these compounds were constant and did not increase during the stability study (Figure 5.5 and 5.6). The presence of dynorphin metabolites in Dyn A 1-17 standards could be contaminants from the synthetic process. The metabolite peaks were seen even when fresh Dyn A 1-17 standards were made and analyzed immediately. The concentrations also did not change over time which would have been expected if the Dyn A 1-17 was undergoing degradation in mPBSA.

If the peaks were due to contaminants from the synthetic process, one would expect an increase in the fragment concentrations when higher Dyn A 1-17 concentrations were used. However, the same concentrations were observed when both 1 ìM and 25 ìM Dyn A 1-17 stocks were analyzed. Another explanation is that in-source fragmentation is occurring, producing smaller peptidic ions at the electrospray source. This is a commonly reported phenomena when analyzing peptides by electrospray and is especially common for peptides with multiple charge sites [36-38]. Data for these fragments (1-8, 1-13, and 2-17) is therefore presented as percent increase in concentration during the study duration (4 hours) to account for the initial metabolite concentrations present due to contamination or in-source fragmentation.

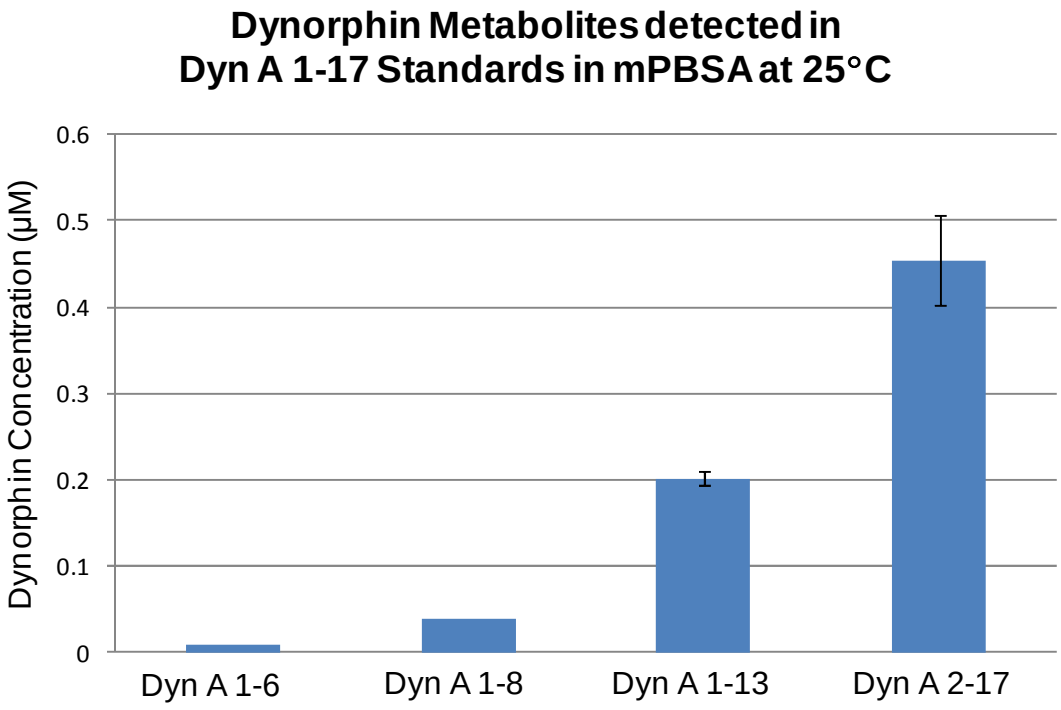

Dynorphin Metabolite	Average Conc (µM)	Standard Deviation
Dyn A 1-6	0.008	0.00018
Dyn A 1-8	0.039	0.00038
Dyn A 1-13	0.202	0.00758
Dyn A 2-17	0.454	0.05171

Figure 5.5 Dynorphin metabolite concentrations in Dyn A 1-17 standards (1 ìM) in mPBSA at 25 °C. Values were constant over time as represented by the standard deviations (n=10).

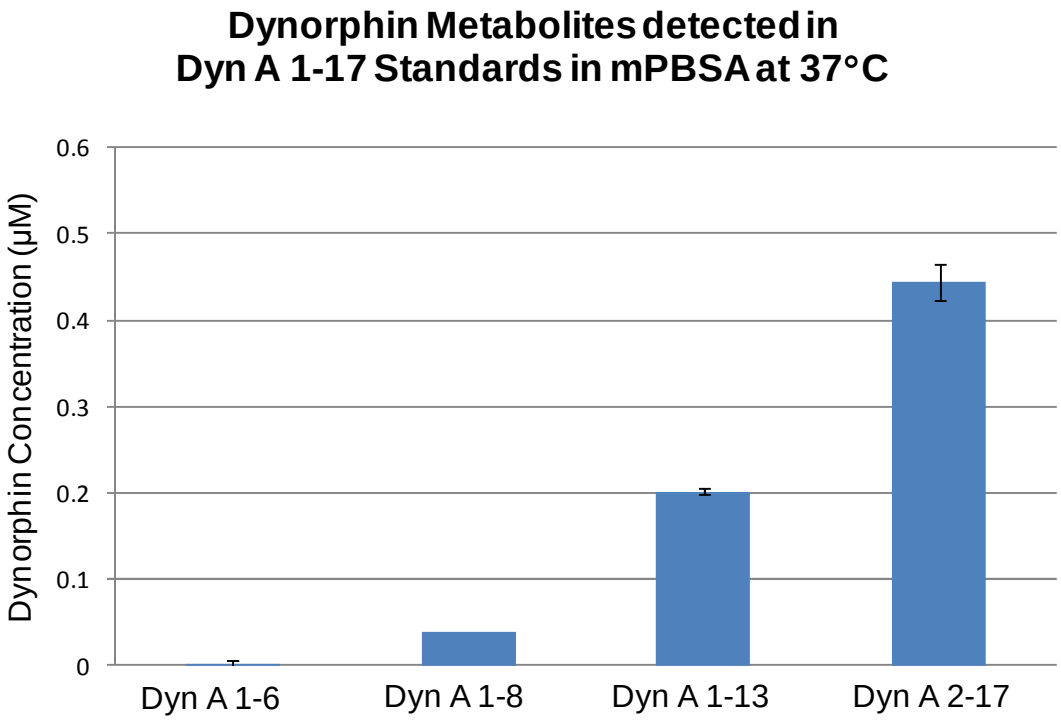

Dynorphin Metabolite	Average Conc (µM)	Standard Deviation
Dyn A 1-6	0.002	0.00053
Dyn A 1-8	0.038	0.00007
Dyn A 1-13	0.202	0.00337
Dyn A 2-17	0.443	0.02070

Figure 5.6 Dynorphin metabolite concentrations in Dyn A 1-17 standards (1 ìM) in mPBSA at 37 °C. Values were constant over time as represented by the standard deviations (n=10).

For Dyn A 1-6 which is not present as a contaminant, the change in concentration from t =0 to t = 240 minutes is plotted.

Once the stability of the parent peptide was established, *in vitro* metabolism could be investigated in rat brain and rat spinal cord samples. The tissue slice was placed in mPBSA and prior to the addition of Dyn A 1-17, a basal sample was collected and analyzed via LC-MS/MS. No dynorphin peaks were observed in this sample with either tissue (Figure 5.7 A & B). Dyn A 1-6 was the most abundant metabolite of Dyn A 1-17 in the presence of three separate rat brain slices, although the overall concentrations and time course of metabolism varied as can been seen in Figure 5.8. Dyn A 1-13 and Dyn A 2-17 were produced to a much lesser extent than Dyn A 1-6, exhibiting 23.0% and 27.8% increases, respectively, from the initial levels observed due to in-source fragmentation. Dyn A 1-8 did not significantly increase over time. The average percent increase for Dyn A 1-8, 1-13, and 2-17 following 4 hour incubation with rat brain slices is summarized in Table 5.1.

Dyn A 1-6 is produced by the cleavage of the Arg^{6}-Arg^{7} bond by dynorphin converting enzyme (DCE) [39, 40]. DCE was first isolated from human cerebral spinal fluid (CSF) and human spinal cord. The presence of Dyn A 1-6 as a metabolite in rat brain was previously confirmed in Chapter 3 of this thesis via analysis by copper complexation with capillary electrophoretic separation and UV detection [41]. Dyn A 1-6 has also been identified as a metabolite in the rat striatum via microdialysis sampling by Reed *et al* [23]. Dyn A 2-17 is thought to arise following cleavage of the N-terminal tyrosine by a non-specific aminopeptidase [42-43]. Dyn A 1-13 was previously identified in human plasma [41], however it has not previously been detected in rat brain. The cleavage of the Lys^{13}-Trp^{14} bond to produce this metabolite may be due an endopeptidase present in the brain tissue [17, 23].

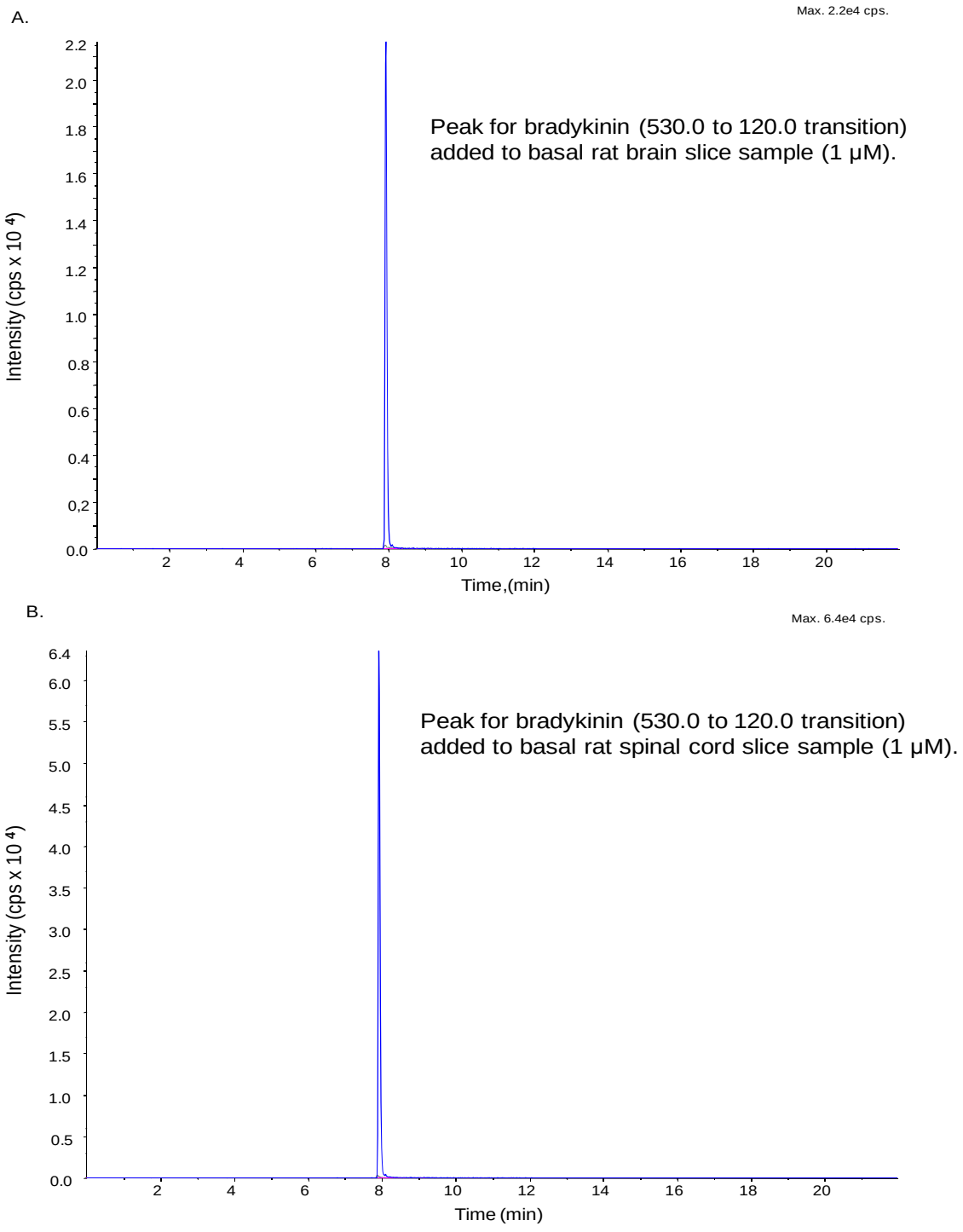

Figure 5.7 Basal rat brain (A) and rat spinal cord (B) slices spiked with 1 ìM internal standard (bradykinin). Overlays of extracted ion chromatograms for Dyn A 1-6, 1-8, 1-13, 1-17, 2-17, and bradykinin. Only one peak is observed for bradykinin.

A.

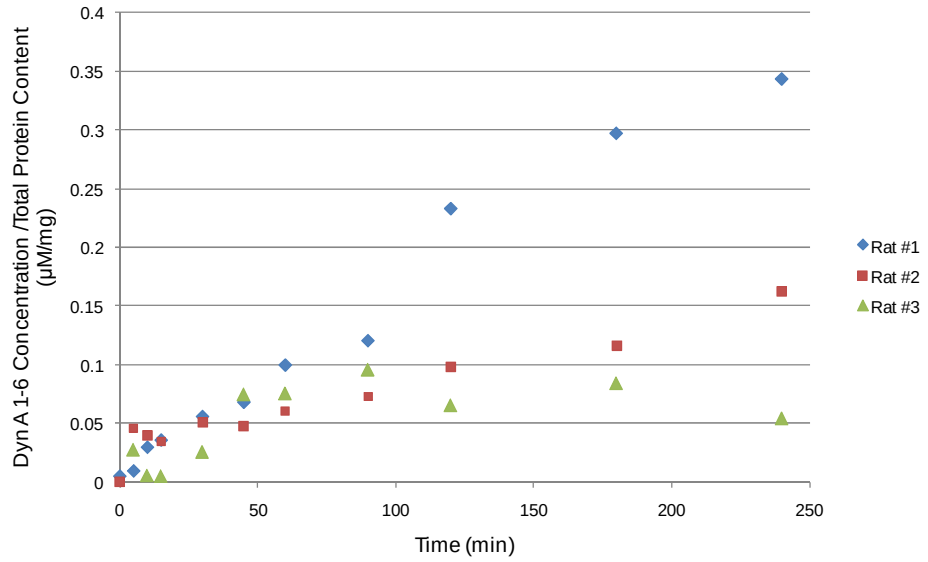

B.

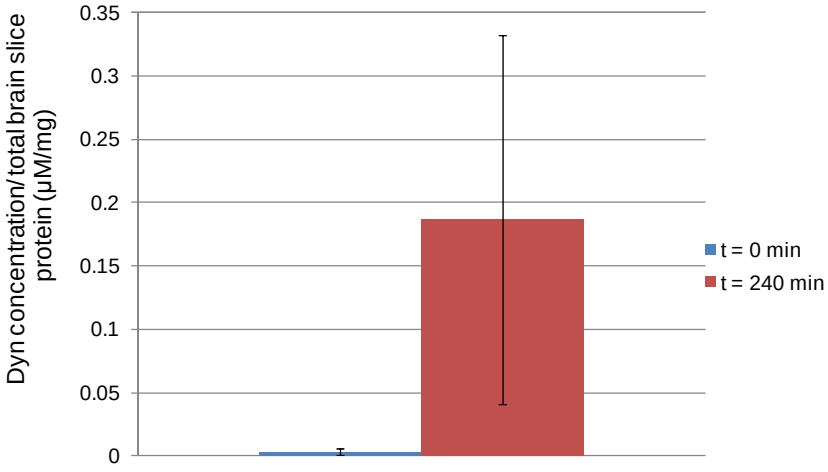

Figure 5.8 Appearance of Dyn A 1-6 in rat brain slices following incubation with 25 ìM Dyn A 1-17. Each graph represents data from 1 rat (A). Concentrations (ìM) are normalized to total protein content. Bar graph plots the average values (ìM peptide/mg of protein) at t = 0 and t = 240 min, standard deviation as error bars n=3. Experiments performed in mPBSA at 25°C.

Dynorphin Metabolite	Average Percent Increase
Dyn A 1-8	2.01% (+/- 1.40)
Dyn A 1-13	23.0% (+/- 4.65)
Dyn A 2-17	27.8% (+/- 11.2)

Table 5.1 Average percent increase of dynorphin metabolites 4 hour following incubation of Dyn A 1-17 with rat brain slices. Standard deviations in parentheses, n = 3.

In addition to investigating the metabolism of Dyn A 1-17 in rat brain slices, the metabolism in rat spinal cord slices was also investigated. Again Dyn A 1-6 was observed as the most abundant metabolite. The time course of Dyn A 1-6 appearance was even more varied than in the rat brain samples (Figure 5.9). In the first rat (Figure 5.9, blue diamonds), the Dyn A 1-6 appears to undergo additional metabolism itself after two hours in the presence of rat spinal cord, shown by the decrease in concentration after the two hour sample. In the third rat (Figure 5.9, green triangles), Dyn A 1-6 is only produced to a small degree (less than 0.1 ìM/mg of protein) until just after 2 hours when a rise in the metabolite concentration occurs. Dyn A 1-13 and 2-17 were also produced, only to a much lesser degree. Again, an increase in Dyn A 1-8 concentration was not observed. The average percent increase for Dyn A 1-8, 1-13, and 2-17 following 4 hour incubation with rat spinal cord slices is summarized in Table 5.2.

Some of the differences observed here can be attributed to inter-animal variability. Factors such as the age and weight of the animal can alter their metabolism. The isolation of the spinal cord was also a more tedious surgery. Unlike the brain (which is easily removed as a whole organ and then sliced in a reproducible way), often the spinal cord was removed in small segments. Therefore, there was more variability with regard to the section of the spinal cord that was used in each experiment. Additionally, the viability of the tissues over the course of the study also plays a significant role in these studies. Rat central nervous system tissues are known to degrade more rapidly than the CNS tissues of other mammalian species (bovine and human for example). This would explain the increase in variability observed at the later timpoints of the metabolism studies. Interestingly, Dyn A 1-6 was not observed in rat spinal cord using the CE method [41]. The detection of this peptide in these experiments is most likely due to the improvements in sensitivity when using mass spectrometry versus UV detection. The limits of

A.

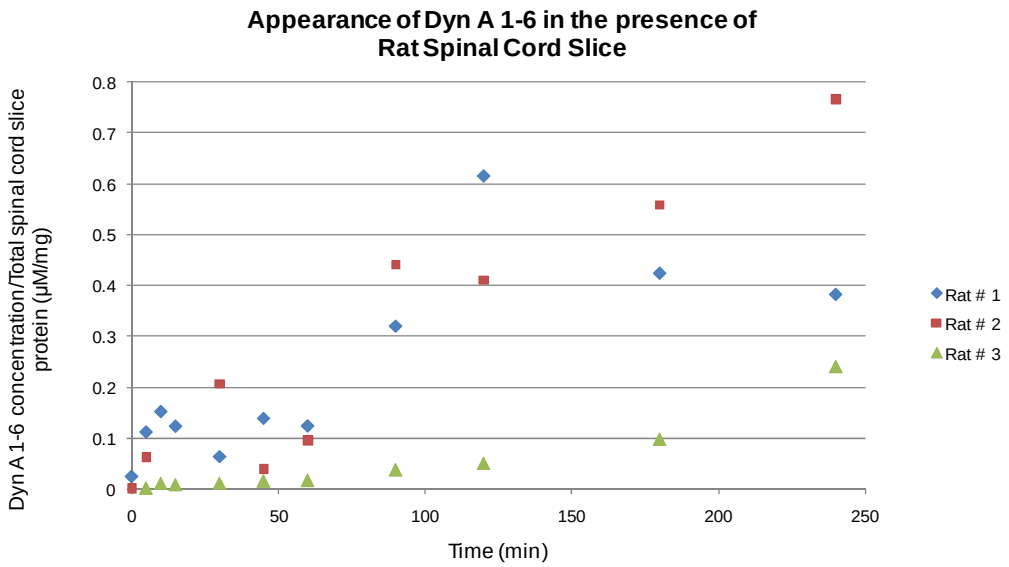

B.

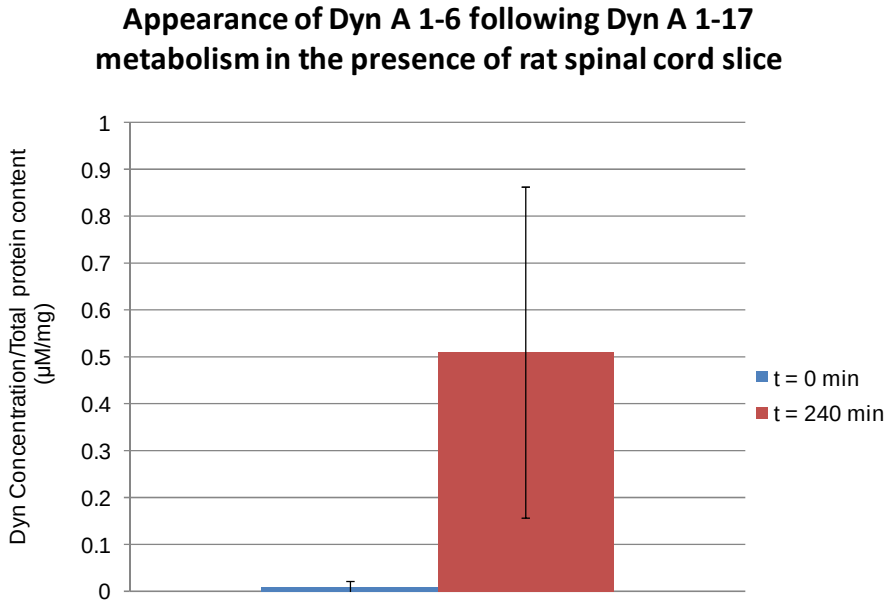

Figure 5.9 Appearance of Dyn A 1-6 in rat spinal cord slices following incubation with 25 ìM Dyn A 1-17. Each graph represents data from 1 rat (A). Concentrations (ìM) are normalized to total protein content. Bar graph plots the average values (ìM peptide/mg of protein) at t = 0 and t = 240 min, standard deviation as error bars n=3 Experiments performed in mPBSA at 25°C.

Dynorphin Metabolite	Average Percent Increase
Dyn A 1-8	1.04% (+/- 0.14)
Dyn A 1-13	35.6% (+/- 20.8)
Dyn A 2-17	17.4% (+/- 0.88)

Table 5.2 Average percent increase of dynorphin metabolites 4 hour following incubation of Dyn A 1-17 with rat spinal cord slices. Standard deviations in parentheses, n = 3.

detection are 0.2 nM using LC-MS/MS versus 2.5 ìM with the CE UV method. Sensitivity as well as selectivity are further increased by using MRM.

5.3.2 *In vitro* metabolism of Dyn A 1-17 in the presence of BBMECs

In addition to investigating the metabolism of Dyn A 1-17 in the presence of rat brain and spinal cord, the metabolism in the presence of BBMECs was also explored. Wells without added Dyn A 1-17 were used as a control, and no dynorphin peaks were observed in the control wells throughout the duration of the experiment (data not shown). Percent increase in each of the metabolites was again calculated to account for the initial levels of fragmentation produced at the electrospray source.

The time course of Dyn A 1-17 metabolism is seen in Figure 5.10. A clear decrease in Dyn A 1-17 concentration over time is apparent. In order to identify the appearance of metabolites over time, LC-MS/MS data is presented as percent increase over the duration of each four hour study. No appreciable increase in Dyn A 1-8, 1-13, or 2-17 concentrations were observed as summarized in Table 5.3. Low amounts of the peptides were present for the duration of the study due to in-source fragmentation; however, in each of the wells, the concentration did not change over time. The concentration of Dyn A 1-6 however did increase over time as can be seen in Figure 5.11. The presence of Dyn A 1-6 as a major metabolite of 1-17 agrees well with the previously reported metabolism in the rat brain and rat spinal cord. Therefore characterizing the transport of this metabolite at the blood brain barrier could contribute to a better understanding of the role dynorphin may play in neuropathic pain and other neurological disorders.

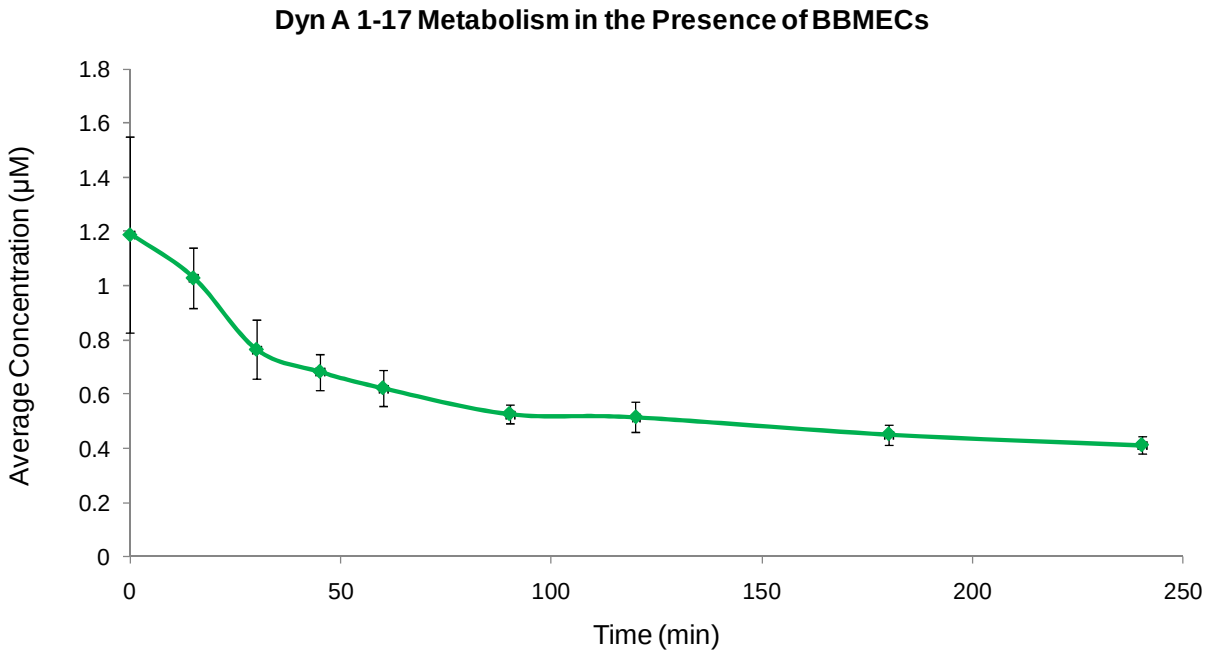

Figure 5.10 Metabolism of Dyn A 1-17 in the presence of BBMECs following a 1 ìM spike (n = 3). Experiment performed in mPBSA at 37 °C.

Dynorphin Metabolite	Average Percent Change
Dyn A 1-8	2.19% (+/- 0.503)
Dyn A 1-13	-0.869% (+/- 1.31)
Dyn A 2-17	-1.15% (+/- 0.903)

Table 5.3 Average percent increase of dynorphin metabolites 4 hour following incubation of Dyn A 1-17 with BBMECs. Standard deviations in parentheses, n = 3.

A.

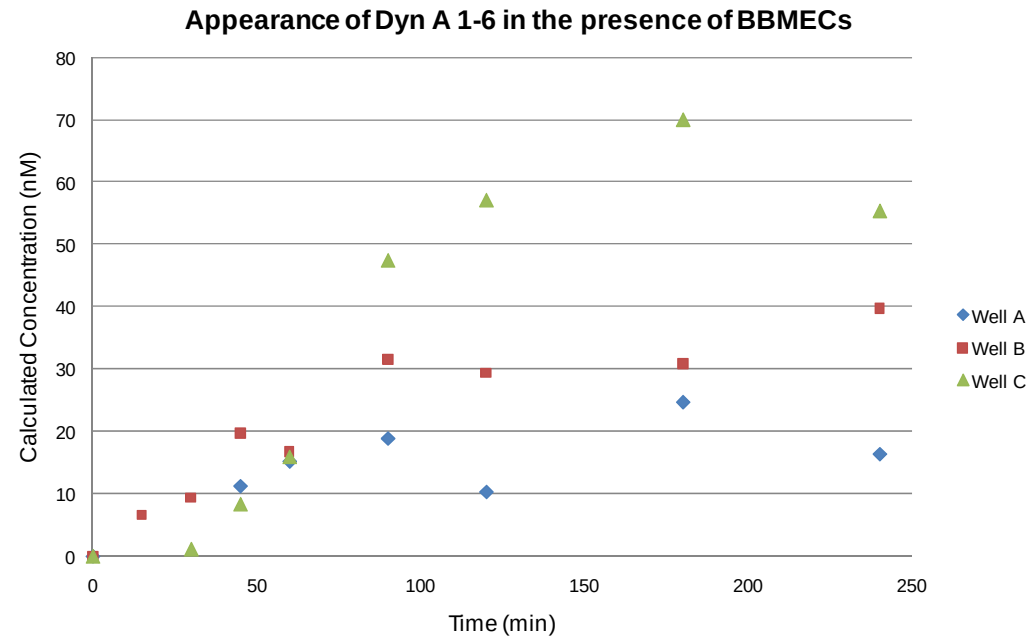

B.

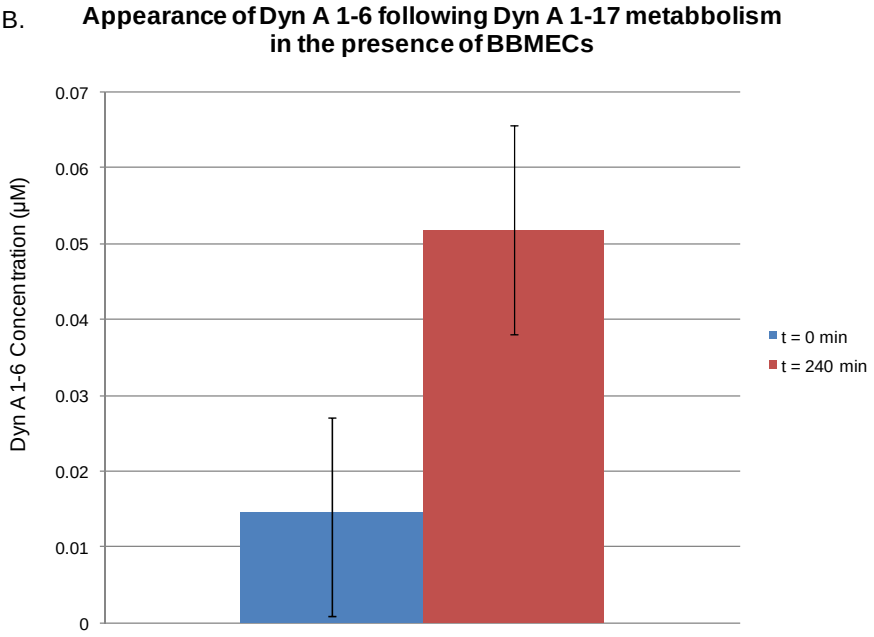

Figure 5.11. Appearance of Dyn A 1-6 in the presence of BBMECs following incubation with 1 ìM Dyn A 1-17. Each trace is the data from 1 well of a 12 well cell culture plate (A). Average concentration (n = 3) in the initial sample (t = 0 min timepoint, blue) and the concentration following a 4 hour incubation (t = 240 min, red) (B). Experiment performed in mPBSA at 37 °C.

5.3.3 Blood brain barrier permeability of Dyn A 1-6, a major metabolite of Dyn A 1-17

Dyn A 1-6 has been identified as a major metabolite of the parent peptide Dyn A 1-17 in both the central nervous system [17, 41, 44] (brain and spinal cord) as well as in peripheral tissues (blood and plasma) [41, 45-47]. For this reason, the BBB permeability of Dyn A 1-6 was investigated, using BBMECs grown on polycarbonate membranes and mounted in Side-by-Side^{TM} diffusion chambers. Fluorescein was utilized as a low permeability control following all experiments to examine monolayer integrity.

Most permeability experiments performed with Side-by-Side^{TM} diffusion chambers use PBSA; however, as described in Chapter 4, the more basic dynorphin peptides exhibited ion suppression likely due to sulfate and/or phosphate adduct formation in PBSA. Therefore, modifications were made to the cell media to decrease this effect and improve ionization. The concentration of phosphate was decreased and magnesium chloride was substituted for magnesium sulfate. Table 5.4 lists the components of PBS and PBSA as well as the components of the modified media (mPBSA). To ensure that mPBSA did not alter the integrity of the cell monolayer, the permeability value for fluorescein was determined before commencing with the Dyn A 1-6 transport experiments. Fluorescein permeability was calculated to be 3.42×10^{-5} cm/s ($^{+}$/- 2.90×10^{-5} n = 4). This value agrees well with previously reported literature [33, 34] indicating that the modifications did not have a negative impact on tight junction integrity.

Next, Dyn A 1-6 permeability was screened by the above method. Both the directional and temperature dependence of Dyn A 1-6 permeability were determined. The apparent permeability coefficient of Dyn A 1-6 was calculated to be $P_{app} = 6.59 \times 10^{-5}$ cm/s ($^{+}$/- 1.74×10^{-5} n = 4), in the apical to basolateral direction, and $P_{app} = 6.43 \times 10^{-5}$ cm/s ($^{+}$/- 1.61×10^{-5} n = 4), in

PBS	PBSA	mPBSA
129 mM NaCl	129 mM NaCl	144 mM NaCl
2.5 mM KCl	2.5 mM KCl	4.0 mM KCl
7.4 mM Na_2HPO_4	7.4 mM Na_2HPO_4	0.74 mM Na_2HPO_4
1.3 mM KH_2PO_4	1.3 mM KH_2PO_4	0.13 mM KH_2PO_4
	0.63 mM $CaCl_2$	0.63 mM $CaCl_2$
	0.74 mM $MgSO_4$	0.74 mM $MgCl_2$
	5.3 mM Glucose	5.3 mM Glucose
	0.1 mM Ascorbic Acid	0.1 mM Ascorbic Acid
		10 mM HEPES

Table 5.4. A comparison of phosphate buffered saline (PBS), phosphate buffered saline with additives (PBSA, typically used for transport studies), and the modification of PBSA employed in these studies to improve electrospray ionization of highly basic dynorphin peptides.

the basolateral to apical direction. There was no difference in the permeability based on direction (Figure 5.12). A decrease in permeability was observed at 4°C, P_{app} = 1.11 x 10^{-5} cm/s ($^{+}$/- 2.90 x 10^{-6}, n = 4, $p < 0.005$) indicative of a carrier-mediated transport system (Figure 5.13). Fluorescein was utilized as a control following the end of each experiment. Values for fluorescein permeability are presented in Figure 5.14.

An interesting observation was made when the fluorescein permeability controls were analyzed following studies with Dyn A 1-6. It was found that the permeability values for fluorescein were increased following the Dyn A 1-6 exposure at 37°C. However, at 4°C the permeability coefficient of fluorescein was not affected by the peptide. This effect was further investigated by incubating mounted monolayers for 2 hours in mPBSA at 37 °C. Following the 2 hour incubation, 0, 20, and 100 ìL of mPBSA were removed and replaced with Dyn A 1-6 resulting in final concentrations in the chamber of 0, 18.6, and 46.6 ìM. The fluorescein permeability increased in a linear fashion with increasing exposure to Dyn A 1-6, R^2 = 0.9995 (Figure 5.15). The permeability values for Dyn A 1-6 in the apical to basolateral and basolateral to apical directions fall along this line, as shown by the purple and orange data points in Figure 5.16, suggesting that this peptide is responsible for increasing BBB permeability. A similar phenomenon was observed by Thompson and Audus with the opioid peptide leucine enkephalin [33, 34], and the reported values for fluorescein permeability both with and without leucine enkephalin pretreatment are also plotted in Figure 5.16.

It has been reported previously that leucine enkephalin can increase the permeability of low molecular weight, membrane impermeant molecules such as sucrose and fluorescein in a concentration-, energy-, and temperature-dependent manner [33, 34, 48]. Metabolites of Leu-enkephalin did not exhibit this effect nor did metabolically stable analogs. It is also well known

that there exists a saturable peptide transport system for small, N-tyrosinated peptides at the blood brain barrier [49-51], and that this system is responsible for the brain to blood efflux of the small opioid peptide leucine enkephalin. Thompson and Audus found that non-opioid peptides capable of utilizing this transport system did not alter BBB permeability to fluorescein or sucrose suggesting that binding this efflux system is not responsible for BBB opening. However, the use of naloxone, a mu- and delta-opioid antagonist, was shown to attenuate the increased transport caused by the Leu-enkephalin [33-34]. This indicates that opioid receptor activity (delta or mu) may play a role in the ability of these peptides to open the BBB. Dyn A 1-17 preferentially acts at the kappa-opioid receptor, while Dyn A 1-6 shares affinity for the kappa, mu, and delta receptors. Dyn A 1-6 has not been implicated in the neurotoxicity of Dyn 1-17; however, it may be responsible for opening the blood brain barrier, allowing for increased transport of the parent peptide. Further studies would be necessary to determine the mechanism responsible for the Dyn A 1-6-induced increase in BBB permeability.

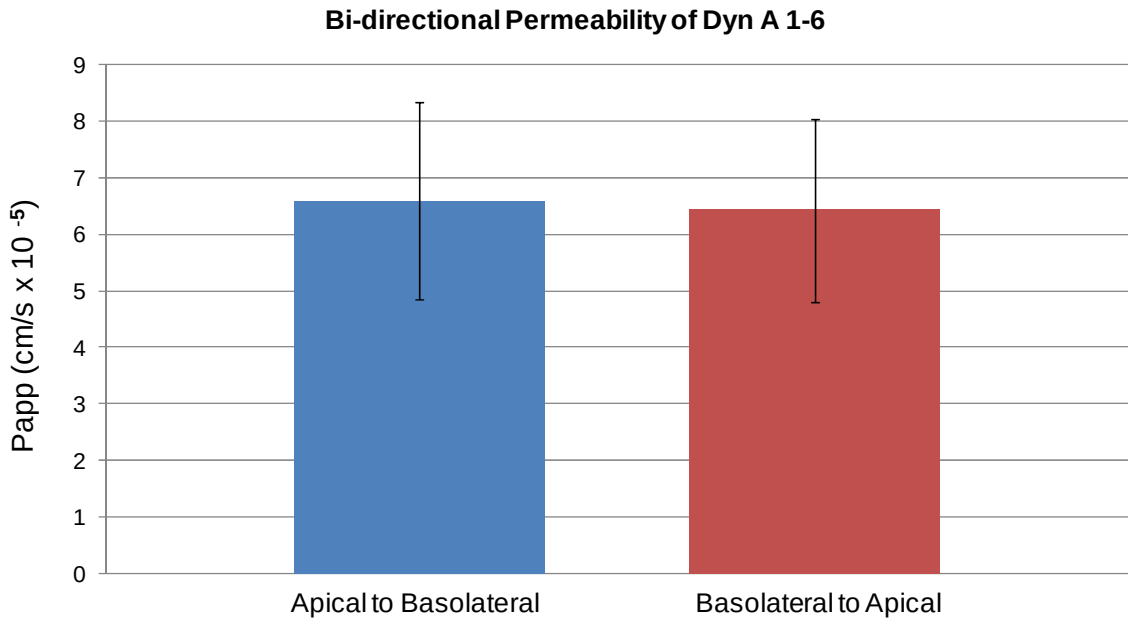

Figure 5.12 Bi-directional apparent permeability coefficients of Dyn A 1-6 (n =4 in each direction).

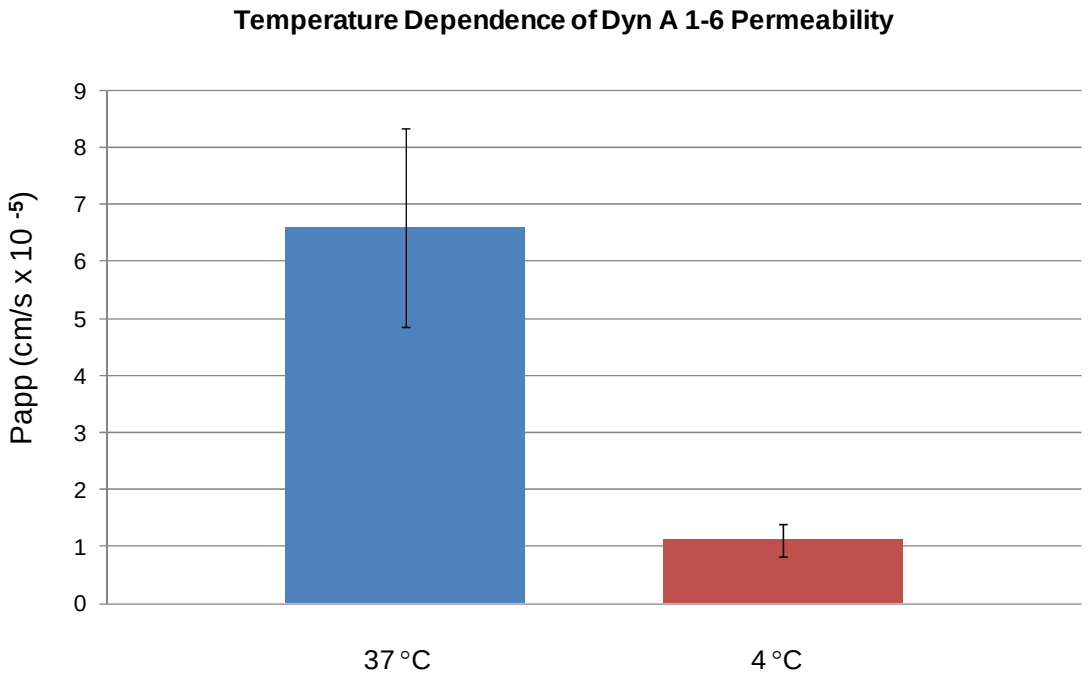

Figure 5.13 Temperature dependence of the apical to basolateral transport of Dyn A 1-6 (n =4 at each temperature) $p < 0.005$.

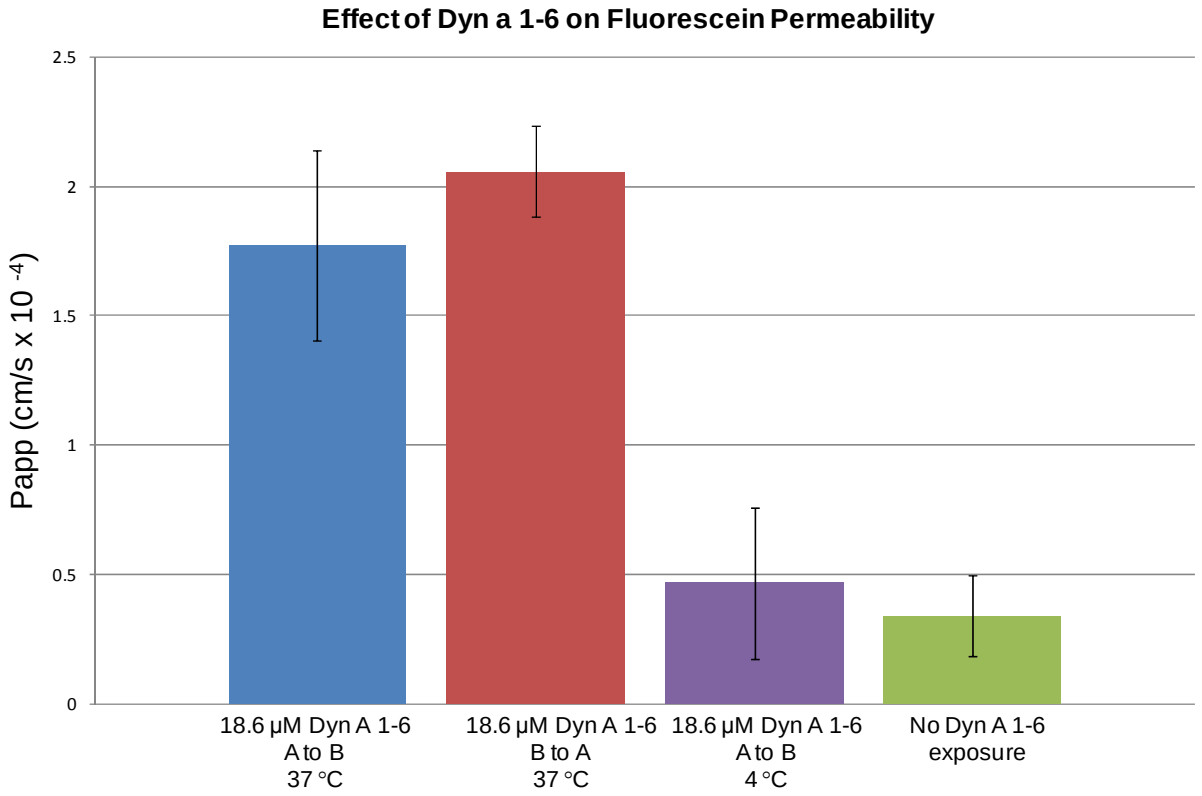

Figure 5.14 Effect of pre-treatment with 18.6 ìM Dyn A 1-6 on the BBB permeability of the low molecular weight, low permeability marker, fluorescein (10ìM), n=4.

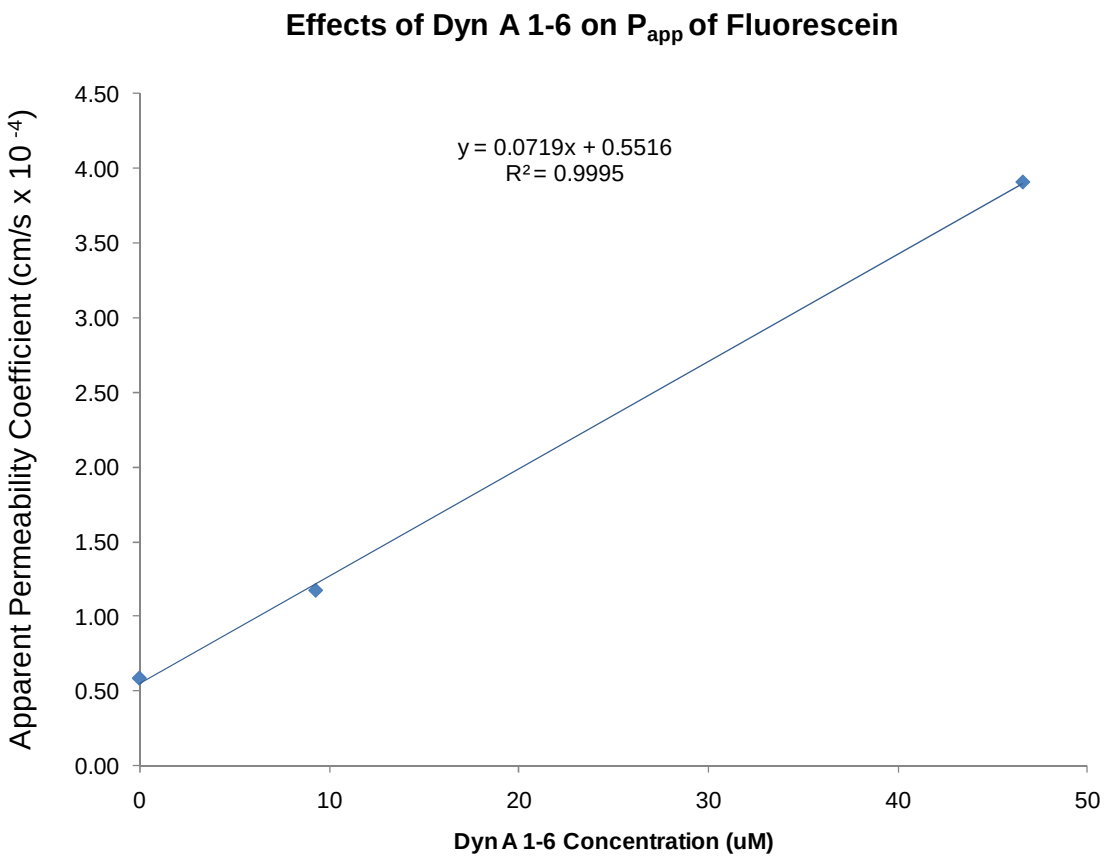

Figure 5.15 Effect of pre-treatment with varying Dyn A 1-6 concentrations on the BBB permeability of the low molecular weight, low permeability marker, fluorescein (10 ìM), n = 1 for each data point.

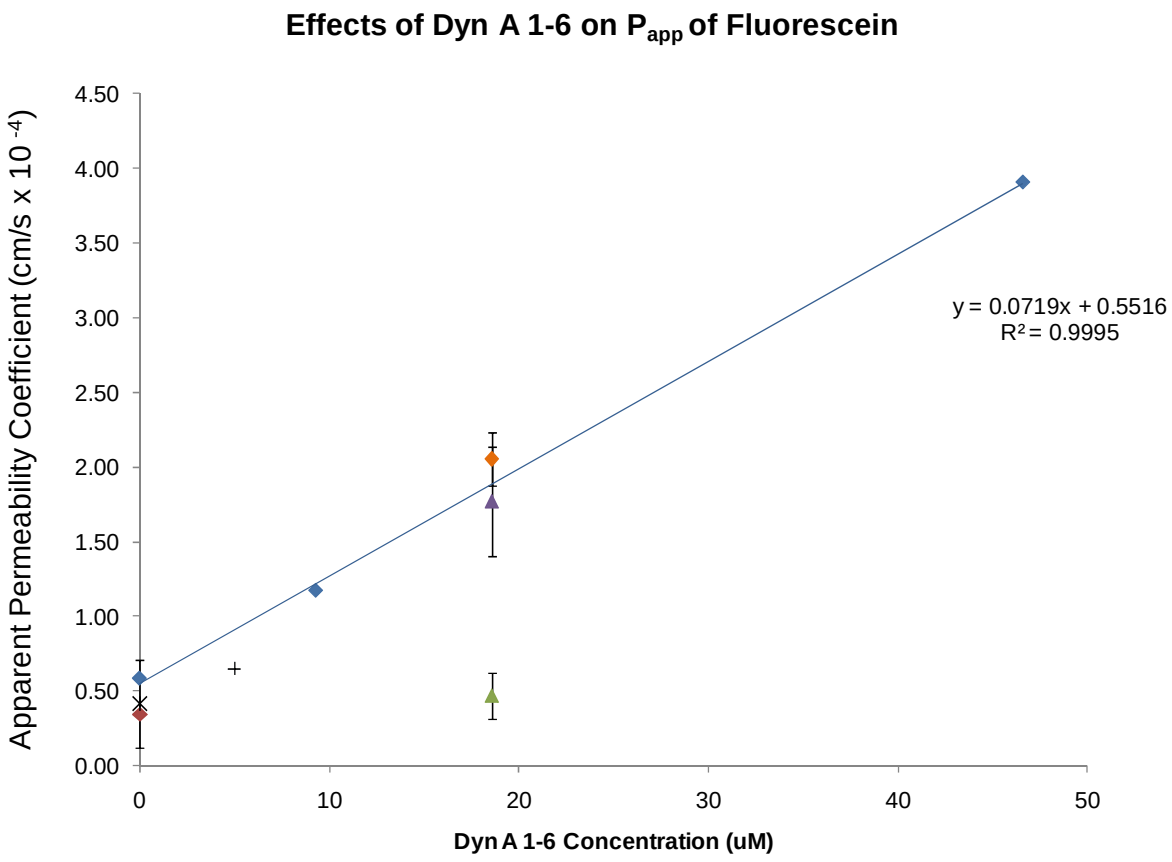

Figure 5.16 Effect of pre-treatment with varying Dyn A 1-6 concentrations (◆) on the BBB permeability of the low molecular weight, low permeability marker, fluorescein (10 ìM). Fluorescein permeability without Dyn A 1-6 incubation (◆), fluorescein permeability following 240 min Dyn A 1-6 pretreatment A to B (▲) and B to A (◆), and fluorescein permeability following 120 min Dyn A 1-6 pretreatment at 4 °C (▲). Also shown are literature values for the permeability of fluorescein alone (**x**) and following pre-treatment with leucine enkephalin (+).

5.4 Summary

The metabolism of Dyn A 1-17 has been characterized in the presence of rat brain and spinal cord slices as well as in the presence of BBMECs, an *in vitro* model of the BBB. Dyn A 1-6 was found to be the predominant metabolite in each of these systems. The transport of this metabolite across the BBB was then characterized and was found to be bi-directional. Dyn 1-6 transport was decreased at 4°C indicating energy (ATP) driven transport mechanism. The metabolite was also found to increase the permeability of the blood brain barrier to a low molecular weight, low permeability control substance, fluorescein. Such effects suggest a role of this dynorphin metabolite in the opening of the blood brain barrier, and potentially a role of the metabolite in the neurotoxic effects of Dyn A 1-17. Further studies would be necessary to determine the mechanism by which this opening occurs.

5.5 References

[1] Brightman, M. W., Reese, T. S., *Journal of Cell Biology* 1969, *40*, 648-677.

[2] Reese, T. S., Karnovsky, M. J., *Journal of Cell Biology* 1967, *34*, 207-217.

[3] Abbott, N. J., Roennbaeck, L., Hansson, E., *Nature Reviews Neuroscience* 2006, *7*, 41-53.

[4] Spatz, M., Mrsulja, B. B., *Advances in Cellular Neurobiology* 1982, *3*, 311-337.

[5] Thompson, S. E., Audus, K. L., *Peptides* 1993, *15*, 109-116.

[6] Baranczyk-Kuzma, A., Raub, T. J., Audus, K. L., *Journal of Cerebral Blood Flow and Metabolism* 1989, *9*, 280-289.

[7] Baranczyk-Kuzma, A., Audus, K. L., *Journal of Cerebral Blood Flow and Metabolism* 1987, *7*, 801-805.

[8] Augustijns, P. F., Ng, K., Williams, T. M., Borchardt, R. T., *Biochemical and biophysical research communications* 1995, *210*, 987-994.

[9] Brownson, E. A., Abbruscato, T. J., Gillespie, T. J., Hruby, V. J., Davis, T. P., *The Journal of Pharmacology and Experimental Therapeutics* 1994, *270*, 675-680.

[10] Hegemann, E. J., Bauer, H. C., Kerbel, R. S., *Cancer Research* 1992, *52*, 6969-6975.

[11] Huai-Yun, H., Secrest, D. T., Mark, K. S., Carnery, D., Brandquist, C., Elmquist, W. F., Miller, D. W., *Biochemical and Biophysical Research Communications* 1998, *243*, 816-820.

[12] Tatsuta, T., Naito, M., Oh-hara, T., Sugawara, I., Tsuruo, T., *Journal of Biological Chemistry* 1992, *267*.

[13] Audus, K. L., Borchardt, R. T., *Pharmaceutical Research* 1986, *3*, 81-87.

[14] Gumbleton, M., Audus, K. L., *Journal of Pharmaceutical Sciences* 2001, *90*, 1681-1698.

[15] Audus, K. L., Borchardt, R. T., *Journal of Neurochemistry* 1986, *47*, 484-488.

[16] Yakovleva, T., Marinova, Z., Kuzmin, A., Seidah, N. G., Haroutunian, V., Terenius, L., Bakalkin, G., *Neurobiology of Aging* 2006, *14*, 1700-1708.

[17] Klintenberg, R., Andren, P. E., *Journal of Mass Spectrometry* 2005, *40*, 261-270.

[18] Lai, J., Ossipov, M. H., Vanderah, T. W., Malan, J., T. P. , Porreca, F., *Molecular Interventions* 2001, *1*, 160-167.

[19] Shirayama, Y., Ishida, H., Iwata, M., Hazama, G., Kawahara, R., Duman, R. S., *Journal of Neurochemistry* 2004, *90*, 1258-1268.

[20] Ghazarossian, V. E., Chavkin, C., Goldstein, A., *Life Sciences* 1980, *27*, 75-86.

[21] Freed, A. L., Cooper, J. D., Davies, M. I., Lunte, S. M., *J. Neurosci. Methods* 2001, *109*, 23-29.

[22] Reed, B., Bidlack, J. M., Chait, B. T., Kreek, M. J., *Journal of Neuroendocrinology* 2008, *20*, 606-616.

[23] Reed, B., Zhang, Y., Chait, B. T., Kreek, M. J., *Journal of Neurochemistry* 2003, *86*, 815-823.

[24] Chappa, A. K., *Pharmacedutical Chemistry*, The University of Kansas, Lawrence 2007.

[25] Stenken, J. A., Lunte, C. E., Southard, M. Z., Staahle, L., *J. Pharm. Sci.* 1997, *86*, 958-966.

[26] Smith, Q. R., *Pharmaceutical Biotechnology* 1996, *8*.

[27] Baranczyk-Kuzma, A., Audus, K. L., Borchardt, R. T., *Journal of Neurochemistry* 1986, *46*, 1956-1960.

[28] Yazdanian, M., Bormann, B. J., (2000), Immortalized Brain Endothelial Cells, Patent Number: 6093553. Boehringer Ingelheim Pharmaceuticals, I. United States.

[29] de Boer, A. G., Gaillard, P. J., *Current Medicinal Chemistry* 2002, *2*, 203-209.

[30] Reinhardt, C. A., Gloor, S. M., *Toxicology in vitro* 1997, *11*, 513-518.

[31] Takakura, T., Audus, K. L., Borchardt, R. T., *NIDA research monograph* 1992, *120*, 138-149.

[32] Shah, M. V., Audus, K. L., Borchardt, R. T., *Pharmaceutical Research* 1989, *6*, 624-627.

[33] Thompson, S. E., Audus, K. L., *Pharmaceutical Research* 1994, *11*, 1366-1369.

[34] Thompson, S. E., Cavitt, J., Audus, K. L., *Journal of Cardiovascular Pharmacology* 1994, *24*, 818-825.

[35] Chappa, A. K., Audus, K. L., Lunte, S. M., *Pharmaceutical Research* 2006, *23*, 1201-1208.

[36] Katta, V., Chowdhury, S. K., Chait, B. T., *Analytical Chemistry* 1991, *63*, 173-178.

[37] Lanckmans, K., Sarre, S., Smolders, I., Michotte, Y., *Talanta* 2008, *74*, 458-469.

[38] Williams, J. D., Flanagan, M., Lopez, L., Fischer, S., Miller, J. A. D., *Journal of Chromatography A* 2003, *1020*, 11-26.

[39] Nyberg, F., Nordstrom, K., Terenius, L., *Biochemical and biophysical research communications* 1985, *131*, 1069-1074.

[40] Silberring, J., Castello, M. E., Nyberg, F., *The Journal of Biological Chemistry* 1992, *267*, 21324-21328.

[41] Kuhnline, C. D., Lunte, S. M., *Journal of Separation Science* 2010, *33*, 2506.

[42] Benuck, M., Berg, M. J., Marks, N., *Neurochemical Research* 1984, *9*, 733-749.

[43] Berg, M. J., Marks, N., *Journal of Neuroscience Research* 1984, *11*, 313-321.

[44] Reed, B., Zhang, Y., Chait, B. T., Kreek, M. J., *Journal of Neurochemistry* 2003, *86*, 815-823.

[45] Chou, J. Z., Chait, B. T., Wang, R., Kreek, M. J., *Peptides* 1996, *17*, 983-990.

[46] Chou, J. Z., Kreek, M. J., Chait, B. T., *American Society for Mass Spectrometry* 1994, *5*, 10-16.

[47] Yu, J., Butelman, E. R., Woods, J. H., Chait, B. T., Kreek, M. J., *The Journal of Pharmacology and Experimental Therapeutics* 1996, *279*, 507-514.

[48] Baba, M., Oishi, R., Saeki, K., 1988.

[49] Banks, W. A., Kastin, A. J., Michals, E. A., *Peptides* 1987, *8*, 899-903.

[50] Banks, W. A., Kastin, A. J., Fishman, A. J., Coy, D. H., Strauss, S. L., *American Journal of Physiology* 1986, *251*, E477-E482.

[51] Banks, W. A., Kastin, A. J., Nager, B. J., *Neuropharmacology* 1988, *27*, 174-179.

Chapter Six:

Work towards the development of an immunoaffinity microchip electrophoresis device for the investigation of the neuropharmacology of Dyn A 1-17

6.1 Introduction

The past decade has led to an increasing interest in combining the fields of immunochemistry and separation science, in particular capillary and microchip electrophoresis (CE and ME respectively), and there are several comprehensive reviews published on the advances in this area [1-4]. One of the touted advantages of capillary- and microchip-based electrophoretic separation techniques is the small sample volume requirements, especially in the case of volume-limited biological samples. In the case of the detection of low abundance biomarkers, however, this is also its significant drawback. Nanoliter injection volumes characteristic of CE and ME can result in only a few molecules of low concentration compounds being injected. This necessitates sufficiently concentration-sensitive detection options and/or concentration prior to analysis. Thus, improvements in limits of detection are essential for the use of CE and ME for the analysis of low concentration compounds of interest. Immunoaffinity techniques have been employed in combination with electrophoresis in a variety of formats. Offline immunoextraction prior to separation is a common method; however, this chapter will focus on the coupling of immunoextraction directly to the separation technique. This can be accomplished in both the capillary and microchip format and several approaches will be detailed.

Many depictions of antibody immobilization on the surfaces of such devices use a similar cartoon, characteristically a Y-shaped molecule, to illustrate the entire antibody chemically attached to the capillary or microchip substrate. Figure 6.1 depicts a cartoon antibody structure indicating important structural elements including the Fc or constant fragment, the two FAb fragments responsible for antigen binding, and the flexible hinge region joined by disulfide bonds. While intact antibodies can be immobilized directly, the orientation of the antibody on

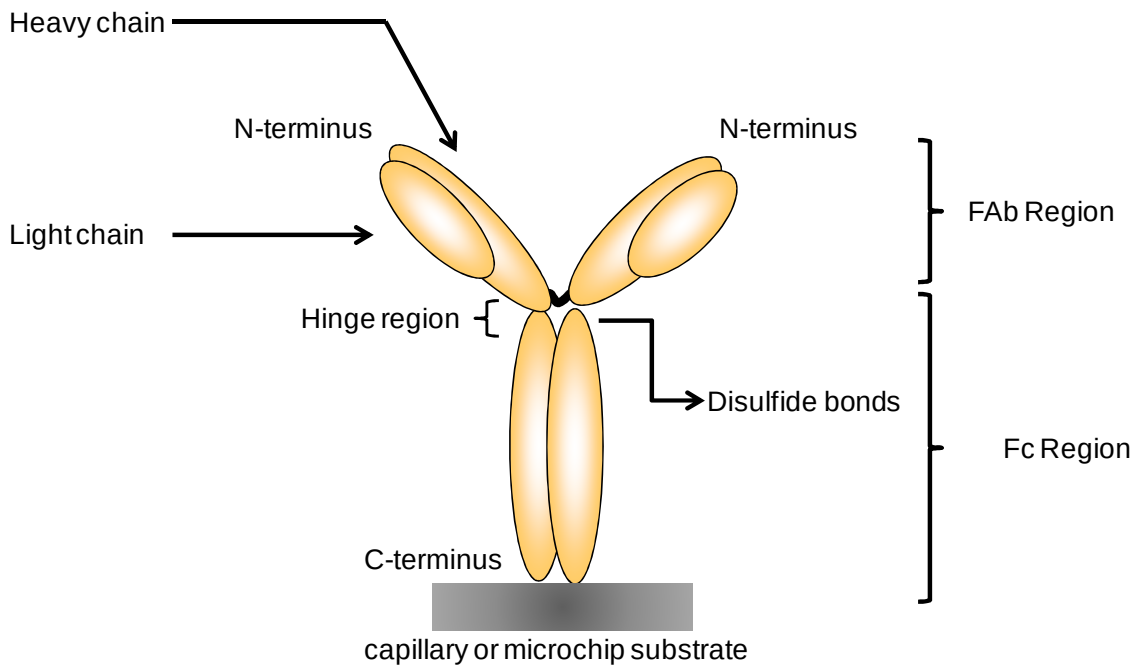

Figure 6.1 Typical antibody schematic illustrating several important regions of the molecule. Figure adapted from [27].

the support surface can be problematic. If attachment chemistries are not specific, antibodies can in effect "lay down" on the support, hindering the availability of the binding site and decreasing the available surface area on which other antibodies can bind [1]. In order to reproducibly immobilize intact antibodies, modifications must be made to both the immobilization surface and the Fc portion of the antibody. One method of immobilizing whole antibodies is to use proteins expressed in the coat of bacteria, namely protein A and G. These proteins are expressed in bacteria to protect the organisms from immune responses in their host organism. Both proteins recognize the Fc portion of the antibody. When these proteins are immobilized onto solid supports they can ensure the proper orientation of antibodies; however, reactivity between protein A and protein G and antibodies is not ubiquitous. The IgG antibodies of some species, for example, do not react with protein A.

Another popular method for immobilizing intact antibodies exploits the high binding affinity of biotin and avidin (or streptavidin). As depicted in Figure 6.2, glass surfaces of capillaries or microchip substrates can be silanized and then activated with a *N*,*N*,'-carbonyl-diimidazole (CDI). Avidin protein is then immobilized via a free amine. Antibodies are biotinylated and will then bind the avidin modified surface. Biotinylation, however, can be carried out at any free amine group and often times this chemistry is not specific enough. Therefore hydrazine chemistries are typically exploited to better control the site of biotinylation. Biotin hydrazine is commercially available. Following oxidation of the carbohydrate moiety on the Fc region of the antibody, preferential biotinylation of the Fc region can be achieved, thus controlling the antibody-surface chemistry. Hage's group utilized this immobilization method to create immunoaffinity restricted access medias (IA-RAM) [5]. Antibodies are first immobilized

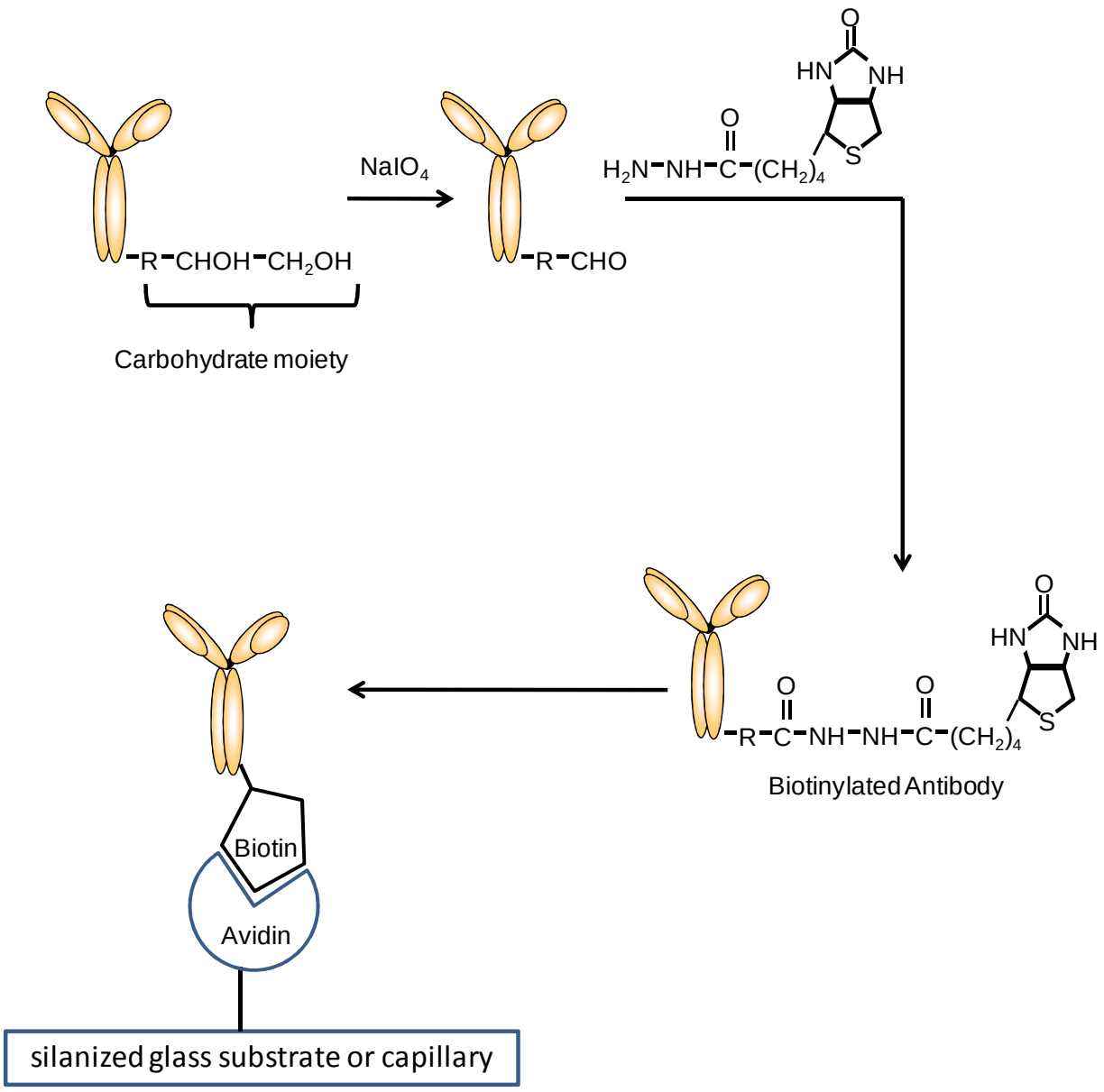

Figure 6.2 Reaction of biotin hydrazine with the carbohydrate moiety on the Fc fragment of an intact antibody. Following this reaction, antibodies are immobilized on a silanized substrate functionalized with avidin. Figure adapted from [27].

on spherical silica particles containing small pores. The spheres are then treated with papain for digestion. Due to steric hindrance, only the antibodies on the outer portion of the supports are digested, thus "disabling" their antigen binding capabilities. The antibodies within the restricted access area remain intact, selectively enabling the devices to capture small analytes of interest and not proteins or other macromolecules (Figure 6.3).

Therefore, antibody fragments are commonly employed in immunosorbent methods. Digestion of antibodies is achieved using either pepsin or papain. The resulting fragments from these two enzymatic reactions are illustrated in Figure 6.4. Pepsin produces one F(Ab') fragment that must be further reduced. FAb fragments retain their antigen binding sites and are more easily immobilized via the free thiol group. Linker molecules are often used to bind the free thiol. This decreases steric hindrance that could interfere with antigen binding. One popular method for the immobilization of FAb fragments onto glass substrates utilizes the bifunctional cross-linker 4-(N-maleimidomethyl) cyclohexane-1-carboxylic-3-sulfo-N-hydroxysuccinimide ester (SSMCC). This is often used when glass capillaries or substrates have been silanized, for example with aminopropyl triethoxy silane. The maleimide functionality of SSMCC reacts with the free thiol groups on the digested antibody fragments, and the succinimide ester is then free to react with amine groups on the substrate surface (Figure 6.5). These chemistries can be performed on the walls of treated capillaries at the sample inlet [6-10] (Figure 6.6) or microchip ports (Figure 6.7).

In addition to direct coupling of the antibodies to the separation device, immobilization on other solid supports such as glass beads [11] and filter papers is feasible. Other examples have utilized sepharose beads [12] functionalized with cyanogens bromide. The beads are

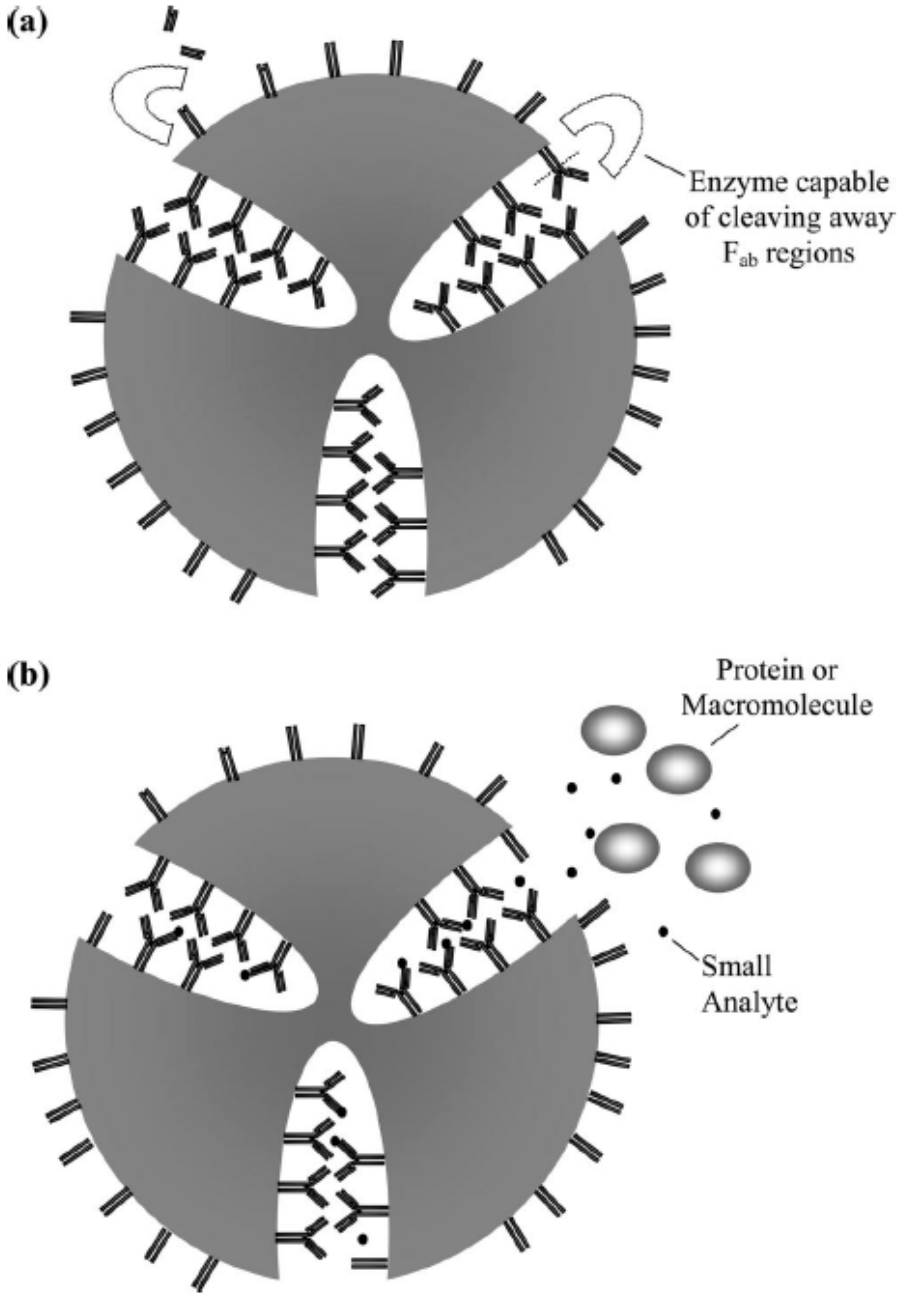

Figure 6.3 Antibodies immobilized via the Fc fragment using hydrazine chemistry. Papain digests the antibodies on the outer sphere (a) while the antibodies within the pores remain intact. This allows the preferential binding of small analytes over large proteins due to steric hindrance. Figure used with permission from [5].

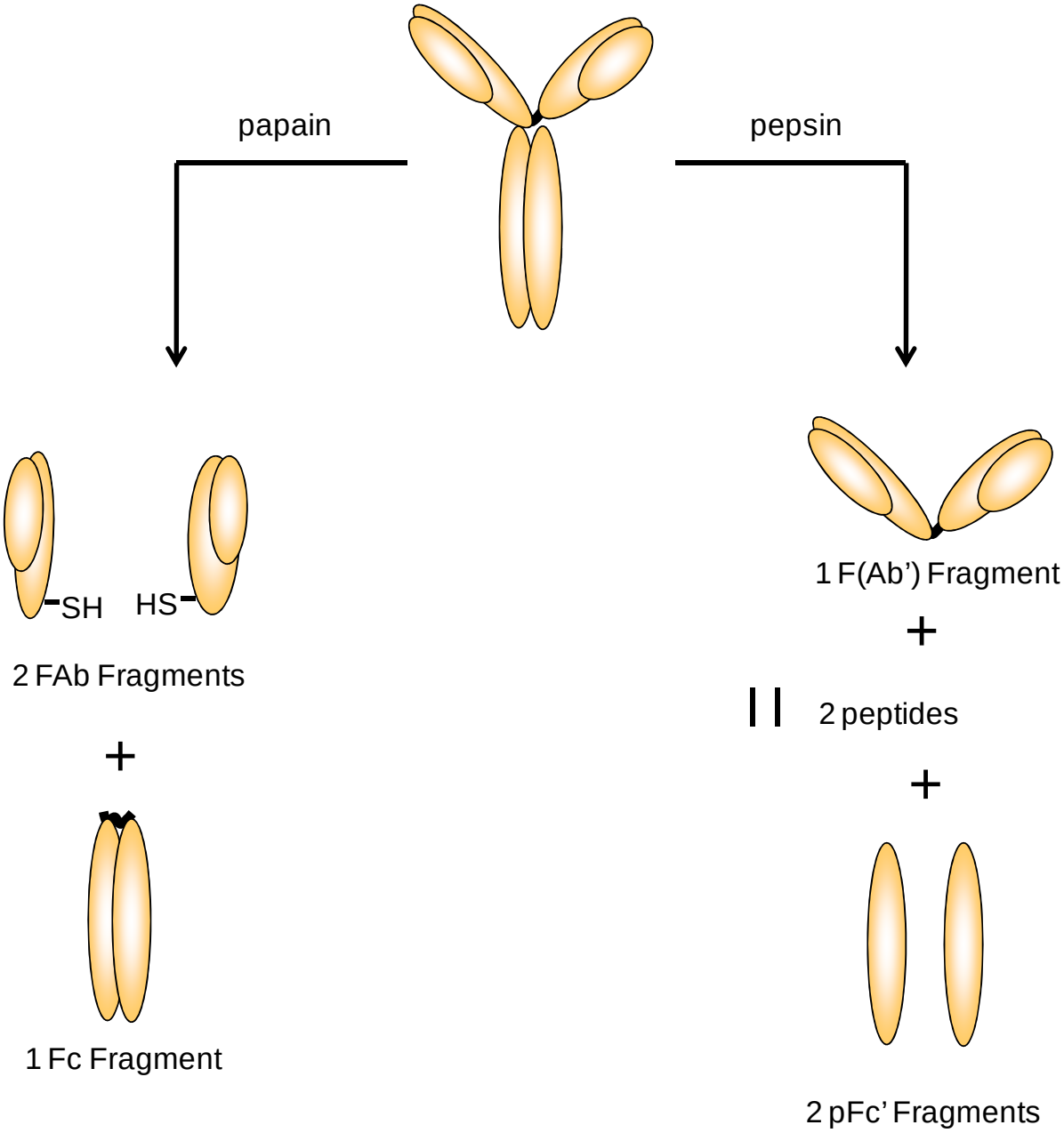

Figure 6.4 Digestion of antibodies with papain and pepsin to produce smaller antigen binding fragments for immobilization via free thiol groups. Figure adapted from [27].

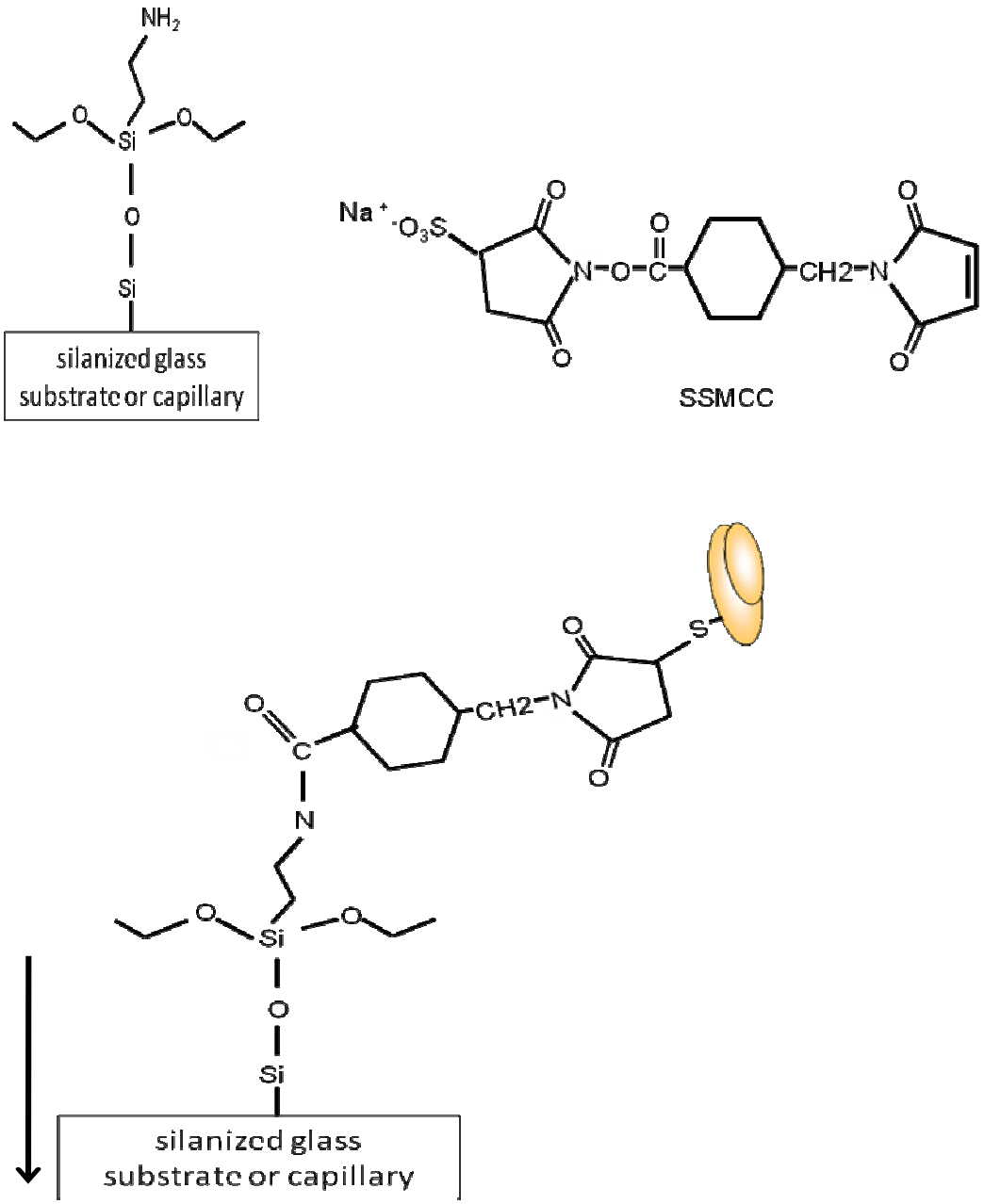

Figure 6.5 Immobilization of FAb fragments via free thiols to a silanized glass surface. SSMCC is used as s linker molecule between the substrate and the antibody. Figure adapted from [27].

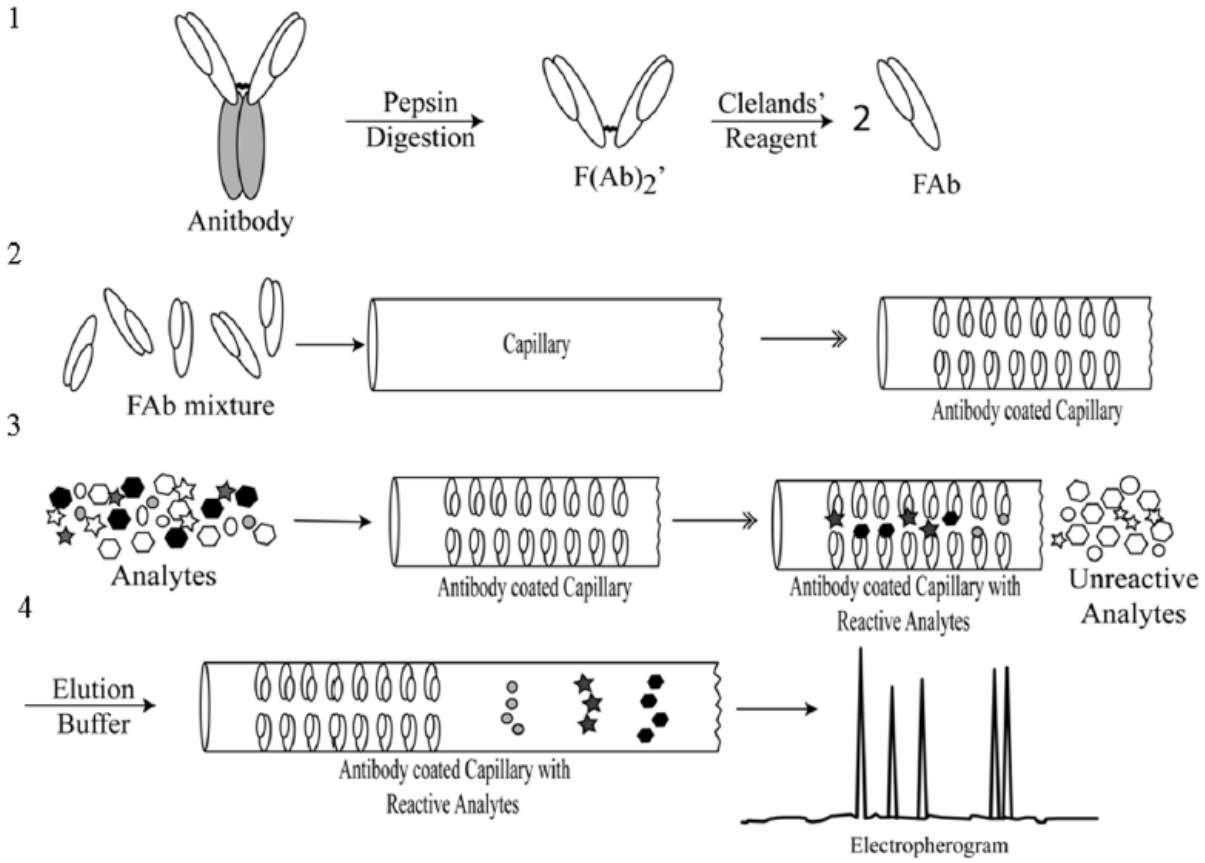

Figure 6.6 Schematic of on-capillary immunoaffinity extraction including antibody digestion (1), antibody immobilization (2), affinity capture of analyte (3), and elution of bound antigen and capillary electrophoresis of bound analytes (4). Figured used with permission from [6].

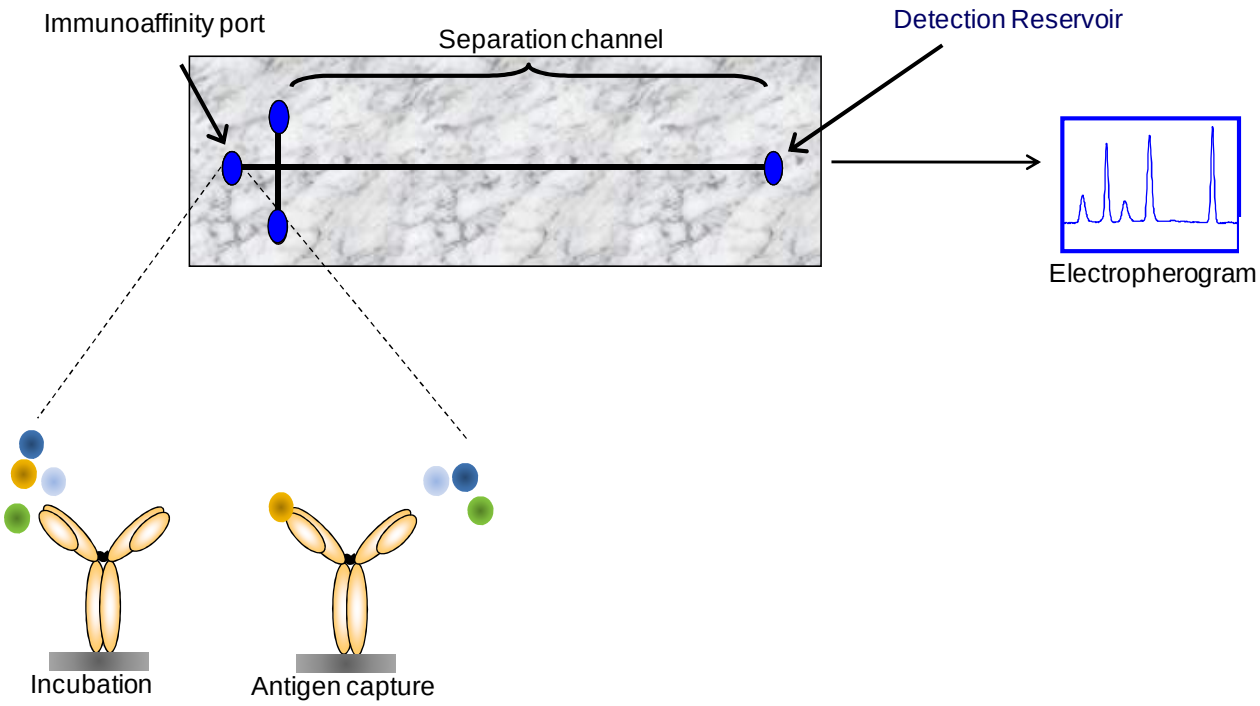

Figure 6.7 Schematic of online microchip immunoaffinity extraction. The process involves several steps including: 1. antibody immobilization, 2. sample incubation, 3. affinity capture of analyte, 4. elution of bound antibody, 5. electrophoretic separation on-chip, and 6. downstream detection.

reacted with the primary amine groups on whole antibodies and then packed into small microreactors or segments of fused silica capillary that are attached to the separation capillary by frits and low volume connectors. Similarly in the microchip systems antibody fragments can be immobilized directly into glass micro-fabricated immunoaffinity ports or onto glass fiber filter papers than can subsequently be placed on chip [13-15]. Monolithic supports have also been functionalized via epoxy groups reacted with the amine groups of whole antibodies in poly(methyl methacrylate) (PMMA) microchips for the detection of human serum albumin (HSA), IgG, green fluorescent protein (GFP), and amino acids [16, 17].

The application of these techniques to pharmaceutical and biological samples of interest has been pioneered largely by the work of Dr. Terry Phillips, Dr. Norberto Guzman, and Dr. David Hage. Research in the Phillip's laboratory has utilized immunoaffinity CE and ME for a variety of applications including the analysis of cellular release following stimulation [6, 8, 9, 18], analysis of proteins and peptides from microdialysates [10], and for clinical applications including analysis from tissue biopsies [15], cytokine clearance profiles in plasma and cerebral spinal fluid (CSF) [19], hormone analysis in blood, saliva, and urine [20], and cyclosporine determination in tears [21]. Kalish and Phillips also reported an immunoaffinity based method for the detection of neurotrophins in the serum of head trauma patients when previously such determinations have only been possible directly from brain tissue or CSF [7]. Guzman and co-workers have utilized immunoaffinity techniques for the determination of endogenous versus exogenously administered erythropoietin (EPO) and EPO analogs [11, 12]. Other groups have utilized immunoaffinity techniques for the quantitation of enatiomeric compounds when immunoassays would not be able to distinguish between such species [22]. Hage's group has developed HPLC immunoaffinity sandwich assays [23, 24]. Using these methods, they were

able to determine free versus bound drugs, such as warfarin, in samples with varying concentrations of serum albumin [23].

While most applications involve antibody immobilization and the detection of labeled antigens, it is also possible to modify supports with the antigen of interest and detect the presence of antibodies. For example, work by Stege *et al* modified magnetic nanobeads with the antigens of Helicobacter pylori (H. pylori), a gram negative bacterium responsible for chronic active type B gastritis and peptic ulcer diseases [25]. Magnetic beads were held in place at the inlet of the capillary by an external magnet. Antigen immobilization, incubation with serum samples, and secondary labeled antibody attachment were all performed on-capillary prior to separation. This method enabled the detection of anti-H pylori IgGs in human serum. Similarly, a microchip method has also been developed for the determination of naproxen in serum of patients taking the anti-inflammatory drug. In this system, anti-naproxen antibodies were fluorescently labeled off-chip. Serum samples were reacted with these antibodies on-chip and the antigen-antibody complex as well as free antibody was detected by laser-induced fluorescence detection (LIF) [26].

Previous chapters in this thesis have described both CE and LC-MS/MS methods for the detection of Dyn A 1-17 and four of its metabolites. These methods, however, still lack the sensitivity necessary to quantitate endogenous concentrations (low picomolar) of the peptides of interest. As stated in previous sections of this thesis, immunoassays are commonly employed for the detection of neuropeptides, and detection limits in the low ng/mL range are typically achieved. While these assays boast low limits of detection, cross-reactivity significantly hinders their applicability to metabolism studies. Therefore, combining the sensitivity of immunoassay with the efficiency of electrophoretic separation has the potential to revolutionize investigations

of peptide metabolism and transport at the blood brain barrier. In particular, the incorporation of immunoaffinity ports onto miniaturized platforms (microchips) enables integrated sample clean-up and preconcentration prior to electrophoretic separation on a single device (Figure 6.7). Further, the inclusion of on-chip labeling and integrated sampling from microdialysis probes will result in a micro total analysis system (μTAS) that has the potential for on-animal applications. Continuous, real-time monitoring of neurochemical processes in awake, freely moving animals can be correlated to animal behavior using telemetry and time-stamped video.

For application of this approach in an on-animal separation based sensor system, the processes described above must be extensively characterized and optimized. To that end, Chapter 2 of this thesis focused on the development of a CE separation of Dyn A 1-17 from several of its metabolites. The current chapter will review immunoaffinity techniques employed for both capillary and microchip electrophoresis (CE and ME respectively), as well as describe the characterization of the immunoaffinity portion of an integrated microchip device for the detection of dynorphin peptides. Some shortcomings of current microchip platforms will be addressed, particularly as they relate to detection options, microchip substrates, and the practicalities of separating closely related species such as peptide metabolites.

6.2 Materials and Methods

6.2.1 Reagents

All dynorphin peptides and antibodies were purchased from Bachem (King of Prussia, PA, USA). Goat anti-rabbit IgG was purchased from Sigma (St. Louis, MO, USA). Alexa Fluor® 633 was obtained from Molecular Probes, Invitrogen (Carlsbad, California, USA). All other reagents were obtained from Sigma (St. Louis, MO, USA).

6.2.2 Antibody screening with traditional microplate ELISAs

A standard enzyme linked immunosorbent assay (ELISA) was performed to screen antibodies to various dynorphin peptides. Several solutions were made including: PBS, PBS with 0.05% Tween 20, carbonate coating buffer and caesin blocking solution (instructions to follow). The carbonate coating buffer consisted of sodium carbonate (40.5 mM), sodium bicarbonate (35.7 mM), and sodium azide (3.0 mM), pH 9.8. Caesin blocking solution was made by combining 5.2 g NaOH, 80.0 g casein (Difco Skim Milk Powder), 4.6 g Tris HCl, 8.0 g sodium azide, and 27.8 g NaCl in 4 L H_2O, pH 7.5. Note: caesin should be added slowly as it will take time to dissolve. Also, when adjusting the pH with HCl, caesin may precipitate. Therefore, add a small amount of HCl, stir to resuspend caesin, and then test the pH.

All reagents plated were 100 μL unless otherwise noted. The procedures used in these studies were adapted for these studies with assistance from Dr. Terry Phillips (NIH) and Dr. Brooke Barrett (Middaugh group, University of Kansas) [27]. All peptides were first diluted in carbonate coating buffer to a final concentration of 10 μg/mL, and incubated in each well of a 96-well plate overnight at 4°C. Samples were removed, and wells were filled with 250 μL caesin blocking solution for 30 minutes at room temperature to prevent non-specific adsorption in the

following steps. Wells were then emptied and the primary antibody diluted in blocking buffer was added at a range of concentrations (0.625, 1.25, 2.5, 5, 10, 20, and 40 μg/mL) and allowed to react for 1 hour at room temperature.

Following incubation with the primary antibody, wells were washed three times with PBS containing 0.05% Tween 20 and once with PBS buffer alone. Then the secondary antibody (goat anti-rabbit IgG) diluted in PBS was added and allowed to react for 30 minutes at room temperature. Next, wells were washed three times with PBS + 0.05% Tween 20 and once with PBS buffer alone. The substrate, 3,3',5'-tetramethylbenzidine (TMB), was added and incubated for 30 min at room temperature. Two molar HCl was then added to quench the reaction. Plates were read with a UV SpectraMax M5 microplate spectrophotometer (Molecular Devices, Sunnyvale, CA) at 450 nm within 10 minutes of HCl addition.

In this work, anti-dynorphin A 1-17 was purchased from Bachem and screened by ELISA in a traditional 96-well plate format. The following dynorphin peptides were screened: Dyn A 1-17, 2-17, 1-13, 1-8, and 1-6 as well as leucine enkephalin. Bradykinin was used as a negative control since this peptide differs structurally from the opioid peptides of interest. Reactivity with bradykinin would be unexpected, and since it is also a neuropeptide, screening for its reactivity with anti-Dyn A 1-17 is of interest. Blank wells (PBS only, no peptide added) are also reported.

6.2.3 Antibody screening with magnetic beads

Dynorphin antibodies were prepared for attachment to magnetic nanobeads via procedures described previously [27]. Commercially available antibodies were reconstituted in 18 MΩ deionized (D.I.) water from a benchtop Milli-Q Synthesis A10 Water Purification System (Millipore, Billerica, MS, USA) as per product instructions. EZ-Link™ Sulfo-NHS-LC-

LC-Biotin (Pierce Biotechnology, Rockford, IL, USA) was dissolved in calcium chloride and heated to 45°C. Equal volumes of antibody and biotin were then combined and allowed to mix for 1 hour. The biotinylated antibody solution was dialyzed overnight at 4 °C against PBS. Streptavidin-coated magnetic beads (Polysciences Inc., Warrington, PA, USA) were washed with PBS and mixed with biotinylated antibody solution in a 1:1 ratio (by volume). After 30 minutes, the beads were washed three times with PBS. When not in use, the modified beads were stored in PBS at 4 °C.

Antibody screening was performed for each dynorphin peptide of interest. Equal volume of antibody-coated beads and peptide were combined in a polypropylene microcentrifuge vial and heated (37 °C) on a benchtop shaker for 2 hours. Following the incubation period, the microcentrifuge vial was placed in a magnetic base collecting the beads and any bound antigen to the side wall of the tube. The unbound fraction was then collected into an empty microcentrifuge vial and the beads were washed three times with PBS. Following the last wash, HCl (0.1 N) was added to the vial to elute the captured antigen. This elution buffer was incubated with the beads and again heated (37 °C) on a benchtop shaker for 15 minutes. The vial was then placed back in the magnetic base and the bound fraction collected for labeling.

Labeling with Alexa Fluor® 633 was then accomplished under basic conditions (10 mM sodium borate, pH 9.5) for efficient labeling. A 200 μL aliquot of the bound fraction was diluted in separation buffer (10 mM sodium borate, pH 9.5) to raise the pH, and then 50 μL of a 1 mg/mL Alexa Fluor® solution (in *N*,*N*-dimethyl formamide, DMF) was added and allowed to mix at 4 °C overnight. The labeled fractions were then analyzed on a Micralyne μTK

microfluidic electrophoresis system (Micralyne, Edmonton, Canada) that is described in more detail in the next section.

6.2.4 Determination of dynorphin and metabolites by microchip electrophoresis

6.2.4.1 ME with LIF Detection

Microchip analysis was performed on a Micralyne μTK microfluidic electrophoresis system (Micralyne, Edmonton, Canada). The system is equipped with eight platinum electrodes and a 635-nm, 8-mW red diode laser. Detection was achieved using an epiluminescence confocal microscope coupled with a Hamamatsu H5773-03 photomultiplier tube and 16-bit data acquisition. The system was also equipped with a chip stage form-fitted to accept Micralyne standard 16 mm x 95 mm x 2.2 mm deep microchips (described below). The entire system was run on a personal computer running Microsoft Windows 2000 with a compiled LabView interface.

Low fluorescence "Borofloat" glass chips were purchased from Micralyne. The standard chip format was made of two 20 μm deep x 50 μm wide semi-circular channels arranged in an offset T. Each channel has a port (2.0 mm diameter x 0.1 mm deep) at its end into which buffers and samples can be loaded. The separation channel was 8 cm in total length (7.5 cm to the detector). A variety of separation voltages were investigated for the separation of the dynorphin peptides. On-chip injections were performed by applying 1.0 kV between the sample (S) and sample waste (SW) reservoir for 5.0 seconds while maintaining the buffer (B) and detection reservoirs at ground to prevent leakage of the sample into the separation channel. Separation and injection of a discrete plug of analytes was achieved by applying a separation voltage (1.0 and

3.5 V) between the buffer and detection reservoirs while maintaining ground at the sample and sample waste reservoirs.

Dynorphin peptides were derivatized with Alexa Fluor® 633 prior to detection. Stock solutions of Alexa Fluor® were made in DMF (1 mg/mL). Dynorphin stock solutions, also 1 mg/mL, were made in PBS. Equal parts (v/v) of peptide and dye were combined and allowed to react overnight at 4 °C. Labeled peptide solutions were stored in 20 μL aliquots at -20 °C and thawed immediately prior to use. Fresh labeled peptides were replaced at the beginning of each week.

6.2.4.2 ME with amperometric detection

The fabrication of glass-PDMS microchips with pyrolyzed photoresist carbon electrodes has been described previously [28, 29]. The following chemicals were used as received for fabrication procedures: AZ 1518 positive photoresist and AZ 300 MIF developer (Clariant, Somerville, NJ, USA); S1818 positive photoresist and Microposit 351 developer (Microchem, Newton, MA, USA); SU-8 10, SU-8 2 negative photoresist and SU-8 developer (MicroChem); 100 and 127mm silicon (Si) wafers (Silicon, Boise, ID, USA); and Sylgard 184 (Ellsworth Adhesives, Germantown, WI, USA). In addition, the following were utilized for microchip construction: Pt wire (22 gauge) (Fisher Scientific, Fairlawn, NJ, USA), high-temperature fused silica glass plates (4 in x 2.5 in x 0.085 in; Glass Fab, Rochester, NY, USA), conductive epoxy (ITW Chemtronics, Kennesaw, GA, USA), and colloidal silver liquid (Ted Pella, Redding, CA, USA).

PDMS electrophoresis channels were fabricated using SU-8 10 negative photoresist that was spin coated on a 100 mm Si wafer and subjected to a soft bake procedure. A negative tone

transparency film was placed over the coated wafer, brought into hard contact, and exposed to a near-UV flood source. Following exposure, both wafers were post-baked, developed in SU-8 developer, rinsed with isopropanol, and dried under nitrogen. A 10:1 ratio of PDMS was used for all analyses. A simple ‘‘T’’ device containing a 3.5 cm separation channel (from the T intersection to the end of the separation channel) and 0.75 cm side arms was employed. The width and depth of the electrophoresis microchannels were 50 and 14 mm, respectively.

Fabrication of pyrolyzed photoresist electrodes has been described previously by our group [29]. Briefly, either AZ 1518 or S1818 positive photoresist was dynamically coated on a fused silica glass plate. The coated plate was prebaked, then covered with a positive transparency film, and exposed to a near-UV flood source. After exposure the plate was developed, rinsed with 18.2 MΩ water, dried under N_2, and subjected to a post-bake procedure. A Lindberg/Blue M Three-Zone Tube Furnace (Cole-Parmer, Vernon Hills, IL, USA) was utilized for pyrolysis. The furnace was continuously flushed with nitrogen at 5 psi to provide an inert atmosphere. The temperature of the furnace started under ambient conditions and was increased at the rate of 5.5 °C/min to 925 °C, held for 1 h, and then allowed to cool to room temperature. The resultant width of the PPF electrodes was 40 mm and the height was determined with a surface profiler to be 0.6 mm.

Electrophoresis was carried out in unmodified PDMS microchannels using a programmable Jenway Microfluidic Power Supply (Dunlow, Essex, UK). The buffer was degassed (Fisher Ultrasonic Cleaner, Fisher Scientific) and filtered with a 0.22 mm teflon filter before use. The PDMS channels were first flushed with 0.1 N NaOH for 3–5 min, then rinsed with 18.2 MΩ H_2O, and finally filled with buffer by applying a vacuum. Electrophoresis was performed by applying a high voltage (+ 1400 V) at the buffer reservoir (B) and a fraction of this

high voltage (+ 1200 V) at the sample reservoir (S), whereas the sample waste and detection reservoirs were grounded. A gated injection method was used for introduction of the sample plug and was achieved by floating the high voltage at the buffer reservoir for the duration of the injection before returning it to + 1400 V.

Amperometric detection was accomplished using a CHI 802B EC analyzer (CH Instruments, Austin, TX, USA) and the current response was recorded using the built-in software package. A three electrode system (working, Ag/AgCl reference, and Pt wire auxiliary) was used. For all data reported, the working electrode was set at a potential of + 900 mV (versus Ag/AgCl) and end channel alignment was used.

6.2.5 Conventional capillary electrophoresis for the separation of pain-related neuropeptides

Separations were performed on a Beckman Coulter PACE/MDQ (Brea, CA, USA) with LIF detection at 488 nm. The system was controlled using 32 Karat software, and all subsequent data analysis was performed with this software as well. Fused-silica capillaries (50 ìm id x 360 ìm od) were obtained from Polymicro Technologies (Phoenix, AZ, USA) and cut to a 50 cm length (40 cm to detector). A small window was burned through the polyimide coating 10 cm from the capillary end for LIF detection. Pressure injections were performed at 6.9 kPa for 5.0 seconds, and a separation voltage of 20 kV was applied with the anode at the injection end. Buffer was composed of 150 mM boric acid, and 7.5 mM sodium dodecyl sulfate (SDS), pH 9.5.

6.3 Results and Discussion

6.3.1 Antibody Screening

Commercial antibodies are available to a variety of dynorphin peptides. Prior to immobilization in a capillary or microchip format, the cross-reactivity of the antibodies were screened to determine the reactivity with Dyn A 1-17 and related compounds (i.e. metabolites). In this work, the reactivity of anti-Dyn A 1-17 towards the dynorphin peptides was determined using the ELISA protocol described in section 6.2.2 of this thesis. The response from incubation with 20 μg/mL antibody is presented in Figure 6.8. As can be seen, significant cross-reactivity with the des-tyrosine metabolite (Dyn A 2-17) occurs. No reactivity was observed with smaller dynorphin peptides, suggesting that the epitope for binding is somewhere at the C-terminal end of the peptide or is contingent upon a structural element that is absent in shorter peptide fragments. Thus if an immunoaffinity microchip analysis system is to be made for the investigation of dynorphin metabolism, additional antibodies must be incorporated that will react with the smaller, N-terminal metabolites.

To this end, an antibody to Dyn A 1-8 was purchased and evaluated in the same ELISA protocol (section 6.2.2) as the above anti-Dyn A 1-17. In this assay, immune-reactivity was not observed with any of the dynorphin metabolites (Figure 6.9). One possible explanation would be that the quality of the antibody itself was poor. However, another possible reason, particularly in the case of such a small antigen, would be that immobilization of the peptide on the microplate actually buried the epitope, preventing the antibody from reacting with even its intended antigen, as seen by the lack of reactivity with Dyn A 1-8. In order to determine if this was the case, an additional assay in a solution format was performed utilizing magnetic beads. Analysis was

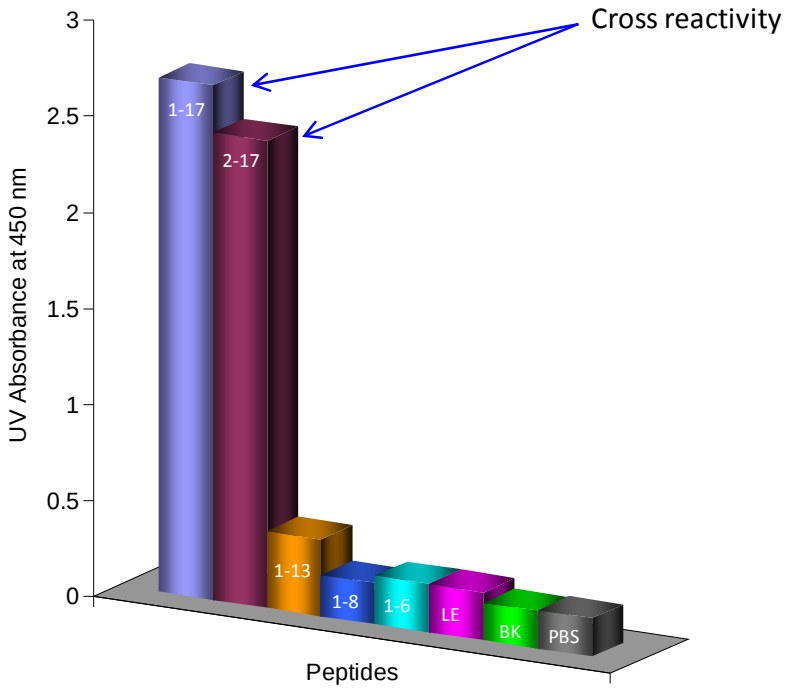

Figure 6.8 Cross reactivity exhibited between Dyn A 1-17 and Dyn A 2-17 following a traditional plate ELISA with anti-Dyn A 1-17

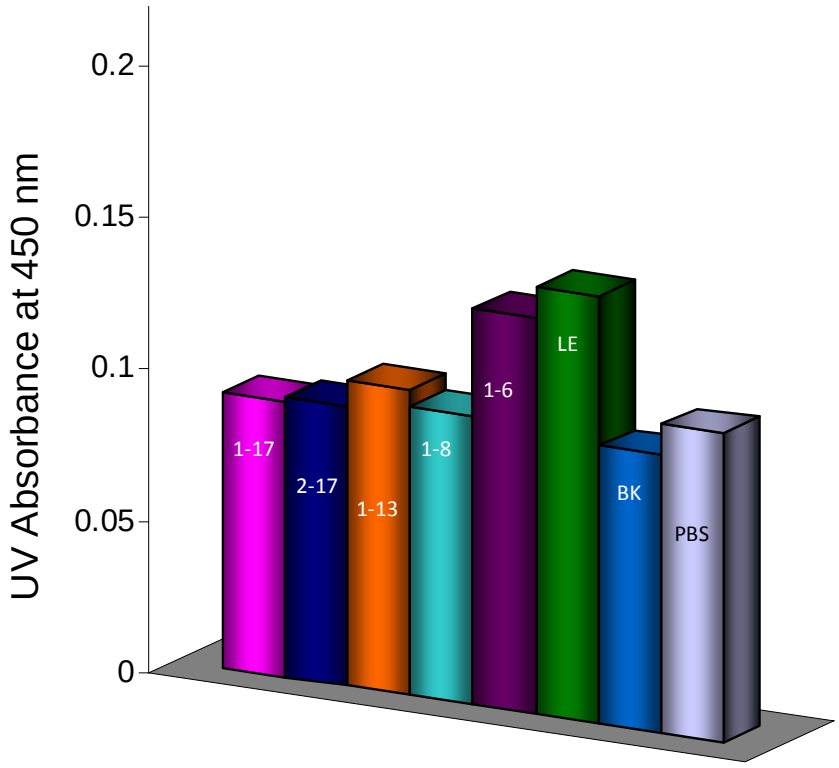

Figure 6.9 Traditional plate ELISA with anti-Dyn A 1-8 exhibiting a lack of reactivity with any of the dynorphin peptides screened.

performed offline by microchip electrophoresis with laser induced fluorescence detection. This protocol is detailed in section 6.2.3 of this thesis. A schematic of the process is shown in Figure 6.10, and the chip design is presented in Figure 6.11. With this assay, reactivity with Dyn A 1-8 was observed; however, cross-reactivity with other N-terminal metabolites was not (Figure 6.12 A and B). Therefore it would still be necessary to screen and immobilize additional antibodies before creating a fully functional immunoaffinity separation device for the investigation of Dyn A 1-17 metabolism.

6.3.2 Determination of dynorphin peptides by microchip electrophoresis

6.3.2.1 Amperometric detection of copper-complexed dynorphins

The simplest microchip substrates for use with amperometric detection are polydimethylsiloxane (PDMS) or PDMS-glass hybrid devices. The PDMS can be reversibly sealed over a glass or PDMS substrate that has a metal or carbon electrode previously microfabricated or micromolded onto it (Figure 6.13). Our group has found a variety of uses for such devices including the detection of reactive oxygen species such as peroxynitrite [30], neurotransmitters [28, 29], and small peptides [31, 32].

Chapter 3 of this thesis described the optimization of a CE separation of dynorphin peptides using copper complexation and UV detection. Copper complexation has the unique capability of rendering even the des-tyrosine metabolites of Dyn A 1-17 electroactive. It has been shown previously in our group, with angiotensin peptides and leucine enkephalin, that amperometric detection of the peptide-copper complexes following CE is feasible and improves limits of detection in comparison to UV detection [33-35]. Gawron *et al* were able to detect des-Tyr Leu-enkephalin at a dual carbon fiber electrode in an all PDMS chip (following

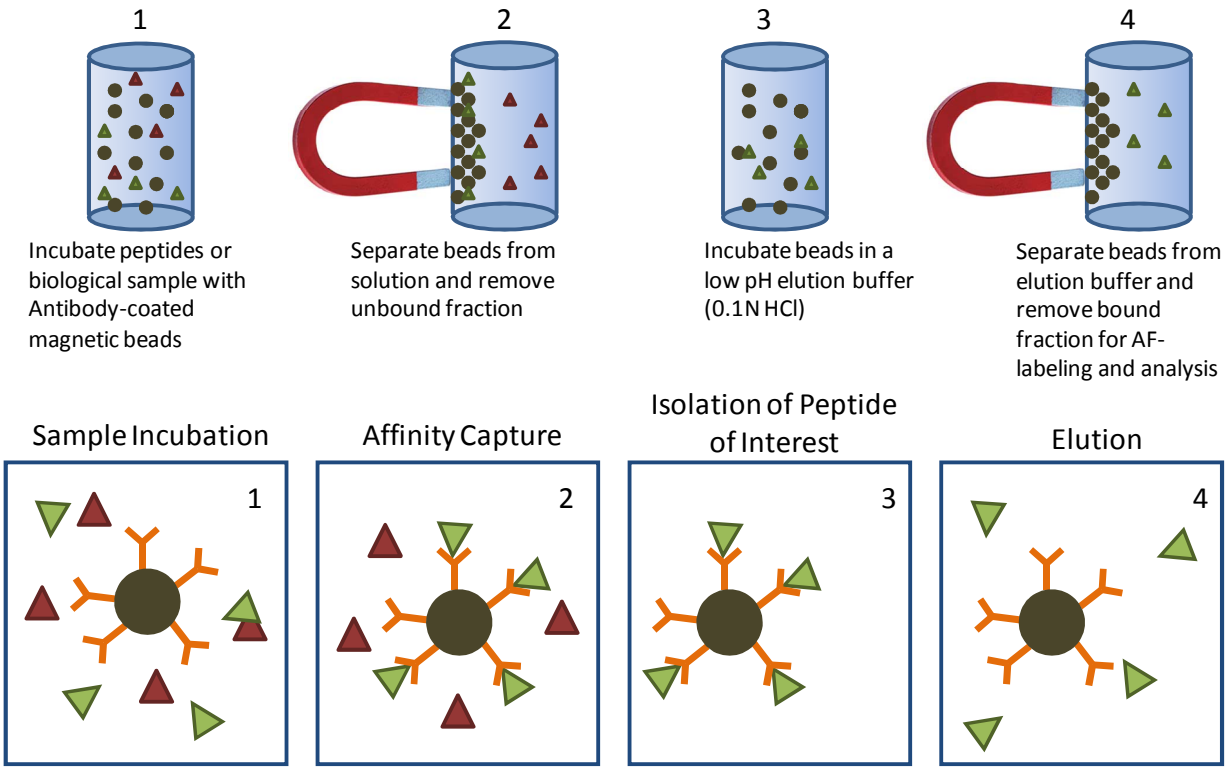

Figure 6.10 Schematic of the offline immunoaffinity extraction with magnetic beads as performed for screening anti-Dyn A 1-8 reactivity. Dyn A 1-8 (green triangles) binds to the antibody-coated beads. Unbound peptides (red triangles) are removed in step 2 of this process.

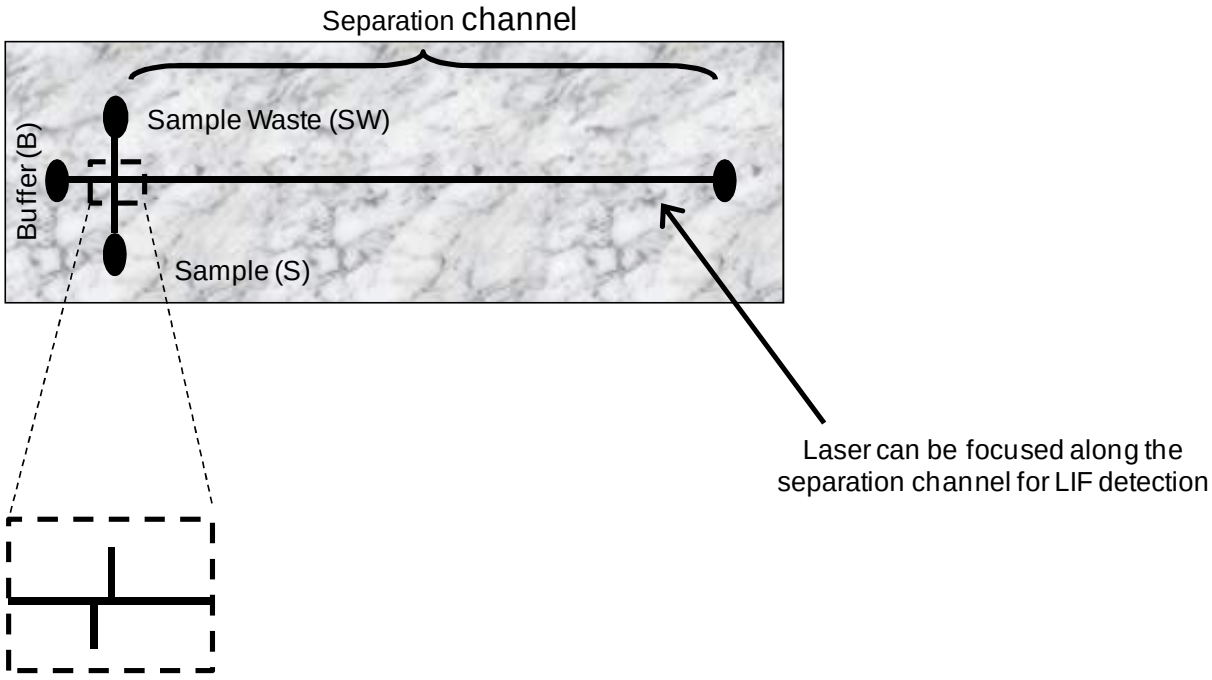

Figure 6.11 Micralyne Standard "borofloat" glass microchip with 8 cm separation channel and an offset 'T' for injection.

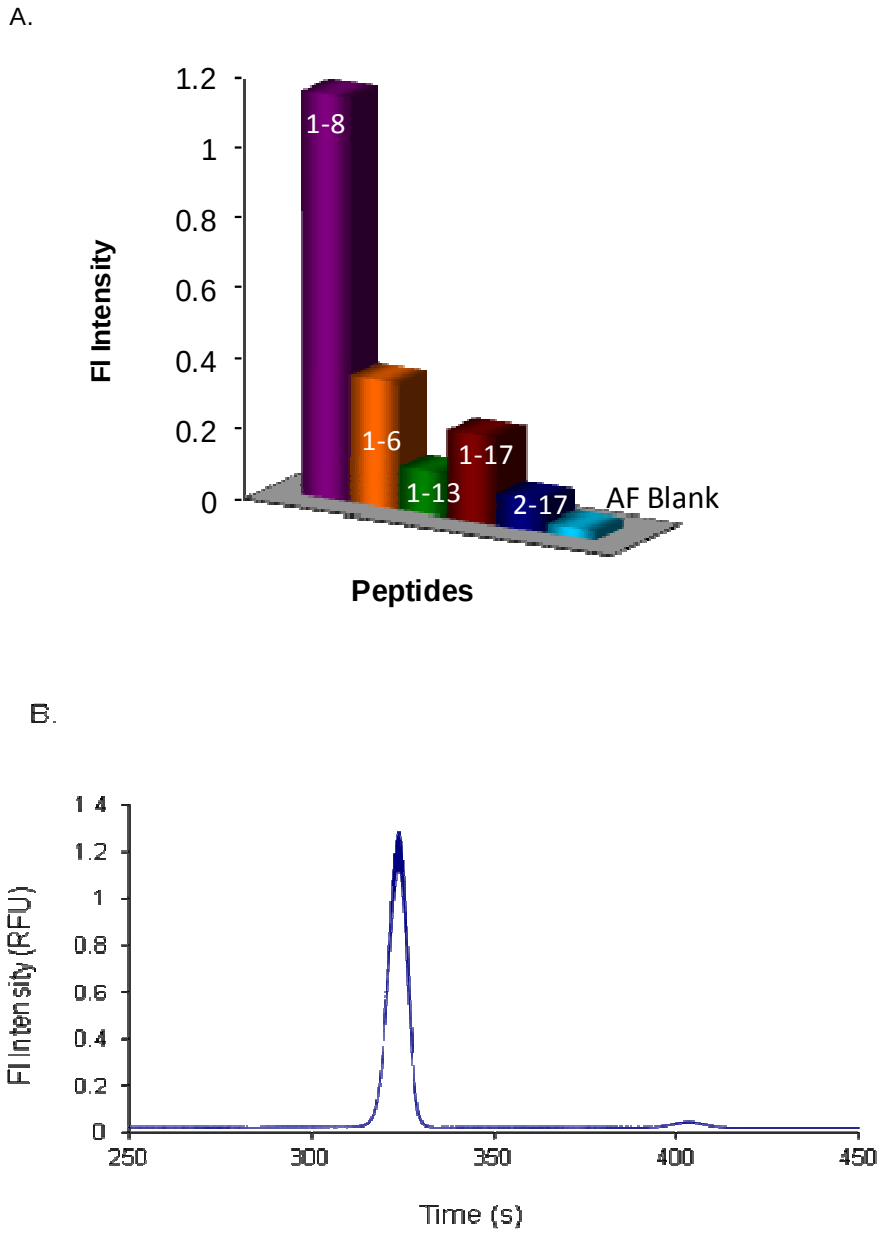

Figure 6.12 Reactivity of dynorphin peptides with anti-Dyn A 1-8 following off-line antibody screening with magnetic bead assay (A). Microchip electropherogram of Dyn A 1-8 following antibody binding, elution, and labeling with Alexa Fluor ® 633 prior to injection and detection on-chip.

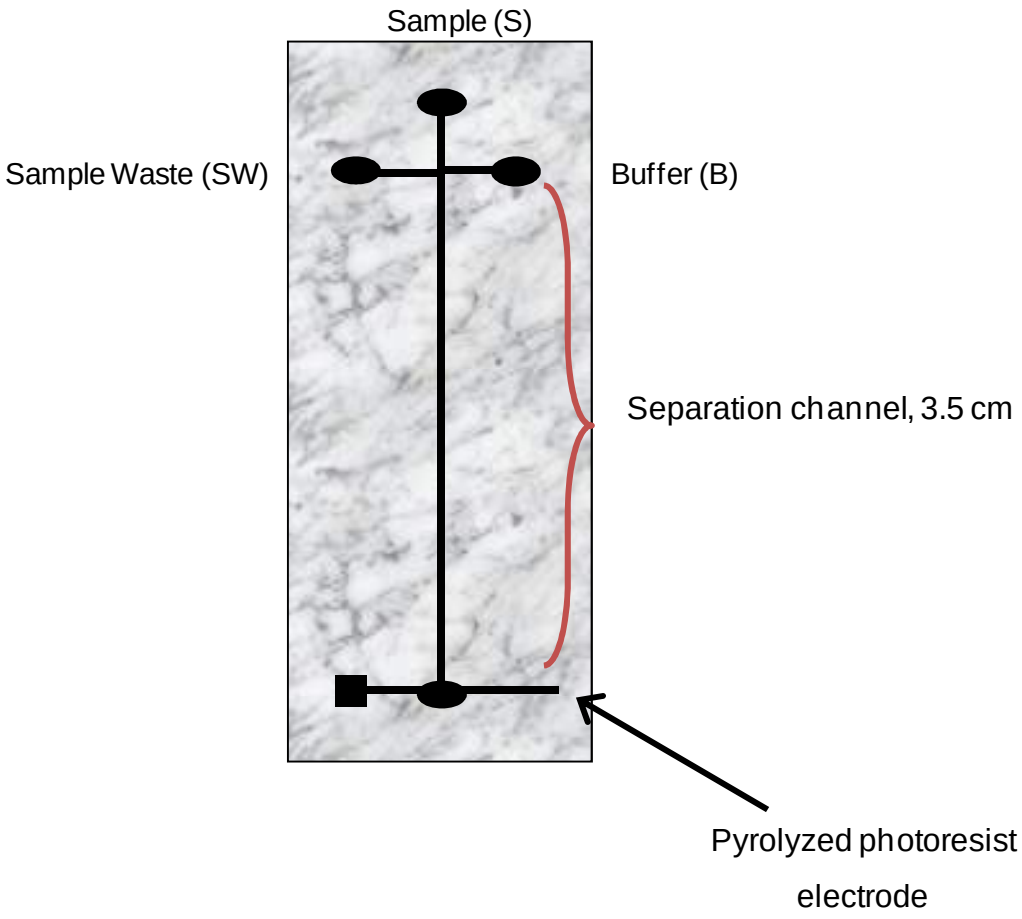

Figure 6.13 Glass-PDMS microchip for amperometric detection with a pyrolyzed photoresist carbon electrode.

precomplexation with copper) [31]. Follow up work demonstrated the use of PDMS microchips with a dual carbon paste electrode for the separation of the tripeptide Tyr-Gly-Gly from des-Tyr-Leu-enkephalin [32]. Both experiments, however, were performed at extremely high concentrations (high hundreds of micromolar) and further characterization was not performed.

Unfortunately, several issues arose when analyzing dynorphin-copper complexed peptides by microchip electrophoresis with amperometric detection. First, even the smallest metabolite investigated, Dyn A 1-6, exhibited extremely broad peaks migrating over minutes as opposed to the seconds normally observed in ME (Figure 6.14). This occurred even with inclusion of the surfactant SDS which has been shown previously to prevent such non-specific adsorption. Secondly, only extremely high concentrations of dynorphin were detected under these conditions. This is likely due to non-specific adsorption of dynorphin peptides to the PDMS surface of the microchip channels. Peptides have been shown previously to adsorb to the surface of PDMS. Lacher *et al* compared the behavior of substance P (SP) on PDMS and Pyrex microchips and observed considerable adsorption of SP to the PDMS surface [36].

One might assume that a simple solution would therefore be to change the microchip substrate material, especially since a commonly stated advantage of such devices is fabrication from a variety of materials. Electrodes for detection, however, are not easily incorporated into other microchip materials such as glass and plastic. The permanent thermal-bonding typically employed for bonding the chips made of these substrates can be disrupted by the raised electrode material. Also the high temperatures used for bonding can destroy the electrodes. Therefore, laser induced fluorescence detection on all glass microchips was investigated in these studies.

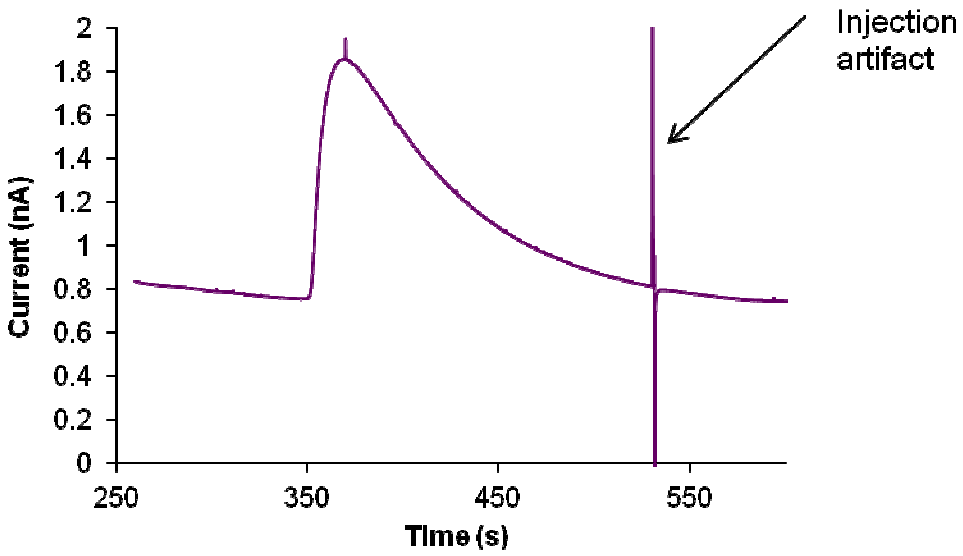

Figure 6.14 Detection of copper complexed Dyn A 1-6 (250 μM) on a glass-PDMS Microchip for amperometric detection with a pyrolyzed photoresist carbon electrode (detection voltage = +900 mV versus Ag/AgCl). Background electrolyte: 25 mM sodium borate, pH 9.0. Sample buffer: 25 mM sodium borate, 3 mM tartaric acid, 2 mM $CuSO_4$, pH 9.0.

6.3.2.2 Laser induced fluorescence detection of Alexa Fluor® tagged dynorphins

The detection of peptides by laser induced fluorescence detection involves tagging of the peptides with a fluorescent moiety prior to analysis. An attractive family of dyes is the Alexa Fluor® tags (Molecular Probes, Invitrogen). These compounds are sulfonated derivatives of commonly used dyes (coumarins, cyanine, rhodamine, and xanthenes, i.e. fluorescein) that offer improved stability and brighter fluorescence. These dyes are also less pH sensitive, making the use of a variety of background electrolytes feasible. Alexa Fluor® 633 has been used extensively by Dr. Terry Phillips in his work with both conventional and microchip separations [6-7, 9, 13-15, 26]. Primarily the applications in his group focus on cytokines, peptides, and proteins of neurochemical interest. Work with small peptides (less than MW = 1000) has not been extensively explored.

Conjugation of this dye to small peptides presents a challenge for the electrophoretic separation, as evidenced by the co-migration of Dyn A 1-6 and Dyn A 1-17 shown in Figure 6.15. This is especially true in a miniaturized device that has a separation channel that is only 8 cm in length. The dynorphin peptides used in these studies range in molecular weight from 711.82 to 2147.52 g/mol. When these small peptides are tagged with Alexa Fluor® (MW = 1200 g/mol), the mass to charge ratios are made increasingly similar. In fact, for some of the peptides of interest, the dye is larger than the peptide itself. For all intents and purposes, the mass to charge ratio of the dye is really what is being altered under such conditions. Ultimately the resulting AF-dynorphin peptides are very similar and therefore difficult to resolve in an 8 cm

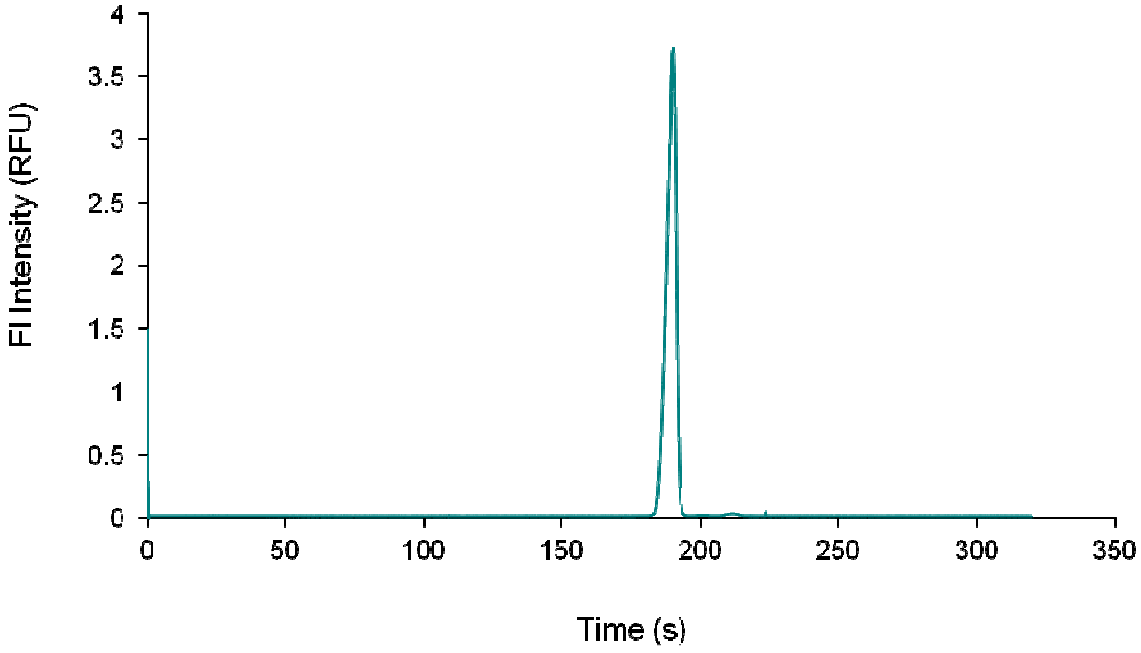

Figure 6.15 Detection of Alexa Fluor® 633-labeled Dyn A 1-6 and Dyn A 1-17 (each 5 μg/mL) on a glass microchip (8 cm separation channel). Run buffer consisted of: 20 mM sodium borate, 0.1% IgePal, pH 9.0, with a 1.0 second injection and 2.5 kV applied separation voltage.

channel. A smaller Alexa Fluor® dye, AF 532 (MW = 721) was therefore investigated. Tagging was performed in the same manner as with the AF-633 and a Micralyne system with a 532 nm laser was utilized. A significant decrease in sensitivity was observed using the AF-532 dye, and there were no improvements with respect to dynorphin resolution observed (Figure 6.16).

To improve upon the resolution of AF-633-tagged dynorphin peptides, a variety of buffer conditions were investigated. These are summarized in Table 6.1. First, different background electrolyte systems, including sodium tetraborate, boric acid, tris borate EDTA, and sodium phosphate, were explored. These investigations included a wide range of buffer concentrations as well as pH values in the hopes of slowing the electroosmotic flow (eof) for improved resolution. Concentrations of buffers greater than 20 mM often resulted in bubble formation and currents that were too high for the system; therefore these were not explored.

In addition to investigating various background electrolytes and fluorescent dyes, two surfactants were evaluated in the run buffers. As discussed in Chapter 2, phytic acid was used to prevent adsorption of the basic peptides to the negatively charge silanol groups of the capillary wall. This compound unfortunately increases the background current significantly which was found to be problematic in the microchip format. Fortunately, a similar effect can be achieved with detergents, without the corresponding increase in current. For these studies, two surfactants were investigated: Brij® 35 and Igepal® CA-630 (structures shown in Figure 6.17). Brij 35 was found to not be very effective at preventing adsorption, and therefore its use was not explored extensively. No peaks were observed upon initial peptide injections with this additive in the run buffer, and then after several runs, the labeled peptide would leach from the glass surface resulting in a large increase in background fluorescence. IgePal®, however, gave more promising results. It is a non ionic, non-denaturing detergent that has been shown to prevent

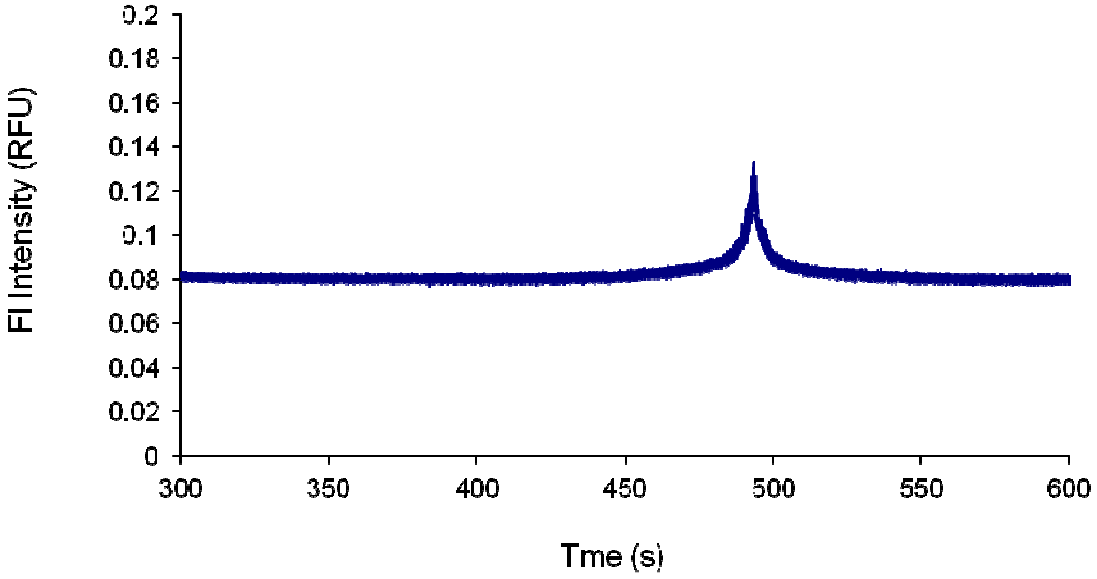

Figure 6.16 Detection of Alexa Fluor® 532-labeled dynorphin peptides, 1-6 , 1-8, 1-13, 1-17, and 2-17 (each 5 μg/mL) on a glass microchip (8 cm separation channel). Run buffer consisted of: 20 mM sodium borate, 0.1% IgePal, pH 9.0, with a 1.0 second injection and 1.0 kV applied separation voltage.

Background Electrolyte	Concentration (μM)	pH	Surfactant(s) (0.1% v/v)	Organic Modifier
Sodium Tetraborate	5	9.0	IgePal®	
Sodium Tetraborate	10	8.0	IgePal®	
Sodium Tetraborate	10	8.5	IgePal®	
Sodium Tetraborate	10	9.0	IgePal®	
Sodium Tetraborate	10	9.0	Brij® 35	
Sodium Tetraborate	10	9.0		Acetonitrile (5%)
Sodium Tetraborate	10	9.5	IgePal®	
Sodium Tetraborate	10	10.0	IgePal®	
Sodium Tetraborate	15	9.0	IgePal®	
Sodium Tetraborate	20	9.5	IgePal®	
Boric Acid	10	9.0	IgePal®	
Boric Acid	20	9.0	IgePal®	
Tris Borate EDTA	10	8.3	IgePal®	
Sodium Phosphate	10	2.5	IgePal®	
Sodium Phosphate	10	7.0	IgePal®	

Table 6.1 Summary of buffer conditions investigated to improve resolution of dynorphin metabolites.

Brij-35

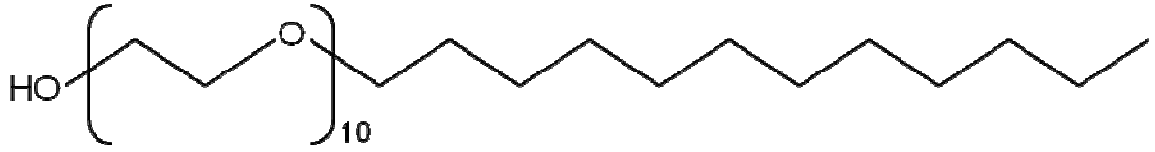

IgePal

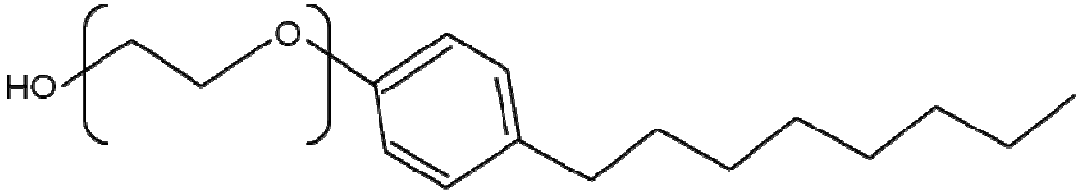

Figure 6.17. Structures of two surfactants (Brij 35 and IgePal) investigated for ME separation of dynorphin and metabolites.

non-specific adsorption onto glass microchip surfaces. Based on the sharp peak shapes observed with the dynorphin peptides, it did in fact prevent adsorption to the glass channels. The most promising separation was achieved with 10 mM sodium borate and 0.1% IgePal, pH 9.0 (Figure 6.18). However, complete resolution of the key metabolites was not achieved under any of the conditions investigated.

Alterations to the chip format or derivatization chemistry could overcome some of this challenge. Serpentine separation channels are a popular means for increasing N by lengthening the separation channel in a microchip device while maintaining the overall small footprint of the microchip. Additionally, investigating peptide tagging with smaller fluorescent probes would potentially enable improved resolution amongst these closely related species.

6.3.3 Future directions toward an immunoaffinity microchip device for pain neuropeptides

Current limitations with the resolution of small peptides after tagging with a large Alexa Fluor® dye, the adsorption of peptides to PDMS, and the difficulties associated with the integration of electrochemical detectors within glass matrices have stalled the progress of an immunoaffinity microchip electrophoresis system for the investigation of Dyn A 1-17 metabolism; however, progress is being made by our group in each of these areas and will be addressed in the following chapter. Additionally, the application of immunoaffinity techniques to a broader biological application is under consideration, that is, an immunoaffinity microchip for the investigation of neuropeptides implicated in neuropathic pain or a “pain pathway chip”. Preliminary work towards that end was accomplished using the conventional CE format utilizing a smaller fluorescent label, fluorescein isothiocyanate (FITC, MW ~ 390 g/mol). A CE separation of two neuropeptides, Dyn A 1-17 and SP, was achieved and is shown in Figure 6.19.

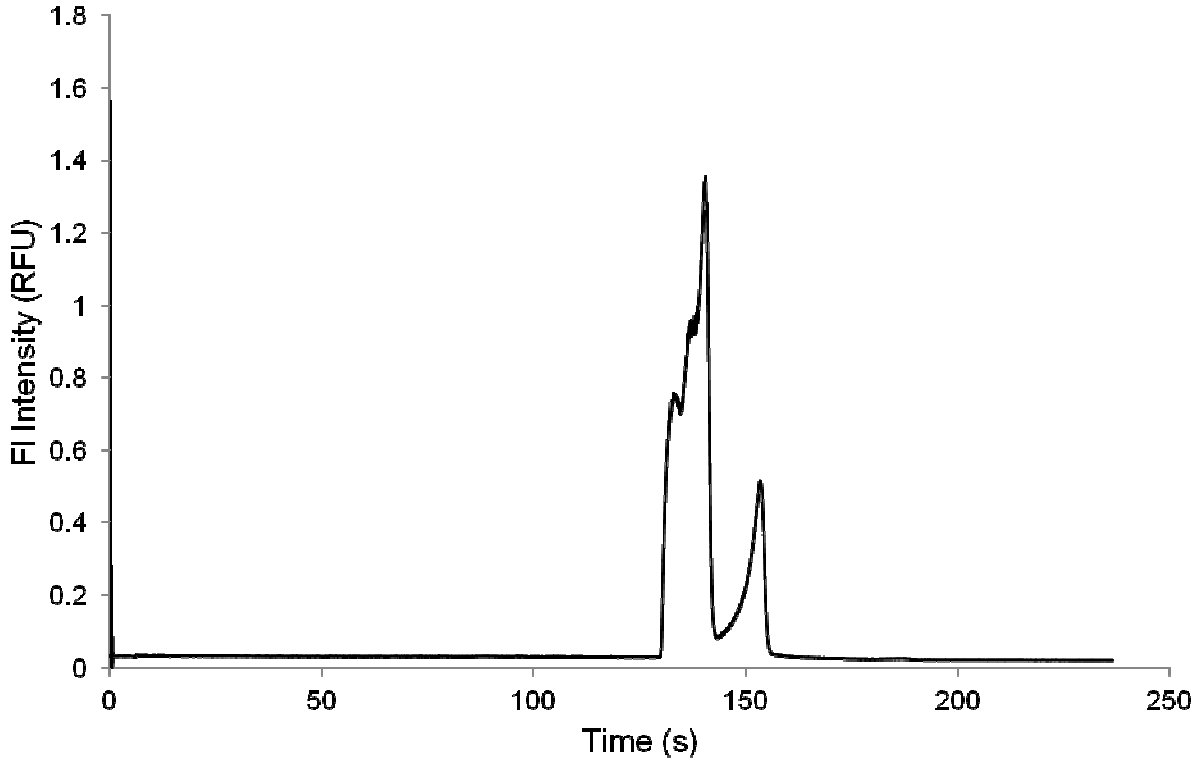

Figure 6.18. Detection of Alexa Fluor® 633-labeled dynorphin peptides, 1-6, 1-8, 1-13, 1-17, and 2-17 (each 2.5 μg/mL) on a glass microchip (8 cm separation channel). Run buffer consisted of: 10 mM sodium borate, 0.1% IgePal, pH 9.0, with a 1.0 second injection and 2.0 kV applied separation voltage.

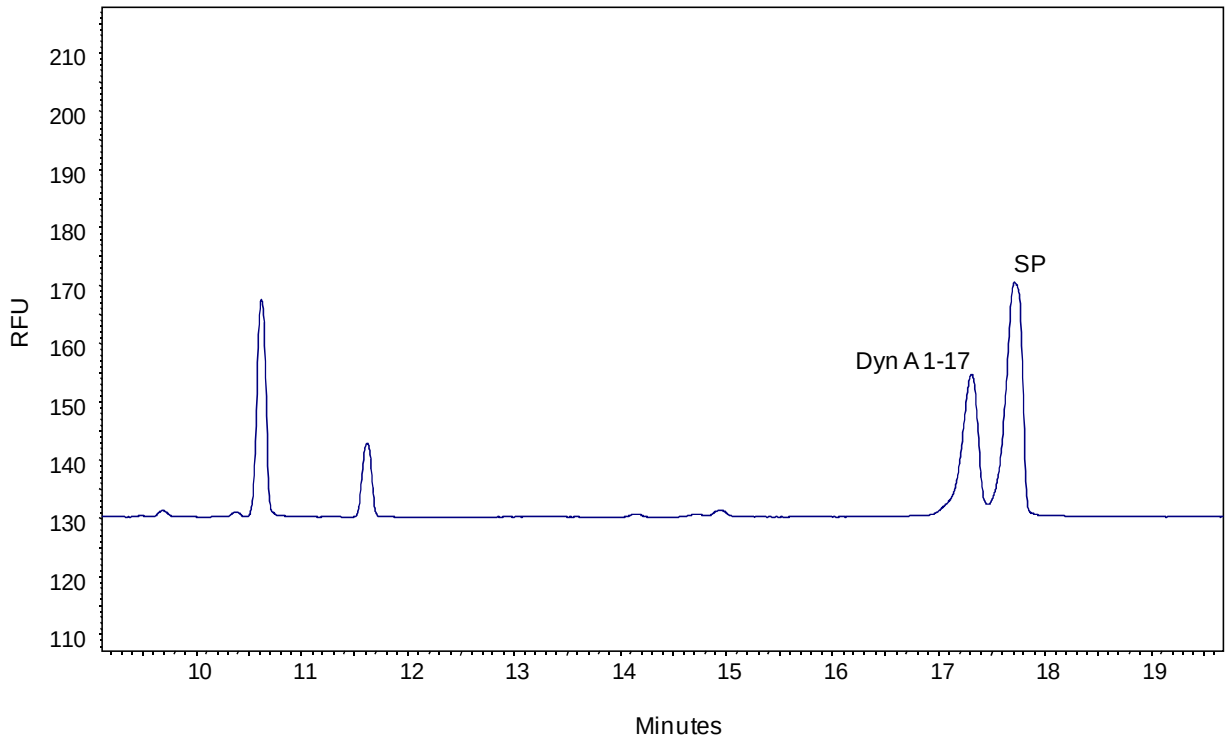

Figure 6.19 Conventional CE separation of FITC-labeled Dyn A 1-17 and substance P (SP), each 500 nM on a 60 cm capillary. Run buffer consisted of: 150 mM boric acid, 7.5 mM SDS, pH 9.5, and a 20.0 kV applied separation voltage.

These results will lay the ground work for future projects investigating the relationship between dynorphin and substance P and their involvement in neuropathic pain.

6.4 Summary

Immunoassays were performed to screen anti-dynorphin antibodies against a panel of dynorphin peptides. Anti-Dyn A 1-17 was shown to cross-react with Dyn A 2-17. Had this assay been performed to quantify the amount of Dyn A 1-17 in a biological sample of interest, a falsely elevated level could easily have been reported for Dyn A 1-17 since any 2-17 present in the sample would have contributed to the overall peptide signal. This observation highlights a key drawback to such techniques for investigations of neuropeptides as biomarkers for disease, especially when the role of a peptide's metabolite(s) is not clearly understood. The work presented here characterizes one component of the overall goal for incorporating a dynorphin immunoaffinity port into a microchip device.

Additionally, a variety of microchip formats have been explored for the separation of Dyn A 1-17 from its metabolites. Each of these experimental designs offers certain advantages. PDMS-glass hybrid chips offer the ease of integrating an electrochemical detector within a chip, which is essential for the future of on-animal total analysis systems. All glass chips with LIF detection exhibit improved sensitivity, which will enable quantitation of endogenous levels of low-abundant neuropeptides. However, each format also carries with it significant drawbacks such as peptide adsorption to PDMS substrates and difficulty resolving tagged-dynorphin peptides on short separation channels. The following chapter will address the future work necessary for the development of such immunoaffinity microchip devices for further

characterization of dynorphin metabolism as well as the applicability of such techniques to neuropeptides in general.

6.5. References

[1] Amundsen, L. K., Siren, H., *Electrophoresis* 2007, *28*, 99-113.

[2] Guzman, N. A., Blanc, T., Phillips, T. M., *Electrophoresis* 2008, *29*, 3259-3278.

[3] Moser, A. C., Hage, D. S., *Bioanalysis* 2010, *2*, 769-790.

[4] Hou, C., Herr, A. E., *Electrophoresis* 2008, *29*, 3306-3319.

[5] Wa, C., Mallik, R., Hage, D. S., *Analytical Chemistry* 2008, *80*, 8751-8762.

[6] Kalish, H., Phillips, T. M., *Journal of Separation Science* 2009, *32*, 1605-1612.

[7] Kalish, H., Phillips, T. M., *Journal of Chromatography B* 2010, *878*, 194-200.

[8] Phillips, T. M., *Luminescence* 2001, *16*, 145-152.

[9] Phillips, T. M., Smith, P., *Biomedical Chromatography* 2003, *17*, 182-187.

[10] Shah, J. P., Phillips, T. M., Danoff, J. V., Gerber, L. H., *Journal of Applied Physiology* 2005, *99*, 1977-1984.

[11] Benavente, F., Hernandez, E., Guzman, N. A., Sanz-Nebot, V., Barbosa, J., *Analytical Bioanalytical Chemistry* 2007, *377*, 2633-2639.

[12] Gimenez, E., Benavente, F., de Bolos, C., Nicolas, E., Barbosa, J., Sanz-Nebot, V., *Journal of Chromatography A* 2009, *1216*, 2574-2582.

[13] Phillips, T. M., Wellner, E. F., *Journal of Chromatography A* 2006, *1111*, 106-111.

[14] Phillips, T. M., Wellner, E. F., *Electrophoresis* 2007, *28*, 3041-3048.

[15] Phillips, T. M., Wellner, E. F., *Electrophoresis* 2009, *30*, 2307-2312.

[16] Sun, X., Yang, W., Pan, T., Woolley, A. T., *Analytical Chemistry* 2008, *80*, 5126-5130.

[17] Yang, W., Sun, X., Wang, H.-Y., Woolley, A. T., *Analytical Chemistry* 2009, *81*, 8230-8235.

[18] Phillips, T. M., Kennedy, L. M., De Fabo, E. C., *Journal of Chromatography B* 1997, *697*, 101-109.

[19] Phillips, T. M., Dickens, B. F., *Electrophoresis* 1998, *19*, 2991-2996.

[20] Wellner, E. F., Kalish, H., *Electrophoresis* 2009, *29*, 3477-3483.

[21] Phillips, T. M., Chmielinska, J. J., *Biomedical Chromatography* 1994, *8*, 242-246.

[22] Miksa, B., Chinnappan, R., Dang, N. C., Reppert, M., Matter, B., Tretyakova, N., Grubor, N. M., Jankowiak, R., *Chem. Res. Toxicol.* 2007, *20*, 1192-1199.

[23] Clarke, W., Chowdhuri, A. R., Hage, D. S., *Analytical Chemistry* 2001, *73*, 2157-2164.

[24] Clarke, W., Hage, D. S., *Analytical Chemistry* 2001, *73*, 1366-1373.

[25] Stege, P. W., Raba, J., Messina, G. A., *Electrophoresis* 2010, *31*, 3475-3481.

[26] Phillips, T. M., Wellner, E. F., *Biomedical Chromatography* 2006, *20*, 662-667.

[27] Phillips, T. M., Dickens, B. F., *Affinity and Immunoaffinity Purification Techniques*, Eaton Publishing, Natick 2000.

[28] Fischer, D. J., Hulvey, M. K., Regel, A. R., Lunte, S. M., *Electrophoresis* 2009, *30*, 3324-2222.

[29] Fischer, D. J., Vandaveer, W. R., Grigsby, R. J., Lunte, S. M., *Electroanalysis* 2005, *17*, 1153-1159.

[30] Hulvey, M. K., Frankenfeld, C. N., Lunte, S. M., *Analytical Chemistry* 2010, *82*, 1608-1611.

[31] Gawron, A. J., Martin, R. S., Lunte, S. M., *Electrophoresis* 2001, *22*, 242-248.

[32] Martin, R. S., Gawron, A. J., Fogarty, B. A., Regan, F. B., Dempsey, E., Lunte, S. M., *The Analyst* 2001, *126*, 277-280.

[33] Gawron, A. J., Lunte, S. M., *Electrophoresis* 2000, *21*, 2067-2073.

[34] Gawron, A. J., Lunte, S. M., *Electrophoresis* 2000, *21*, 3205-3211.

[35] Lacher, N. A., Garrison, K. E., Lunte, S. M., *Electrophoresis* 2002, *23*, 1577-1584.

[36] Lacher, N. A., de Rooij, N. F., Verpoorte, E., Lunte, S. M., *Journal of Chromatography A* 2003, *1004*, 225-235.

Chapter Seven:

Future directions

7.1 Thesis summary

This thesis describes the development of methods for the detection of Dyn A 1-17 and four of its key metabolites: Dyn A 1-6, Dyn A 1-8, Dyn A 1-13, and Dyn A 2-17 in biological samples. In chapter 3, capillary electrophoresis with on-capillary copper complexation and UV detection is used to investigate dynorphin metabolism in human plasma as well as rat brain and spinal cord slices. The method ultimately involved the incorporation of phytic acid to prevent peptide adsorption to the capillary wall and sulfobutyl ether-β-cyclodextrin to improve resolution of such closely related species.

Chapter 4 describes the development of an LC-MS/MS assay for dynorphin peptides from cell culture samples, including special considerations regarding ionization in the cell media. A description of mass spectrometric parameter optimization is thoroughly discussed as well as liquid chromatographic conditions for the separation of dynorphin peptides and an appropriate internal standard. This method is utilized in Chapter 5 to characterize the dynorphin metabolism in rat brain and spinal cord slices as well as with a cell culture model of the blood brain barrier (BBB). Dyn A 1-6 is identified as the major metabolite of Dyn A 1-17. Its transport was then characterized at the blood brain barrier using the bovine brain microvessels endothelial cell (BBMEC) BBB model.

Chapter 6 lays the groundwork for developing an immunoaffinity microchip device for determining dynorphins. Traditional ELISAs were used for antibody screening to determine reactivity. Initial studies using a PDMS-glass hybrid microchip with amperometric detection demonstrated significant peptide adsorption. An all glass microchip with LIF was also investigated, following tagging with Alexa Fluor® 633. However, incomplete resolution was

obtained under a variety of buffer conditions that were investigated. Future directions of the project will continue optimization of the microchip separation and will further develop an immunoaffinity microchip for investigating neuropeptides implicated in neuropathic pain. These experiments are described in more detail in the next section.

7.2 Future directions

7.2.1 Mass spectrometric detection of dynorphin peptides

In addition to the studies described in Chapter 5 of this thesis, additional mass spectrometry studies could further confirm the presence of Dyn A 1-6 as the major metabolite of Dyn A 1-17. Matrix-assisted laser desorption ionization mass spectrometry (MALDI MS) would also be an additional method to confirm the presence of the Dyn A 1-6 metabolite. While not quantitative, the molecular weight identification would provide additional support to the data presented in chapters. Identification of the 7-17 fragment would further confirm the presence of this metabolite as well.

The effect of opioid peptides on low molecular weight peptide transport could further be investigated using the BBMEC culture model described in Chapter 5. Additional dynorphin peptides should be evaluated for their propensity to alter the integrity of the blood brain barrier. Studies to elucidate the mechanism by which this opening occurs would also be useful in examining the role this family of peptides may play in the central nervous system.

7.2.2 Microchip modifications for improved resolution of dynorphin metabolites

While the studies presented here demonstrate the difficulties in separating closely related species on miniaturized devices, several design modifications could potentially alleviate these complications. Considerable attention in microchip research has been devoted to increasing separation length while maintaining the desirable small footprint of these devices using serpentine channels [1-4]. In this way, improved resolution can be accomplished without compromising the portability of the device.

Peptide adsorption was the most significant drawback to the use of a PDMS microchip. This further hinders the use of electrochemical detection since the incorporation of electrodes is most easily accomplished in a PDMS device where reversible sealing over the electrode is rather simple. Electrode materials typically produce defect sites during glass bonding and leaking around the electrode is a significant issue. Our group is working to fabricate electrodes embedded into a glass substrate to alleviate this effect. Additionally investigating smaller fluorescent tagging systems could help with the assay as well. Because dynorphin peptides are relatively small (molecular weights of 700-2100), the large Alexa Fluor® tags (MW = 1200) used in these studies, significantly diminish any differences in the mass to charge ratio of these compounds, decreasing resolution by CE.

7.2.3 Immunoaffinity microchip electrophoresis for neuropeptides implicated in neuropathic pain

Dynorphin is one of several neuropeptides involved in pain signaling pathways [5]. Substance P (SP) is also known to play a role in pain processing. Capsaicin-stimulated release of SP has been previously reported and some work suggests that dynorphin facilitates this release [6]. Therefore, in addition to investigating the role of dynorphin in chronic conditions such as neuropathic pain, the interplay between dynorphin and substance P should be considered (Figure 7.1). Immunoaffinity microchip electrophoresis is an attractive method for such applications. In particular some of the complications with separating dynorphin metabolites can be avoided. Dynorphin and substance P differ structurally (Figure 7.2) making separation an easier task even if large fluorescent tags are utilized. Antibody characterization is also simplified considerably when investigating two un-related species. An antibody to capture each of these compounds should still be screened for cross-reactivity in a conventional immunoassay for comparison with a novel chip-based assay.

Prior to the fabrication of a fully integrated device, the separation of the two peptides on a microchip device should be optimized. As an intermediate step, off-line extraction (most conveniently using antibody-functionalized magnetic beads) can be performed to assure that elution conditions do not alter the eletrophoretic behavior in any way. Both SP and Dyn A 1-17 antibodies can then be incorporated into a microchip device for a fully integrated immunoaffinity pain microchip. This would make it possible to investigate the interaction between these two peptides at the blood brain barrier. The effect of both peptides on BBB transport would be of interest to the role that each plays in neuropathic pain, as well as the *in vivo* role of the peptides on the release of excitatory amino acids and the effect on fluorescein permeability.

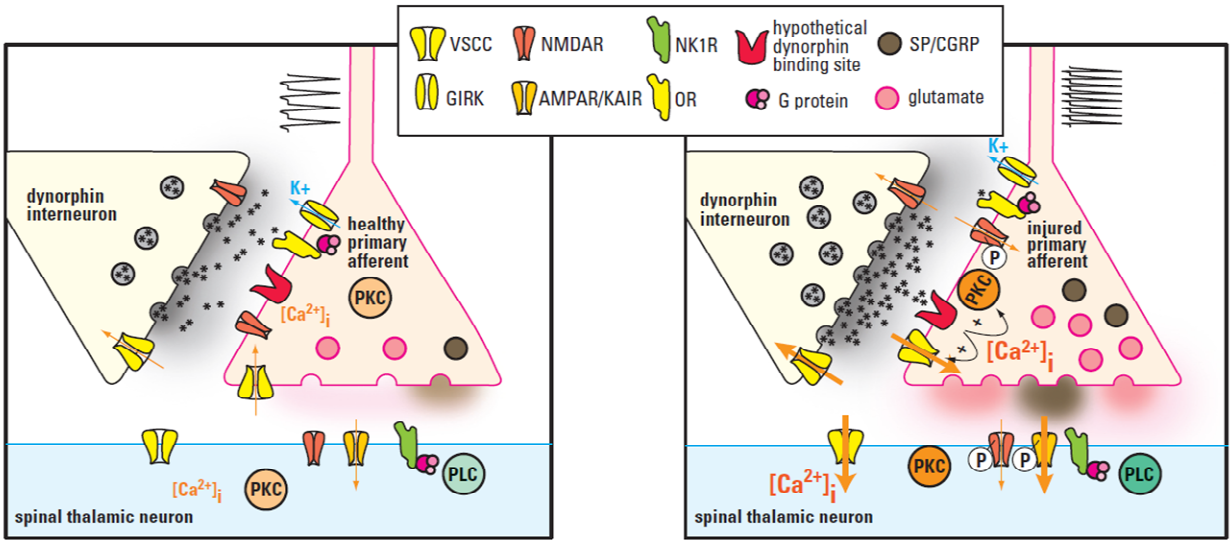

Figure 7.1. Cartoon depiction of the possible mechanism by which dynorphin potentiates neuropathic pain. Normal conditions are represented on the left and the downstream effects of dynorphin upregulation, following nerve injury, is represented on the right. Used with permission from [5].

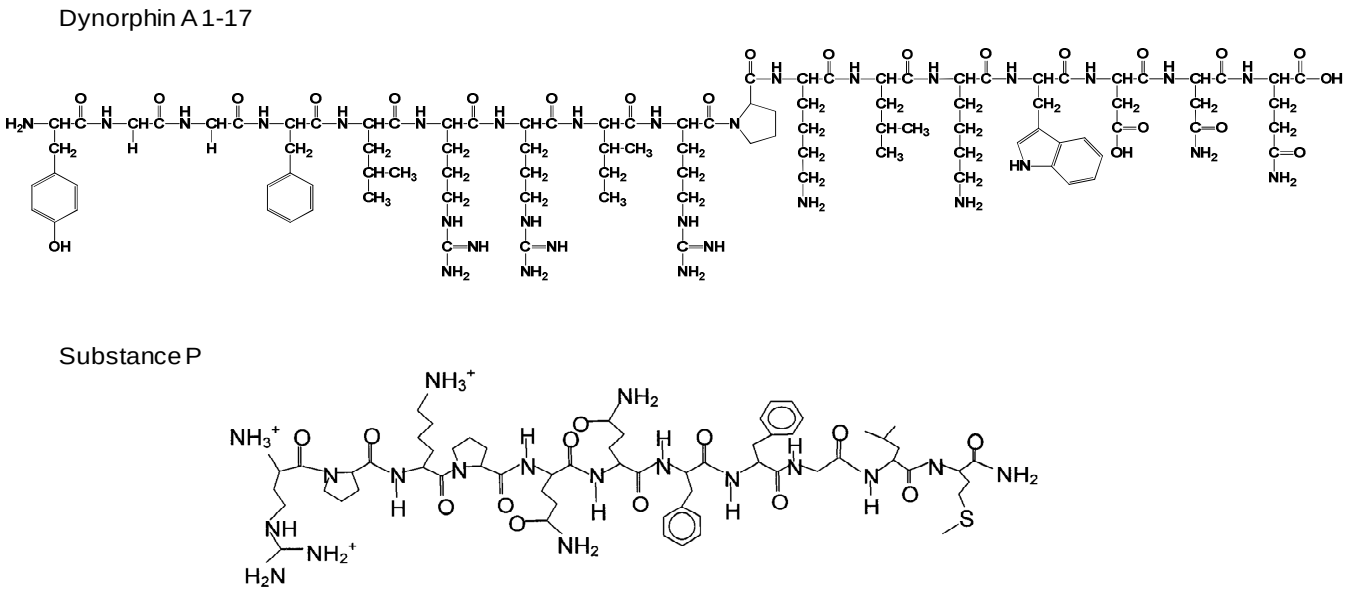

Figure 7.2 Structures of Dyn A 1-17 (NH_2-Tyr-Gly-Gly-Phe-Leu-Arg-Arg-Ile-Arg-Pro-Lys-Leu-Lys-Trp-Asp-Asn-Gln-OH) and SP (NH_2-Arg-Pro-Lys-Pro-Gln-Gln-Phe-Phe-Gly-Leu-Met-$NH_{2)}$

As mentioned in previous sections of this thesis, miniaturization of an electrophoresis system enables portability and improved temporal resolution. Previous work in our group has developed a microchip device capable of on-line microdialysis sampling and on-chip derivatization with NDA/CN^- [7-9]. Therefore, the long term goal of this project, in addition to other projects in our group, is the creation of a fully functional on-line microdialysis immunoaffinity microchip electrophoresis device for on-animal studies to correlate animal behavior with the physiological role of neuropeptides (SP and Dyn A 1-17) and excitatory amino acids (glutamate and aspartate).

7.3 References

[1] Ramsey, J. D., Jacomson, S. C., Culberston, C. T., Ramsey, J. M., *Anal. Chem.* 2003, 75, 3758-3764.

[2] Roman, G. T., McDaniel, K., Culberston, C. T., *The Analyst* 2006, 131, 194-201.

[3] Skelley, A. M., Mathies, R. A., *Journal of Chromatography A* 2003, 1021, 191-199.

[4] Skelley, A. M., Scherer, J. R., Aubrey, A. D., Grover, W. H., Ivester, R. J., Ehrenfreund, P., Grunthaner, F. J., Bada, J. L., Mathies, R. A., *PNAS* 2005, 102, 1041-1046.

[5] Lai, J., Ossipov, M. H., Vanderah, T. W., Malan, J., T. P. , Porreca, F., *Mol. Interventions* 2001, 1, 160-167.

[6] Arcaya, J., Cano, G., Gomez, G., Maixner, W., Suarez-Roca, H., *European Journal of Pharmacology* 1999, 366, 27-34.

[7] Huynh, B. H., Fogarty, B. A., Martin, R. S., Lunte, S. M., *Anal. Chem.* 2004, 76, 6440-6447.

[8] Huynh, B. H., Fogarty, B. A., Nandi, P., Lunte, S. M., *J. Pharm. Biomed. Anal.* 2006, 42, 529-534.

[9] Nandi, P., Desai, D. P., Lunte, S. M., *Electrophoresis* 2010, 31, 1414-1422.